Regulation and Neutralisation of Adrenomedullin in Cancer

PhD

Mary Brindha Ashok Kumar

Department of Human Metabolism

April 2014

Acknowledgements

It is a pleasure to thank the many people who made this thesis possible.

The financial support from SURE, Dorothy Hodgkin Postgraduate Awards, BBSRC and Medella Therapeutics are gratefully acknowledged.

My sincere thanks to my supervisor, Prof. Tim Skerry for his constant encouragement, inspirational guidance and sound advice. Tim once let me drive his tractor whilst sitting next to me and steering me in the right direction when necessary. This is precisely how Tim would guide me during the entire course of my research. Many thanks to him for giving me full freedom to think and design experiments and for teaching me to learn from my mistakes. I would like to extend my gratitude to his wife, Donna for always welcoming me with her cheerful smile and warm hug. Every visit to the Skerrys' always reminded me of my home back in India.

The good advice, support and friendship of my second supervisor Dr. Gareth Richards, has been invaluable to me. He believed that I had the potential to do a PhD while I was a master's student, many thanks for that and for his patience even when I tried him the most.

My deepest gratitude extends to Dr. Dave Roberts and Dr. Ning Wang for their constant help in calculations however trivial they might be.

I would like to thank Dr. Alison Gartland and Dr. Peter Grabowski for their untiring support and guidance. Warm thanks to Clive Buckle for helping me with qPCR. Thanks to Orla Gallagher for preparing sections with my tumour samples for immunohistochemistry. I also wish to thank Dr. Ingunn Holen and Hannah Brown for helping me with ordering mice and inter-cardiac injections.

Warm thanks to my friend and colleague Aditya Desai for being there for me in and out of lab. Special thanks to my student Nasim Eskandari for her work in

the 2nd chapter of this thesis and her continuous enthusiasm she showed in this project. I am grateful to my friends Viji, Vini, Susanna, Carlos, Sindhu, Juhi Suruchi and Sandeep for their friendship and encouragement.

I want to express my appreciation to my family for their unending love, constant support and for having faith in me.

My loving thanks to my husband Shravanth, for being understanding, loving, caring and encouraging. It would have been impossible for me to finish my research and thesis but for his constant love, emotional support and never failing faith in me. I cannot thank him enough for enduring this long process with me.

I would like to dedicate this thesis to my loving father whom I miss very much.

Abstract

Adrenomedullin (ADM) is an evolutionarily conserved peptide hormone that is essential for a wide variety of physiological functions. Deregulation of ADM has been implicated in many pathological conditions including sepsis, cardiovascular diseases and cancer. Published data suggest ADM may play a role in up to 80% of cancers by acting as an apoptosis survival factor, a proliferative agent, an angiogenic factor and helping tumour cells evade the immune system. Receptors for ADM are composed of a G protein Coupled Receptor called the Calcitonin Like Receptor (CLR) which complexes with either Receptor Activity Modifying Protein (RAMP) 2 or 3 resulting in two distinct receptors for ADM (RAMP2+CLR or RAMP3+CLR). Since ADM plays a crucial role in tumour progression, it was hypothesized that neutralising ADM would have a significant impact on reducing tumour growth and its angiogenic potential.

Under hypoxia, cells expressed significantly high levels of ADM, possibly to withstand the potentially lethal microenvironment. The effect of over-expression of ADM was studied on cell proliferation, migration and invasion. ADM over-expressing cells migrated faster than control cells in scratch test assay. Preliminary analysis on cell proliferation showed no significant difference in cells transfected with ADM. Results from these studies demonstrated that ADM contributes to cancer cell progression.

An anti-RAMP3 antibody, JF2, developed in our lab was used to inhibit ADM action. A decrease in cell proliferation was seen in Glioblastoma, Pancreatic, Breast and Prostate cancer cells when compared to isotype controls. *In vivo* experiments using NOD-SCID mice subcutaneously injected with pancreatic cancer cells resulted in significant reduction in tumour size and volume.

Collectively, it is demonstrated that ADM is elevated in a malignant setting and targeting ADM activity would significantly reduce tumour progression. Further research on the affinity, toxicity, mechanism of action and downstream effects in signalling of JF2 could elucidate its potential as a drug in cancer treatment.

Table of Contents

List of Figures

List of Tables

Abbreviations

µg -	microgram
µl -	microlitre
µm -	micromolar
A/bis A -	Acrylamide / Bis - Acrylamide
ADCC -	Antibody - dependent cellular toxicity
ADM -	Adrenomedullin
ADMR -	Adrenomedullin Receptor
Akt -	Protein Kinase B
AMBP1 -	Adrenomedullin Binsing Protein -1
AMY -	Amylin
ANOVA -	analysis of variance
ARD -	Acetyle transferase arrest-defective
ATP -	Adenosine triphosphate
BCA -	Bicinchoninic acid
BLAST -	Basic Local Alignment Tool
bp -	base pair
BSA -	Bovine Serum albumin
cAMP -	cyclic Adenosine monophosphate
CaSR -	Calcium Sensing Receptor
cDNA -	complementary Deoxyribonucleic acid
CGH -	Comparitive Genomic Hybridization
CGRP -	Calcitonin Gene Related peptide
CH -	continous hypoxia
CLR -	Calcitonin Like Receptor
cm^2 -	centimetre square
CO_2 -	Carbon di oxide
$CoCl_2$ -	Cobalt Chloride
CRE -	cAMP Regulated Enhancer
CT -	Calcitonin
CTLA4 -	Cytotoxic T-lymphocyte associated antigen
CTR -	Calcitonin Receptor
ddH_2O -	double distilled water
DEPC -	Diethylpyrocarbonate
dH_2O -	distilled water
DMEM -	Delbecco's Modified eagle Medium
DNA -	Deoxyrobonucleic acid
ECD -	Extracellular Domain
ECL -	Extracellular loop
ECL -	Enhanced Chemiluminescent
ECM -	Extracellular Matrix

EDTA - Ethylene diaminetetraacetic acid
EGF - Epidermal Growth Factor
EMMPRIN - Extracellular Matrix Metalloproteinase inducer
EMT - Epithelial Mesenchymal transition
ER - Endoplasmic Reticulum
ERK - Extracellular signal-regulated konases
Fv - Fragment variable
Fab - Fragment antigen binding
FACS - Fluorescent Activated Cell Sorting
FAK - Focal Adhesion Kinase
Fc - Fragment constant
FGF - Fibroblast Growth Factor
fig - Figure
FIH - Factor Inhibiting Hypoxia Inducible Factor
FITC - Fluorescein isothiocyanate
fmol - femtomole
g - gravity
g - Gram
G - Gauge
GBM - Glioblastoma multiforme
GDP - Guanosine diphosphate
GFP - Green Fluorescent Protein
GPCR - G Protein Coupled Receptor
GRKs - G Protein Coupled Receptor Kinase Family
GRP - Gastrin Releasing Peptide
GTP - Guanosine triphosphate
h - Hours
H&E - Haemotoxylin & Eosin
H_2O - Water
hCASMC - human Coronary Artery Smooth Muscle Cells
HEK - Human Embryonic Kidney
HEPES - (4-(2-hydroxyethyl)-1-piperazineethanesulfonic acid
HIF - Hypoxia Inducible Factor
HMECs - Human Microvascular Endothelial Cells
HPRT - Hypoxanthine phosphoribosyltransferase
HRE - Hypoxia Response element
HRP - Hors raddish peroxidase
hrs - Hours
HUVECs - Human Umbilical Vein Endothelial Cells
iADM - immature Adrenomedullin
Ig - immunoglobulin
IgCAMs - Immunoglobulin domain cell adhesion molecules
IGF - Insulin Like Growth Factor
IH - Intermittent Hypoxia

IL - Interleukin
IMS - Industrial Methylated Spirit
IRES-eGFP - Internal ribosomal entry site -enhanced Green Fluorescent Protein
JNK - c-Jun N-terminal kinases
KCl - Potassium Chloride
kDa - kilo Dalton
Kg - kilogram
KOD - Thermococcus kodakaraensis
L - Litre
LB - Luria Broth
LOX - Lysyl Oxidase
LOXL - Lysyl Oxidase Like Protein
mAb - monoclonal Antibody
MAC - Membrane Attack Complex
mADM - mature Adrenomedullin
MAPK - Mitogen Activated protein kinase
MEM - Minimum Essential Media
mg - milligram
$MgCl_2$ - Magnesium Chloride
MHC - Major Histocompatibility complex
min - minute
ml - millilitre
mm - millimetre
mmHg - millimetre mercury
MMP - Matrix Metalloproteinase
mRNA - messenger Ribonucleic acid
MTT - (3-(4,5-dimethylthiazol-2-yl)-2,5-diphenyl tetrazolium bromide
N_2 - Nitrogen
NaOH - Sodium Hydroxide
NEP - Neutral Endopeptidase
NHERF - Na^+/H^+ Exchanger Regulatory Factor
NK - Natural Killer
NO - Nitric Oxide
NOD - SCID - Non-Obese diabetic Severe Combined Immunodeficieny
NOS - Nitric Oxide Synthase
NSF - N-ethylmaleimide - Sensitive Factor
O_2 - Oxygen
^oC - degree Celsius
OD - Optical Density
PAC - Pancreatic adenocarcinoma cells
PAGE - Poly Acrylamide Gel Electrophoresis
PAL - Peptidyl-α-hydroglycine α-amidating lysase
PAM - Peptidylglycine α-monooxygenase
PAMP - pro Adrenomedullin N Terminal 20 peptide

PBS - Phosphate Buffered Saline
PCR - polymerase chain reaction
PDGF - Platelet Derived Growth Factor
PFA - Paraformaldehyde
pg - picogram
PHDs - Prolyl-4-hydroxylases
PI-3k - Phosphoinositide 3-kinase
PIP3 - phosphatidylinositol (3,4,5) - triphosphate
pm - pico molar
PTEN - Phosphatase and tension homolog
PTH - Parathyroid Hormone
PTYK - Protein tyrosine Kinase
PVDF - Polyvinylidene difluoride
qPCR - quantitative polymerase chain reaction
RAMPs - Receptor Activity Modifying Proteins
RCC - Renal Cell Carcinoma
RCP - Receptor Component Protein
REC - Rat Endothelial Cells
RMCs - Rat Mesangial Cells
RNA - Ribonucleic acid
ROS - Reactive Oxygen Species
rpm - rotation /revolution per minute
RPMI - Roswell Park Memorial Institute
RT - Reverse Transciption
RTPCR - Reverse Transcription Polymerase Chain Reaction
ScFv - Single Chain Variable fragment
SDS - Sodium dodecyl sulfate
secs - seconds
SEM - Standard error mean
SRK1/2 - Signal Regulated Kinase
TAM - Tumour Associated Macrophages
TB - Tris Borate
TK - Tyrosine Kinase
TNF - Tumour Necrosis Factor
TS - Tumour Suppressor
UV - Ultraviolet
V - Volts
VEGF - Vascular Endothelial Growth Factor
VEGFR - Vascular Endothelial Growth Factor Receptor
VHL - Von Hippel Lindau
VSMCs - Vascular Smooth Muscle Cells
w/v - weight / volume
γ-GCL - γ-glutamate cysteine ligase
ZG - Zona Glomerulosa

CHAPTER I: INTRODUCTION

1.1. Cancer

Cancer is a multifactorial disease characterised by uncontrollable proliferation of cells, leading to the formation of tumours. The lifetime risk of developing cancer is one in three (Futreal et al. 2001). Figure 1 shows the top 20 most common causes of cancer deaths worldwide estimated in 2008 by Cancer Research UK. When the tumour reaches a certain mass, a small number of cells are capable of being carried from the primary tumour by blood or the lymphatic system to other parts of the body leading to the formation of secondary cancer termed as metastases. Cancers are classified according to their tissue of origin and histology. Since there are over 200 types of cells, there are over 200 types of cancers (Hanahan and Weinberg 2000).

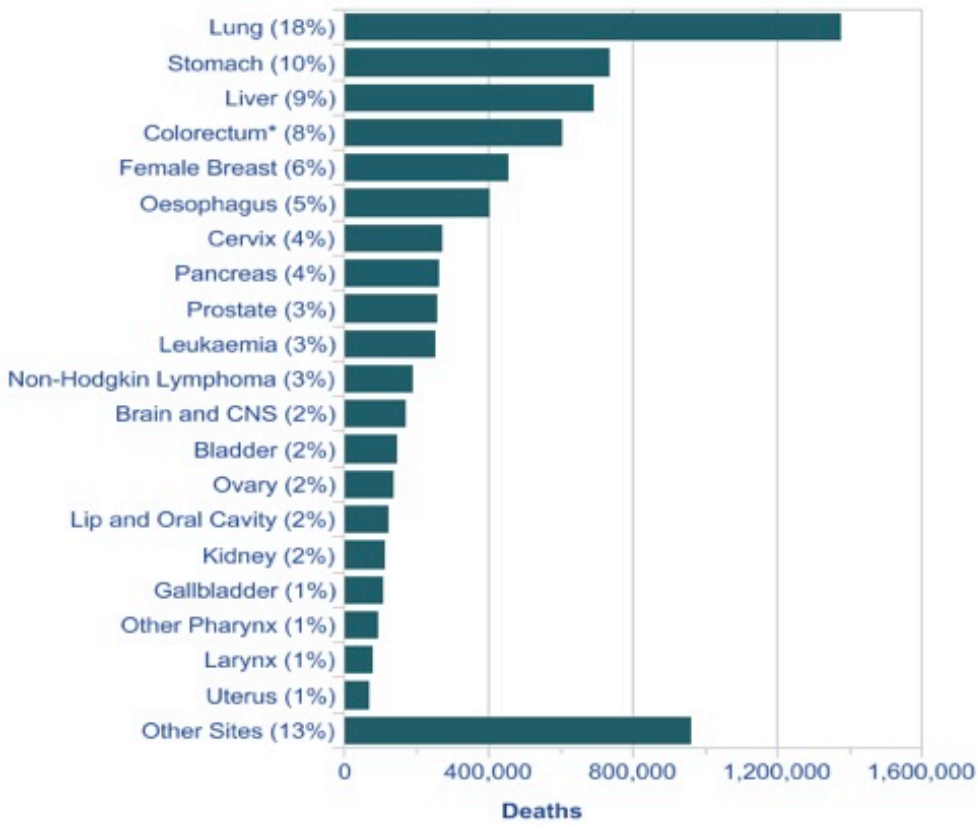

Figure 1: Top 20 most common causes of cancer deaths world wide estimated in 2008. Picture taken from Cancer Research UK.

There are many factors that influence the pathogenesis of cancer, such as carcinogens (Gibbs and Berry 2008; O'Reilly et al. 2007; Robert and Dubertret 1995), lifestyle (Bradley et al. 2002; Salaspuro 2007; Witschi et al. 1997), environment (Kampa and Castanas 2008; Ward 1995), viruses (Blattner 1999; Frazer 2004; Narisawa-Saito and Kiyono 2007), genetic make-up (Rahman and Stratton 1998) and age (Hanahan and Weinberg 2000). All of these factors play a role that directly or indirectly alter the normal functioning of the DNA. All through life DNA is exposed to various mutagens that alter the replication and causes certain mutations in the sequence of the DNA. Studies have shown that an average of six to seven mutations are needed to convert a normal epithelial cell into an invasive carcinoma (Futreal et al. 2001). The common genes that undergo mutations by the above mentioned factors can be broadly classified into two categories:

- Proto-oncogenes – When the gene undergoes mutations it becomes an oncogene and promote uncontrolled cell proliferation. For example, when the RET proto-oncogene undergoes mutations, it becomes an oncogene resulting in multiple endocrine neoplasia type 2 which is a syndrome for cancer (C. Eng 1999).

- Tumour Suppressor (TS) genes – these genes aid in suppressing the events leading towards cancer. They help the inappropriate cell cycle progression and maintain low mutation rates by ensuring accurate replication and repair, mutation in these genes results in cancer. In order to change the normal behaviour of the cell, both alleles of this gene must be inactivated / mutated. An example of such a gene is, TP53 that codes for p53 which is a tumour suppressor protein and has many anti-cancer mechanisms. 60% of cancers have mutations in p53 gene (Bourdon 2007).

Studies have shown that mutations in the genes lead to cancerous phenotypes (Blume-Jensen and Hunter 2001) by amplification of proto-oncogenes (Pinkel and Albertson 2005), point mutations (Lowy and Willumsen 1993) and chromosomal translocations (Rabbitts 1994). Genes involved in the

development of cancer show a wide variety in structure and function. Due to this wide variety, cancer has proved to be a difficult condition to treat (Futreal et al. 2001). Cancer cells exhibit various characteristics to sustain themselves. Hanahan and Weinberg in 2000 and 2011 (Hanahan and Weinberg 2000, 2011) outlined the characteristic features of cancer cells which is illustrated in figure 2.

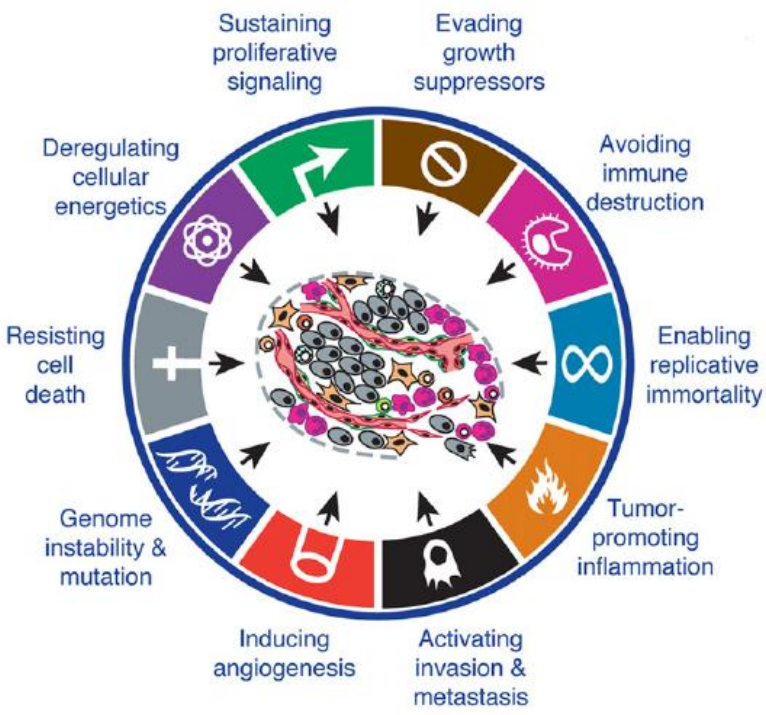

Figure 2: The different characteristic features of a cancer cell. Picture taken from Hanahan and Weinberg, 2010.

Studies on cancer cells reveal that many signalling pathways contribute to its pathogenesis. Once a cell has undergone the mutations to make it neoplastic, it needs to have cell-cell signalling that is dependent on growth factors, cytokines and hormones. Cancer cells acquire the ability to proliferate uncontrollably by either producing excessive growth factors or by sending signals to stimulate non-cancerous cells within the tumour-associated stroma to produce growth factors (Bhowmick et al. 2004; Cheng et al. 2008). Cancer cells in turn up-regulate the expression of receptor proteins to respond to the excessive

production of growth factor ligands (Hanahan and Weinberg 2011). One of the growth regulatory peptide that is over produced in cancer is Adrenomedullin (F. Cuttitta et al. 2002; Martinez et al. 1997; Satoh et al. 1995; Zimmermann et al. 1996).

1.2. Adrenomedullin

Adrenomedullin (ADM) is a hypotensive peptide discovered in the pheochromocytoma of humans which are tumours present in the adrenal medulla, thus giving this peptide its name. It belongs to the Calcitonin super family of peptides (Kitamura et al. 1993). ADM is known to elicit the levels of cAMP which resulted in elevated blood pressure in rats. ADM is evolutionarily conserved for over millions of years playing an important role in various physiological functions thereby contributing to survival (Frank Cuttitta et al. 1999). Some of the physiological functions that ADM plays a role are cell growth (Frank Cuttitta et al. 1999), blood pressure, hormone regulation (T. Yamaguchi et al. 1995), angiogenesis (Y. Zhao et al. 1998) and apoptosis (H. Kato et al. 1997).

1.2.1. Structure

ADM is a 52 amino acid peptide, having a disulphide bond between two cysteine residues located at positions 16 and 21, as illustrated in figure 3. The amidation of the C terminal end and the cysteine ring structure is important for the biological activity of the peptide. These structures are responsible for the receptor binding and subsequent cAMP generation (Kitamura et al. 1993). The C-terminal fragment ADM_{22-52} does not contain the disulphide ring and does not show any activity upon binding to the ADM receptors, so it is used as an ADM receptor antagonist (Eguchi et al. 1994). ADM circulates in plasma with concentrations between 2-10pM (Kitamura et al. 1993). Circulating ADM is bound to an ADM binding protein-1 (AMBP-1) – complement factor H; this complex makes it hard to estimate the amount of ADM in plasma (Pio et al. 2001), therefore circulating ADM levels maybe more than 2-10pM.

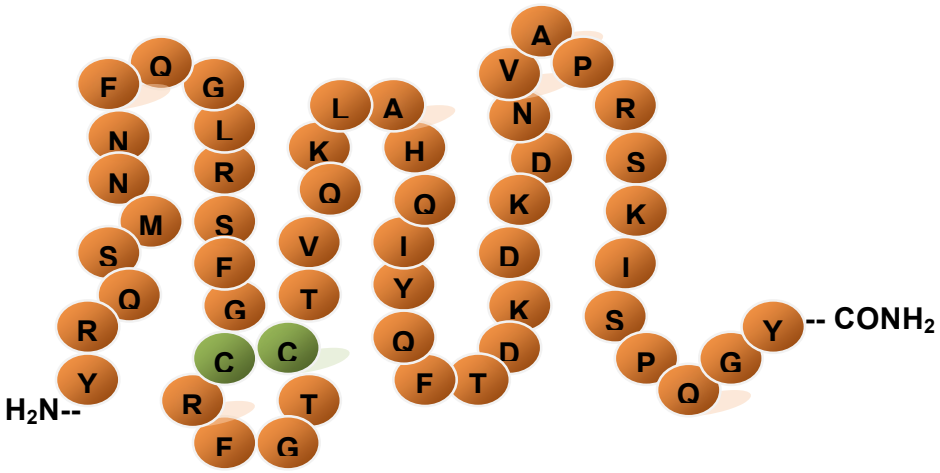

Figure 3: Structure of Adrenomedullin showing the two cysteine residues in green where the disulphide bond exists. The figure also shows the amidated C terminal end. Figure drawn by self, adapted from Beltowki & Jamroz, 2004 .

1.2.2. Expression, Release and Clearance

The gene that encodes ADM in humans, is present on chromosome 11 and is made up of a single locus and consists of four exons and three introns. The 5' flanking region consists TATA (-653), CAAT (-755) and GC boxes. There are multiple binding sites for Activator Protein -2 (AP-2), Activator Protein -1 and a cAMP Regulated Enhancer (CRE). Protein kinase C and cAMP mediate transcription activation through AP-2. A binding site for the promoter Sp factor 1 (Spf1) is also adjacent at -682 position. These elements are responsible for binding of RNA polymerase 2 and basal activity of the gene (Ishimitsu et al. 1994). The gene also contains 16 putative Hypoxia Response elements (HREs) in the promoter region (Garayoa et al. 2000).

ADM is derived from preproADM which is made up of 185 amino acids. After cleaving of the 21 residue signal peptide, preproADM is converted to proADM having 164 amino acids, which is the precursor of ADM and another peptide called proADM N terminal 20 peptide (PAMP) (Beltowski and Jamroz 2004; Bunton et al. 2004; Ishimitsu et al. 1994). Figure 4 illustrates the

ADM gene and the transcribed mRNA that is 1.6kb long and the translated region. When ADM is cleaved from PAMP, it is a glycine-extended 53 amino acid peptide, which is an immature ADM (iADM) that is functionally inactive. An amidating enzyme called the Peptidylglycine α-Monooxygenase (PAM) converts the iADM to mature ADM (mADM) by amidating the glycine in the C-terminal end (Beltowski and Jamroz 2004).

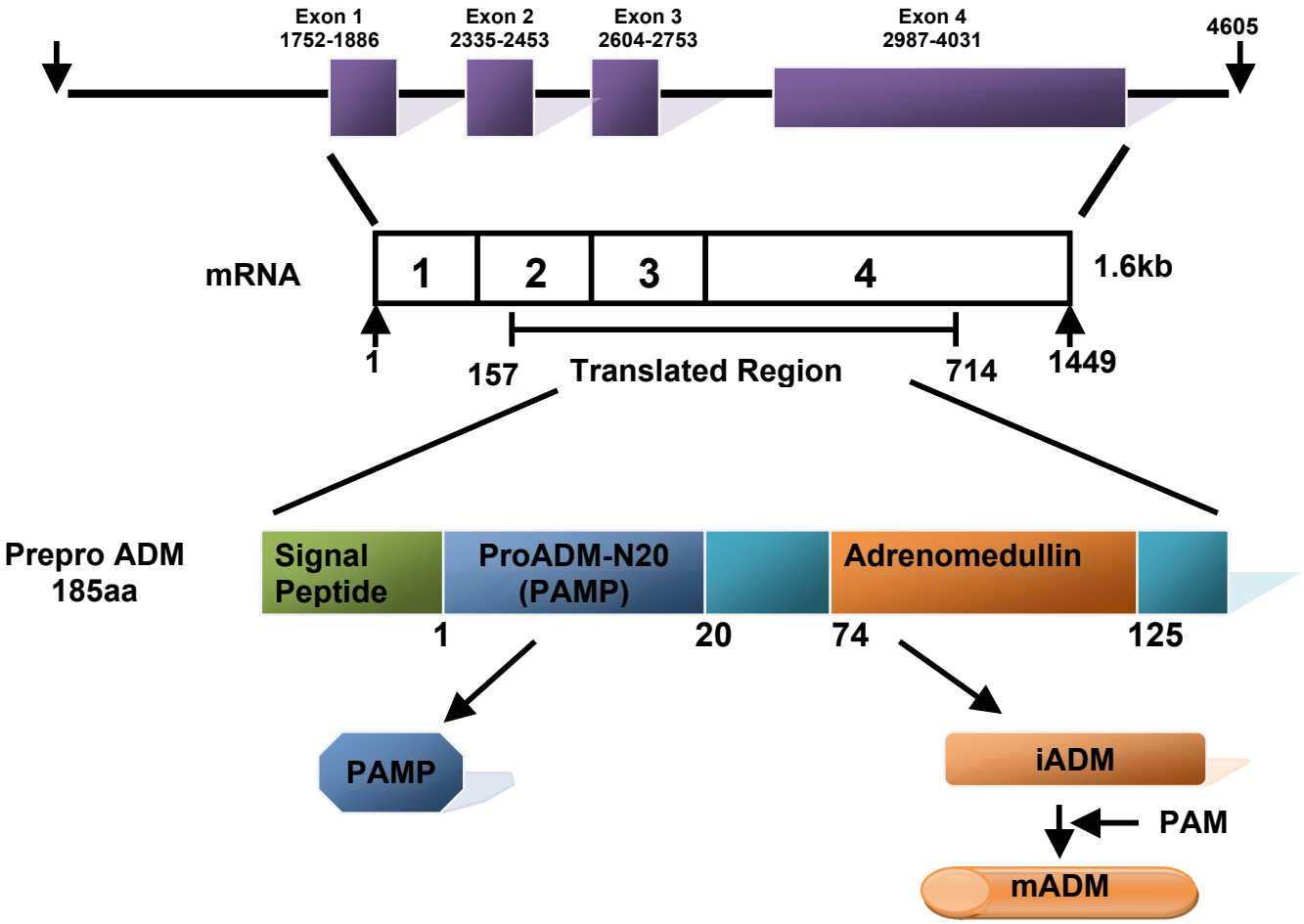

Figure 4: Expression of ADM – gene/mRNA/protein. The gene has 4 exons and 3 introns. The mRNA is 1.6kb and is translated into 185 amino acid protein that codes for two peptides – PAMP and ADM. The iADM (immature ADM) is converted to mADM (mature ADM) by PAM. Figure adapted from Ishimitsu *et al*, 1994 and Beltowski and Jamroz, 2004.

ADM is a ubiquitously expressed peptide which is largely secreted by the adrenal glands (Kitamura et al. 1993). Since ADM is present in almost all of the organs, it is a biologically important peptide (Marutsuka et al. 2003). Smooth muscle cells are said to produce 3-4 times more ADM than endothelial cells, but the plasma ADM is predominantly secreted from endothelial cells (Sugo et al. 1994b; Sugo et al. 1994a; Yamaga et al. 2003). Several factors such as Nitric Oxide (NO) (Hofbauer et al. 2002), IL-1 α and β, TNF α and β (Chini et al. 1995; Sugo et al. 1995b), endotoxin (So et al. 1996), bradykinin, adrenaline (Sugo et al. 1995a), dexamethasone, thyroid hormones (Kureishi et al. 1995), have been shown to stimulate the production of ADM from Vascular Smooth Muscle cells (VSMCs). Factors such as forskolin, interferon-γ, thrombin, transforming growth factor β are said to inhibit the secretion of ADM (Bunton et al. 2004).

Circulating ADM has a half-life of ~20 minutes. Lungs are known to be the largest site where ADM is metabolised. Another site of clearance are the kidneys since the ADM concentration in urine is 15 times the concentration found in plasma (Beltowski and Jamroz 2004). In the kidney, ADM is filtered by the glomeruli and is broken down by Neutral Endopeptidase (NEP) suggesting that the high level of ADM in the urine is not from the systemic circulation, but due to the intrarenal production of ADM (Beltowski and Jamroz 2004). This diversity in expression and release of ADM in various organs shows that ADM plays numerous roles in each of these organs/cells.

1.2.3. Signal Transduction

Unlike the classical concept of single ligand – single receptor, ADM functions through a combination of a G-Protein Coupled Receptor and an accessory protein (McLatchie et al. 1998; Pinto et al. 1996; Zimmermann et al. 1996). The signalling mechanism of ADM is extensively reviewed in the following sections.

1.2.3.1. G-Protein Coupled Receptors (GPCRs)

GPCRs are the largest receptor family and are the most common signalling mechanism through which a plethora of proteins, genes and other secondary messengers are activated (Kohout and Lefkowitz 2003). The GPCR superfamily has been classified into 6 families (Kristiansen 2004),these are:

- Family A, the rhodopsin family – Family A is the largest GPCR family and consists of 20 conserved residues that are confined to the transmembrane region. Examples of this family are rhodopsin receptors, platelet activating factor.

- Family B, the secretin receptor family – Family B, has a large extracellular domain that consists of 6 conserved cysteine residues along with 20 conserved residues present in their transmembrane region. An example of this family is calcitonin receptor, parathyroid hormone receptor.

- Family C, the metabotropic glutamate/pheromone receptor family – Family C, has a long extracellular domain consisting of 20 cysteine residues along with the 20 conserved residues present in the transmembrane domain. An example for this family of receptors are, taste receptors, calcium-sensing like receptors.

- Family D – fungal pheromone receptors

- Family E – cAMP receptors and

- Family F – frizzled/smoothened receptors

Approximately 80% of neurotransmitters/hormones transduce their signal by activating GPCRs (Kristiansen 2004). Due to their wide variety and distribution, dysfunction of GPCRs are involved in diseases and are very important therapeutic targets. For example anti-depressants and β-blockers are two of the best known drugs. An example of a β-blocker is Nebivolol in the

treatment of hypertension; it targets the β-adrenergic receptor kinase of the G-protein Coupled Receptor Kinases family (GRKs) (M. A. Weber 2005). Elevated levels of GPCRs and their ligands are found in cancer cells suggesting that they are involved in tumour growth and progression (S. Li et al. 2005). For example, 61% of colon tumours and 53% of ovarian tumours over-express GPR49, which is a GPCR. Knockouts of GPR9 receptors in tumours induced apoptosis; this is just one example showing the involvement of GPCR in cancer (McClanahan et al. 2006).

Structure

As illustrated in figure 5, GPCRs have seven transmembrane helices that are linked with both extracellular and intracellular loops. The extracellular domain contains the ligand binding pocket while the intracellular domain conveys the signal to secondary messengers (Rios et al. 2001).

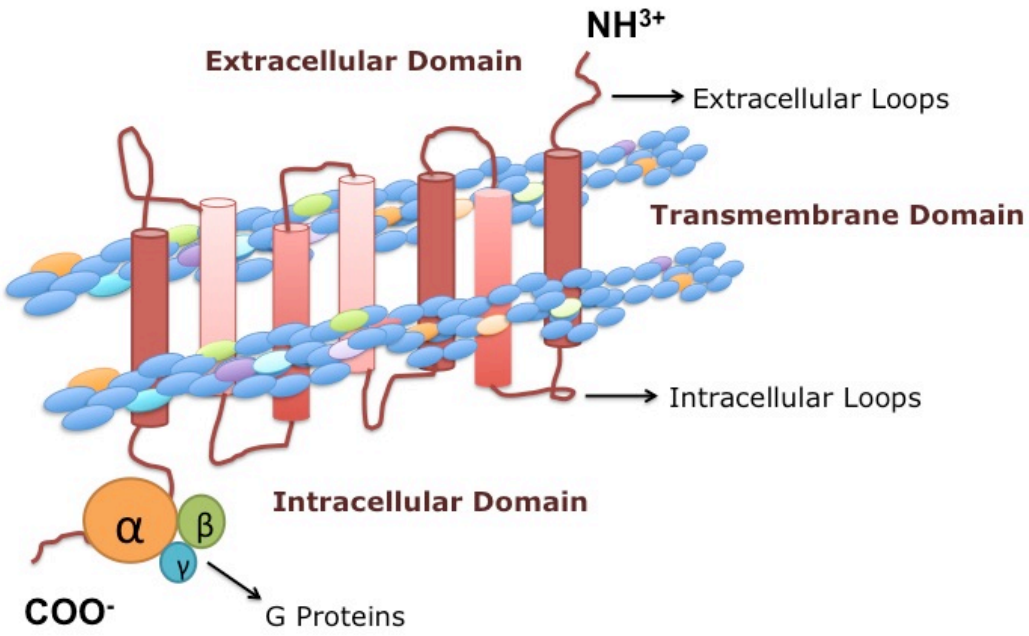

Figure 5: Structure of GPCR showing the seven transmembrane helices and the G proteins attached to the C terminal end of the receptor. Figure drawn by self, adapted from Rios *et al,* 2001.

The GPCRs mediate their action through the G proteins which reside at the C terminal tail of GPCRs.

G Proteins

G proteins convey signals from GPCRs to a variety of targets. G proteins upon activation, cause the induction of secondary messenger systems via various effector proteins. This system allows amplification *ie*, one ligand is able to activate GPCRs that in turn activate effectors that are able to stimulate a secondary messenger system resulting in the amplification of the entire signal (Kristiansen 2004)**.**

The G proteins are comprised of α, β and γ subunits, and the molecular weights are approximately, 39-45, 35-39 and 6-8kDa respectively (Kristiansen 2004)**.** In the resting state of the receptor, the G proteins are bound to each other and the α_s has GDP (Guanosine diphosphate) bound to it. When a ligand binds to the extracellular domain of the GPCR, conformational changes take place activating the bound G proteins and α subunit to dissociate and it activates an effector molecule (example, adenylate cyclase) and since it is a GTPase it converts GDP to GTP (Guanosine triphosphate). βγ subunits exist together and in some cases they may also activate a few effector molecules (Cabrera-Vera et al. 2003) such as type I and type II adenylate cyclase, phosphoinositide-specific phospholipase A beta (Ueda et al. 1994). In order to terminate the signalling, the Gα subunit converts GTP back to GDP thereby restoring the inactive state of the G protein. Another mechanism of GPCR activation is through phosphorylation of the receptor by a kinase, which decreases its ability to respond to the ligand. This phosphorylation triggers β-arrestin binding which desensitizes the receptor and leads to the down-regulation and either degradation or recycling of the receptor back to the membrane. In the resting state, α subunit reunites with βγ subunits once again (Strader et al. 1994).

There are a wide range of G proteins that interact with different receptors and control different effectors. There are about 28 different Gα proteins to which

the GPCR can associate with (Kristiansen 2004).The α subunits are classed in four groups such as α_s (G_s and G_{olf}), α_i (G_{tf}, G_{tc}, G_g, $G_{il\text{-}3}$, G_0 and G_z), α_q (G_q, G_{11}, G_{14} and $G_{15/16}$) and α_{12} (G_{12} and G_{13}). Even the β and γ subunits have been subdivided into 12 and 5 subunits respectively, to date (Kroeze et al. 2003). Various combinations of these sub-units make up different types of functional G-proteins, which make them diverse and specific for their signalling (Cabrera-Vera et al. 2003). Each of these subunits has been further sub classified according to the oncogene they stimulate. For example, studies have shown that when there is an increase in intracellular cAMP level, there is increase in proliferation. Therefore, in tissues expressing high cAMP levels, hyperplasia is induced by the $G\alpha_s$ subunit and this acts on the oncogene called the gsp oncogene, while $G\alpha_{i2}$ induces the gip2 oncogene (Gutkind 1998).The effector proteins through which the GPCRs control different aspects of cell functions are

- Adenylatecyclase – $G\alpha_s$, the enzyme responsible for cAMP formation.

- Phospholipase C – $G\alpha_{q,}$ the enzyme responsible for inositol phosphate and diacylglycerol formation

- Ion channels – $G\alpha_{iz}$, specifically calcium and potassium channels (Kristiansen 2004).

The family of GPCRs that ADM receptors belong to are the class B GPCR family, which include receptors for 30-50 amino acid peptides like the Calcitonin family (CT family) of peptides which includes ADM, Amylin (AMY), Calcitonin Gene Related Peptide (CGRP). The receptor for these peptides has been found to be Calcitonin Receptor (CTR) and Calcitonin Like Receptor (CLR) (McLatchie et al. 1998).

1.2.3.1.1. Calcitonin Like Receptor (CLR)

The gene for human CLR is located in chromosome 2q31 and contains fifteen exons and spans approximately 100kbps (Conner and Poyner 2001; Nakazawa et al. 2001; Nikitenko et al. 2003).

CLR similar to other members of class B GPCRs, contain large N terminal domain consisting of highly conserved six cysteine residues resulting in the formation of disulphide bonds (Gether 2000). This N-terminal domain is involved in ligand binding and function similar to that of other class B GPCRs such as receptors for secretin, glucagon and parathyroid hormone (Chauhan et al. 2005). CLR shares 50% and 54% sequence identity with rat and human CTR respectively (Aiyar et al. 1996; Chang et al. 1993; Fluhmann et al. 1995). CLR is expressed in high levels in lungs, heart and kidneys (Elshourbagy et al. 1998).

Mice deficient in CLR die at mid-gestation due to Hydrops Fetalis and severe cardiovascular defects. Figure 6a shows the edema seen throughout the body of the embryo at E12.5 days. Figure 6b shows the edema being progressed to severe Hydrops Fetalis at E13.5 days. There was a significant reduction in proliferation of cells in ventricles for $CLR^{-/-}$ when compared to wild type. Similarly there was a high rate of apoptosis in $CLR^{-/-}$ mice when compared to wild type. This suggests that CLR is required for the embryonic development and mediate growth and proliferation of cardiac and vascular smooth muscle cells (R. T. Dackor et al. 2006).

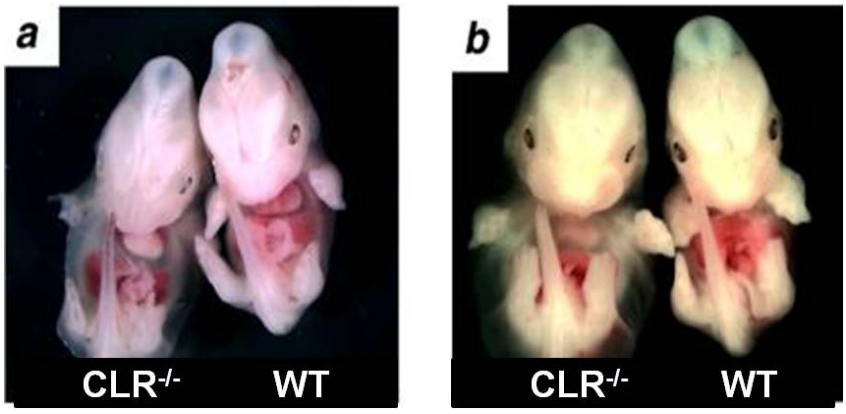

Figure 6: CLR knock out mice. Figure A shows the edema throughout the body at E12.5 days, and figure B shows the progression of the edema to severe Hydrops Fetalis at E13.5 days. Picture taken from Dackor *et al*, 2006.

CLR unlike most GPCRs requires the association with Receptor Activity Modifying Proteins (RAMPs) to traffic from endoplasmic reticulum to cell surface and for ligand specificity (McLatchie et al. 1998). RAMPs confer ligand specificity to CLR by regulating glycosylation of CLR. There are three types of RAMPs that associate with CLR and the details of RAMPs are reviewed under section 1.2.3.1.2. Glycosylation is important for receptor transportation and function (Ho et al. 1999; Liu et al. 1993; Mery and Boulay 1993; Ray et al. 1998; Walsh et al. 1998). RAMP1 confers terminal glycosylation while RAMP2 and RAMP3 confer core glycosylation of CLR (McLatchie et al. 1998). CLR has three putative Asn glycosylation sites in its extracellular domain at positions 66, 118 and 123 (Aiyar et al. 1996; Fluhmann et al. 1995).

The implication of glycosylation at Asn66 and/or Asn118 is currently unclear as one data suggest that glycosylation at these sites are important for the cell surface expression (Buhlmann et al. 2000) while another group contradict this report (Kamitani and Sakata 2001). In order to confer binding of ADM, CLR has to be glycosylated at position Asn123 (Kamitani and Sakata 2001).

CLR consists of N-terminal α helix (named α1) and two anti-parallel β sheets (named β1 and β2) that are connected by five loops. The structure is stabilized by three disulphide bonds that exist between Cys-48-Cys74, Cys 65-Cys105 and Cyc88-Cys127 (Kusano et al. 2011). The extracellular loop 3 (ECL3) has shown to be important in ADM binding and subsequent signal transduction (Kuwasako et al. 2011a). The ECLs in family A and B GPCRs are known to be important in ligand binding and receptor activation (Hawtin et al. 2006; Kuwasako et al. 2003b; Lawson and Wheatley 2004; Peeters et al. 2011). ECL1 and ECL2 in family B GPCRs are known to contain a conserved disulphide bond which determines the stability of the receptor (Kuwasako et al. 2003b). Helix8 of CLR has already been shown to be involved in Gs signaling (Kuwasako et al. 2010), recent evidence has shown that ECL3 controls the activation of Gs resulting in the accumulation of cAMP (Kuwasako et al. 2011a).

The transmembrane domains 1 to 5 of CLR have been shown to be important in transportation of RAMP+CLR to the plasma membrane. The difference in trafficking interactions between the three RAMPs might be determined by the N terminal domain and/or the third intracellular loop and/or transmembrane domain (Kuwasako et al. 2009). The role of transmembrane domains and loops in CLR are still unknown (Walker et al. 2010; Wheatley et al. 2011).

Since CLR is unable to mediate signal transduction on its own as mentioned above, it requires an association with RAMPs for trafficking to the cell surface and conferring ligand specificity (McLatchie et al. 1998). RAMPs are needed for the cell surface expression and receptor phenotype of CLR. For example, the CLR-RAMP complexes originating from the endoplasmic reticulum and golgi are co-trafficked to the cell surface and are important for receptor activation (Conner et al. 2004; Parameswaran and Spielman 2006).

1.2.3.1.2. Receptor Activity Modifying Proteins (RAMPs)

RAMPs are single transmembrane proteins that associate with GPCRs to facilitate ligand binding and trafficking of the receptor to the cell surface. This family of proteins has 3 members – RAMP1, RAMP 2 and RAMP3. RAMP 1 and RAMP 3 are 148 amino acids long; while RAMP 2 is 175 amino acids long (McLatchie et al. 1998). Puffer Fish expresses five RAMPs, from RAMP1 to RAMP5, three CLRs – CLR1 to CLR3 and five ADM proteins – ADM1 to ADM5 (Nag et al. 2006; Ogoshi et al. 2003).

The genes that code for RAMP1, RAMP2 and RAMP2 in humans are present in between 2q33 and 2q37, chromosome 17 and 7p11-7p13 respectively (Sexton et al. 2001). Mammalian RAMPs share 30% sequence identity and their basic structures are similar. Mouse and human amino acid sequence identity for RAMP1, RAMP2 and RAMP3 are 70%, 68% and 84% respectively (Husmann et al. 2000).

RAMPs have three main structural domains, this is illustrated in figure 7 (McLatchie et al. 1998). Each RAMP has a short C terminal end that is made up of ten amino acids and the transmembrane domain is made up of approximately 20 amino acids and the N terminal end is the largest and contains the signal peptide. RAMP2 has 26 amino acids longer extracellular domain than the other RAMPs (Conner et al. 2004). One of the important features that are common to all three RAMPs is that the extracellular domain contains two disulphide bonds, and if this bond is disturbed RAMPs lose their activity. The disulphide bonds are important for stabilizing the receptor in order to facilitate ligand binding and activation (Parameswaran and Spielman 2006). For RAMP1, residues 91-103 are essential for CGRP binding, residues 86-92 and residues 59-65 are needed for RAMP2 and RAMP3 for ADM binding respectively (Conner et al. 2004). RAMPs are abundantly distributed throughout the body, although certain organs and tissues have different RAMP phenotypes. For example, the aortic endothelial cells respond to ADM but express only RAMP2 (Parameswaran and Spielman 2006).

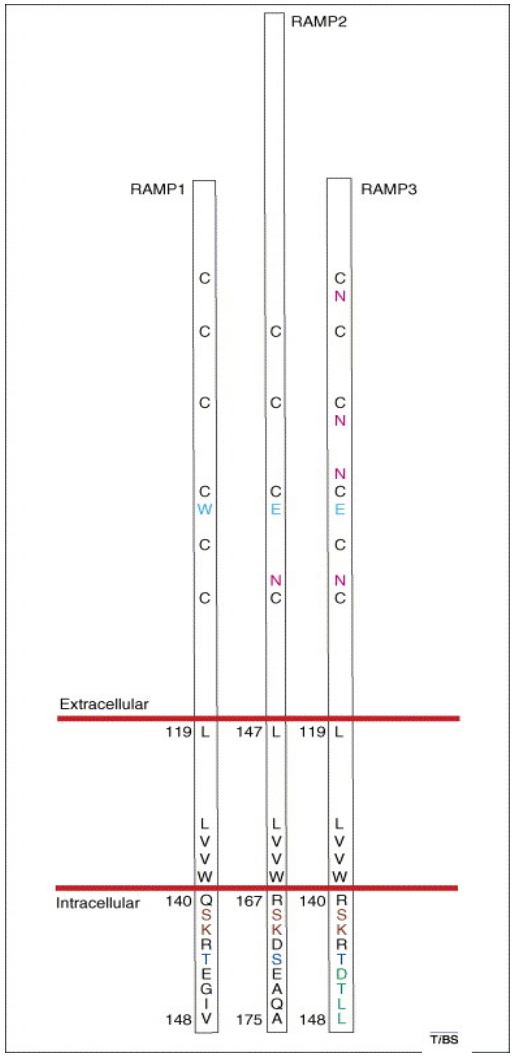

Figure 7: Structural domains of RAMP1, RAMP2 and RAMP3. Conserved cysteine residues and glycosylation sites are shown as C and N respectively. Conserved amino acids in the transmembrane domains are shown. The putative phosphorylation sites are shown in blue and the PDZ motif in RAMP3 is shown in green. Picture taken from Parameswaran & Spielman, 2006.

The distribution of RAMPs is broader than ADM and CLR, indicating that RAMPs also interact with other class B GPCRs. Besides class B GPCR family receptors, RAMPs also associate with class C GPCR family, for example Calcium-Sensing Receptor (CaSR) requires association with either RAMP1 or RAMP3 for transport from ER to golgi and co-expression to the cell surface. This receptor plays a crucial role in calcium homeostasis (Bouschet et al. 2005). Studies have

shown that RAMP2 interacts with glucagon and PTH1 parathyroid hormone receptors and while RAMP3 interacts with PTH2 receptor (Christopoulos et al. 2003). Microarray analysis of human and mouse transcriptomes showed that RAMP2 is predominantly expressed in lungs, female reproductive organs and adipocytes besides other tissues. RAMP3 is expressed highly in heart, thyroid and lungs in humans and female reproductive organs in mice (Su et al. 2002). It is suggested that RAMP3 may have differential functions in human and mouse (Gibbons et al. 2007).

RAMPs and their receptor partners' gene expression is altered under various pathological conditions such as cardiovascular diseases, renal failure and hypoxia (Kuwasako et al. 2004; Morfis et al. 2003; Udawela et al. 2004). For example, in models of heart failure ADM and RAMP2 mRNA were present in high levels when compared to controls (Nishikimi et al. 2003; Totsune et al. 2000). Experimental models of sepsis showed a 40 fold increase in RAMP3 expression and 95% decrease in RAMP2 and CLR expression in lungs (Ono et al. 2000).

In an experiment of cardiac hypertrophy induced by volume overload by aortocaval shunt and/or pressure overload by aortic banding, there was an increase in ADM1 (RAMP2+CLR) and ADM 2 (RAMP3+CLR) receptor expression under pressure overload. But in volume overload induced models there was an increase in ADM1 receptor mRNA. Data from these experiments suggest that RAMP2 and RAMP3 are transcribed under different pathophysiological conditions (Onitsuka et al. 2004).

RAMP1

Association of RAMP1 and CLR results in a receptor for Calcitonin Gene Related Peptide (CGRP) (McLatchie et al. 1998). RAMP1 knockout mice showed elevated blood pressure without change in heart rate (Tsujikawa et al. 2007). This shows that RAMP1+CLR induced CGRP signaling is important in the regulation of blood pressure.

The extracellular domain (ECD) of RAMP1 chimerised with platelet-derived growth factor (PDGF) transmembrane domain resulted in a functional CGRP receptor with CLR. This suggests that the ECD is responsible for the response of ligand and also for the glycosylation of CLR receptor (Fitzsimmons et al. 2003). Amino acids Phe93, Tyr100 and Phe101 of RAMP1 are involved in binding with CLR and Phe92 and Tyr74 form part of ligand binding pocket of CLR+RAMP1 heterodimer (Simms et al. 2006). Deletion of amino acid residues from 101-103 in RAMP1 has shown to abolish the formation of the CGRP receptor (Kuwasako et al. 2003a).

RAMPs contain three serine or threonine residues in their intracellular domain, which could be possible phosphorylation sites. Upon CGRP induction on CLR+RAMP1 in HEK293 cells, there was no phosphorylation seen in RAMP1 but there was phosphorylation of CLR (Hilairet et al. 2001). This suggests that RAMP1 phosphorylation might not play a role in agonist induced signal transduction.Targeted deletion of RAMP1 cytoplasmic tail does not inhibit the trafficking of CLR to the cell surface. Since the cytoplasmic tail of RAMP1 has no effect on CGRP signaling, it has been suggested that it is not necessary for CLR function (Fitzsimmons et al. 2003).

RAMP2

RAMP2 associates with CLR to form a functional receptor for ADM called ADM1 receptor (McLatchie et al. 1998). RAMP2$^{-/-}$ is embryonically lethal as the mice die *in utero* due to severe interstitial edema and defects in development of vasculature (R. Dackor et al. 2007; Fritz-Six et al. 2008; Ichikawa-Shindo et al. 2008). RAMP2$^{+/-}$ mice showed elevated blood pressures with ~10mmHg more than wild type. Reduced litter size (R. Dackor et al. 2007) and edema was observed in brain and skin due to impaired neovascularisation (Ichikawa-Shindo et al. 2008). Figure 8 shows the RAMP$^{-/-}$ embryos showing severe Hydrops Fetalis and hemorraghes (Ichikawa-Shindo et al. 2008).

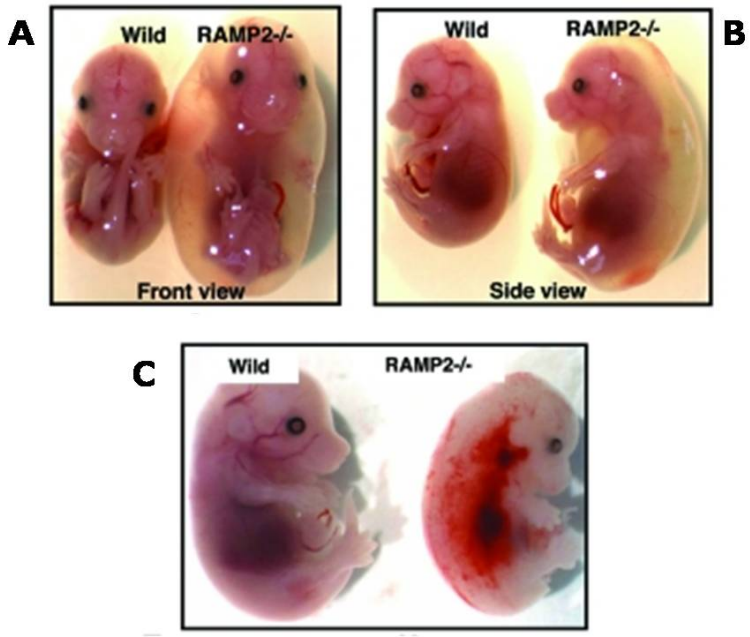

Figure 8: RAMP2$^{-/-}$ mice. RAMP2 mice died *in utero* at E14.5 days due to severe edema resulting in Hydrops Fetalis as it can be seen from pictures A and B. Mice suffered severe cardiovascular defects resulting in haemorraghes as it can be seen in figure C. Reprinted with permission from Ishikawa-Shindo *et al,* 2008.

The ECD of RAMP2 is composed of three α-helices (named as α1, α2 and α3) connected by two loops as shown in figure 9. α2 and α3 of RAMP2 interact with α1 helix of CLR (Kusano et al. 2011). Two disulphide bonds at Cys68-Cys99 and Cys-84-Cys131 stabilise the structure of RAMP. These amino acid residues cys68, cys84, cys99 and cys131 are important for N-glycosylation and mutations in these cysteine residues result in reduced ADM binding (Kuwasako et al. 2003b).

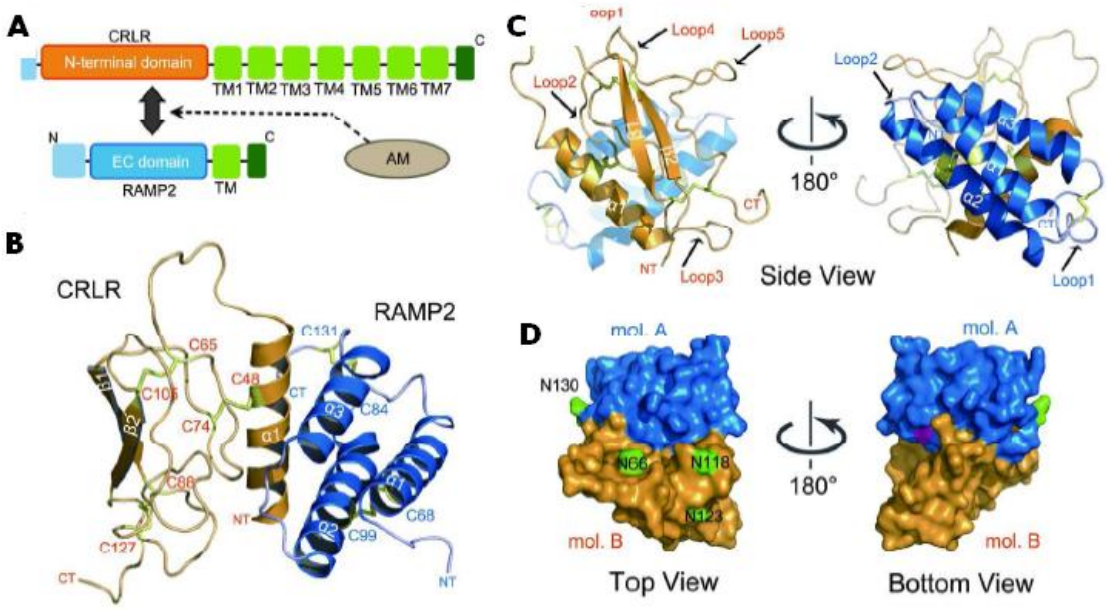

Figure 9: Crystal Structure of CLR and RAMP2 extracellular domain required for ADM binding. (A) Schematic representation of where ADM binds to in CLR+RAMP2 complex. (B) Cartoon images of CLR in orange and RAMP2 in blue. Disulphide bonds are shown as yellow sticks and the α-helices and β-sheets in each are numbered. (C) loop position in CLR and RAMP2 (D) Representation of Molecular surface of CLR+RAMP2 complex. Glycosylation sites are shown in green. Reprinted with permission Kusano *et al*, 2011.

Recent Studies have shown that the binding pocket of CLR+RAMP2 is different from the binding pocket of CLR+RAMP1 (figure 9) (Kusano et al. 2011). Residues that are conserved between RAMP1 and RAMP2 do not play a role in

ligand binding as they engender different specificities for ligands. Amino acid residues 77-101 of RAMP2 has been shown to be involved in the interaction with CLR, the residues 86-92 is known to play a vital role (Kuwasako et al. 2001). His124Ala and His127Ala in RAMP2 ECD is important in ADM binding and activation of receptor (Qi et al. 2008). Studies have shown that the cytoplasmic tail of RAMP2 is needed for ADM1 receptor expression and function (Hay et al. 2006; Kuwasako et al. 2006). Deletion of cytoplasmic tail of RAMP2 inhibits the trafficking of CLR to cell surface (Fitzsimmons et al. 2003).

RAMP3

CLR associates with RAMP3 to form ADM2 receptor (McLatchie et al. 1998). RAMP3$^{-/-}$ mice did not have a significant phenotype as that of RAMP2$^{-/-}$ and CLR$^{-/-}$ mice. The RAMP3$^{-/-}$ mice appeared normal upto six months of age after which the weights of 9-10 months old RAMP3$^{-/-}$ mice were significantly lower (~9g) than wild type controls (R. Dackor et al. 2007). From this study, it has been suggested that RAMP3 has a different signaling that is not necessary for growth and survival and that it may be induced when necessary for example in a diseased condition. For example, in mouse models of sepsis where RAMP3 expression was elevated in lungs, spleen and thymus (Ono et al. 2000), it has been suggested that RAMP3 maybe involved in immune function (Kuwasako et al. 2011b). Addition of Platelet Derived Growth Factor (PDGF) in Rat Mesangial Cells (RMCs) increased the half life of RAMP3 mRNA from 66.5mins to 331.6mins. This resulted in an increase in the cell surface expression of RAMP3, resulting in increased adenylate cyclase activity (Nowak et al. 2002).

Besides binding ADM, ADM2 receptor can also effectively bind CGRP with atleast 10 fold more affinity than ADM1 receptor. This affinity is suggested to be due to the disulphide bond at cys27 and cys82 which is present in RAMP1 and RAMP3 but not RAMP2 (Hay et al. 2006; Kuwasako et al. 2011b). One plausible reason for this difference in signalling between RAMP2 and RAMP3 is suggested by the presence of a PDZ motif (Thr-Leu-Leu) that can interact with N-

ethylmaleimide-Sensitive Factor (NSF) and Na^+/ H^+ Exchanger Regulatory Factor-1(NHERF). This interaction is known to aide in receptor internalization and recycling (Bomberger et al. 2005b).

Glu74 residue in the ECD of RAMP3 is known to be involved in ADM binding (Qi et al. 2011). Six Cysteine residues in RAMP3 and four N-Glycosylated residues play a vital role in ADM binding. This was shown by performing a site-directed mutagenesis on the N- glycosylation sites in RAMP3, which resulted in no ADM binding. The glycosylated residues of RAMP3 are Asn28 and Asn54 (Flahaut et al. 2003). Amino acid residues 59-65 in RAMP3 are suggested to be involved in the interaction with CLR to form a functional ADM receptor (Kuwasako et al. 2001). Deletion of RAMP3 cytoplasmic tail does not affect the trafficking of CLR to cell surface (Fitzsimmons et al. 2003) but is required for ADM2 receptor internalization and recycling (Hay et al. 2006; Kuwasako et al. 2006).

ADM1 Receptor and ADM2 Receptor

The association of RAMP2 and RAMP3 with CLR forms two ADM receptors. The ADM antagonists ADM_{22-52} and $CGRP_{8-37}$ have specific affinity for RAMP2 and RAMP3 respectively. The differences in affinities between these receptors are explained by the structures of these proteins. RAMP3 shows greater similarities to RAMP1 than RAMP2. RAMP2 is N-terminally extended compared to RAMPs 1 and 3; on the other hand, RAMP3 have an extra pair of conserved cysteines that may create a disulphide-bonded loop that is absent in RAMP2. The consensus sequences at either end of this putative loop (NH_2CN/QE..GCY/FW..) are very different from the RAMP2 sequence (..GTV…DLGF..), and may contribute to the different pharmacologies shown by the CLR/RAMP2 and CLR/RAMP3 complexes (Hay et al. 2004).

Another protein found to be involved in the ADM signalling is the Receptor Component Protein (RCP). It has been shown that to form a receptor for ADM signaling it must have at least three proteins namely CLR, RAMP2/3 and RCP

(Prado et al. 2001). Figure 10 shows the schematic representation of activation of ADM receptors by ADM, and the dissociation of Gα that triggers the Adenylate cyclase pathway resulting in the accumulation of cAMP and activation of signalling cascade (Beltowski and Jamroz 2004; Kuwasako et al. 2000; Prado et al. 2001). Site-directed mutagenesis carried out at the amino acid positions 86-92 in RAMP2 and 59-65 in RAMP3 contributed to a loss of ADM binding, showing that certain conserved residues exist in RAMPs that specifies ligand binding (Kuwasako et al. 2001). Most studies suggest that ADM1 receptors mediates most ADM signaling, therefore there is a need to understand the signaling mechanisms mediated by ADM1 and ADM2 receptors (Gibbons et al. 2007).

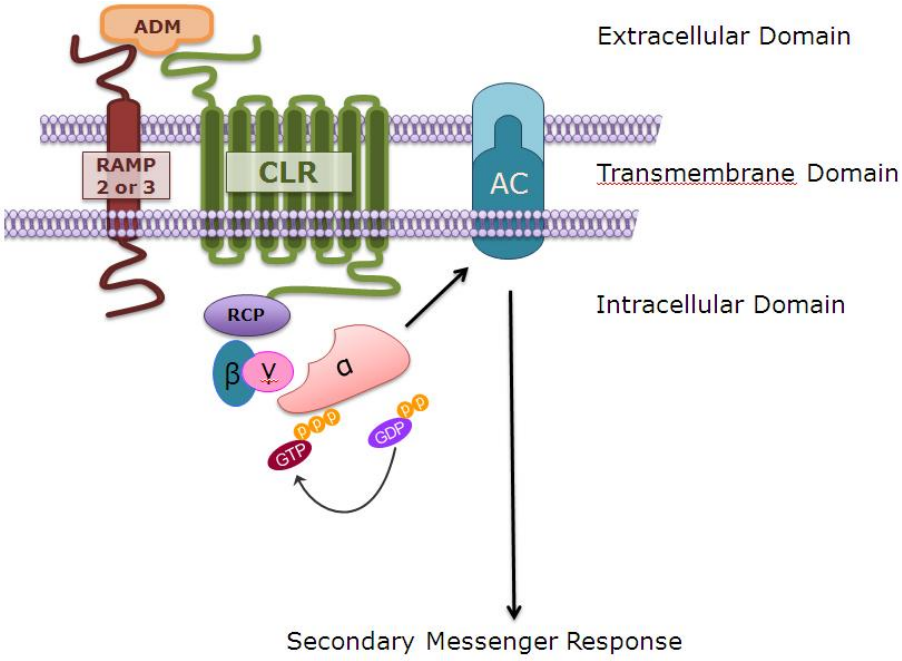

Figure 10: Activation of adenylate cyclase pathway by the association of CLR and RAMP2 or 3 upon ADM binding. Picture shows the dissociation of G proteins where Gα activates the adenylate cyclase pathway resulting in the activation of a signalling cascade. Figure drawn by self, adapted from Kuwasako *et al*, 2000 and Prado *et al,* 2001.

1.2.4. Biological Functions of ADM

One of the main functions of ADM is its vital role in vasodilation, which can be mediated via both endothelium-dependent and endothelium-independent mechanisms (Nuki et al. 1993). NO has a partial role to play in the vasodilation effects of ADM in humans (Nakamura et al. 1997).

ADM has important functions during embryogenesis, organogenesis and differentiation in various cell types during the developmental stage (Jahnke et al. 1997; H. Kato et al. 1997; Montuenga et al. 1997; Morrish et al. 1996). This data is supported by ADM knockout studies. ADM knockout mice showed that ADM is essential for vascular morphogenesis, since ADM knockout mice died at embryonic day 14, as seen in figure 11. The heterozygotes survived until adulthood having elevated blood pressure (Caron and Smithies 2001; Fritz-Six et al. 2008; Ichikawa-Shindo et al. 2008; Shindo et al. 2001). ADM is expressed high in angiogenesis and vasculogenesis of the foetus during early stages of pregnancy, showing that it is an important peptide in foetal development (Nikitenko et al. 2000). ADM also protects organs such as liver, kidney, heart, vasculature from pathological conditions such as hypertension, septic shock, ischemia etc, by up-regulating the expression of NO (Shimosawa et al. 2003).

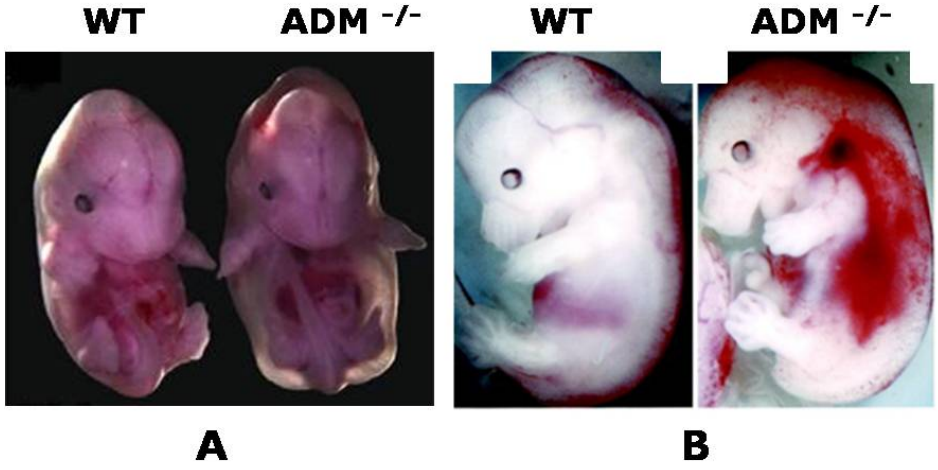

Figure 11: Comparison of wild type and ADM$^{-/-}$ mice embryos at E14. Edema and hemorrhagic changes were observed in various organs (under skin). Picture reprinted with permission from Ishikawa-Shindo *et al,* 2008and Caron *et al,* 2001.

Since similar embryonic lethality and phenotypic defects are seen in $ADM^{-/-}$, $RAMP2^{-/-}$ and $CLR^{-/-}$ mice, it can be concluded that ADM is required for embryonic development and its actions are primarily mediated through ADM1 receptor (Czyzyk et al. 2005). Based on these findings, it has been suggested that ADM1 receptor is required for the basal activity of ADM, while ADM2 receptor is up-regulated under a pathological condition (Czyzyk et al. 2005; R. T. Dackor et al. 2006).

Besides being important in the development of vasculature during embryogenesis as outlined above, ADM is known to play a vital role in various physiological functions such as acting as a bronchodilator (Kanazawa et al. 1994), regulator of blood glucose metabolism and insulin secretion (Martinez et al. 1996), hypotensive effector on ocular pressure (Taniguchi et al. 1999), regulator of bone growth (Naot et al. 2001), regulator of stress response hormone, corticostrone (Taylor and Samson 2004), dilates blood vessel and reduces blood pressure (Nagaya et al. 2000), increases natriuretic response (Jougasaki et al. 1995) and increases Glomerular Filtration Rate (GFR) in kidneys (Majid et al. 1996) (shown in figure 12).

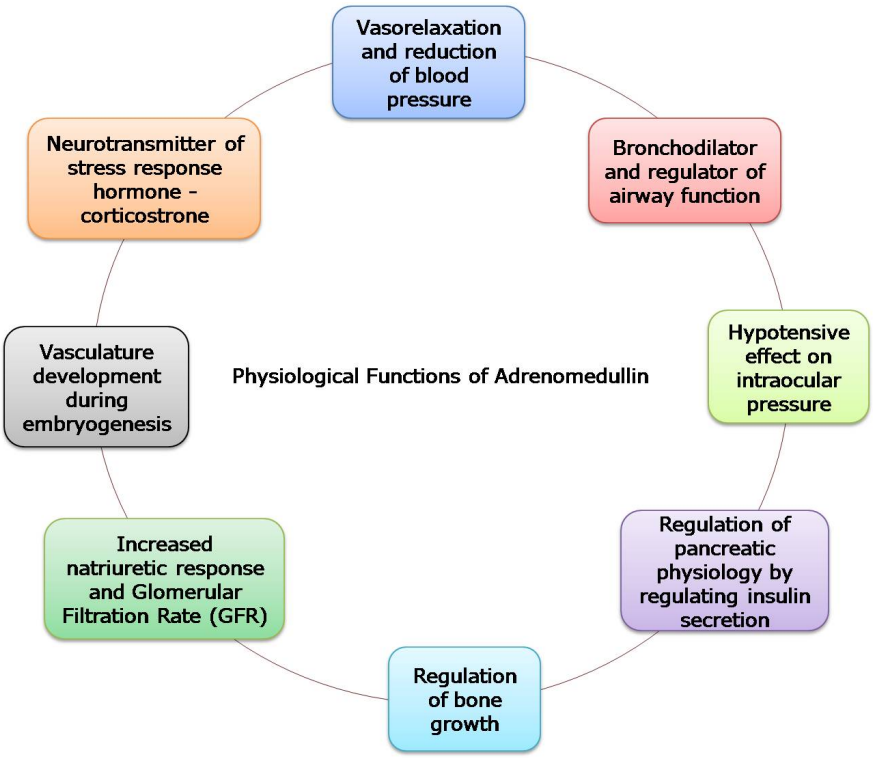

Figure 12: Some of the many physiological functions where Adrenomedullin plays a vital role. Figure drawn by self, adapted from Kanazawa *et al*, 1994, Martinez *et al*, 1996, Taniguchi *et al,*1999, Naot *et al*, 2001, Taylor and Samson, 2004, Caron and Smithies, 2001, Nagaya *et al,*2000, Jougasaki *et al*, 1995 and Majid *et al,* 1996.

Evidence suggests that the CLR-RAMP2/3 elicit its response via the G protein Gs subunit thereby increasing cAMP (figure 8) (Buhlmann et al. 1999). ADM when discovered was found to elevate cAMP levels in most of the cell types (Eguchi et al. 1994; Kitamura et al. 1993). The most prevalent second messenger that is activated by ADM actions is cAMP (Hinson et al. 2000). Increase in intracellular cAMP in endothelial cells and VSMCs elevates the intracellular concentration of Ca^{2+} resulting in the activation of Nitric Oxide Synthase (NOS) triggering the secretion of NO (Moncada et al. 1991).

ADM also increases the intracellular Ca^{2+} mobilisation via the ADM receptors. Human Embryonic Kidney293 (HEK293) cells, when transfected with

CLR and any RAMPs, increased the intracellular Ca^{2+} levels (Kuwasako et al. 2000). ADM increases /decreases intracellular Ca^{2+} levels independently of cAMP (Mazzocchi et al. 1996; Shimekake et al. 1995). Whilst ADM increases Ca^{2+}, many calcium dependent mechanisms up-regulate the expression of ADM (Bunton et al. 2004).

In Human Microvascular Endothelial Cells (HMECs), exogenously added ADM up-regulated the expression of CLR and RAMP2 but not RAMP3. ADM stimulated HMECs had an increase in CLR and RAMP2 mRNA levels immediately after stimulation (Schwarz et al. 2006). There are many examples where the ligand up-regulates/down-regulates the expression of its own receptors (Hukovic et al. 1999; Inoue et al. 1999; Siegrist et al. 1994). For example, the expression of the somatostatin receptor 1 is up-regulated by somatostatin (Hukovic et al. 1999) and calcitonin down-regulates the expression of calcitonin receptor mRNA (Inoue et al. 1999). Similarly it is hypothesised that ADM may up-regulate the expression of CLR and RAMP2, although RAMP3 might have a different mechanism (Schwarz et al. 2006).

Since ADM plays an important role in physiology, deregulation of ADM has been implicated in various pathological conditions, some of which are reviewed in the following sections.

1.3. Adrenomedullin and Diseases

Elevated levels of ADM have been shown to be associated with many disease conditions some of which are arterial hypertension (Kohno et al. 1996), heart failure (Hirayama et al. 1999), renal diseases (Kinoshita et al. 2000), diabetes mellitus (Hayashi et al. 1997), septic shock (Nishio et al. 1997) and cancer (Kitamura et al. 1993; Satoh et al. 1995; Zimmermann et al. 1996).

1.3.1. ADM and Septic Shock

ADM is over-expressed 13 fold more than normal in patients with septic shock. Plasma ADM in septic shock patients, (107+/- 139 fmol/ml in sepsis patient, while normal subjects range from 7.9+/- 3 fmol/ml) is the highest in any pathological condition (Hirata et al. 1996; Nishio et al. 1997). This ADM contributes to hypotension and vasodilation (So et al. 1996; P. Wang et al. 1999). The two stages of septic shock where ADM contributes to progression is the,

- Early hyperdynamic phase where there is increase in cardiac output, reduction in peripheral resistance and hyperfusion of tissues – ADM associated reduction in response to vasculature contributes to this phase (Koo et al. 2001; P. Wang et al. 1999).

- Hypodynamic phase where there is reduction in cardiac output and high vascular resistance. This results in hyperfusion of tissues and ultimately damage of the organ. There is reduction to ADM sensitivity in this phase due to the reduction in circulating levels of ABMP-1 – complement factor H (S. Yang et al. 2002; Zhou et al. 2002).

RAMP3 expression is also found to be elevated in hyperdynamic stage (Ornan et al. 2002). Exogenously added AMBP-1 restores the effect of ADM in blood vessels delaying the transition from hyperdynamic phase to hypodynamic phase thereby delaying organ damage. Therefore ADM and AMBP-1 is suggested as a therapy for septic shock (S. Yang et al. 2002).

1.3.2. ADM and Diabetes Mellitus

ADM is known to exert an inhibitory effect on insulin secretion. In diabetes mellitus, there is an increase in plasma ADM levels resulting from endothelial activation and impaired renal clearance in patients with diabetic nephropathy (Garcia-Unzueta et al. 1998). ADM deregulation is not the underlying cause of

diabetes but it contributes to disease progression (Hayashi et al. 1997; Turk et al. 2000).

1.3.3. ADM and Renal Diseases

Increase in plasma ADM levels and decrease in urinary excretion of ADM is observed in glomerulonephritis (Kinoshita et al. 2000; Kubo et al. 1998). Plasma ADM levels also increase in patients with renal failure. Whether this increase is due to over production or reduction in ADM clearance is unclear (Ishihara et al. 1999; Nitta et al. 2000). Different groups have seen both increase (Cases et al. 2000) and decrease (Mallamaci et al. 1998) in plasma ADM levels in patients undergoing hemodialysis.

1.3.4. ADM and Heart Failure

Studies have shown that there is a correlation between increased plasma ADM levels and the severity of congestive heart failure (Hirayama et al. 1999; C. M. Yu et al. 2001a). Studies have shown that patients with elevated plasma ADM levels benefit from β-adrenergic antagonists (Richards et al. 2001).

In different animal models of heart failure, ADM and its receptor components (CLR, RAMP2 and RAMP3) were up-regulated (Cueille et al. 2002; Nishikimi et al. 1997; Totsune et al. 2000; Yoshihara et al. 2000). It has been suggested that prolonging the half life of natriuretic proteins by inhibiting NEP could augment ADM effect in heart failure (Corti et al. 2001).

1.3.5. ADM and Cancer

As described previously, ADM is deregulated in cancer. Evidences show that ADM influences tumour growth, survival and angiogenesis. For example cancers like breast cancer, glioblastoma, prostate cancer, lung cancer and almost 80% of cancers have been shown to have high levels of ADM expression (Miller et al. 1996). ADM contributes to cancer cells lymph node metastasis in

breast cancer (Oehler et al. 2003). ADM is a clinically important peptide in cancer since it is a characteristic feature of cancerous cells (Bunton et al. 2004). Various characteristics of cancer where ADM contributes in tumour progression are illustrated in figure 13.

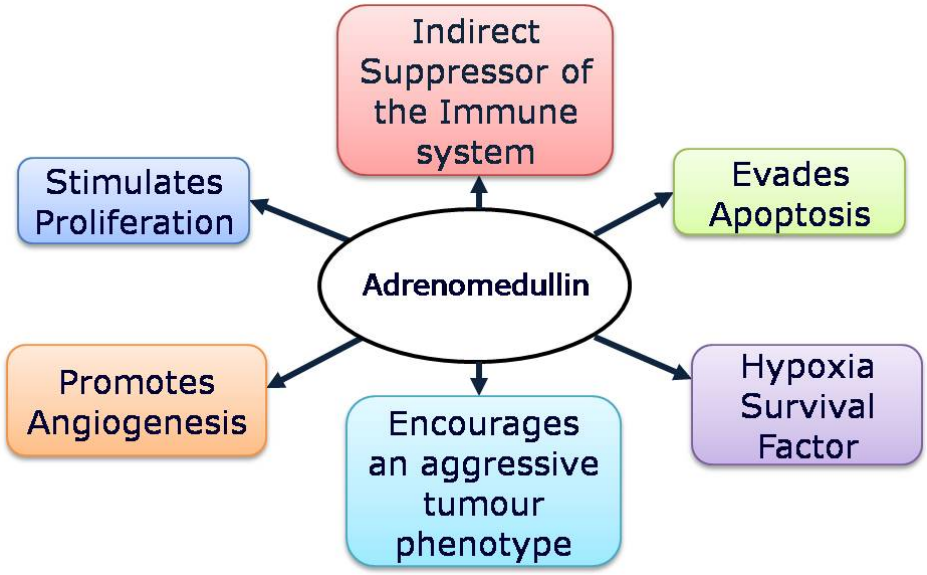

Figure 13: Various roles played by ADM in cancer progression. Original sketch by Dr. Gareth Richards.

1.3.5.1. ADM and Proliferation

ADM was found to promote proliferation for the first time in Swiss 3T3 mouse fibroblasts, where it increased the intracellular level of cAMP (Withers et al. 1996). ADM also elicits the mobilisation of Ca^{2++} in bovine aortic endothelial cells (Shimekake et al. 1995), although it had no effect in the Swiss 3T3 mouse fibroblasts (Withers et al. 1996).

ADM either induces cell proliferation or growth inhibition depending on the cell type. ADM induces cell proliferation in Vascular Smooth Muscle Cells by activation of Protein Tyrosine Kinase (PTYK)-MAPKB pathway. In cells lacking MAPK signalling, ADM inhibits cell proliferation by activation of cAMP through

adenylate cyclase (Iwasaki et al. 1998; Iwasaki et al. 2001; Shichiri and Hirata 2003). Figure 14A shows the growth stimulatory effects of ADM via MAPK signalling, resulting in the activation of C-Src where Sos catalyses GDP to GTP in Ras resulting in the activation of Raf which activates the MAPK signalling, resulting in cell proliferation (Shichiri and Hirata 2003). Figure 14B shows the growth inhibitory effects of ADM via activation of adenylate cyclase pathway.

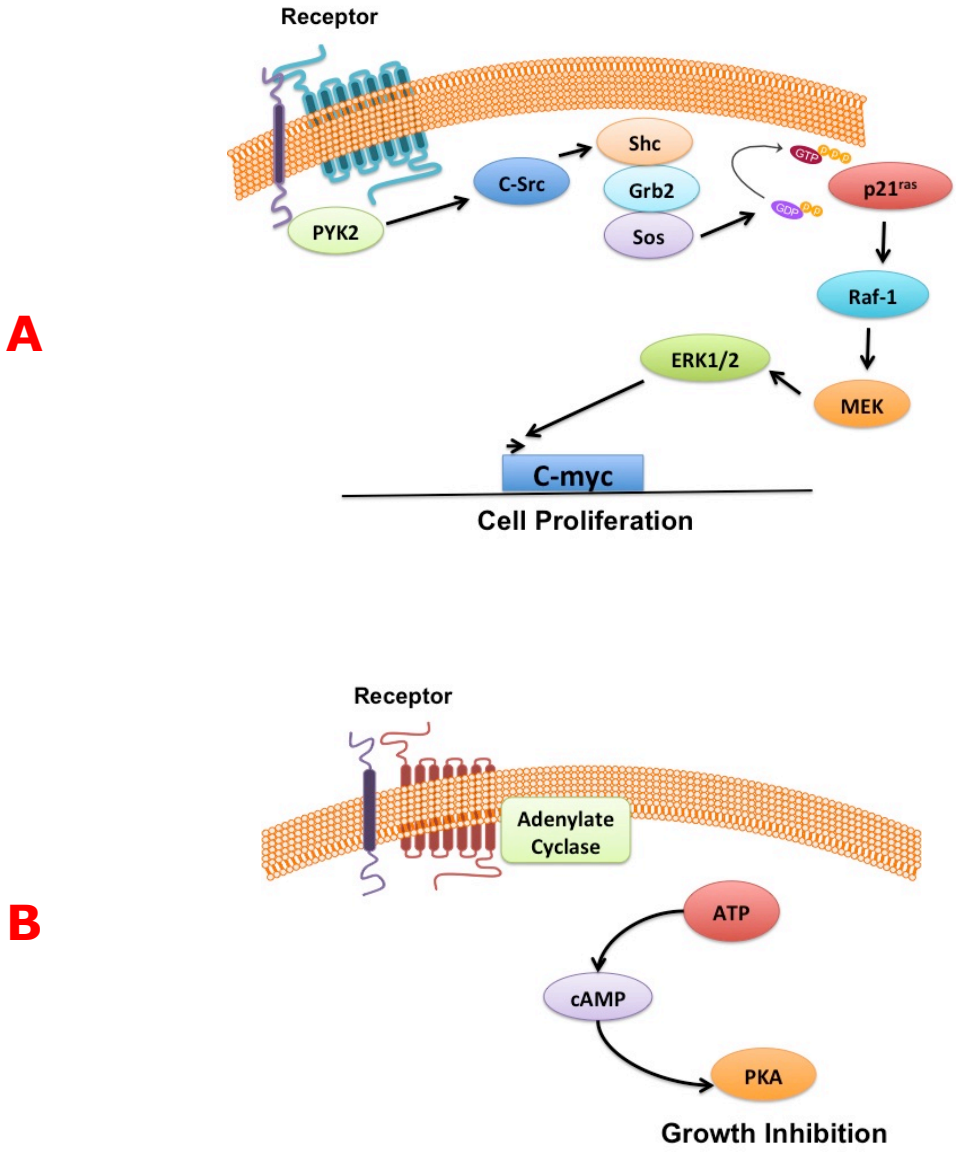

Figure 14: Cell proliferation and growth inhibition effects of ADM. Figure A shows the cell proliferation effects of ADM via MAPK pathway by activation of Protein Tyrosine Kinase. Figure B shows the growth inhibition effects of ADM in cells lacking MAPK signalling, via adenylate cyclase pathway. Figure drawn by self, adapted from, Shichiri *et al*, 2003 and Iwasaki *et al*, 2001.

Human Umbilical Vein Endothelial Cells (HUVECs) express ADM receptor – both CLR RAMP2 and CLR RAMP3 (Fernandez-Sauze et al. 2004) and ADM induces proliferation of HUVEC cells (Fernandez-Sauze et al. 2004; Y. Zhao et al. 1998) and helps them to prevent apoptosis in rat endothelial cells (H. Kato et al. 1997). ADM has been shown to promote proliferation of cancer cells by various groups (Beltowski and Jamroz 2004; Bunton et al. 2004; Frank Cuttitta et al. 1999; Fernandez-Sauze et al. 2004; Martinez et al. 1997; Martinez et al. 2002; Miller et al. 1996). In order to show that ADM promotes proliferation of cancer cells, compromising ADM activity by addition of ADM antagonist -ADM_{22-52} or an anti-ADM antibody, has shown a growth suppressing effect in human Glioblastoma cells (Ouafik et al. 2002), lung, breast and ovarian cell lines (Miller et al. 1996), human oral squamous cell carcinoma cell line (Kapas et al. 1997). ADM has also been shown to promote proliferation in non-cancer cells; *in vitro* and *in vivo* proliferative effects in rodent osteoblasts (Cornish et al. 1997), vascular endothelial cells, rat vascular smooth muscle cells (Iwasaki et al. 1998).

1.3.5.2. ADM and Apoptosis

As suggested by Hanahan and Weinberg, cancer cells have the capacity to evade apoptosis, and ADM is one such factor that helps cancer cells achieve this (H. Kato et al. 1997). Similar to cell proliferation effects of ADM, it can act both as an anti-apoptotic (Oehler et al. 2001) and a pro-apoptotic factor (Parameswaran et al. 1999b; Parameswaran et al. 1999a).

Studies have showed that during serum deprivation, cultured rat endothelial cells (RECs) released ADM which helped them survive. They showed that ADM acts via a cAMP independent mechanism to evade apoptosis, by studying the effects of cAMP agonists and antagonists where they did not affect growth or apoptosis of RECs inspite of ADM inducing cAMP levels (H. Kato et al. 1997; Sata et al. 2000). ADM inhibited hypoxia induced apoptosis by up-regulation of BCL2 in endometrial cancer cells (Oehler et al. 2001). It has been shown that cells that over-express ADM have lower levels of factors that bring about apoptosis, like bid, bax, caspase 8 (Martinez et al. 2002).

Published data suggests that ADM acts as an apoptosis survival factor via many pathways which are dependent on the cell type. One such method of apoptosis survival induced by ADM is by up-regulation of Max. Figure 15, shows the apoptosis survival mechanism induced by ADM. Under normal conditions Max forms a complex with c-myc which is a proto-oncogene. This complex binds to DNA sequence – CACGTG called E Box, which upon activation results in cell proliferation, transformation and apoptosis. When ADM expression is high, it results in over-production of Max, which then forms dimers with Mxi and Mad and homodimers with other Max and competes in binding to E Box (Amati et al. 1993; Shichiri et al. 1999).

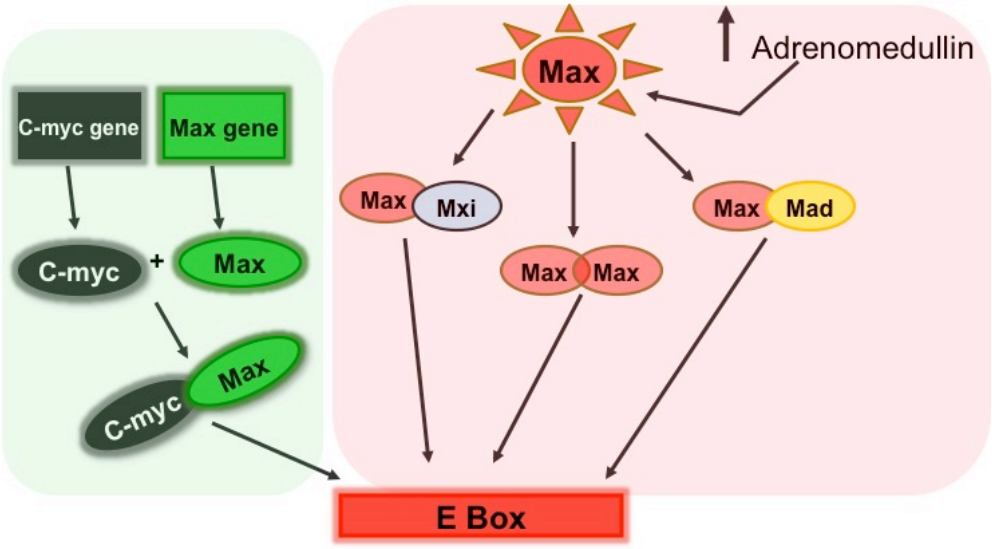

Figure 15: Apoptosis survival mechanism induced by ADM. Green shaded area shows the induction of apoptosis under normal circumstances, where Max forms dimers with c-myc to bind to E box resulting in apoptosis. Red shaded area shows when ADM expression is high, it results in the over-production of Max which binds to Mxi and Mad and other Max to bind to E box which act as an antagonist to C-myc-Max activity. Picture drawn by self, adapted from Shichiri *et al*, 1999.

1.3.5.3. ADM and Angiogenesis

Angiogenesis is a mechanism by which blood vessels sprout from pre-existing ones, which is observed in many physiological process and pathological conditions (Risau 1997). Angiogenesis is a process that is needed for tumour growth and survival (Hanahan and Weinberg 2000). As the tumour size grows bigger, the centre of the tissue is deprived of oxygen, which results in hypoxia. This triggers the expression of many angiogenic factors, one of which is ADM (Martinez et al. 2002; Y. Zhao et al. 1998). Figure 16 shows the angiogenesis pathways triggered by ADM.

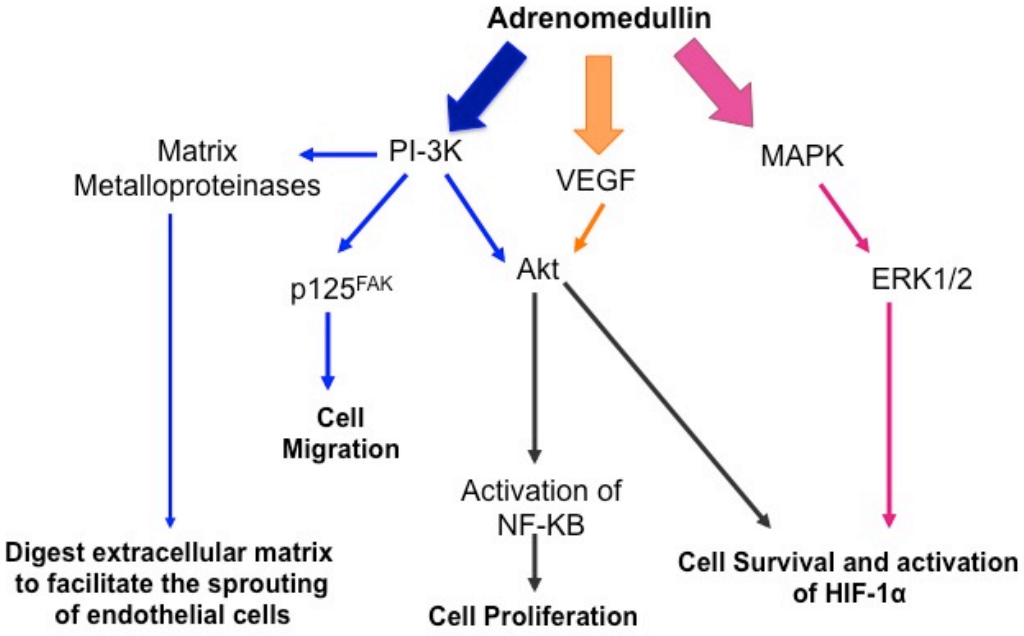

Figure 16: ADM and Angiogenesis pathways. ADM activates PI-3K and MAPK and transactivates VEGF resulting in the cell survival, proliferation, migration and digestion of extracellular matrix. Picture drawn by self, adapted from Iimuro *et al*, 2004.

There are many growth factors that promote angiogenesis – Vascular Endothelial Growth Factor (VEGF), Fibroblast growth Factor (FGF), angiopoietin-1 (Carmeliet 2000; W. Kim et al. 2003a; W. Kim et al. 2003b). Another mediator of angiogenesis via ADM administration is NOS (Abe et al. 2003; Iimuro et al.

2004). Like ADM, VEGF is also expressed in high levels in case of hypoxic stress (Garayoa et al. 2000). It was shown that ADM did not have any effect on the expression of the growth factors mentioned above, although it was shown that ADM was able to elicit an angiogenic response on par with VEGF. The ADM secretion also occurs in the normal uterine endometrium, where it helps in the proliferation of endothelial cells (W. Kim et al. 2003a; Nikitenko et al. 2000). Neutralising activity of VEGF using anti-VEGF antibody on HUVEC cells, does not alter the tube formation on matrigel, showing that ADM acts independently of VEGF during angiogenesis (Fernandez-Sauze et al. 2004; Guidolin et al. 2008) although ADM is said to up-regulate the expression of VEGF in *in vivo* models (Carmeliet 2000) and *in vitro* [HMECs (Schwarz et al. 2006) and HUVECs (Iimuro et al. 2004)]. ADM induced angiogenic effects can be reduced when the tyrosine kinase activity of VEGF Receptor2 (VEGFR2) is selectively inhibited (Guidolin et al. 2008), since many GPCRs transactivate Receptor Tyrosine Kinases (RTKs) like Epidermal Growth Factor (EGF) (Daub et al. 1996), Insulin-Like Growth Factor-1 (IGF-1) (Lowes et al. 2002; Luttrell et al. 1999; Marinissen and Gutkind 2001).

1.4. Background to Project

The cancer models that were used in this project are – Glioblastoma, Breast, Prostate and Pancreatic cancers. The role of ADM in each of these cancers are reviewed next.

1.4.1. ADM and Glioblastoma

Glioblastomas are aggressive tumours affecting the glial cells of the brain (Leon et al. 1996). ADM is one of the peptides that is predominantly over-expressed in glioblastoma and is known to contribute to tumour progression (Ouafik et al. 2002).

Cytokines such as interferon-γ, tumour necrosis factor-α and interleukin-1β is known to induce ADM expression in T98G glioblastoma cells. This induction was inhibited by addition of dexamathasone, which is a glucocorticoid used in the

treatment of glioblastoma (K. Takahashi et al. 2003). Therefore it has been suggested that cytokines are one of the important factors that influence the production of ADM in glioblastoma (K. Takahashi et al. 2003).

ADM is known to up-regulate cyclin D1 protein by activating C-Jun/JNL/AP-1 pathway and transits U87 cells through cell cycle (Ouafik et al. 2009). JNK pathway is known to play a significant role in cell transformation and growth (Khatlani et al. 2007) and contributes to tumour development and progression (Ouafik et al. 2009) in glioblastomas (Cui et al. 2006; Mangiola et al. 2007), breast cancer (Davidson et al. 2006) and Melanoma (Jorgensen et al. 2006).

Highly malignant glioblastomas result in loss of PTEN activity (Furnari et al. 1997; Knobbe et al. 2002; Rasheed et al. 1995). PTEN inhibits PI-3K pathway by blocking Akt activity (Stambolic et al. 1998; X. Wu et al. 1998). PTEN was found to inhibit the expression of ADM (Betchen et al. 2006). Since ADM expression is increased in highly malignant glioblastoma, *in vitro* addition of ADM to U87 cells resulted in increased proliferation (Ouafik et al. 2002). Besides blocking ADM expression, PTEN blocks the expression of CLR by 4-fold in U251 glioblastoma cells (Betchen et al. 2006).

Studies have shown that neutralising ADM activity using specific antibodies for ADM (Ouafik et al. 2002) and its receptors (Kaafarani et al. 2009) have significantly reduced glioblastoma cells growth. *In vivo* data using these antibodies have shown decrease in tumour volume, tumour vascular density and increase in tumour cell apoptosis (Kaafarani et al. 2009).

1.4.2. ADM and Breast Cancer

Breast cancer is the most common cancer, affecting women and the lifetime risk of developing cancer for women in UK is 1 in 8 (Cancer Research UK).

Studies have shown that ADM is up-regulated in breast cancer (Disa et al. 1998; Martinez et al. 2002; Oehler et al. 2003). Although much is not known about the role of ADM in breast cancer, ADM levels of patients with breast cancer is significantly higher than controls (132.2±74.3 pg/ml in patients and 107.9±32.7 pg/ml in controls) (Oehler et al. 2003). It has been seen that breast cancer cells transfected with ADM produced more oncoproteins such as Ras, Raf, PKC and decreased production of apoptotic factors such as Bax, Bid and caspase 8 (Martinez et al. 2002). It has been suggested that plasma ADM levels in breast cancer patients could be an indicator of tumour severity (Oehler et al. 2003).

1.4.3. ADM and Pancreatic Cancer

Pancreatic cancer is one of the leading causes of deaths worldwide which are usually detected at a late stage due to the location of the pancreas and non-specific symptoms (Cancer Research UK). The lifetime risk of developing pancreatic tumour for men and women in UK is 1 in 77 and 1 in 79 respectively (Cancer Research UK).

ADM is required for the development of pancreas in rats and is therefore an important endocrine factor (Martinez et al. 1998). Microarray analysis have shown ADM is over-expressed in pancreatic cancer (Logsdon et al. 2003). Studies using ADM antagonists resulted in reduced vascular density of pancreatic tumour (Ishikawa et al. 2003; Miseki et al. 2007). It has been shown that the level of ADM secreted by tumour correlates with tumour growth and metastasis (Ramachandran et al. 2007), and it could be a diagnostic marker in cancer (Keleg et al. 2007).

1.4.4. ADM and Prostate Cancer

Prostate cancer is the most common cancer affecting men and the lifetime risk of developing cancer for men in UK is 1 in 9 (Cancer Research UK).

ADM is expressed in both normal prostate epithelial cells and in prostate cancer cells (Calvo et al. 2002; Jimenez et al. 1999). PAM is also up-regulated in prostate carcinomas suggesting a significant role played by biologically active ADM (Jimenez et al. 2003; Rocchi et al. 2001). Prostate cancer cell lines DU145 and PC3 both express ADM1 receptor, but only DU145 and not PC3 expresses ADM2 receptor. It has been suggested that DU145 cells resemble prostate epithelial cells more than PC3 cells (Mazzocchi et al. 1996). Studies have shown that ADM increased cell proliferation in DU145 cells but not in PC3 cells, suggesting involvement of ADM2 receptor (Rocchi et al. 2001). It was also seen that ADM inhibits proliferation in PC3 cells transfected with ADM (Abasolo et al. 2004)

ADM enhances IL-13α2 expression both *in vitro* and *in vivo* in PC3 cells treated with ADM peptide (Joshi et al. 2008). Interleukin-13 (IL-13) is a cytokine that regulates immunity. The receptors for IL-13 are over-expressed in various cancers such as glioma, renal cell carcinoma and ovarian cancers. (Debinski et al. 1999; Joshi et al. 2000; Obiri et al. 1995; Obiri et al. 1997). Over-expression of ADM has known to change the phenotype of cells (Martinez et al. 2002), in prostate cancer cells, it was found to increase the appearance of neuroendocrine phenotype (Berenguer et al. 2008; Martinez et al. 2002). ADM over-expressing PC3 cells were found to up-regulate ~100 genes that were involved in apoptosis, cell adhesion, cell cycle arrest, transcription, immune function and extracellular matrix (Gonzalez-Moreno et al. 2005).

1.5. Hypotheses and Aims

Based on the literature, it is hypothesised that,

ADM is up-regulated under a malignant setting and Inhibition of ADM would significantly reduce tumour progression.

In order to test the hypothesis, three different hypotheses were proposed. They were,

1. Hypoxia up-regulates the expression of ADM and its receptors

2. ADM and its receptors increases tumour progression and regulates receptor expression

3. Neutralising ADM using anti-RAMP3 antibody significantly reduces tumour growth.

Since ADM is physiologically important, completely abolishing its activity would result in adverse complications. Therefore our strategy was to target one of its receptor systems, which we hypothesize to be of more pathological importance – the RAMP3+CLR receptors. This anti-RAMP3 therapeutic target would be beneficial to neutralise ADM mediated effects in cancer progression.

CHAPTER II: HYPOXIC REGULATION OF ADM AND RECEPTORS

2.1. HYPOTHESIS

Hypothesis

Hypoxia up-regulates the expression of ADM and its receptors.

The aim is to determine the mRNA and protein expression of HIF-1α, ADM and its receptors in different cancer cell lines under hypoxia.

2.2. INTRODUCTION

2.2.1. Hypoxia and Cancer

Hypoxia is a classical feature of large and solid tumours, since the vasculature is unable to cope up with the increasing demands of the steadily growing tumour mass (Brown and Giaccia 1998; Hockel et al. 1991). The ability of cells to adapt to hypoxia is mainly mediated by Hypoxia Inducible Factor family of various transcription factors. These transcription factors either enable angiogenesis so that there is supply of oxygen or enable cells to sustain hypoxia for regulating various growth regulatory factors. The important regulatory factor that is stabilised under hypoxia is Hypoxia Inducible Factor-1α (HIF-1α) (Ivan et al. 2001; Jaakkola et al. 2001). Since hypoxic regions of tumour require oxygen to sustain, there is activation of various angiogenic factors, most notably VEGF (Folkman 1992; Shweiki et al. 1992). As shown in figure 17 tumour hypoxia enables cancer cells to adapt to low oxygen levels by changing gene expression, resulting in an aggressive phenotype and increase in tumour mass (Vaupel 2004). This vicious cycle is further fuelled by various angiogenic factors.

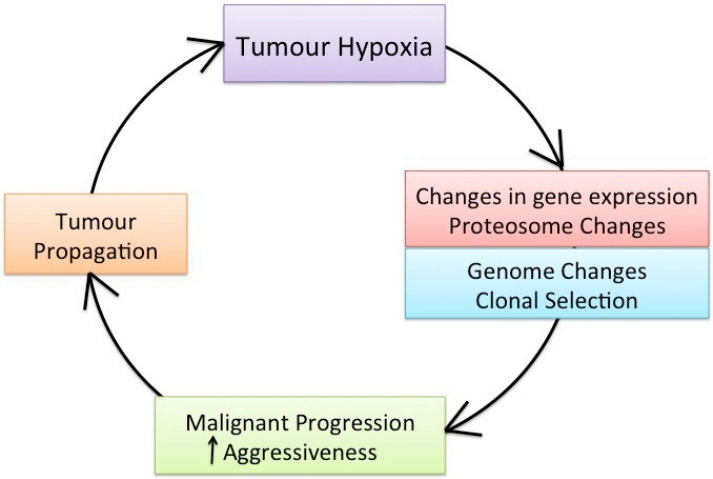

Figure 17: Hypoxia and cancer progression. Tumour hypoxia results in changes in proteosomal changes that give tumours an aggressive phenotype that results in an increase in tumour mass. Picture taken from Vaupel, 2004.

2.2.2. Effect of hypoxia on cancer treatment

In cancer therapy, hypoxia plays a crucial role as it enables cancer cells to be more resistant to radiotherapy and chemotherapy (Brown and Giaccia 1998).

Hypoxia and Radiotherapy

Radiotherapy requires oxygen to cause breaks in the DNA double strand which is cytotoxic thereby resulting in cell death (Hall 1994; Kallman and Dorie 1986). Study by Hockel *et al* (Hockel et al. 1993) on cervical carcinomas demonstrated that patients with partial oxygen pressure more than 10mmHg responded well to radiotherapy resulting in increased survival rate and reduced tumour reoccurrence than patients with less than 10mmHg partial oxygen pressure. Therefore a well oxygenated tumour is more likely to respond to radiotherapy which is hindered by hypoxia.

Hypoxia and Chemotherapy

Chemotherapeutics which are usually administered intravenously requires blood vessels to deliver drug to the actively dividing tumour cells. Since hypoxia results in a deficiency in a proper vasculature development in the tumour mass, this provides an inability to the drug to induce cytotoxicity. Hypoxic regions contain cells that are slow dividing therefore anti-cancer drugs are unable to be efficacious as they require actively proliferating cells (Comerford et al. 2002). Hypoxia has also shown to induce the expression of various multidrug transporters which enable the drugs to be transported out the cell thereby ensuring resistance to drugs (Wartenberg et al. 2003).

2.2.3. Hypoxia Signalling

HIF-1α undergoes post-translational stabilisation process and act as transcription factor for various hypoxia inducible genes (Ivan et al. 2001; Jaakkola et al. 2001). As tumour progresses from being a benign tumour-to-tumour metastases, level of HIF-1α has shown to markedly increase (Harris

2002; Ke and Costa 2006; Zhong et al. 1999). HIF-1α signalling at normoxia and hypoxia are illustrated in figure 18.

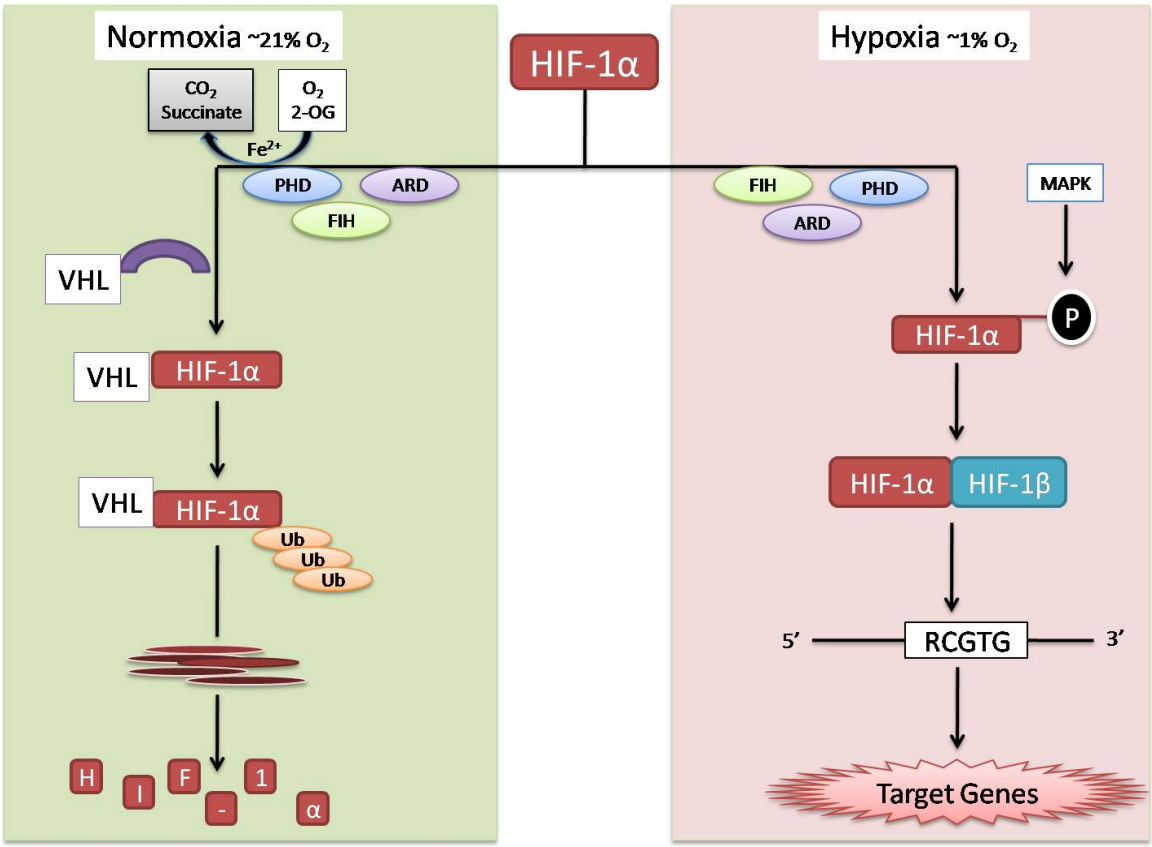

Figure 18: Regulation of HIF-1α under normoxia and hypoxia. Under normoxia HIF-1α is rapidly degraded by ubiquitination. Under hypoxia HIF-1α is stabilised, forms a dimer with HIF-1β and act as a transcription factor for various hypoxia inducible genes. Picture was adapted from Ke and Costa, 2006.

Under Normal conditions, HIF-1α is hydroxylated at two proline residues by Prolyl-4-hydroxylases (PHDs) and Factor Inhibiting HIF-1 (FIH-1) (Chan et al. 2002; Chan et al. 2005; Hewitson et al. 2002; Lando et al. 2002b; Masson et al. 2001). This reaction is catalysed by hydroxylases which require O_2, 2-oxoglutarate, iron and ascorbate (Bruick and McKnight 2001; Masson et al.

2001) to act as substrates and co-factors. Upon hydroxylation HIF-1α is recognised by Von Hippel Lindau (VHL) tumour suppressor which is favoured by acetyle transferase Arrest-Defective-1 (ARD-1) (Jeong et al. 2002). This VHL-HIF-1α association results in the addition of ubiquitin ladders that undergo proteosomal degradation (Huang et al. 1998; Semenza 1999; F. Yu et al. 2001b).

Under Hypoxia, PHDs and FIH-1 are inhibited due to lack of oxygen. Therefore, HIF-1α-VHL interaction is inhibited resulting in the stabilisation of HIF-1α (Huang et al. 1996; Kallio et al. 1997; Lando et al. 2002a). The stabilised HIF-1α binds to HIF-1β, which is constitutively expressed regardless of oxygen levels (Kallio et al. 1997). This complex acts as transcription factor by binding DNA consensus element - 5' RCGTG 3', and regulate various factors to help cells to adapt to hypoxia (Goldberg et al. 1988; Semenza et al. 1991).

Besides PHDs that sense oxygen and regulate HIF-1α, it is also activated by phosphorylation, mediated by MAPK (Minet et al. 2001; Richard et al. 1999; Sodhi et al. 2000). Phosphorylated HIF-1α has been demonstrated to have increased transcriptional activity (Richard et al. 1999). Other factors affecting HIF-1α regulation are cytokines, growth factors and other signalling molecules under normoxic conditions (Feldser et al. 1999; Gorlach et al. 2001; Haddad and Land 2001; Richard et al. 2000). The common pathway that transactivates HIF-1α and synthesis is via MAPK or PI-3K pathways (J. Li et al. 2004; Zelzer et al. 1998).

2.2.4. Effects of HIF-1α

HIF-1α$^{-/-}$ is embryonically lethal at E11 due to developmental defects of the vasculature (Iyer et al. 1998; Ryan et al. 1998). HIF-1α$^{+/-}$ mice survives until adulthood but when exposed to hypoxia, they had reduced physiological responses (Kline et al. 2002; A. Y. Yu et al. 1999). HIF-1α is important in various physiological and pathological processes as illustrated in figure 19 (Brahimi-Horn and Pouyssegur 2007; Hickey and Simon 2006; Semenza 1999).

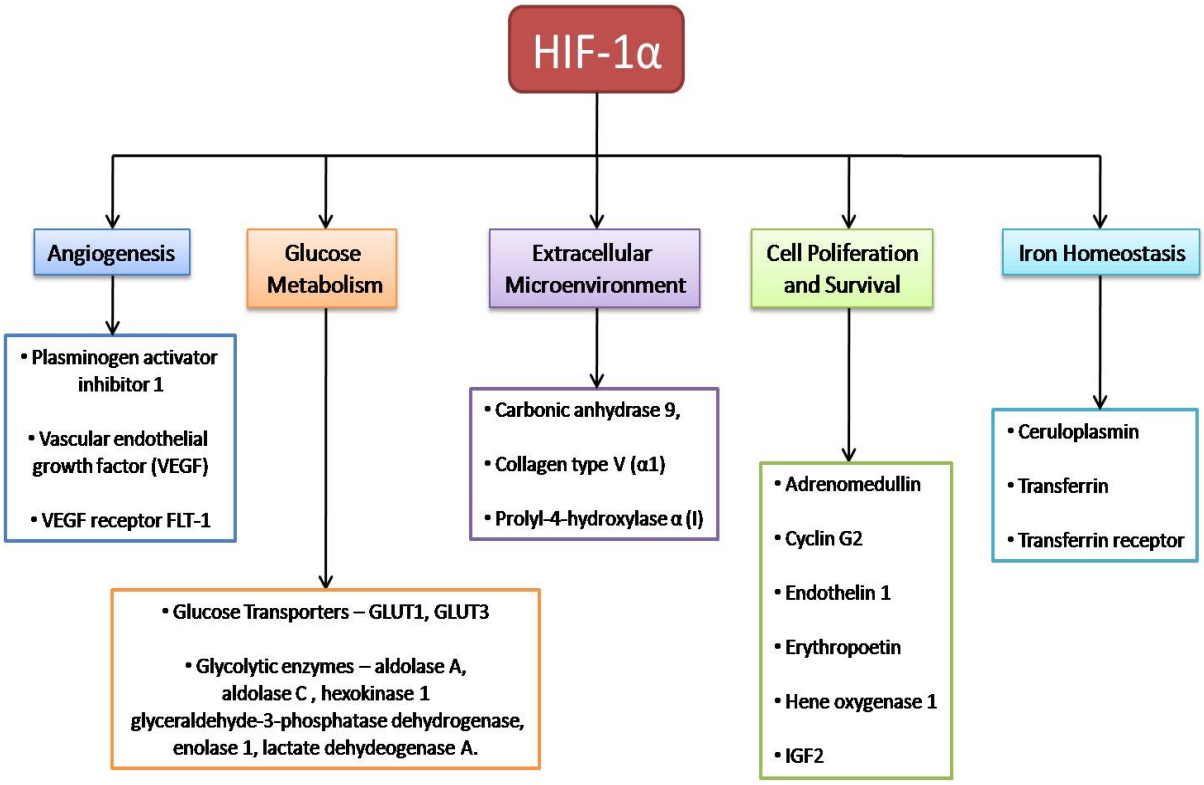

Figure 19: Example of some of the genes regulated by HIF-1α. Picture was adapted from Semenza *et al*, 1991, Rolfs *et al,* 1997, Levy *et al,* 1995, Grosfeld, 2002, Melillo *et al,* 1995, Feldser *et al,*1999, Krishnamachary *et al,* 2003 and Cormier-Regard *et al,* 1998.

Hypoxia and Apoptosis

Growing tumour mass has diminished apoptotic potential, and hypoxia plays a crucial role in enabling this. Reduced oxygen in cells results in apoptosis, but since cancer cells contain mutations in various apoptosis regulating pathways such as p53, caspase-9, Apaf-1, this results in survival (Graeber et al. 1996; Soengas et al. 1999). Hypoxia has also shown to increase genomic stability making tumour cells more aggressive (Bindra and Glazer 2005; Huang et al. 2007; Koshiji et al. 2005).

Hypoxia and Angiogenesis

Angiogenesis is one of the initial responses to hypoxia (Conway et al. 2001). VEGF is the most important angiogenic factor that recruits and stimulates the proliferation of endothelial cells (Bunn and Poyton 1996; Forsythe et al. 1996; Giordano and Johnson 2001; Josko et al. 2000; Levy et al. 1995). Besides VEGF, HIF-1α regulates the expression of nitric oxide synthase 2 (NOS2) (Melillo et al. 1995), heme oxygenase 1 (P. J. Lee et al. 1997), endothelin-1 (Hu et al. 1998), ADM (Nguyen and Claycomb 1999) and α_{1B}-adrenergic receptor (Eckhart et al. 1997). These contribute to angiogenesis and result in tumour survival.

Hypoxia - Cell Proliferation and Survival

HIF-1α regulates various growth factors such as IGF-1 and TGF-α (Feldser et al. 1999; Krishnamachary et al. 2003). These growth factors activate various signalling pathways that result in the accumulation of HIF-1α. This vicious cycle eventually results in cell proliferation and survival leading to cancer progression (Semenza 2003). Besides angiogenesis, apoptosis and cell proliferation, HIF-1α acts as a transcription factor for various genes such as genes involved in iron metabolism that results in increase in haemoglobin level thereby enabling oxygen transport (Rolfs et al. 1997; Semenza et al. 1991), glucose metabolism (Chen et al. 2001; O'Rourke et al. 1996; Semenza et al. 1996) and matrix metabolism (Ben-Yosef et al. 2002; Y. Takahashi et al. 2000) as illustrated in figure 19.

Aim

Based on these data, the aim of this chapter is to study the effect of hypoxia on ADM, its receptors, PAM and Akt regulation. It is hypothesized that ADM and its receptors are up-regulated under hypoxia and PAM is also up-regulated to render ADM active. Since ADM mediates its pro-tumourigenic action via Akt signalling, it is hypothesized that under hypoxia Akt is activated by up-regulation of ADM.

2.3. METHODS

Materials and Recipes for solutions used are given in Chapter 6, Appendix.

2.3.1. Cell Culture

Cell culture was carried out under aseptic conditions on Nunclon treated tissue culture plastics. The different cell lines and the respective media used during the project are outlined in table 1.

S.No	Cell Line	Cancer Type	Media
1	MDA-MB-231	Breast Cancer	RPMI
2	MDA-MB-436		
3	Meso	Mesothelioma	
4	Hela	Cervical Cancer	
5	U-87	Glioblastoma	MEM
6	PC-3	Prostate Cancer	DMEM
7	Panc2.3	Pancreatic Cancer	
8	Sw-13	Adenocarcinoma	
9	HT-29	Colon Cancer	
10	HCT-116		

Table 1: Different cancer cell lines used in this project. The media used for each cell line is also shown.

The media were supplemented with 10% heat inactivated Fetal Bovine Serum and 5% Penicillin/Streptomycin antibiotic.

The frozen cells were thawed in water bath at 37°C for 2 minutes and transferred to 75 cm^2 flasks with the required amount of media. The culture was

incubated at 37°C with 5% CO_2 to attain confluency. The media was changed every three days and subcultured after reaching 80-90% confluency.

A. Subculture of Cells

Cells were washed with PBS in order to clear any media and dead cells left over in the flask. 10% Trypsin EDTA was added to dislodge cells adhered to the flask. Cells were centrifuged at 1000 rpm for 3 minutes and the supernatant was discarded, the resulting cell pellet was resuspended in fresh media and subcultured into the appropriate number of flasks as required for the experiments.

B. Cell Counting

Cells were washed with PBS, trypsinised and centrifuged as mentioned above. The cell pellet was resuspended in 1ml of appropriate media and a further 1:10 or 1:100 dilution was made using PBS or media, depending on cell density. Cells from this dilution were counted using a haemocytometer. Cells in four corner squares (each containing 16 squares) of the haemocytometer was counted and averaged. The total number of cells in 1ml of the cell suspension was calculated as follows:

Total number of cells = Average of four squares x 10,000 x dilution factor

2.3.2. Induction of Hypoxia

Hypoxia was induced using three different methods as follows:

A. Cobalt Chloride ($CoCl_2$)

Since $CoCl_2$ is widely used to mimic hypoxia, 300μM $CoCl_2$ made up in PBS was used to induce hypoxia at 0, 2, 5, 7, 24 and 48hrs time points. Cells were seeded (~80,000 cells) in a 35mm petriplate the day before treatment was

started. At desired time points, the culture media were collected for further analysis and cells were extracted using 1ml Tri reagent and frozen at -80°C until RNA extraction.

B. Incubator containing 0.1% O_2

An incubator containing 0.1% O_2, 5% CO_2 and 94.9% N_2 at 37°C was used to induce hypoxia. Cells were cultured in T25cm^2 flasks till 60% confluent and incubated for 24 and 48hrs. As a control for hypoxia, cells were incubated in a regular incubator for 0, 24 and 48hrs. 0hrs was done as a control to see the basal level of protein expression. At the appropriate time points, cells were extracted using 1ml Tri regent and frozen at -80°C until RNA extraction.

C. Hypoxic media

Two T175cm^2 flask containing 200ml MEM media each was left in the hypoxic incubator with conditions as mentioned above for two days. The T175cm^2 flask was half filled with media so that there was enough space to displace O_2. Meanwhile, cells were cultured in T25cm^2 flasks under regular condition until 60% confluent. After two days, the now hypoxic media was added to the cells in T25cm^2 flasks. The media was added to the brim, so that O_2 does not get stabilised during the time points. The lids of the flasks containing filters were then secured with parafilm. Normoxic controls contained regular media filled to the brim and lids secured with parafilm. The time points used were 0, 15mins, 30mins, 45mins, 1, 2 3 4 6 and 16hrs. At the appropriate time points, cells were extracted using 1ml Tri regent and frozen at -80°C until RNA extraction.

2.3.3. RNA isolation

The frozen cell extracts were thawed at room temperature and RNA was extracted using the protocol as described by Sigma Aldrich.

200µl chloroform was added to the thawed cell extracts and incubated for 5-10 minutes in room temperature. The samples were centrifuged at 12,000xg for 15 minutes at 2°C. The upper aqueous phase containing RNA was carefully transferred to an RNase free tube. 500µl isopropyl alcohol was added and incubated for 15 minutes at room temperature and centrifuged at 12,000xg for 10 minutes at 2°C. The RNA was washed with 75% ethanol and air-dried. The pellet was resuspended in DEPC treated water.

2.3.4. DNase treatment

In order to eliminate genomic DNA contamination from the RNA sample, DNAse treatment was carried out according to the protocol from Applied Biosystems.

0.1 volume of 10xDNase buffer and 2Units of DNase was added to the RNA and incubated for 30mins at 37°C. 0.1volume of DNase inactivation reagent was added to the RNA and incubated for 5mins at room temperature. The RNA was then centrifuged at 10,000xg for 90secs and the RNA was carefully transferred to a UV treated tube.

2.3.5. Quantification of RNA

The concentration of RNA was quantified using a nanodrop spectrophotometer. DEPC water that was used to resuspend RNA was used as blank and 1µl of RNA was used to quantify RNA. The quality of RNA was determined by the value of 260/280 ratio as determined by the spectrophotometer. 260/280 ratio lying between 1.8 and 2 was considered to be a good quality RNA and was used for cDNA synthesis.

2.3.6. cDNA Synthesis

1µg of RNA was used for cDNA synthesis. cDNA was synthesised according to the protocol from Applied Biosystems.

To 1µg of RNA, 10µl of 2X RT buffer and 1µl of enzyme mix was added. Water was added to make the final volume to 20µl. A no Reverse Transcriptase control (RT-) was done by replacing the enzyme mix with water. The mixture was briefly vortexed and centrifuged to eliminate any air bubbles. Reverse Transcription was allowed to take place by incubating the tubes for 1hour at 37°C. The reaction was stopped by heating to 95°C for 5mins and transferred to ice for subsequent PCR analysis or frozen for long term storage. The incubation steps were carried out using a thermal cycler.

2.3.7. Real Time PCR (qPCR)

To quantitate the expression of the gene of interest, quantitative PCR (qPCR) was carried out using ABI 7900HT sequence detection system from Applied Biosystems. Taqman assays (primers) for RAMP2, RAMP3, CLR, ADM, HIF-1α, HPRT1 and β-Actin were inventoried from Applied Biosystems, their assay ID and amplicon length can be obtained from table 2. In order to exclude any genomic DNA amplification, the taqman assay belonged to m1 group, which spans the exon-exon junction thereby eliminating the amplification of genomic DNA (gDNA).

The reaction mixture per well contained 5µl of 2x Taqman gene expression master mix, .5µl tagman assay, 2.5µl water and 2µl cDNA/RT-/H_2O

The qPCR reaction was carried out in triplicates and the standard PCR reaction cycle used is as follows:

Step 1: 50°C for 2 min
Step 2: 95°C for 10 min
Step 3: 95°C for 15sec
Step 4: 60°C 1 min

The reaction was carried out for 40 cycles.

S.No	Gene name	Assay ID	Amplicon length
1	RAMP2	Hs00359352_m1	117
2	RAMP3	Hs00234665_m1	82
3	CLR	Hs00173787_m1	130
4	ADM	Hs00181605_m1	76
5	HIF-1α	Hs00936368_m1	87
6	HPRT1	Hs01003267_m1	72
7	β-Actin	Hs99999903_m1	171

Table 2: Gene specific taqman assays, their ID and amplicon length.

A. qPCR Data Analysis

qPCR data was analysed using SDS 2.2.1 software. There are two methods of calculating qPCR data depending on whether a fold change in expression is required or relative quantification of mRNA to a control is required.

The Ct values obtained from the ABI 7900HT system was used for analysis using both the methods determine either fold change or the relative expression of a gene of interest. Both the methods require that the Ct value of the gene of interest be normalised to an endogenous control, whose expression is unchanged in any experimental condition. For this project β-actin and HPRT1 were used as an endogenous controls.

Fold change in expression is calculated using the ΔCt method. The formula for calculating fold change is $2^{-\Delta Ct}$, where,

ΔCt = Average Ct of target gene – Average Ct of endogenous control

Relative Quantification is calculated using the ΔΔCt method. The formula for calculating relative quantification is $2^{-\Delta\Delta Ct}$, where,

ΔΔCt = ΔCt of target gene – ΔCt of endogenous control

2.3.8. Hoechst Staining

In order to measure the cell death index after $CoCl_2$, morphological assessment of the apoptotic cells was done using Hoechst 33258 stain.

Cells were seeded on a glass coverslip placed in a standard clear bottom 6 well plates. 300μM of $CoCl_2$ was added to all the wells belonging to time points 0h, 2h, 5h, 7h, 24h and 48h. Once the cells are confluent on the coverslips, cells were washed with PBS and fixed using Clarke's fixative (ethanol:aceticacid=3:1) for 10 minutes at room temperature. The fixative was then discarded and cells were washed with PBS and Hoechst stain (1:1000 dilution) was added to the coverslips and incubated for 20 minutes at room temperature. The stain was discarded and coverslips were washed with PBS, air dried and mounted using mowiol [1 part of Phenylenediamine + 9 parts of mowiol]. The slides were viewed under an inverted widefield fluorescence microscope (Leica DFC300FX). The apoptotic cells were counted using ImageJ software and an apoptotic index was created using the formula,

$$\text{Cell Death Index, \%} = \frac{100 \text{ X apoptotic cells}}{200 \text{ cells}}$$

2.3.9. Western Blotting

A. Protein Extraction

Cells cultured in T175cm^2 flask was briefly washed with PBS and 10% Trypsin EDTA was added to dislodge cells from flask. The cells were then centrifuged at

1000 rpm for 5mins. The cell pellet was resuspended in 500µl of NP-40 cell lysis buffer containing freshly added protease inhibitors. Cells were incubated on ice to swell for 20mins. Cells were then sonicated in an ultrasonic water sonicator for 10mins. Cells were then centrifuged at 1000 rpm for 5mins. The supernatant was transferred to a fresh tube for quantification.

B. BiCinchonic Acid (BCA) Assay

Protein samples were quantified using BCA assay. BCA reagent A and B were mixed in 1:50 ratio. 2µl and 5µl of protein samples were added to 1ml of AB mixture, in duplicates. Varying dilutions of BSA was used as a standard to measure concentration of protein samples. All samples were incubated for 30mins at 65°C. The absorbance was measured using a spectrophotometer at 562nm. Linear Regression analysis was done using GraphPad Prism software to interpolate concentrations of protein samples from BSA standards.

C. Gel Casting

Gels were cast in a 9cmx9cm glass slides with 1.5mm spacer slide. Resolving and stacking gels were cast according to the recipe given in chapter 7, appendix.

D. Sample Preparation

70µg of protein sample was mixed with 10x protein loading buffer and heated to 90°C for 5mins to denature proteins. Biotinylated protein ladder was also heated along with the samples. In order to ensure homogenous migration of samples, the final volume of samples was kept the same.

E. PolyAcrylamideGel Electrophoresis

Samples were loaded into the wells of the gel. A Kaleidoscope ladder was also run alongside the biotinylated ladder to track the migration of samples. Samples were run in the presence of running buffer at 150V for 30mins or until

the dye front reached the bottom of the gel. For 7% gels where ADM was to be probed, gel was run half way since the molecular weight of ADM was ~7kDa. For 15% gels where HIF-1α and PAM was to be probed, gel was run longer since the molecular weights were >100kDa.

Protein samples were then transferred to PVDF (Polyvinylidene Difluoride) membrane in the presence of transfer buffer at 100V for 1hr.

PVDF membrane was blocked with 5% milk solution for an hour to reduce non-specific binding of antibodies. PVDF membranes were then incubated with appropriate antibodies.

F. Primary Antibody dilutions

PVDF membranes were incubated with the appropriate primary antibodies diluted in 1% milk solution overnight at 4°C with gentle agitation. The antibody dilutions were: RAMP2 = 1/200 to 1/1000; RAMP3 = 1/200 to 1/1000; CLR = 1/500; ADM = 1/500 to 1/1000; HIF-1α = 1/100; Akt = 1/1000; Phospho-Akt =1/2000; PAM = 1/200; β-Actin =1/2000.

G. Secondary Antibody dilutions

PVDF membranes were washed with wash buffer two times 5mins each with gentle agitation to remove any non-specific binding of primary antibodies. HRP conjugated secondary antibodies were diluted in 1% milk solution and PVDF membranes were incubated for 1hr at room temperature with gentle agitation. The antibody dilutions used were 1/15,000 for both anti-rabbit and anti-goat HRP. 1/1000 dilution of HRP conjugated anti-biotin antibody was used for biotinylated ladder.

H. Protein Detection

After secondary antibody incubation, PVDF membranes were washed thrice 5mins each with wash buffer. Membranes were incubated with Enhanced Chemiluminescent (ECL) substrate for a 1min and sandwiched between two

acetate sheets. ECL sensitive Hyperfilm was exposed to membrane for different durations and the film was developed and fixed manually.

I. Data Analysis

Western blots were scanned as .jpeg images. The intensity of bands was measured using ImageJ software. Rectangular box encompassing spaces little above, below and sides of the bands were drawn and the same box was used for every band to measure intensity of pixels. Similarly pixel intensity was measured for controls and test and relative intensity of the test bands were quantified by normalizing to control (β-actin).

2.3.10. Flow Cytometry

Cells for flow cytometry were cultured in T175cm^2 flasks until 90% confluent. Cells were washed with PBS and fixed with 5ml of 4% PFA for 10mins at room temperature. Cells were scrapped gently using cell scrapper and transferred into 15ml falcon tubes. Cells used to determine total protein expression were permeabilised by incubating with 0.5% Tween/PBS for 15mins. Cells used to determine the cell surface expression were not permeabilised. Both permeabilised and non-permeabilised cells were blocked with 10% rabbit serum for 30mins at room temperature. Cells were centrifuged at 1000xg for 5mins at 4°C and resuspended in 1ml of 2% rabbit serum. Cells were counted as mentioned in section 3.3.1.

A. Antibody dilutions

Primary antibody was diluted in 500ul of cell suspension in 2% rabbit serum. The antibody dilutions used were, 1ug/1x10^6 cells for RAMP2, RAMP3, CLR and isotype control. Cells were incubated with primary antibodies for 1hr at room temperature with gentle agitation.

Cells were washed with wash buffer thrice, 5mins each at 1000xg at 4°C. Cells were incubated with FITC labelled secondary antibodies in 500µl volume of wash buffer for 45mins at room temperature with gentle agitation. Secondary antibody dilutions were same as primary antibodies.

B. Cell Sorting

Cells were washed with wash buffer thrice, 5mins each and finally resuspended in 500ul wash buffer. Quantiquest software was used to sort the cells in flow cytometer. Cells with no antibody treatment were sorted first to optimise for background fluorescence. Optimal cell population was gated and 10,000 cells were counted from the gated population.

C. Data Analysis

Quantiquest flow cytometry software was used to analyse the flow cytometric data. From the scatter plot of the cells, optimal cell population in order to exclude dead cells and cell clumps was chosen. Histometric data analysis was done to nullify any fluorescence from isotype control and the same statistics was applied to test antibody treated cells. Therefore, number of cells more fluorescent than isotype antibody treated cells was considered to be positive for test antibody (RAMP2, RAMP3 and CLR).

2.3.11. Statistical Analysis

Statistical analysis was carried out for data obtained from the number of experimental repeats and not the number of repeats done per experiment (for example, duplicates and triplicates). For qPCR anaylsis One Way Analysis of Variance (ANOVA) was done to gain statistical analysis. Tukey post hoc test was done to compare between groups. Data is expressed as mean±SEM, and p value <0.05 was considered to be statistically significant. Linear Regression analysis was done for qPCR to test the efficacy of taqman assays where, the slope of the line, $R^2<1$ was considered to be significant.

2.4. RESULTS

2.4.1. HIF-1α Expression

In order to test the protein expression of HIF-1α under hypoxia, glioblastoma cells were cultured in an incubator containing 0.1% O_2 and whole cell lysate was used for western blotting.

Figure 20 shows the western blotting for HIF-1α in glioblastoma when exposed to hypoxia. It can be seen that HIF-1α protein expression was up-regulated under hypoxia. β-actin used as a loading control is shown in figure 21. Upon normalising and quantifying the intensity of the bands, it can be seen in figure 22 that the cells responded to hypoxia by up-regulating HIF-1α. Cells produced 34% and 92% more HIF-1α under hypoxia at 24 and 48hrs respectively when compared to their normoxic counterparts.

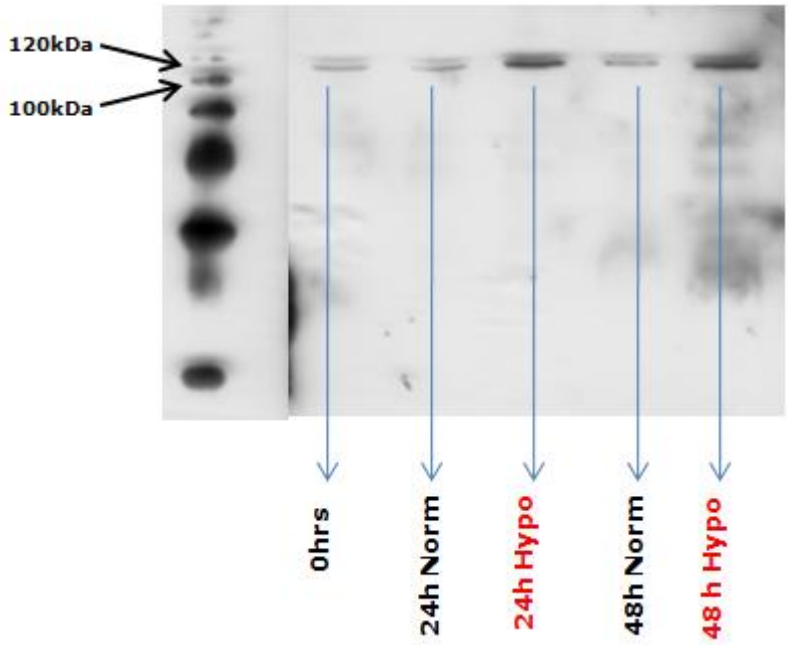

Figure 20: Western blotting result for HIF-1α at normoxia and hypoxia. The blots were exposed for 5 minutes and developed. The HIF-1α bands belong to 120kDa as shown in the picture.

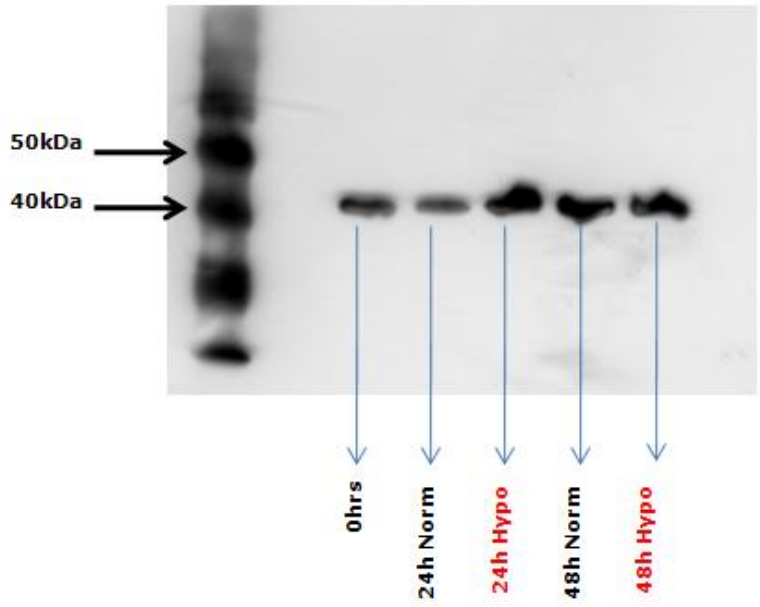

Figure 21: Western blotting result for β-actin expression in the glioblastoma cells when exposed to hypoxia and normoxia. The blots were exposed for 5 mins and developed. The β-actin bands belong to 45kDa as shown in the picture.

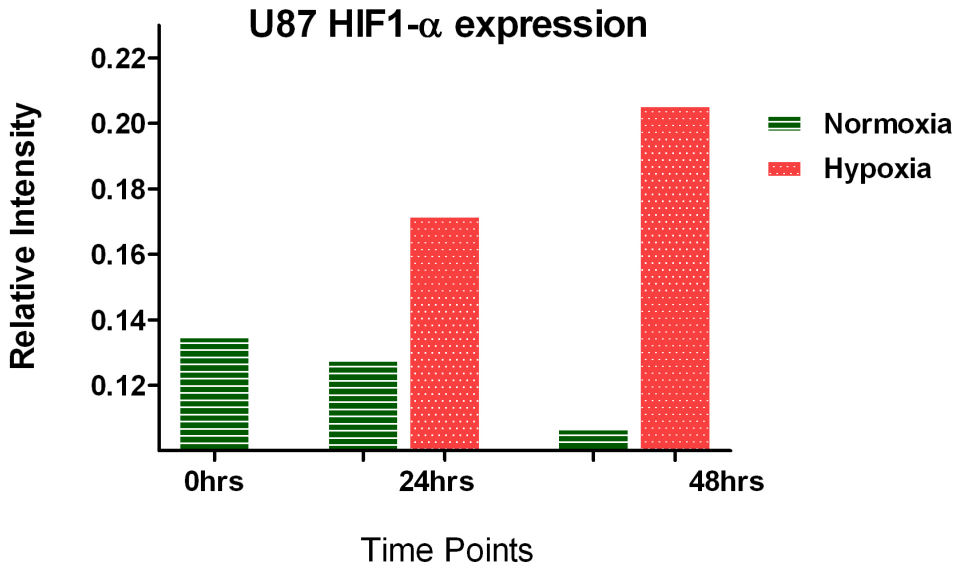

Figure 22: Quantification of HIF-1α expression in the Glioblastoma cells when exposed to hypoxia and normoxia. The band intensities were quantified as pixels using ImageJ and normalised to β-actin. n=1.

2.4.2. ADM Expression under Hypoxia

Since the cells were responding to hypoxia by up-regulating HIF-1α, next the expression of ADM mRNA was quantified using qPCR.

Figure 23A shows the ADM mRNA expression in glioblastoma cells when exposed to hypoxia. At 24hrs cells produced 7 fold more than normoxia and at 48hrs there was a 26.3 fold increase in ADM expression. The graphs are shown as a relative expression to 0hrs.

Figure 23B shows the ADM mRNA expression in prostate cancer cells. Cells up-regulated ADM at 7.6 fold and 16.6 fold at 24 and 48hrs hypoxia respectively when compared to their normoxic counterparts.

Figure 23C and D show the ADM mRNA expression in the two breast cancer cell lines – MDA-MB-436 and MDA-MB-231. In MDA-MB-436 cells (fig 23C) ADM mRNA expression was increased by 9.4 and 158 fold at 24 and 48hrs respectively. MDA-MB-231 (fig 23D) produced 20 fold increase at 24hrs and 29 fold at 48hrs.

Figure 23E shows the ADM mRNA expression in pancreatic cells. Cells produced an 8.5 fold increase in ADM expression at 24hrs hypoxia and 5.5 fold increase at 48hrs.

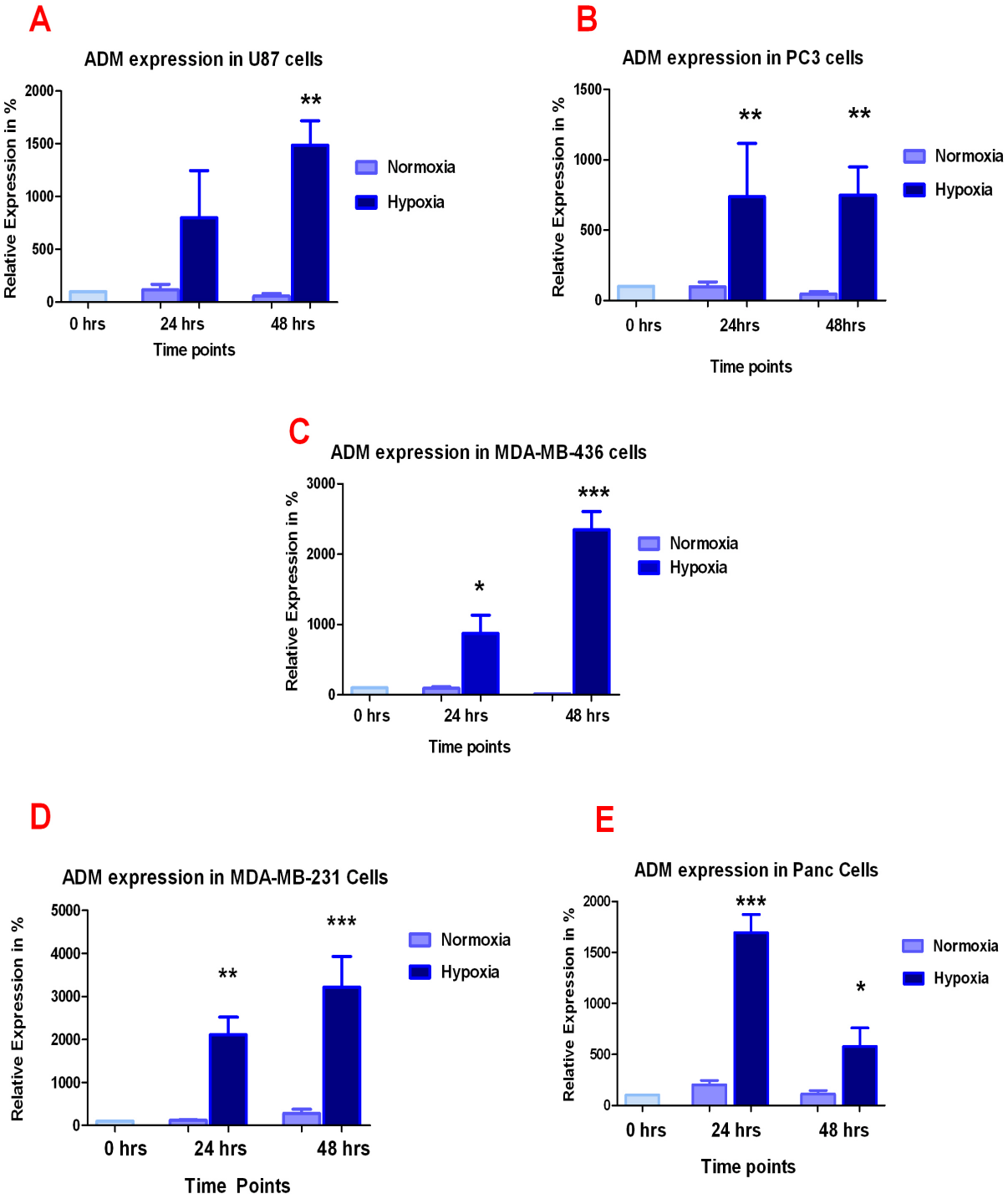

Figure 23: mRNA expression of ADM under normoxia and hypoxia at 24hrs and 48hrs in Glioblastoma, n=4 **(A)**, prostate cancer, n=4 **(B)**, breast cancer – MDA-MB-436, n=4 **(C)**, MDA-MB-231, n=3 **(D)** and pancreatic cancer, n=3 **(E)** cells measured by qPCR. The bars are represented in relative to the expression at 0hrs, which is 100%. Data is expressed as mean ± SEM. ANOVA and Tukey post test was performed to gain statistical significance. $p < 0.001$

2.4.3. ADM Receptor Expression under Hypoxia

2.4.3.1. CLR Expression

Figure 24 shows the CLR mRNA expression in glioblastoma cells, when exposed to hypoxia. CLR expression was down-regulated by 75% at 24hrs and 50% at 48hrs hypoxia when compared to the normoxic counterparts.

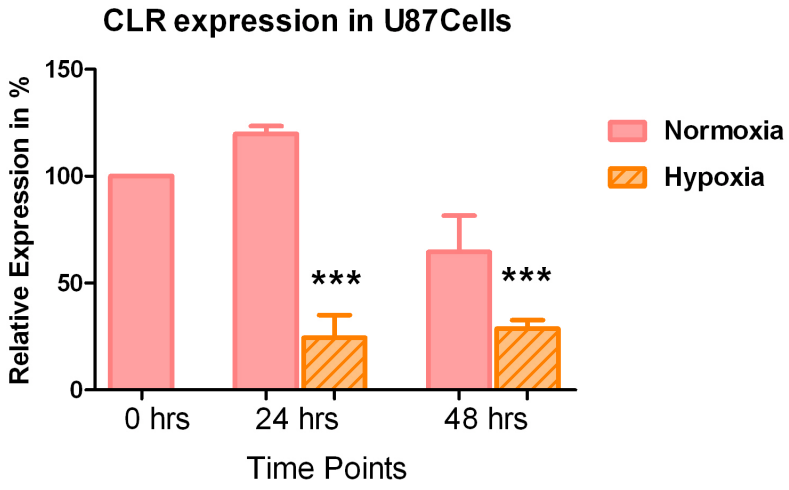

Figure 24: mRNA expression of CLR in the glioblastoma cells when exposed to hypoxia and normoxia measured by qPCR. The bars are represented in relative to the expression at 0hrs, which is 100%. Data is expressed as mean ± SEM. ANOVA and Tukey post test was performed to gain statistical significance. n=4, $p < 0.001$

Next the protein expression of CLR was measured using western blotting. 50µg of whole cell lysate was separated in a 12% gel. Figure 25 shows the western blot for CLR expression on glioblastoma cells. Bands belonging to CLR can be seen in between 40kDa and 50kDa.

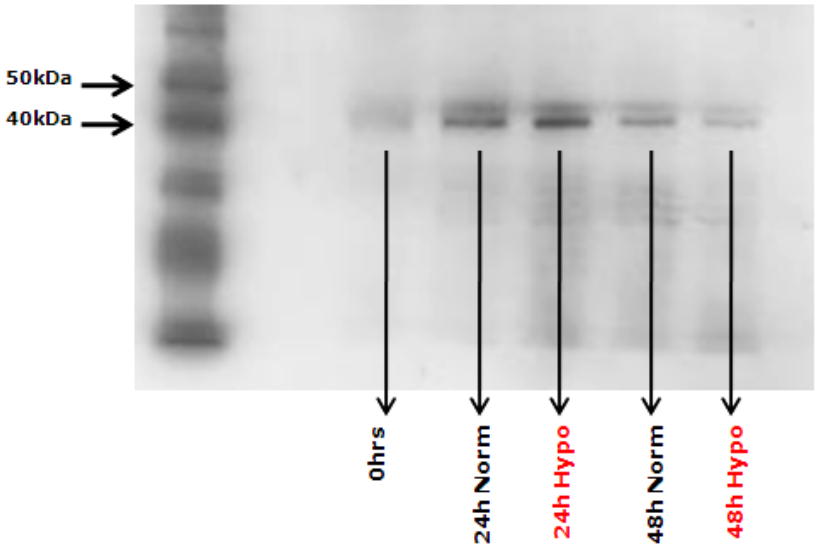

Figure 25: Western blot for CLR expression in glioblastoma cells when exposed to hypoxia and normoxia. The blots were exposed for 5 mins and developed. The CLR bands belong to 42kDa as shown in the picture.

Figure 26, shows the relative intensity of CLR expression normalised to β-actin. There was no significant difference between CLR protein expression under hypoxia when compared to normoxia.

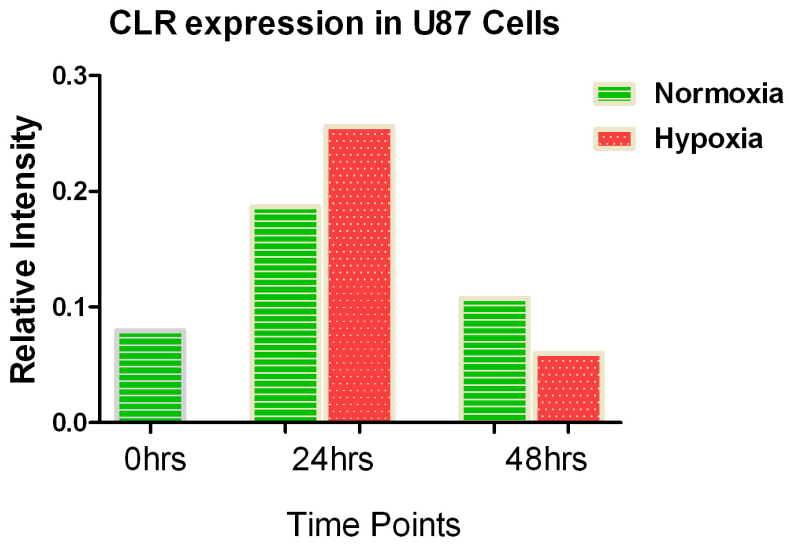

Figure 26: Protein expression of CLR under hypoxia and normoxia in Glioblastoma cells. The bars are shown relative to the band intensity of β-Actin at each of these time points, measured as pixels using ImageJ software. n=1.

Figure 27A shows the mRNA expression of CLR in prostate cancer cells. There was a significant down-regulation of 40 fold at 24hrs and no significant difference at 48hrs.

Figure 27B shows the mRNA expression of CLR expression in breast cancer cells. There was no significant difference between cells exposed to hypoxia when compared to normoxic controls at 24hrs and 48hrs. The expression of CLR in both hypoxia and normoxia at 24hrs and 48hrs was significantly lower when compared to the expression at 0hrs.

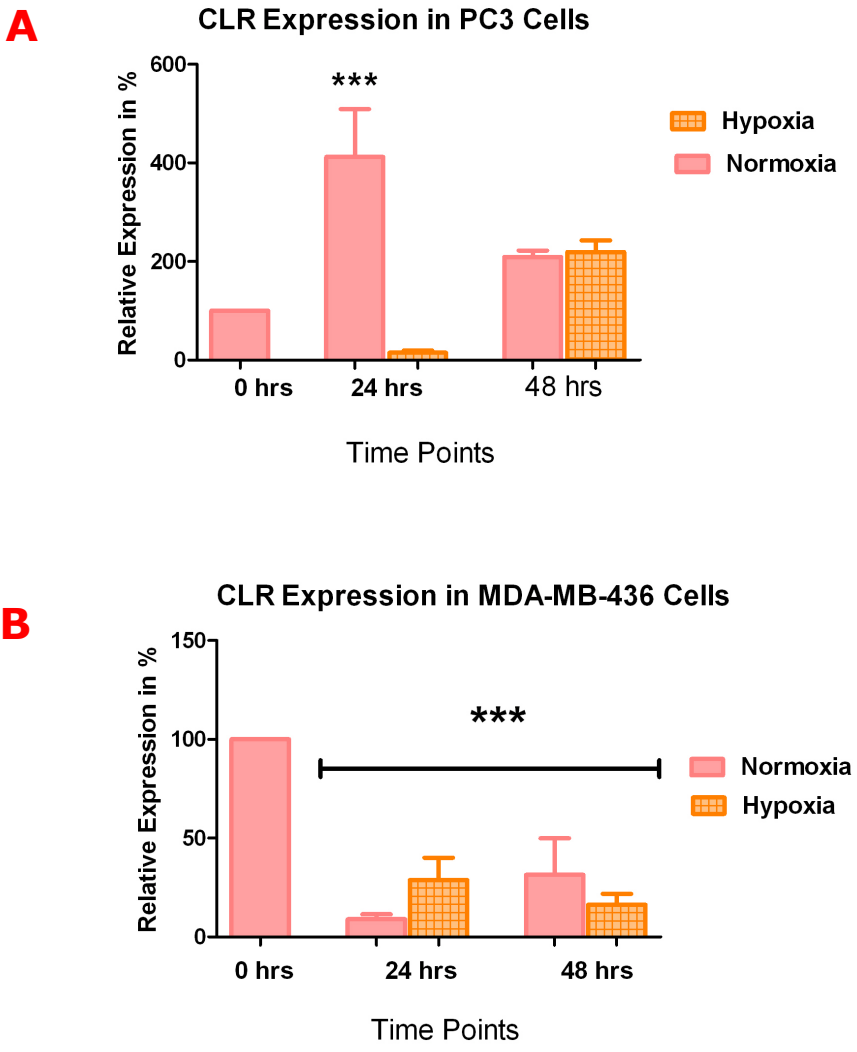

Figure 27: mRNA expression of CLR in prostate (A) and breast cancer (B) cells when exposed to hypoxia and normoxia measured by qPCR. The bars are represented in relative to the expression at 0hrs, which is 100%. Data is expressed as mean ± SEM. ANOVA and Tukey post test was performed to gain statistical significance. n=4, $p < 0.001$

2.4.3.2. RAMP2 and RAMP3 Expression

Please Note: This section contains supplementary figures that were been included here at the request of examiners.

mRNA

qPCR done using taqman assays on different cancer cell lines were usually undetermined or sometimes greater than 35 which were inconsistent.

Primers were tested on COS-7 cells stably transfected with RAMP2 and RAMP3. Supplementary figure 2.4.3.2.1. shows that the primers were amplifying RAMP2 and RAMP3 in COS-7 cells transfected with RAMP2+CLR and RAMP3+CLR.

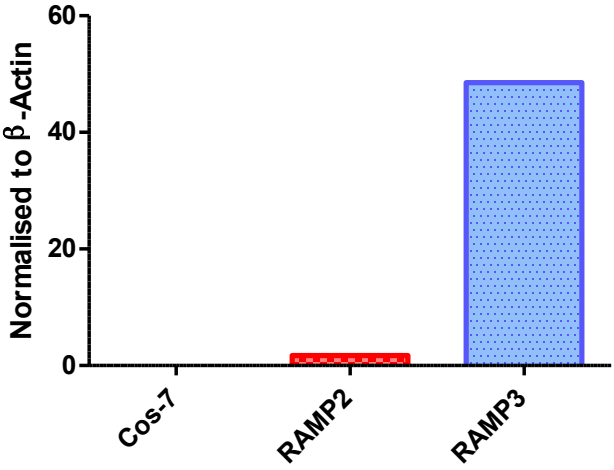

Supplementary Figure 2.4.3.2.1 : mRNA expression of RAMP2 and RAMP3 detected in stably transfected COS-7 cells. Non-transfected COS-7 cells showed no expression of RAMP2 and 3.

Since the RAMP2 and RAMP3 primers were detecting the mRNA expression, during cDNA synthesis, instead of random primer, gene specific primers from Primer Design was used for RAMP2 and RAMP3. RAMP 2 and RAMP 3 could still not be detected in different cancer cell lines.

Since the mRNA expression of RAMP2 and RAMP3 could not be detected, the protein expression of RAMPs were done using rat brain protein sample as a positive control.

Protein Quantification – Western Blotting

Supplementary figure 2.4.3.2.2 shows the western blotting for RAMP2 in rat brain sample. The bands correspond to 20kDa which could be the monomer RAMP2 and the 60kDa band could be RAMP2 + CLR heterodimer.

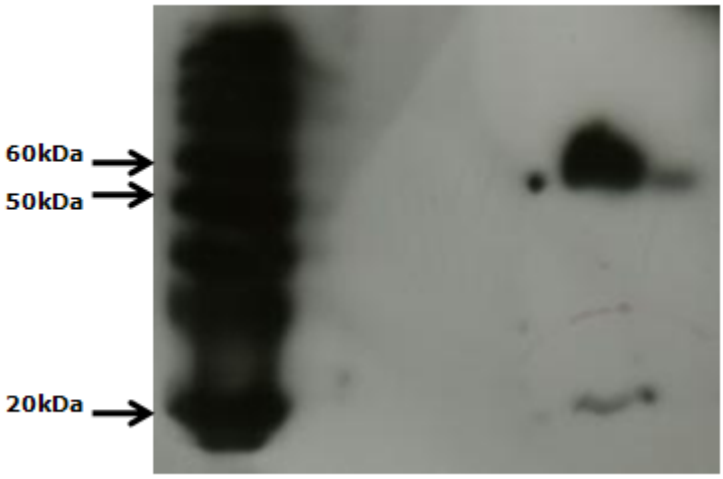

Supplementary Figure 2.4.3.2.2 : Western blot for RAMP2 in rat brain brain. RAMP2 monomer belongs to 20kDa and the CLR+RAMP2 heterodimer belongs to 60kDa.

Supplementary figure 2.4.3.2.3 shows the western blotting for RAMP3 in rat brain sample. The band at approximately 16kDa could be the RAMP3 monomer and the band at approximately 28kDa could be glycosylated form of monomer RAMP3 and the band corresponding to approximately 32kDa could be a homodimer of RAMP3.

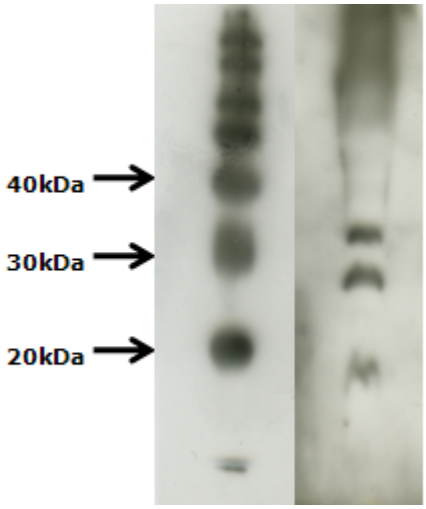

Supplementary Figure 2.4.3.2.3 : Western blot for RAMP3 in rat brain sample. Monomer RAMP3 band can be seen at ~16kDa. RAMP3 homodimer can be seen at 28kDa and the band at 32kDa could belong to glycosylated RAMP3 homodimer.

Next western blotting was done for RAMP2 and RAMP3 in whole cell lysate of glioblastoma cells when exposed to hypoxia.

Supplementary figure 2.4.3.2.4 shows the different western blotting results obtained from probing glioblastoma cells with RAMP2 antibody. The different lanes belong to 0hrs, 24hrs normoxia, 24hrs hypoxia, 48hrs normoxia and 48hrs hypoxia. (A) shows a single band varying in intensities over hypoxia and normoxia at ~55kDa. (B) shows a prominent band at ~40kDa and bands at ~22kDa, ~28kDa, ~31kDa, ~50kDa and ~55kDa. (C) shows two bands at ~40kDa and ~55kDa. (D) shows three bands at ~20kDa, ~40kDa and ~55kDa.

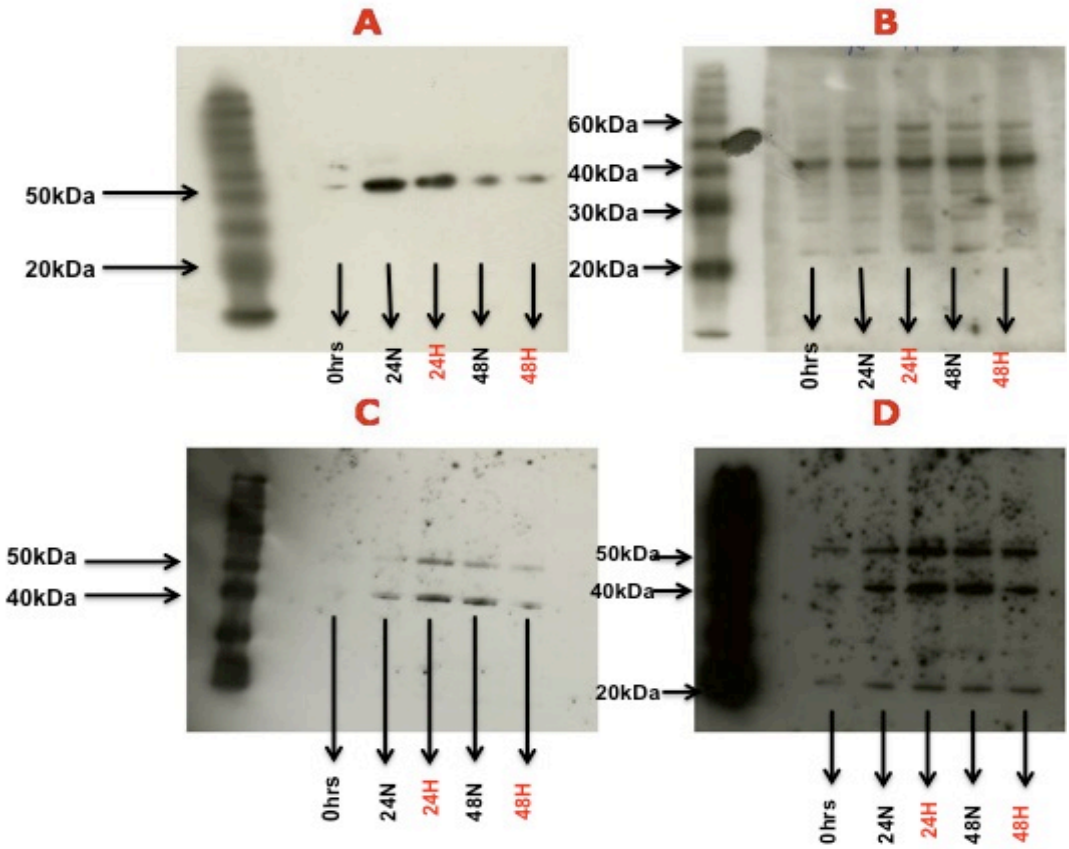

Supplementary Figure 2.4.3.2.4: Western blotting results when probed for RAMP2 antibody on glioblastoma (U87) cells when exposed to hypoxia. The results were different each time western blotting was done for the same samples. 24N, 48N = 24 Normoxia, 48 Normoxia. ; 24H, 48H = 24 Hypoxia, 48 Hypoxia.

Supplementary figure 2.4.3.2.5 shows the different western blotting results when probed for RAMP3 antibody on Glioblastoma cells when exposed to hypoxia. (A) shows multiple bands at ~20kDa, ~30kDa, ~42kDa, ~55kDa and ≈60kDa. (B) shows multiple bands from ~20kDa to ~80kDa. (C) shows similar multiple bands pattern as that of picture B.

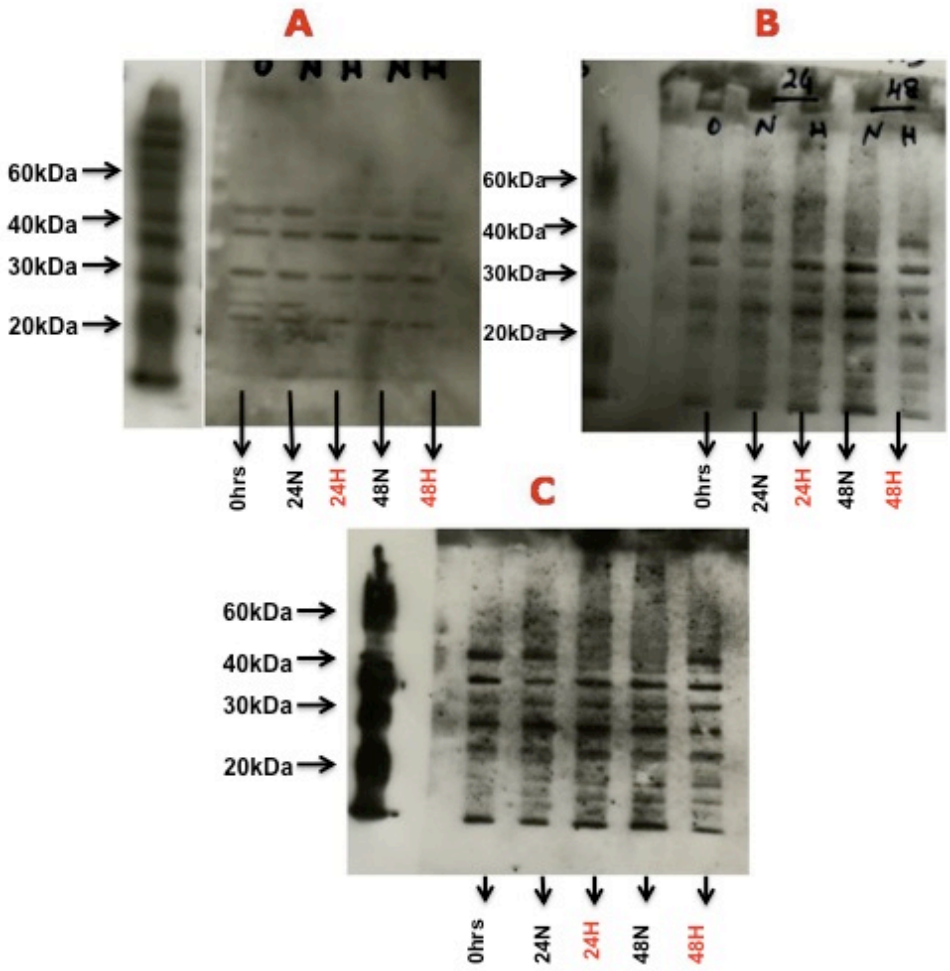

Supplementary Figure 2.4.3.2.5 : Western blotting results when probed for RAMP3 antibody on glioblastoma (U87) cells when exposed to hypoxia. The bands were different each time western blotting was done for the same samples. 24N, 48N = 24 Normoxia, 48 Normoxia ; 24H, 48H = 24 Hypoxia, 48 Hypoxia.

Since the RAMP2 and RAMP3 western blotting could not be construed as specific bands, flow cytometry was carried out to determine the expression of RAMP2 and RAMP3 in both permeabilised and non-permeabilised cells.

Protein Quantification – Flow Cytometry

Supplementary figure 2.4.3.2.6 shows the quantified flow cytometry results. The bars are the mean protein expression of 10,000 cells. Bars are drawn after normalising the receptor expression values to that of isotype control.

Cos-7 cells show 18% expression of RAMP2, 19% expression of RAMP3 and 3% expression of CLR.

U87 cells showed 96% expression of RAMP2, 86% expression of RAMP3 and 78% expression of CLR.

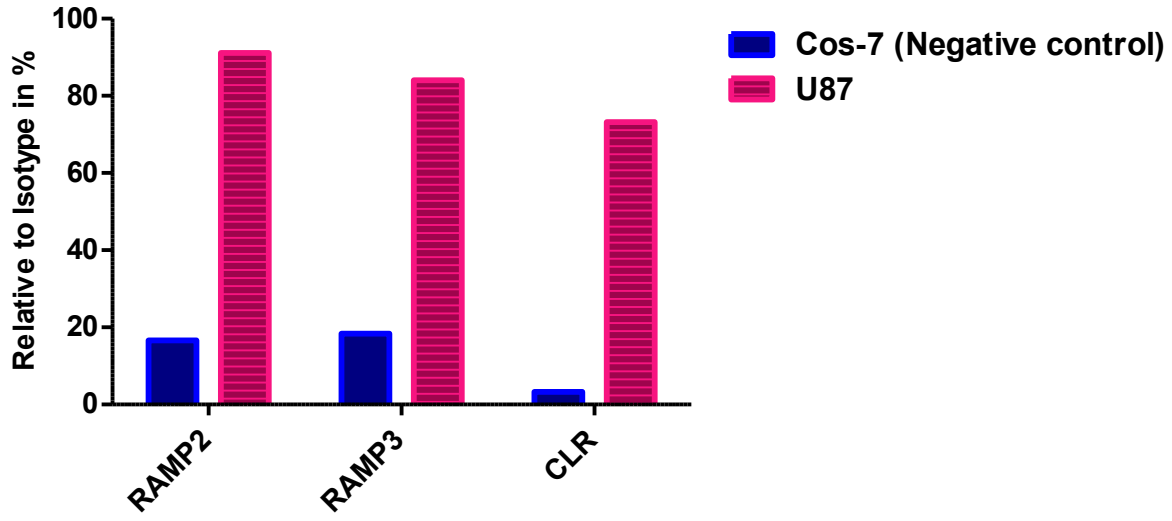

Supplementary Figure 2.4.3.2.6 : Percentage of total receptor expression in permeabilised glioblastoma (U87) cells after normalising with the isotype controls in Cos-7 and U87 cells.

Figure 28 shows the quantified flow cytometric results of U87 cells exposed to hypoxia.

The total expression at 0hrs was 50% RAMP2, 80% RAMP3 and 10% CLR.

At 24hrs normoxia, there was 58% RAMP2, 1% RAMP3 and 18% CLR.

At 24hrs hypoxia, there was 10% RAMP2, 42% RAMP3 and 8% CLR.

At 48hrs normoxia and hypoxia as it can be seen from figures 102 and 103 under Appedix section, there was a huge shift in fluorescent intensity in control antibody probed cells. The fluorescent intensities of receptors were same as control antibody; therefore the protein expression could not be evaluated.

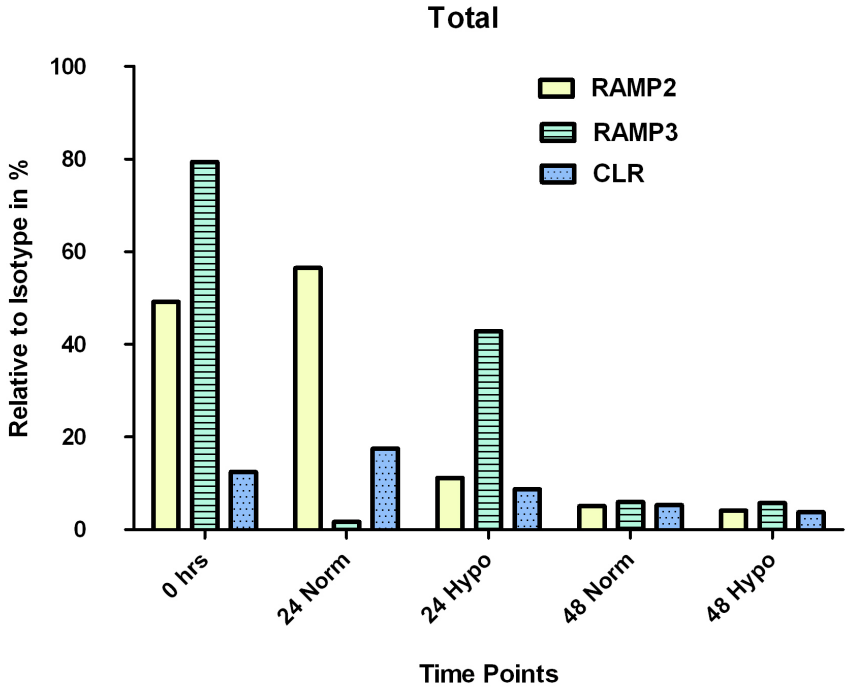

Figure 28: Total receptor expression when exposed to hypoxia in permeabilised glioblastoma (U87) cells. Bars are drawn after being normalised to antibody control, and are the mean of values from 10,000 cells.

The cell surface receptor expression shown in figure 29 at 0hrs was 47% for RAMP2, 28% for RAMP3 and 11% for CLR.

At 24hrs normoxia, there was 21% RAMP2, 13% RAMP3 and 8% CLR.

At 24hrs hypoxia, there was 23% RAMP2, 22% RAMP3 and 8% CLR.

As mentioned above, at 48hrs normoxia and hypoxia there was control antibody background, the protein expression could not be evaluated.

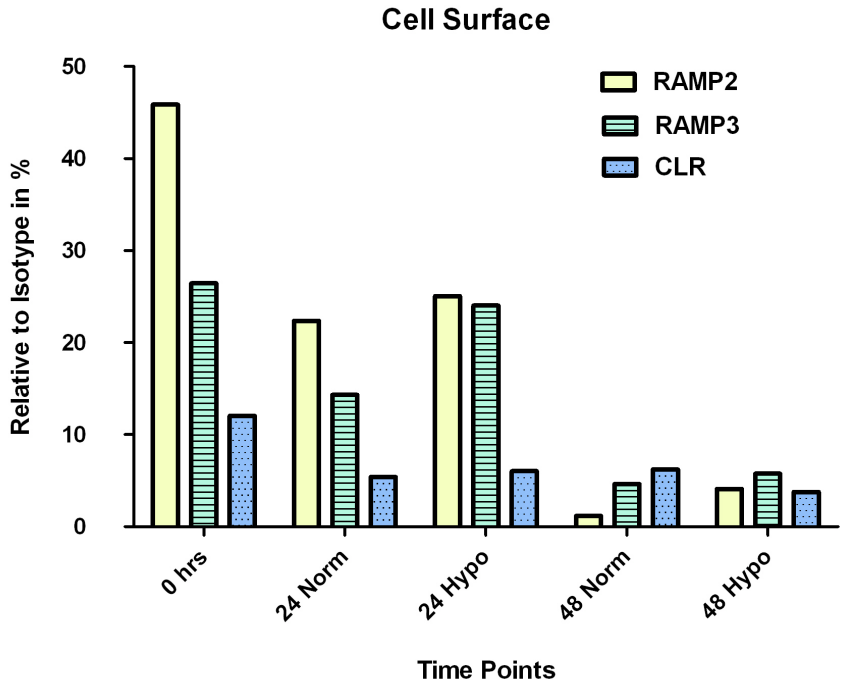

Figure 29: Cell surface receptor expression when exposed to hypoxia in non-permeabilised glioblastoma (U87) cells. Bars are drawn after being normalised to antibody control, and are the mean of values from 10,000 cells. n=1.

Receptor Expression in MDA-MB-231 cells under hypoxia

The effect of hypoxia on receptor expression was tested on breast cancer cells.

Upon normalising and quantifying, figure 30 shows that the receptors are down-regulated under hypoxia.

At 24hrs normoxia, there was 80% of RAMP2, 89% RAMP3 and 90% CLR.

At 24hrs hypoxia, there was 20% RAMP2, 27% RAMP3 and 18% CLR.

At 48hrs normoxia, there was 45% RAMP2, 78% RAMP3 and CLR.

At 48hrs hypoxia, the expression of RAMP2 was 9%, RAMP3 was 3% and CLR was 4%.

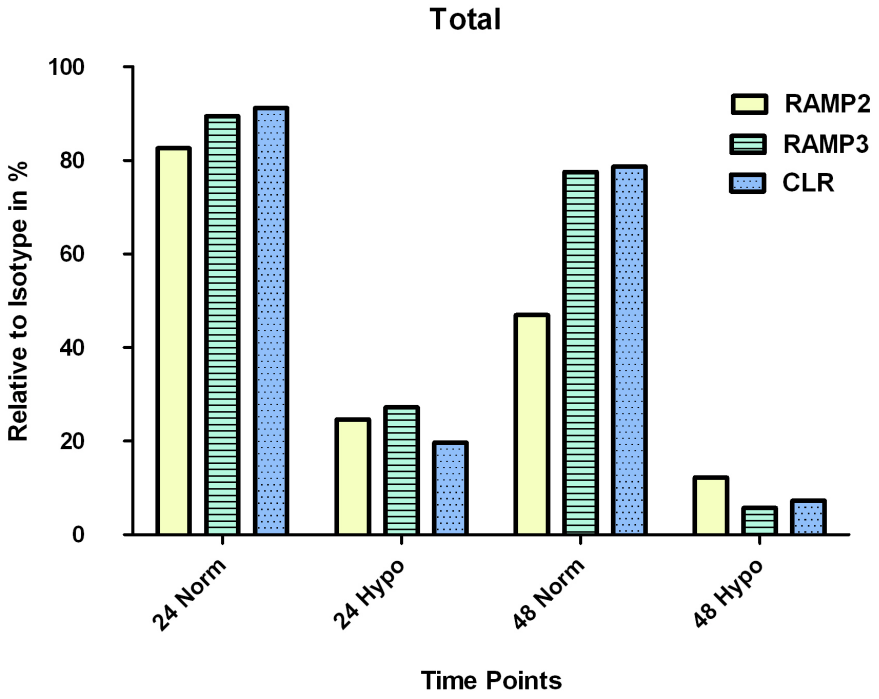

Figure 30: Total protein expression in permeabilised breast cancer (MDA-MB-231) cells when exposed to hypoxia. The bars are drawn as a mean expression after being normalised to the respective control antibodies. n=1

Figure 31 shows the quantified flow cytometric results of receptors expression at the cell surface.

At 24hrs normoxia, there was 30% RAMP2, 69% RAMP3 and 72% CLR.

At 24hrs hypoxia, there was 24% RAMP2, 41% RAMP3 and 14% CLR.

At 48hrs normoxia, there was 49% RAMP2, 62% RAMP3 and 69% CLR.

At 48hrs hypoxia, there was 8% RAMP2, 10% RAMP3 and 11% CLR.

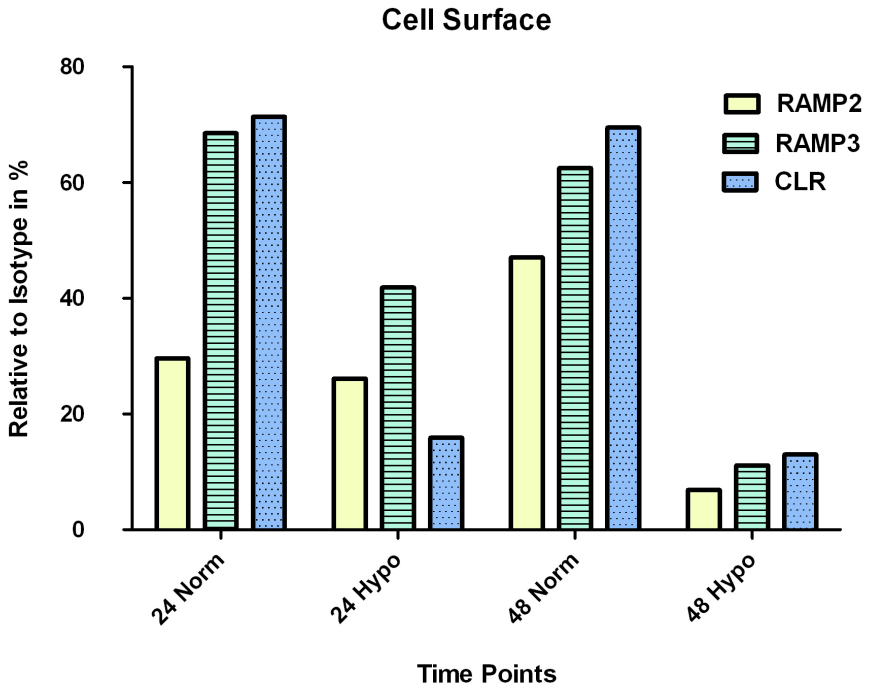

Figure 31: Cell Surface receptor expression in non - permeabilised breast cancer (MDA-MB-231) cells when exposed to hypoxia. The bars are drawn as a mean expression after being normalised to the respective control antibodies. n=1

2.4.4. Effect of hypoxia on PAM expression

ADM when being secreted is expressed as an immature peptide as previously mentioned. In order to render it active, the C terminal of ADM has to be amidated by an enzyme called PAM. Therefore, the effect of PAM expression under hypoxia was tested.

Figure 32 shows the western blotting result for glioblastoma cells probed for PAM expression. The size of PAM is 100kDa. It can be seen from the intensities of the bands that PAM expression was up-regulated at 24hrs hypoxia when compared to normoxia.

At 48hrs hypoxia, PAM expression was completely down-regulated when compared to normoxia at 48hrs.

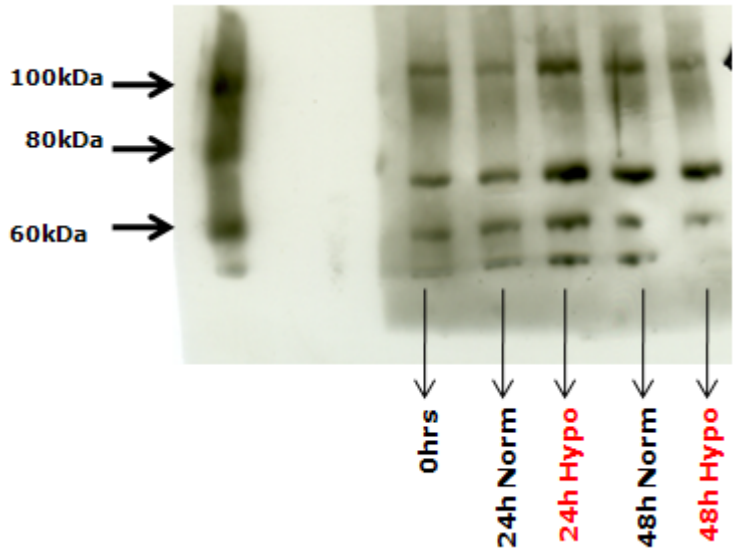

Figure 32: Western blotting for glioblastoma cells probed for PAM under hypoxia and normoxia. Bands belonging to 100kDa belong to PAM whereas bands between 50kDa to 70kDa are non-specific bands.

2.4.5. Akt Signalling under Hypoxia

In order to test if Akt signalling is turned on under hypoxia, western blotting was done for glioblastoma samples.

Figure 33 shows the western blotting for Akt and phosphorylated Akt as indication for Akt activation. It can be seen that under hypoxia Akt

phosphorylation is down-regulated when compared to normoxia at both 24 and 48hrs.

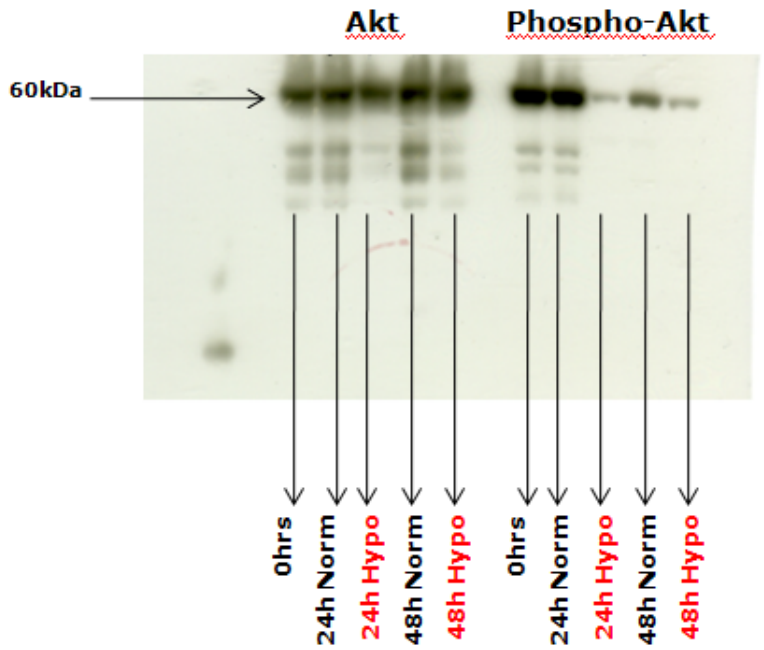

Figure 33: Western blotting for glioblastoma cells probed for Akt and phosphorylated Akt under hypoxia and normoxia. Blots were exposed for 15 mins and developed. n=1

Since ADM is up-regulated under hypoxia, the effect of ADM treatment was tested on Akt phosphorylation. Glioblastoma cells cultured at normal conditions were treated with 1μM ADM for 2hrs and whole cell lysate was used for western blotting.

Figure 34 shows the western blotting results for glioblastoma cells treated with ADM. Akt phosphorylation was down-regulated in ADM treated cells when compared to non-treated cells.

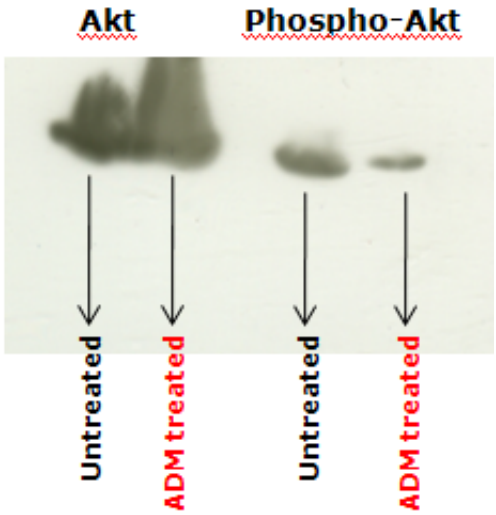

Figure 34: Western blotting for glioblastoma cells probed for Akt and phosphorylated Akt when treated with 1μM of ADM for 2hrs. Blots were exposed for 15mins and developed.

2.5. TECHNICAL DISCUSSION

This part of the project was aimed at determining ADM expression under hypoxia and to determine the receptor regulation under hypoxia.

2.5.1. ADM expression under hypoxia

ADM mRNA expression was significantly up-regulated under hypoxia.

In glioblastoma, breast, prostate and pancreatic cancer cell lines ADM mRNA expression was significantly higher under hypoxia when compared to normoxic counterparts at same time points. Various studies have shown that ADM expression is up-regulated under hypoxia *in vivo* and *in vitro* (Boudouresque et al. 2005; Cormier-Regard et al. 1998; Drimal et al. 2006; Garayoa et al. 2000; Hofbauer et al. 2000; Hwang et al. 2007; Iimuro et al. 2004; Jogi et al. 2004; Keleg et al. 2007; Kitamuro et al. 2000; Kitamuro et al. 2001; Krieg et al. ; Nakanishi et al. 2004; Nakayama et al. 1999; Nguyen and Claycomb 1999; Park et al. 2008; Serrano et al. 2008; Steiner 1975; Uemura et al. ; S. M. Wang and Yang 2009; B. C. Yang et al. 1996; L. Zhao et al. 1996). ADM contains 16 HREs in its gene, out of which 4 to 8 genes are known to contribute to ADM expression under hypoxia (Cormier-Regard et al. 1998). Various studies have shown that ADM is up-regulated 1.3 to 25 fold under hypoxia at different time points in different cell lines (Zudaire et al. 2003). One of the targets for HIF-1α is ADM (Cormier-Regard et al. 1998) that results in ADM production under hypoxia. Under hypoxia, expression of ADM is stabilised at both mRNA and protein levels (Zudaire et al. 2003).

Besides ADM mRNA regulation, studies have demonstrated that ADM protein expression is also up-regulated under hypoxia (Keleg et al. 2007; Zudaire et al. 2003). But I was unable to quantify the protein expression of ADM by western blotting using both whole cell lysate and cell culture media. Different concentrations of ADM antibody was used to detect ADM in both these samples. Figures 89 in appendix section is a representative western blotting result using whole cell lysate to probe for ADM. Molecular weight of ADM is 6kDa (Kitamura et al. 1993) and no matching bands were observed.

Next, ADM present in cell culture media was quantified using western blotting in glioblastoma cells cultured under normoxia and hypoxia. In figure 90 in appendix section, bands at ~6kDa were observed, which could be ADM, but this western blotting result was not reproducible for the same sample under the same experimental conditions. Therefore this result was not considered as a conclusive protein band for ADM. Various studies showing western blotting for ADM do not mention about any additional higher molecular weight at 50-60kDa bands as I have seen. Groups have reported ADM precursor bands at ~14kDa (Collantes et al. 2003; Jimenez et al. 1999).

Many studies have shown the expression of ADM under hypoxia. My specific aim was to determine which RAMP was specifically regulated under hypoxia so as to determine the RAMP involved in ADM actions under stress.

2.5.2. Receptor Expression under Hypoxia

CLR Expression under hypoxia

There was no significant increase in CLR mRNA expression in glioblastoma, prostate and breast cancer cell lines. Why CLR mRNA levels at normoxia are highly variable is unclear. In glioblastoma cells, CLR expression at 48hrs normoxia was significantly lower than 0hrs and 24hrs. In prostate cancer cells CLR expression at 24hrs normoxia was significantly higher than other samples at both normoxia and hypoxia. In breast cancer cells, 24hrs and 48hrs normoxia, the CLR expression was significantly lower than CLR expression at 0hrs. In U87, MDA-MB-436 and PC3 cell lines tested, CLR mRNA was significantly lower under hypoxia when compared to normoxia (figure 24 and figure 27).

Protein expression of CLR was quantified in U87 cells using western blotting. Similar to mRNA data, there was no significant difference in CLR expression under hypoxia when compared to hypoxia. Various studies have shown different CLR responses in cells under hypoxia both *in vitro* and *in vivo*. In human Coronary Artery Smooth Muscle cells (hCASMC), there was a 3.5 fold

increase in CLR protein levels under 1hr of hypoxia. The mRNA levels only increased after 3-6hrs of hypoxia, during which time the protein levels decreased (Cueille et al. 2005). When neuroblastoma cells were cultured under hypoxia, CLR was not detected (Kitamuro et al. 2001), even though there was an increase in ADM expression. In pancreatic cancer cells, there was 2.5 fold increase in CLR mRNA (Keleg et al. 2007). Rats exposed to chronic hypoxia resulted in increase in both mRNA and protein CLR levels *in vitro* and *in vivo* in both left and right ventricles. Therefore it is suggested that CLR protein levels that can be functionally active are regulated independent of transcription. CLR mRNA may have an increased half-life by various factors (Cueille et al. 2005).

RAMP2 and RAMP3 expression under hypoxia

RAMP2/3 protein expression under hypoxia was measured by flow cytometry. Glioblastoma cells produced more RAMP3 than RAMP2 at 0hrs although no RAMP3 could be detected at 24hrs normoxia. This could be due to poor sensitivity of the antibody at this particular time point. At 24hrs hypoxia, there was 4 times more RAMP3 than RAMP2 total protein expression.

At cell surface, there was a no difference between RAMP2 and RAMP3 expression at 24hrs normoxia. There was a 1.7 fold increase in RAMP3 cell surface expression at 24hrs hypoxia when compared to its normoxic counterpart, whereas there was no difference in RAMP2 and CLR expression at 24hrs between normoxia and hypoxia.

Although there are no results from various experimental repeats, due to reasons discussed later in this chapter, these are results from 10,000 cells. From this FACS data, it was seen that the glioblastoma cells up-regulate RAMP3 than RAMP2 when subjected to hypoxic stress.

Breast cancer cells (MDA-MB-231) when subjected to hypoxia, resulted in reduction in the expression of RAMP2, RAMP3 and CLR at both 24hrs and 48hrs

hypoxia. The total protein expression was down-regulated over time under hypoxia. RAMP2, RAMP3 and CLR produced similar levels of reduction under hypoxia. At 24hrs, 4 fold decrease in RAMP2, 3.3 fold decrease in RAMP3 and 5 fold decrease in CLR total protein expression. At 48hrs there was 5 fold, 26 fold and 19.5 fold decrease in RAMP2, RAMP3 and CLR protein expression respectively.

Cell surface expression of receptors showed similar decrease in expression under hypoxia. At 24hrs 1.2 fold, 1.7 fold and 5.1 fold decrease in RAMP2, RAMP3 and CLR expression respectively. At 48hrs, there was 6.1 fold, 6.2 fold and 6.3 fold reduction in RAMP2, RAMP3 and CLR expression respectively.

In vitro hypoxia studies using human neuroblastoma cells resulted in 46% decrease in RAMP2 mRNA although there was an increase in ADM levels. RAMP3 on the other hand was not determined (Kitamuro et al. 2001). In hCASMC, an increase in RAMP2 mRNA was observed after 4hrs of hypoxia, around the same time when CLR mRNA levels had increased (Cueille et al. 2005). RAMP3 could not be measured due to its low level of expression (Cueille et al. 2005). Lung endothelial microvascular cells when subjected to 16hrs of hypoxia resulted in elevation of ADM and CLR mRNAs but no changes in both RAMP2 and RAMP3 mRNAs (Nikitenko et al. 2003). In chronic heart failure rat model, there was an increase in RAMP3 mRNA and protein levels which could be due to hypoxia in this model (Cueille et al. 2002).

In vivo studies on hypoxic rat lungs resulted in increase in RAMP3 mRNA with no observable changes in CLR and RAMP2 mRNA (Qing et al. 2001). Increase in RAMP2 and RAMP3 proteins were observed in both ventricles of rats exposed to hypobaric hypoxia (barometric pressure = 505hPa; inspired partial oxygen pressure = 106hPa). The mRNA levels on the other hand showed that RAMP3 expression was high at day 1 and RAMP2 was elevated from day 14 of exposure (Cueille et al. 2005). Other studies have shown an increase in ADM and CLR mRNA, but a 7.3 fold decrease in RAMP3 mRNA and no changes in RAMP2 mRNA. Protein levels on the other hand showed prominent staining for RAMP2

but RAMP3 was not detected (Keleg et al. 2007); this could mean that the mRNA levels for RAMPs are not always the measure for their protein levels.

From my results and from other studies it can be understood that RAMP3 mRNA is expressed at low levels in cell lines and are not measured. RAMP2 mRNA levels could be measured in other studies, using primers designed by individual groups.

From *in vivo* hypoxic studies it is learnt that RAMP3 responds first after which RAMP2 levels are elevated (Cueille et al. 2005). This could mean that RAMP3 is up-regulated under stress to convey ADM mediated signalling to aide cell survival. Once cell survival is stabilised, RAMP2 which seems to be the preferred receptor partner for ADM is then up-regulated to mediate its functions. RAMP3 could have other receptor partners for hypoxia response proteins and could be up-regulated first hand under hypoxia.

The reason why RAMP3 could be up-regulated under pathophysiological conditions may be due to the presence of a PDZ motif which is not present in other RAMPs. PDZ motif which binds to NHERF and NSF is responsible for receptor trafficking and internalisation (Bomberger et al. 2005b; Bomberger et al. 2005a). Studies on RAMP knockouts have shown that the deletion of RAMP3 gene does not have an impact on the expression of RAMP2 and CLR (R. Dackor et al. 2007), showing that RAMP2-CLR is necessary for the basal activity of ADM while under stress, RAMP3-CLR is regulated.

Studies have shown that Platelet Derived Growth Factor (PDGF) stabilises RAMP3 mRNA and also increases its half-life from 66.5mins to 331.6mins (Nowak et al. 2002). This maybe the reason why RAMP3 mRNA remains at low levels since it is rendered stable and may continue expressing the protein. Studies have shown that HIF-1α regulates the expression of PDGF in glioblastoma cells (Yoshida et al. 2006), endothelial cells (Kourembanas et al. 1990), glomerular capillary endothelial and mesangial cells (E. Eng et al. 2005), breast cancer (Bos et al. 2005), neuronal cells (S. X. Zhang et al. 2003), lungs,

kidneys, heart and liver of hypobaric exposed rats (Bucher et al. 1996) and human pulmonary arterial smooth muscle cells (hPASMC) (ten Freyhaus et al.). PDGF is over-expressed in many cancers induced by hypoxia (P. Guo et al. 2003; Le et al. 2004) and contributes to angiogenesis thereby increasing tumourigenecity (Carmeliet and Jain 2000).

2.5.3. PAM expression under hypoxia

Secreted ADM is expressed as an immature peptide as previously described. In order to render it active, the C terminal of ADM has to be amidated by an enzyme called PAM. In order to see if the ADM that is being over-expressed under hypoxia is functionally active, since ~85% of plasma ADM is iADM and requires amidation to make it active. Therefore the aim was to test the effect of hypoxia on PAM using western blotting to measure the ratio between mADM to iADM.

In the western blotting, for PAM expression is glioblastoma cells under hypoxia PAM (~100kDa) was up-regulated at 24hrs hypoxia and almost disappeared at 48hrs hypoxia. Although the no house-keeping gene was probed for in these blots, the conclusions drawn are merely from the appearance of the blots. Other bands ranging from 50kDa to 70kDa could belong to PHM and PAL domains of PAM (Eipper et al. 1992; Sharma et al. 2009). It has been suggested that in different cell types PAM undergoes specific proteolytic processing (Eipper et al. 1992).

PAM consists of two domains that are required for its functional activity of amidating peptides. Peptidyl glycine α-hydroxylating monooxygenase (PHM) domain is located at the N-terminal of PAM and at the mid region is located the peptidyl-α-hydroglycine α-amidating lysase (PAL) (Perkins et al. 1990). PAM requires O_2 to amidate its target peptides (Sharma et al. 2009). Since ADM is elicited under hypoxia, an increase in PAM expression could mean that the ADM is biologically active.

Studies have reported that intermittent hypoxia increases the activity of PAM catalysed by PHM domain. Continuous hypoxia did not result in increase in PAM activity (Sharma et al. 2009).

PAM that is up-regulated at 24hrs hypoxia could render ADM active to aide cell survival. Since PAM is possibly down-regulated at 48hrs, it maybe that ADM at 48hrs is not functionally active or functionally active ADM at 24hrs could have an increased half-life to help in cell survival. Studies have shown that intermittent hypoxia elevates the expression of PAM than continuous hypoxia (Sharma et al. 2009).

2.5.4. Akt Signalling under hypoxia

Akt phosphorylation was measured in glioblastoma cells under hypoxia. At both 24hrs and 48hrs a very evident reduction in Akt phosphorylation was noticed. Since ADM expression was up-regulated under hypoxia, I wanted to determine Akt phosphorylation.

Akt is activated by binding of phospholipid and when phosphorylated at Thr308 in the activation loop by PDK1 (Alessi et al. 1996) and/or phosphorylation at Ser473 at the C terminus (Nielsen et al. 1990; Sarbassov et al. 2005). Various studies have shown that under hypoxia Akt is phosphorylated and contributes to cell survival and provide resistance to apoptosis (W. Kim et al. 2003a; Krishnaswamy et al. 2006). ADM has been shown to activate Akt by enabling Akt phosphorylation (W. Kim et al. 2002; W. Kim et al. 2003a; J. Y. Kim et al. 2006; Okumura et al. 2004; Park et al. 2008; Yin et al. 2004). In hepatocellular carcinoma cells, hypoxia induced ADM has shown to stimulate cell proliferation by activation of Akt (Park et al. 2008). Akt remained in activated state until 60mins and the level of phosphorylated Akt dropped at 120mins (Park et al. 2008). ADM has shown to protect cells from hypoxia by activating γ-glutamate cysteine ligase (γ-GCL) resulting in up-regulation of glutathione (J. Y. Kim et al. 2006). Glutathione is required in cellular redox balance (Arrigo 1999;

Meister and Anderson 1983). γ-GCL is activated by PI-3K/Akt pathway (J. Y. Kim et al. 2006).

In mannitol induced apoptosis which is a therapy used in brain edema and ischemic brain swelling, ADM produced an anti-apoptotic effect mediated by PI-3K/Akt phosphorylation (W. Kim et al. 2002).

Although Akt phosphorylation was shown to be down-regulated in my samples, studies have shown that Akt phosphorylation is an instant reaction which usually trails off at 24hrs (Ardyanto et al. 2006; Grymer et al. 1991; W. Kim et al. 2003a; S. M. Lee et al. 2006).

In order to test if excessive ADM resulted in down-regulation of Akt phosphorylation, glioblastoma cells were treated with 1μM ADM (Park et al. 2008). Glioblastoma cells treated with ADM peptide for 2hrs down-regulated Akt phosphorylation. This result was similar to the result obtained in cells cultured under hypoxia. This result correlates with results obtained from other studies where Akt phosphorylation had peaked at 30mins and trailed off at 2hrs (Park et al. 2008).

Akt activation under hypoxia is an event that occurs instantly and this up-regulation is sufficient to trigger events that enable cells to survive. Therefore the time points that I have chosen would result in elevation of ADM, but its downstream signalling might not be active at 24hrs and 48hrs hypoxia.

2.5.5. Validation and Optimisation

Induction of Hypoxia

$CoCl_2$ is a widely used hypoxia mimetic agent that is used in many hypoxic studies. $CoCl_2$ does not induce hypoxia per se, but mimics the hypoxic situation. One mechanism of action of how it mimics hypoxia is that $CoCl_2$ stabilises HIF-1α by inhibiting PHD enzymes that degrade HIF-1α under normoxic conditions

(Vengellur and LaPres 2004). Another mechanism is by changing the redox state of heme proteins (Gleadle et al. 1995).

HIF-1α expression was taken as a measure to determine if the cells were undergoing hypoxia. Therefore, when U87 cells exposed to 300μM $CoCl_2$ did not induce an increase in HIF-1α mRNA (figure 80 in appendix), Hoechst staining was carried out to determine if 300μM $CoCl_2$ induced cell death due to toxicity. Since prolonged exposure or overdose of $CoCl_2$ results in cobalt induced toxicity (Vengellur and LaPres 2004). Since $CoCl_2$ stabilises HIF-1α, sustained HIF-1α expression results in signalling of BNIP3 and NIX death genes. BNIP3 leads to increase in chromatin condensation. Therefore BNIP3 causes activation of caspase-3, an early marker for apoptosis (Vengellur and LaPres 2004). Therefore as seen in figure 81 in appendix, the cell death index is higher for cells treated with 300μM $CoCl_2$. At that time, it was concluded that cell death was the reason why there was no increase in HIF-1α mRNA expression. It was noted during the experiment that dead cells belonging to 7h-48h hypoxia had got washed away during the wash step in Hoechst staining. This might be the reason why the apoptotic index went down from 7hrs onwards (figure 81).

Therefore three doses of $CoCl_2$ were used to determine if hypoxia was induced (figure 82). Since there was no increase in HIF-1α expression, hypoxia was then induced using an incubator containing ~0.1% O_2.

A hypoxic incubator uses N_2 to control the O_2 in the incubator. Although using a hypoxic incubator is the closest to mimic real time hypoxic situations, the actual onset of hypoxia in cells cannot be determined (Millonig et al. 2009). An experimental problem I faced with using hypoxic incubator is that every time the incubator is opened, the O_2 levels go up and it takes a while (how long it takes exactly is not known) to stabilise the O_2 levels to 0.1%. Therefore, 24 and 48hrs were chosen to be the time points for this experiment.

U87 and MDA-MB-436 cell lines were incubated in hypoxic incubators and again there was no HIF-1α mRNA response to hypoxia (figure 83 in appendix).

As the time points for inducing hypoxia were 24 and 48hrs, HIF-1α mRNA response at 2hrs when exposed to ~0.1% O_2 was tested (figure 84 in appendix). As there was no increase in HIF-1α mRNA, a different approach to induce hypoxia was carried out.

Hypoxia induced by using hypoxic media did not result in increase in HIF-1α mRNA (figure 86 in appendix), although the cells containing hypoxic media was undergoing some kind of stress (figure 85 in appendix).

At this stage, literature search revealed that HIF-1α mRNA remains unaltered under hypoxia (Huang et al. 1996; Kallio et al. 1997; Salceda and Caro 1997). Therefore protein expression of HIF-1α was determined in U87 cells when exposed to 0.1% O_2. Cells expressed 34% and 92% more HIF-1α at 24hrs and 48hrs hypoxia respectively, when compared to their normoxic controls (figure 22). Since cells were responding to hypoxia by up-regulating HIF-1α, regulation of ADM and its receptors were studied.

qPCR

Firstly taqman assays were tested on positive controls. A standard curve using plasmid DNA as template was done for RAMP2, RAMP3, CLR and ADM was carried out. As seen in figure 87 in appendix, concentrations ranging from 1pg to 1μg in $\log_{10}$ increases were used. Once the accuracy of taqman assays was confirmed, ADM expression in different cancer cell lines was carried out to test the efficiency of taqman assays on cell lines.

ADM Protein Expression

ADM protein expression could not be determined by western blotting in both whole cell lysate and in cell culture media. Despite repeats in western blotting, a 6kDa band could not be detected in whole cell lysate. Western blotting on cell culture media contained various non-specific bands.

RAMP2 and RAMP3 protein expression

Western blotting for RAMP2 and RAMP3 on rat brain sample as shown in supplementary figures 2.4.3.2.2 and 2.4.3.2.3 showed bands that corresponds to homodimers and heterodimers. But using the same antibodies on glioblastoma whole cell lysate showed multiple non-specific bands. Despite changing antibody concentrations and protein extraction methods, each western blotting showed multiple bands or non-specific bands that cannot be reproduced or construed as specific bands for RAMP2 or RAMP3 (supplementary figures 2.4.3.2.4 and 2.4.3.2.5). Therefore the same antibodies were treated on fixed cells for flow cytometry.

Flow Cytometry

RAMP2 and RAMP3 protein expression was quantified on fixed cells by flow cytometry. Glioblastoma cells were used to quantify the expression and Cos-7 cells were taken as negative control. The antibody concentrations used were as previously described (Granholm et al. 2008). Control antibody was used to exclude any non-specific background. From supplementary figure 2.4.3.2.6 in appendix it can be seen that there was very little background in Cos-7 cells and over 80% expression of RAMP2 and RAMP3 and over 60% expression of CLR. These were tested on fixed permeabilised cells. Figures 91 and 92 in appendix show the histograms of receptors in Cos-7 and Glioblastoma cells respectively.

Figures 93 to 97 in appendix, show the histograms of total and cell surface expression of receptors in glioblastoma cells under normoxia and hypoxia. Figures 98 and 99 in appendix show the histograms of receptors in breast cancer cells under normoxia and hypoxia.

Flow cytomtery was repeated thrice for each cell line, although after first time for each cell line, there was high control antibody background. Despite several rounds of washing, reducing antibody concentrations, the control antibody background could not be reduced. Therefore the flow cytometry results

taken for calculating receptor expression belong to n=1 that accounts for 10,000 cells. It was noted that the control antibody background was dependent on cell type.

2.5.6 Conclusion

Collectively, the hypoxia data suggest that ADM is up-regulated under hypoxia. The receptor for ADM in breast cancer cells were down-regulated. And in glioblastoma cells at 24hrs hypoxia, cells produced more RAMP3 than RAMP2. These results show that the expressions of RAMPs are cell type and microenvironment dependent. Although my results show a decrease in Akt signalling, it cannot be concluded that ADM does not activate this signalling pathway, as Akt activation as a response to hypoxia is instantaneous.

CHAPTER III: EFFECT OF ADM OVER-EXPRESSION ON TUMOUR PROGRESSION

3.1. HYPOTHESIS

Hypothesis

Over-Expression of ADM increases tumour progression and over-expresses receptor expression.

The objectives are to:

1. Determine the effect of ADM over-expression on cell proliferation, migration and invasion

2. Determine the regulation of ADM receptors in cells over-expressing ADM

3. Determine regulation of cells over-expressing ADM receptors

4. Determine the bone homing features in cells over-expressing ADM

3.2. INTRODUCTION

3.2.1. Background

Adrenomedullin (ADM) is a pluripotent hormone composed of a 52 amino acid peptide and carries structural similarity with the calcitonin/CGRP gene family. ADM is secreted by various malignant cells such as breast, lung, and prostate. The hormone is known to display its physiological effects by paracrine, autocrine or endocrine mechanisms. Along with mediating pathological conditions like cardiovascular disorders, renal problems, sepsis and inflammation, ADM plays an important role in the progression of cancer and metastasis. Over-expression of ADM in different tumours aggravates the molecular and physiological features of malignant cells. ADM hormone is pro-proproliferative, anti-apoptotic, pro-angiogenic, and induces new bone formation (Zudaire et al. 2003).

This chapter was aimed at studying the role of ADM in tumour progression. Elevated levels of ADM are a characteristic feature of tumour cells (Bunton et al. 2004). ADM contributes to cancer cells lymph node metastasis in breast (Oehler et al. 2003), pancreatic (Ramachandran et al. 2007) and ovarian cancers (Deng et al. 2012). Tumour metastasis is known to be the primary reason for cancer fatalities in about >90% of cancers (Gupta and Massague 2006; Jemal et al. 2010; Steeg 2006). Metastasis of tumour cells involves a complex signalling cascade that is controlled by inhibitory growth factors, apoptotic factors, hypoxia and extracellular matrix in tumour microenvironment (Geiger and Peeper 2009). In order to metastasise successfully, tumour cells undergo various stages that are summarised in figure 35.

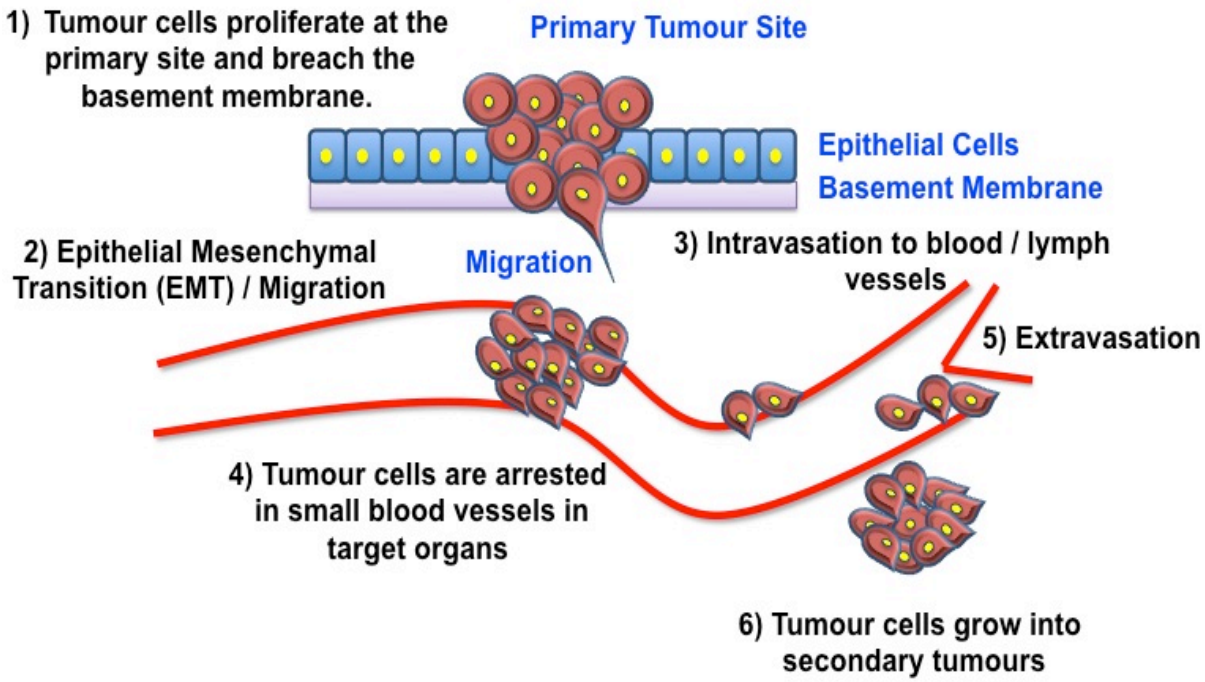

Figure 35: Metastastic Cascade – 1) Tumour cells at the site of the primary tumour proliferate and dissociate by invading the basement membrane. 2) Tumour cells acquire spindle shaped morphology as that of mesenchymal cells that enables them to migrate. 3) This process is followed by invasion of tumour cells into blood/lymph vessels. 4) After circulation in blood vessels, tumour cells are arrested in small blood vessels in target organ and 5) extravasate and 6) grow to a secondary tumour. Picture adapted from Geiger and Peeper, 2009.

Tumour metastasis cascade briefly involves the following steps (Fidler 2003; Valastyan and Weinberg 2011).

1. Invasion and migration of cells into extracellular matrix
2. Intravasate into blood vessels
3. Transportation through the vasculature
4. Arrest in organs due to small vessels
5. Extravasate into distant tissues
6. Survive in metastasized environment by rapid proliferation

Since ADM is known to contribute to tumour progression, effect of ADM in cell proliferation, migration and invasion was tested in this chapter. An invasive cancer cell line (MDA-MB-231) was used to test the effects of ADM over-expression on bone metastasis *in vivo*.

3.2.2. Tumour Metastasis

A "seed-to-soil" hypothesis by Paget in 1889 suggested thar tumour cells were like seeds and when they encounter a tissue with appropriate growth promoting factors, which is termed as soil, the tumour cells get lodged in the tissue and start growing. There seems to be an interaction between tumour cells and distal organs. For example, when prostate and breast cancer metastasize to bone, there seems to be a communication between tumour cells, osteoblasts and osteoclasts. Figure 36 shows the metastatic cascade where primary breast or prostate cancer cells migrate and invade into the tumour microenvironment via vasculature. The communication seems to result in bone destruction and release of various tumour promoting factors (Mundy 2002). In bone microenvironment a pre-metastatic niche is established that enables the tumour cells to lodge. The tumour cells then trigger a vicious cycle to enable them to grow by interacting with bone cells (Palmer et al. 2011; Peinado et al. 2011).

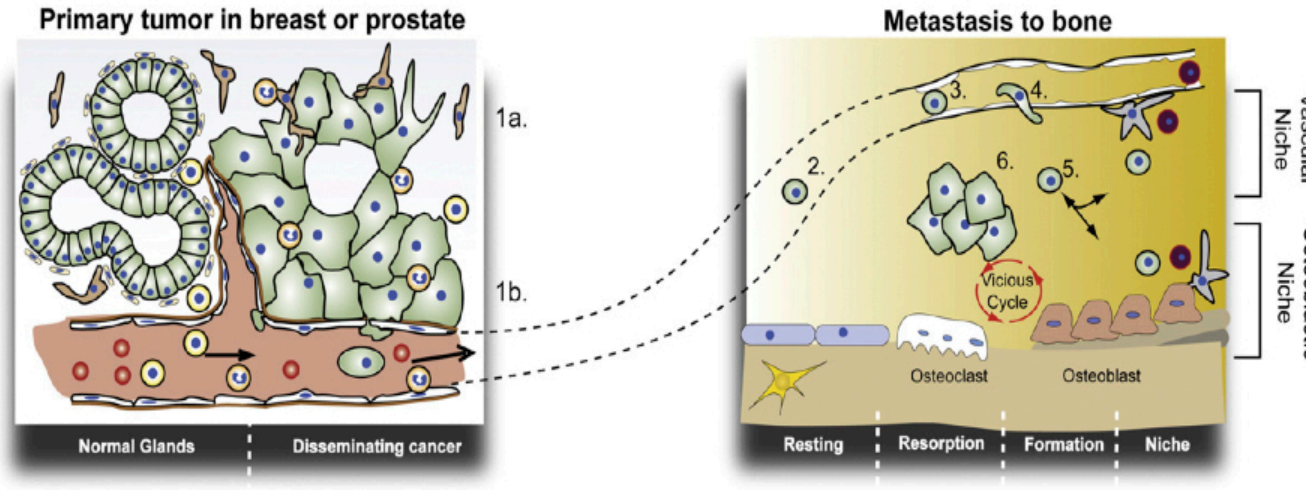

Figure 36: Schematic representation of bone metastasis from primary tumour. It shows the tumour cells migrating and invading into the bone microenvironment via vasculature. A niche is established in the bone where the tumour cells lodge themselves. The tumour cells then trigger a vicious cycle to enable them to grow by interacting with the bone cells. Picture taken from Palmer *et al,* 2011.

Primary tumours lack the properties of a metastatic cell. These properties are acquired when epithelial derived cancers undergo Epithelial-Mesenchymal Transition (EMT). During EMT, there is change in the cytoskeletal proteins and various transcription factors that enable invasion and migration (Feinberg 2007; Kalluri and Weinberg 2009). Absence of EMT results in invasive tumour cells migrating as clusters or sheets. This intracellular adhesion is brought about by Cadherins and other cell-cell adhesion molecules (Bates et al. 2000; Friedl and Wolf 2003). One of the characteristic features of tumour cells during the transition is the loss of E-Cadherin which is an important cell-cell adhesion molecule (Berx and van Roy 2009; Cavallaro and Christofori 2004). While E-Cadherin is suppressed, other adhesion molecules, example N-Cadherin that is associated with cell migration, is up-regulated (Kalluri and Weinberg 2009). Since one of the initial step in metastasis is migration, inhibiting the molecular determinants that cause cell motility has been suggested to be a viable therapeutic target (Palmer et al. 2011). Integrins, CD44, Immunoglobulin – domain Cell Adhesion Molecules (IgCAMs) and various other adhesion and

signalling molecules play a crucial role in cell migration and invasion (Cavallaro and Christofori 2004; W. Guo and Giancotti 2004; Ponta et al. 2003; G. F. Weber 2008).

For a cell to migrate, the cell membrane protrudes as a result of both polymerisation and depolymerisation of actin (Condeelis and Segall 2003). The membrane protrusions alongside cofilin pathway result in cell migration. The cofilin pathway consists of adhesion of ECM due to cell contraction mediated by integrin, FAK containing complexes and actin-myosin2 complexes (Ghosh et al. 2004). For example, in melanoma, a scaffolding protein called NEDD9 modulates RAC1 activity resulting in cell invasion (Sanz-Moreno et al. 2008).

Intravasation is when tumour cells enter blood vessels. The tumour cells align towards the vessels and migrate towards it (C. Y. Li et al. 2000; Sahai 2007; J. B. Wyckoff et al. 2000). Tumour Associated Macrophages (TAMs) help the tumour cells intravasate via an interaction between a CSF1 receptor on the macrophages and an EGFR on the tumour cells, this is called the paracrine loop (Lin et al. 2001; J. Wyckoff et al. 2004; J. B. Wyckoff et al. 2007).

In the previous chapter, it was seen that hypoxia promotes angiogenesis resulting in an invasive and metastatic phenotype (Sullivan and Graham 2007). Angiogenesis plays an important part during tumour cell migration and invasion, with help from bone marrow derived vascular and hematopoietic progenitor cells (Rafii et al. 2002). HIF-1α and HIF-2α contribute to cell migration and invasion. For example, in Renal Cell Carcinoma (RCC), *in vitro* tests show HIF-1α promotes CXCR4 receptor activity resulting in cell migration. It has been known that high level of CXCR4 is correlated with poor prognosis in patients with RCC (Staller et al. 2003). HIF-1α activates FAK resulting in accumulation of lysyl oxidase (LOX) which promotes EMT (Higgins et al. 2007). HIF-1α also activates various factors that promote EMT, such as snail, ZEB1, ZEB2 and twist in head, neck and breast cancers (Evans et al. 2007; Imai et al. 2003; Krishnamachary et al. 2006; M. H. Yang et al. 2008).

Besides blood vessels, tumour cells also intravasate into the lymphatic system (Cao 2005; Stacker et al. 2002). Signalling molecules promoting tumour

hemangiogenesis also contribute to lymphangiogensis, example VEGFR3 (Kopfstein et al. 2007; Mandriota et al. 2001).

Certain types of tumours which have been studied extensively usually metastasize to the same organs. For example, breast cancer usually leads to metastasis to bone, lung, liver and brain. This ability of these tumours is called metastatic tropism (Fidler 2003). Figure 37 shows the metastatic tropism of six different cancers.

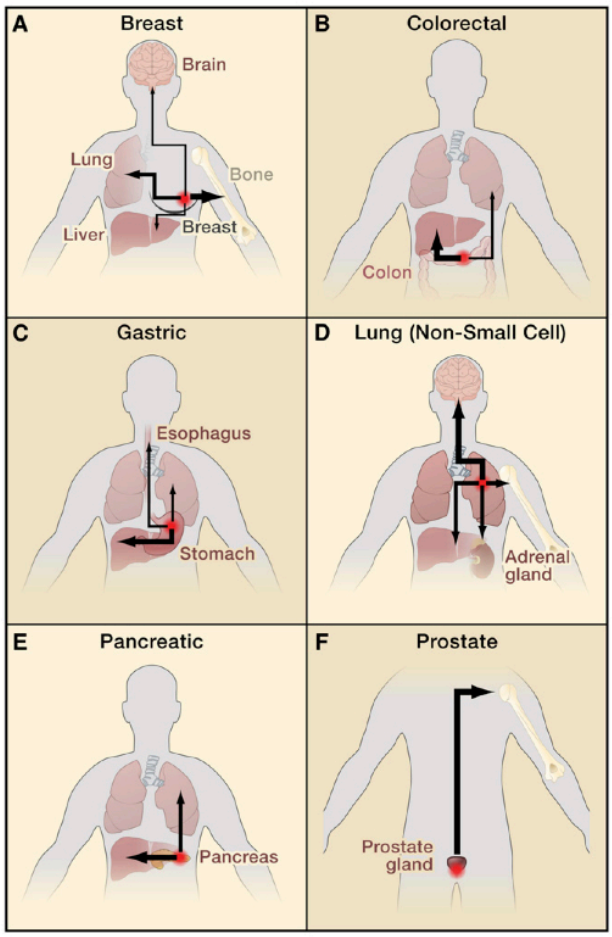

Figure 37: Metastatic Tropism of various cancers. A) The common metastatic sites for breast cancer are lung, bone and liver. B) Colorectal cancer usually metastasises to liver and lungs. C) Gastric cancer metastasises to esophagus, lungs and stomach. D) Non-small cell lung cancer metastasis to lungs, brain and adrenal gland. E) Pancreatic cancer metastasises to liver and lungs. F) Prostate cancer metastasises to bone. Picture taken from Valastyan & Weinberg, 2011.

One of the reasons why tumour cells exhibit metastatic tropism, could be due to the layout of the vasculature. For example, metastasis of colorectal carcinoma into liver. This could be because the portal vein drains the circulation into liver (Gupta and Massague 2006). Besides metastatic tropism, tumour cells have the ability to be passed into arteriovenous shunts thereby enabling them to metastasize into farther organ sites (Valastyan and Weinberg 2011).

3.2.3. ADM and Tumour Metastasis

Results from different range of studies which used many different models have strongly implied that ADM has an important role in tumour growth and metastasis. Clinical data gathered over years of research confirms that ADM is over-expressed in cancer patients. For example, Ehlenz *et al*, (Ehlenz et al. 1997) found that the patients with colon or lung cancer have higher circulating levels of ADM as compared to healthy control subjects. The ovarian tumours observed by Hata *et al* in 2000 (Hata et al. 2000) showed increased expression of ADM mRNA which was statistically significant and correlated with poor prognosis in ovarian cancer patients. The similar effect of ADM over-expression was also seen in prostate cancer where elevated ADM mRNA was associated with high Gleason scores (Rocchi et al. 2001). Udono *et al* (Udono et al. 2000) found that statistically high levels of ADM mRNA is found in intraocular and orbital tumours and high levels of ADM is significantly related to the lesions in eye with cancer. When patients of pituitary tumour were operated for tumour removal, ADM levels drastically reduced in the patients with Cushing's syndrome due to pituitary adenoma (Letizia et al. 2000). This finding suggested that ADM is also over-expressed by pituitary tumours. In patients with leiomyomas, high ADM expression is associated with increased vascular density (Hague et al. 2000).

To understand the proliferative effect of ADM, Andreis *et al* in 2000 (Andreis et al. 2000) investigated rat adrenal cortex *in vivo* using an *in situ* perfusion technique. It was found that during the 180min perfusion cycle, ADM infusion concentration dependently increased the mitotic index and [3H] thymidine incorporation into DNA in the zona glomerulosa (ZG). Interestingly, it

was found that the agents like adenylate cyclase inhibitor SQ-22536 (10^{-4} M), the cAMP blocker Rp-cAMP-S (10^{-3} M), and the protein kinase A inhibitor H-89 (10^{-5} M), which inhibited cAMP in reduced or inhibited ZG proliferogenic effect of 10^{-9} M angiotensin II. The overall findings identified that ADM is capable of promoting cell growth in both normal and malignant cells. Growth promoting effect of ADM is based on Tyrosin kinase/Mitogen activated protein kinase (TK/MAPK) and Akt mechanism. Insulin like growth factor 1 receptor (IGFR1) and protein kinase p42/44 MAPK are the main players of tumour progression by ADM. Prototypic signalling by MAPK induces cyclin D mediated cell cycle transition G0 to G1 and G2 to M and thus promotes cell proliferation (Andreis et al. 2000). ADM being an angiogenic peptide exhibits its activity by phosphorylation of Akt (W. Kim et al. 2003b). Akt phosphorylation in endothelial cells is essential in angiogenesis (Dimmeler and Zeiher 2000; T. Takahashi et al. 1999; L. W. Wu et al. 2000). Akt phosphorylation is a measure of quantifying PI-3K activity (Goel et al. 2004). Activation of Akt has been demonstrated to be important in cell survival (anti-apoptosis) (Fujio et al. 2000). ADM has known to contribute to angiogenesis by activation of Akt (Hinson et al. 2000; Iwase et al. 2005).

A study on a ovarian cell line revealed that addition of synthetic ADM to ECV ovarian tumour cells lead to a dose dependent cell migration through membrane. The study discussed that the projection on the cancerous cells are focus for ADM over-expression and also responsible for an active plasma membrane. The study also recognized elevated levels of gelsolin due to ADM over-expression. Gelsolin protein vigorously participates in cytoskeletal restructuring that underlies morphological changes and lead to reduction in cell adhesion by reducing the cell adhesion molecules like Fak. All of these data, together with the fact that ADM increases tumour cell motility, suggest that tumour cells that express high levels of ADM may be more likely to be involved in metastasis (Martinez et al. 2002).

ADM is known to be involved in the human implantation process via regulating trophoblast proliferation and differentiation. Studies have reported

that ADM, CLR and RAMPs-were greatly expressed by human choriocarcinoma Jar cells and first-trimester cytotrophoblast HTR-8/SV neo cells. It was observed that ADM not only stimulates both JAr and HTR-8/SV neo cell proliferation, but increased gelatinolytic activity and reduction in plasminogen activator inhibitor mRNA expression, increased invasion by the Jar and neo cells thus suggesting invasive properties of ADM (X. Zhang et al. 2005). A study by Keleg et al. (2007) found that in pancreatic cancer patients, ADM was induced by hypoxia and significantly augmented invasiveness in 3/5 human pancreatic cancer cells. Furthermore, the study indicated that blocking of ADM receptor CLR decreased invasiveness in 4/5 human pancreatic cancer cells. The study concluded that due to its characteristic of elevating invasiveness in pancreatic cancer cell lines, ADM over-expression might also influence angiogenesis.

ADM has been reported to cause up-regulation of various receptors. ADM over-expression resulted in up-regulation of M_2 expression on P19-derived cardiomyocytes because of mechanism involving L1/G10D receptor but not CLR/RAMPs receptor complexes (Buys et al. 2003). A different study identified that ADM levels increased in volume overload-induced cardiac hypertrophy rats. The elevated levels of ADM further increased gene expressions of ADM, CLR, RAMP2 and RAMP3 (+27%, +76%, +108% and +131%, respectively) in the rats (Yoshihara et al. 2005). The findings of both these studies together suggested that ADM over-expression has a significant effect on up-regulation of ADM receptors. Similar results were observed by Schwarz *et al* (Schwarz et al. 2006) while observing the effect of ADM over-expression on microvascular endothelial cells. The in-depth study by Schwarz *et al* noticed that within 5-45 minutes of ADM treatment, cAMP levels increased in the cells followed by increased extracellular signal-regulated kinase 1/2 phosphorylation. The entire cascade leads to up-regulation of peptide and mRNA expression for VEGF, RAP2 and CLR, thus increasing receptor population.

3.2.4. ADM and Bone Metastasis

An important physiological effect of ADM which may lead to bone metastasis in various cancers is its efficiency to cause osteoblast proliferation. A study by

Cornish *et al* (Cornish et al. 2001), assessed the effect of systemically administered ADM in male mice. It was found that ADM increased the indices of osteoblast activity, osteoblast and osteoid perimeter in tibia. A 21% increase in cortical width and a 45% increase in trabecular bone volume were observed along with highly significant increase in bone strength. There was also a significant increase in the width of the epiphyseal growth plate. It has been reported that over-expression of ADM stimulated bone formation in a mouse calvarial assay, increased bone metastasis and osteoblastic response in prostate cancer cell line while reduced ADM expression decreased bone metastasis in lung cancer model (Guise 2010). Many patients with cancer develop bone cancer on a longer run. Bone metastasis causes extreme bone pain, skeletal fractures, nerve compression, and hypercalcemia (Siclari et al. 2006). Once the tumour cell enters bone, they secrete ADM inside the bone cells and induce new bone formation. Dose dependent action of ADM stimulates fresh bone formation at picomolar concentration. The hormone exhibits this function by stimulating adenyl cyclase activity after binding to CLR+RAMP2 or CLR+RAMP3. Although, ADM stimulates osteoblast proliferation, it does not induce bone matrix protein mRNA expression. ADM has no direct action on bone sialoprotein, type I collagen, osteocalcin and osteopontin mRNA expression. Furthermore, ADM also lead to an inflammatory cascade in the affected bone as it increases IL-6 mRNA expression in the primary osteoblast (Cornish et al. 2003).

Aim

All these findings confirm ADM as a major regulator of carcinogenesis-tumour progression. The present study is focused on studying the action of ADM on bone metastasis. An invasive cancer line was used for the purpose of the study and the cells were studied for the effects of ADM over-expression. The cell line was observed for changes in cell migration, proliferation, cell invasion, regulation of ADM receptors, and bone homing features.

3.3. METHODS

Materials and Recipes for solutions used are given in Chapter 6, Appendix.

3.3.1. ADM over-expression (*in vitro)*

ADM cDNA construct was obtained from Genecopoeia. ADM cDNA arrived as an insert in pOTB7 vector in filter paper discs. The filter disc was placed in a 1.5ml microcentrifuge tube and 50µl of 1x TE Buffer (pH 8.0) was added and incubated for 30-60mins at room temperature.

pOTB7 vector containing ADM was transformed into E.Coli and cultured for use in downstream applications.

3.3.1.1. Transformation

Top10 E.Coli Chemically Competent cells were thawed on ice and 5-10µl of vector mixture was added and incubated on ice for 30mins. Cells were heat shocked for 30secs at exactly 42°C and immediately transferred to ice. 300µl of room temperature SOC media was added to the cells and incubated for 1hr at 37°C in a shaking incubator at ~225rpm. The transformation mixture was plated out onto pre-warmed agar plates containing the appropriate antibiotic as shown in table 3. The plate was incubated at 37°C overnight for 14-18hrs. A single bacterial colony was picked for inoculating to extract plasmid cDNA for downstream analysis.

Plasmid	Antibiotic	Dose
pOTB7	Chloramphenicol	25µg/ml
pBUDCE4.1	Zeocin	50µg/ml
pcDNA3.1	Ampicillin	100µg/ml
pReceiverM61 (IRES-eGFP)		

Table 3: Table shows the different plasmids used in ADM over-expression studies, their appropriate antibiotics and concentrations.

3.3.1.2. Bacterial Culture

A single bacterial colony was picked for inoculating in LB Broth media containing the appropriate antibiotic. Bacteria were cultured in a shaking incubator at 37°C at ~225rpm overnight for 14-18hrs. Plasmid DNA was extracted following the protocol as described below.

3.3.1.3. Extraction of Plasmid DNA

Depending upon the culture volume, plasmid DNA was extracted using either mini- or midi-prep plasmid DNA extraction kit from Promega.

Bacterial cultures were centrifuged for 10,000xg for 10mins and the pellets were resuspended thoroughly in Cell Resuspension solution. Cells were lysed using Cell Lysis Solution for 3mins at room temperature. Cell Lysis was stopped by adding neutralization solution and incubated for 3-5mins for the white flocculent precipitate to form. Plasmid DNA was separated from rest of the cellular debris by passing through clearing columns by centrifuging at 1500xg for 5mins. The resultant DNA mixture was passed through a binding column to ensure DNA binding. The columns were washed to remove endotoxin, protein, RNA and endonucleases. DNA was eluted in nuclease free water and quantified.

3.3.1.4. DNA Quantification

DNA was quantified by diluting it 1:25 in nuclease free water in a disposable cuvette and quantified in the spectrophotometer at 260nm.

3.3.1.5. Site Directed Mutagenesis (gradient PCR)

In order to clone ADM cDNA into pcDNA3.1 vector, site directed mutagenesis PCR was carried out to incorporate HindIII and XhoI restriction sites on either sides of ADM cDNA. A gradient PCR was done in order to detect the right annealing temperatures as below:

Forward : 5′ GCA TAT AAG CTT ATG AAG CTG GTT TCC GTC GCC 3′
Reverse : 5′ GTC ATA CTC GAG CTA AAG AAA GTG GGG AGC ACT TC 3′

PCR was done using the Kapa PCR kit from KapaBiosystems. The PCR conditions used were as follows:

95°C – 3mins
94°C- 15 secs
gradient 50°C - 60°C – 15secs — 40 cycles
72°C – 1min
72°C – 1min

3.3.1.6. Gel Electrophoresis

1g agarose was dissolved in 100ml of Tris Borate EDTA buffer by briefly heating it in a microwave for 1-2mins. 2µl (0.02%) of Ethidium Bromide was added to agarose and the gel was allowed to set at room temperature. 5µl of PCR product mixed with 1µl of xylene loading buffer was loaded in the wells of the gel and allowed to migrate for 30mins at 200V. A 10kBp ladder was added alongside the PCR Products. The gel was observed on a bio-imaging system under UV light (Bio-rad Gel Doc 2000) using Quantity One Software. The ADM cDNA bands were extracted from the gel as described.

3.3.1.7. Gel Extraction of DNA

DNA was extracted from agarose gels using the Zymoclean Gel DNA Recovery Kit.

In order to recover DNA from agarose gels, DNA was resolved in an agarose gel without ethidium bromide. The resolved DNA was stained with 1% crystal violet made up in distilled water (w/v). The gel was incubated with crystal violet for 30-45mins with gentle agitation. The desired stained DNA bands were

excised using a scalpel and the protocol instructed by the DNA recovery kit was followed.

Three times volume of agarose dissolving buffer was added to the excised gel and incubated for 5-10mins at 37°C until the agarose was completely dissolved. Melted agarose solution was added to a spin column to adhere DNA to the column filters. Agarose and other contaminants were washed off the spin columns using wash buffer by centrifuging at 10,000xg for 30secs. DNA was eluted in 20µl water and quantified by nanodrop spectrophotometer and frozen at -20°C or used for downstream applications.

3.3.1.8. DNA Manipulation

A. DNA Precipitation

DNA was precipitated according to the volume of DNA and not the concentration. Salt Solution during precipitation was added if the DNA was to be precipitated after midi/mini-prep. If the DNA was to be precipitated after PCR, restriction digestion or ligation, salt solution was not added since the buffers contained enough salt to precipitate the DNA.

For 50µl DNA, 70µl isoproponal was added. 15µl of 2mM Sodium Acetate was added if necessary. The mixture was incubated for 15-30mins at -20°C and centrifuged at 20,817xg for 15mins at 4°C. The DNA pellet was washed with either 70% ethanol of DNA>200bp or 95% ethanol if DNA<200bp. The resuspended DNA was centrifuged at 20,817xg for 10mins at 4°C. DNA pellet was air dried, resuspended in water and quantified and used for downstream applications or frozen at -20°C.

B. Restriction Digestion

Restriction digestion was carried out to produce sticky ends in ADM cDNA so as to clone it into the pcDNA3.1 vector. Both the vector and the restriction site incorporated ADM was digested with XhoI and HindIII enzymes.

A 100µl reaction containing vector (10µg) or the precipitated ADM cDNA, 20units* of XhoI and HindIII and appropriate buffers was incubated at 37°C overnight.

Restricted products were either precipitated or gel extracted as per subsequent applications.

** One unit is the amount of enzyme required to digest 1µg of DNA in 1hr at 37°C in 50µl reaction volume.*

C. Dephosphorylation

The restricted vector was precipitated and dephosphorylated to prevent self-annealing. Antarctic Phosphatase was used to dephosphorylate the vector.

A 50µl reaction containing the restricted vector, 10 units* of Antartic Phosphatase and the appropriate buffer was incubated at 37°C overnight.

Dephosphorylated vector was precipitated and resuspended in 20µl water and quantified.

** One unit is defined as the amount of enzyme that hydrolyses 1µmol of p-nitrophenylphosphate to p-nitrophenol in 1ml reaction volume in 1min at 37°C.*

Restricted ADM cDNA was resolved on an agarose gel and DNA was extracted and quantified as mentioned above.

D. Ligation

Cloning of ADM cDNA into pcDNA3.1 vector was carried out using T4 DNA Ligase enzyme.

In a 100µl reaction containing 1µg each of dephosphorylated vector and restricted ADM cDNA, 2000 units* of T4 DNA Ligase and buffers were incubated overnight at room temperature.

** One unit is defined as the amount of enzyme required to give 50% ligation of HindIII fragments of DNA (300µg/ml) in a total reaction volume of 20µl in 30mins at 16°C.*

The ligation mixture was precipitated, resuspended in 50µl water and DNA was gel extracted and resuspended in 20µl water. KOD PCR was carried out as mentioned above to amplify the entire pcDNA3.1 vector containing ADM cDNA using the primers and PCR conditions given below.

Forward: 5' GAA GTG GAA TAA GTG GGC TCT GAG TC 3'
Reverse: 5' GAC TCA GAG CCC ACT TAT TCC ACT TC 3'

PCR Cycle setup:
95°C – 2mins
95°C – 20secs
60°C – 15secs
72°C – 3:30mins
} 18 cycles
72°C – 5mins

E. Removal of methylated DNA

In order to removal any residual vector as a result of incomplete restriction, PCR product was demethylated using DpnI enzyme.

20units* of DpnI enzyme was added to the PCR product and incubated overnight at 37°C.

Demethylated DNA was precipitated and transformed as mentioned above.

** One unit is defined as the amount of enzyme required to digest 1µg of pBR322 DNA (dam methylated) in 1ht at 37°C in a 50µl reaction volume.*

* Definitions of 1 unit is taken from www.neb.com

The bacterial colonies were cultured and plasmid DNA was extracted. 1µg DNA was sent for sequencing using primers for T7 promoter in University of Sheffiled's Core Genetics Facility. DNA was also restricted using XhoI and HindIII enzymes for 1hr at 37°C and resolved in an agarose gel to confirm the size of ADM cDNA.

3.3.1.9. Linearisation of Constructs

pcDNA3.1 vector containing ADM cDNA was linearised prior to tranfection in order to incorporate into the genome of the cells. pBUDCE4.1 vector containing RAMP2+CLR and RAMP3+CLR inserts were kindly provided by Dr.Dave Roberts in Prof.Skerry's lab.

20-30µg of vector was restricted with 20units of FspI enzyme (pcDNA3.1) and MfeI enzyme (pBUDCE4.1) for 1hr at 37°C. The restricted vector was precipitated and quantified.

3.3.1.10. Transfection

Cells were transfected with linearised vectors by electroporation. 4-5 million cells were trypsinised and resuspended in electroporation buffer containing 2mM of ATP and 5mM of glutathione. 400-500µl cell suspension was transferred to a 4mm gap cuvette. 10µg of linearised vector was added and the cuvette was gently flicked to mix the contents. Transfection control cells contained more

electroporation buffer instead of DNA. The cells were electroporated as shown in table 4 depending on the cell type.

Cell Type	Voltage	Capacitance
PC-3	200V (0.2kV)	960µF
MDA-MB-231	230V (0.23kV)	
U-87	400V (0.4kV)	

Table 4: Electroporation voltage and capacitance used for transfecting different cancer cell lines.

After electroporation, cells were left to rest at room temperature for 2-5mins and 300µl warm media was added to the cells and gently transferred into T175cm^2 flasks containing pre-warmed media. Cells were cultured under standard conditions for two days in order to stabilise protein expression for antibiotic selection.

Antibiotic Doses

Transfected cells along with control transfections were treated with antibiotic containing media. The media was replenished every 2 days, with freshly added antibiotics. 1mg/ml of G418 or Zeocin was added for pcDNA3.1 or pBUDCE4.1 transfected cells respectively. Control transfected cells die from 7-15 days from the start of selection. Individual colonies of stably transfected cells were trypsinised and cultured under standard conditions. The media contained 500µg/ml of antibiotics in order to maintain selection pressure.

3.3.1.11. Over-expression of ADM Receptors

pBUDCE4.1 vector containing either RAMP2+CLR or RAMP3+CLR (constructs kindly provided by Dr. Dave Roberts in our lab). The vectors were linearised by using FspI enzyme and transfected into PC3 cells as previously described. Post transfection, media containing 500mg/ml Geniticin antibiotic was added to cells to select for transfected cells. The stably transfected cells were then used for MTT assay and wound healing assay.

3.3.1.12. Cell Proliferation

The assessment of cell proliferation was carried out using the MTT assay kit obtained from ATCC. Cells were counted and $2x10^3$ cells/well were added into 96 well plates in 6 replicates for each cell type. At each time point, MTT reagent was added and incubated for 2hrs at 37°C. Once the purple formazan was visible, detergent was added to dissolve the formazan overnight with gentle agitation. Absorbance at 570nm was measured using a micro plate reader at day 0 to test the seeding consistency between cell types. Thereafter, every two days, absorbance was measured and media was replaced for other time points. Proliferation was assessed for a period of 8-10 days.

3.3.1.13. Wound Healing Assay/Scratch Test

The assessment of cell migration was done by wound healing assay also called as scratch test. Cells were counted and $4x10^6$ cells/well were added to 12 well plates in duplicates for each cell type. Once the cells were 80-90% confluent, which was usually the next day, cells were treated with 30µg/ml Mitomycin C to block cell proliferation. Cells were incubated with Mitomycin C for 30mins at 37°C. A scratch was created in the monolayer using a 200µl pipette tip. The tip was changed for every well so as to maintain consistency in the scratch. The cells were then washed with PBS to get rid of any cell debris and media were added. At each time point, cells were fixed in ice cold methanol for 5mins and stained with 1% crystal violet for 5mins. Excess stain was washed

with water and the wells were air dried and pictures were taken at 10x magnification in Leica DMB4000B microscope using Leica Application Suite V3 software.

There are two methods to assess the migration of cells in scratch test, one by measuring the distance between the edges of the scratch and the other by measuring the area of the scratch.

Measuring Distance

The distance between the edges of the scratch was measured using ImageJ software. For samples where the distance could not be measure due to the closure of the scratch, 0 was taken as the distance.

Initially the scale on the ImageJ software was set to 500μM scale.

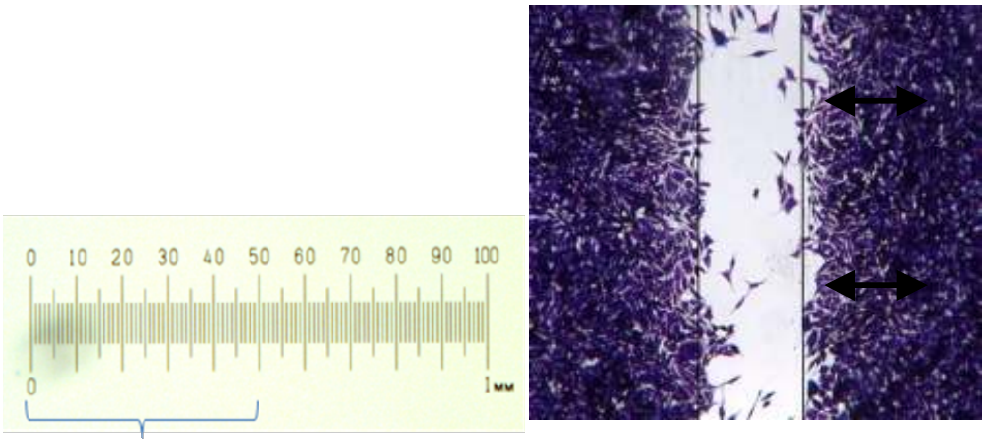

500μM

Figure 38: Measurement of the distance between the edges of the scratch. Lines were drawn on the edges of the scratch and distance was measured at different points and average was taken.

As shown in figure 38, the distance between the edges of the scratch was measured at various points and average taken.

Measuring Area

The area of the scratch was measured using ImageJ software. The image was converted to a black and white image and the outline of the scratch was generated. The accuracy of the analysis was determined by overlaying the outline of the scratch generated with the original image. Figure 39, shows the original image, outline of the scratch and the overlaid image. For scratches, where the area could not be measure due to the closure of wound, it was considered as 0.

Original Image **Scratch Outline** **Image Overlay**

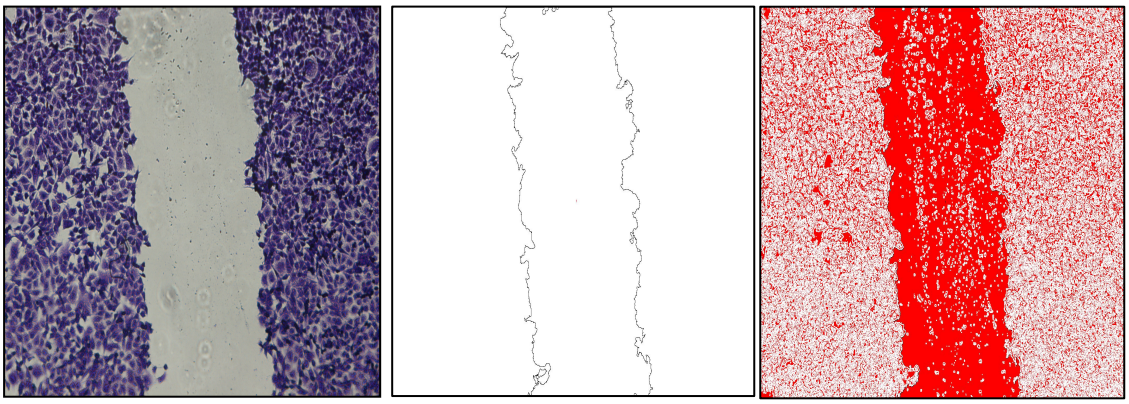

Figure 39: Measurement of area in scratch test. The original image is converted into a black and white image and the outline of the wound is generated in ImageJ. The accuracy of the generated scratch was determined by overlaying the original image with the scratch outline. The original image is shown in gray while the scratch is overlaid in red.

The data are expressed as the distance/area migrated by the cells. A migration index is expressed as the ratio of the percent migration of test cells over the percent invasion of control cells.

a) Percent Migration = $\frac{\text{Mean distance/area of test cells}}{\text{Mean distance/area of control cells}}$ X 100

b) Migration Index = $\frac{\text{\% Migration of Test Cells}}{\text{\% Migration of Control Cells}}$

Test cells = cells transfected with ADM or ADM receptors

Control cells = cells transfected with empty vector (vector control)

3.3.1.14. Cell Invasion

Cell invasion was assessed using Matrigel Invasion Chambers and protocol obtained from BD Biosciences. Cells were counted and $2.5x10^4$ cells were seeded in the insert with media containing 1% serum in duplicates. The wells below the inserts contained media with 10% serum to act as a chemoattractant. Cells were incubated for 20hrs under standard cell culture conditions.

Non-invading cells were removed from the upper surface of the insert membrane by scrubbing with cotton swabs. The cells in the lower surface of the membrane were fixed in methanol and stained with 1% crystal violet. Excess stain was washed with water and the membrane was air-dried, peeled off the inserts and mounted using DPX mountant using glass coverslips. Invaded cells were counted in several fields of duplicate membranes in Leica DMB4000B microscope using Leica Application Suite V3 software.

Data are expressed as the number of cells that invaded through the matrigel matrix. The Invasion Index is also expressed as the ratio of the percent invasion of test cells over the percent invasion of control cells.

a) Percent Invasion = $\frac{\text{Mean number of Test Cells}}{\text{Mean number of Control Cells}}$ X 100

b) Invasion Index = $\frac{\text{\% Invasion of Test Cells}}{\text{\% Invasion of Control Cells}}$

Test cells = cells transfected with ADM or ADM receptors

Control cells = cells transfected with empty vector (vector control)

3.3.1.15. Flow Cytometry

General flow cytometry protocol using antibody incubations was the same as described under section 2.3.10.

To test for GFP intensity, cells cultured in T75cm^2 were trysinised and centrifuged at 1000xg for 3-5mins. The cell pellet was resuspended in 1ml of media and sorted inFL-1 530/30 nm filter. 5x10^6 cells were counted in a population which excluded dead cells and cell clumps. A non-GFP cell line was used to optimise basal level of fluorescence and as a negative control.

3.3.2. ADM Over-Expression (*in vivo)*

3.3.2.1. IRES-eGFP Vector

The vector to over-express ADM to study the effect of over-expression of ADM in bone homing is a bicistronic IRES-eGFP vector, where the expression of GFP is directly proportional to the expression of ADM. The vector map containing the cDNA for ADM is shown in figure 40. The length of ADM ORF is 558bp which lies exclusively in Exon 4 of ADM gene coding sequence.

MDA-MB-231 Cells were transfected with IRES-eGFP vector according to the protocol described in section 3.3.1.10.

Vector Information for EX-T0150-M61

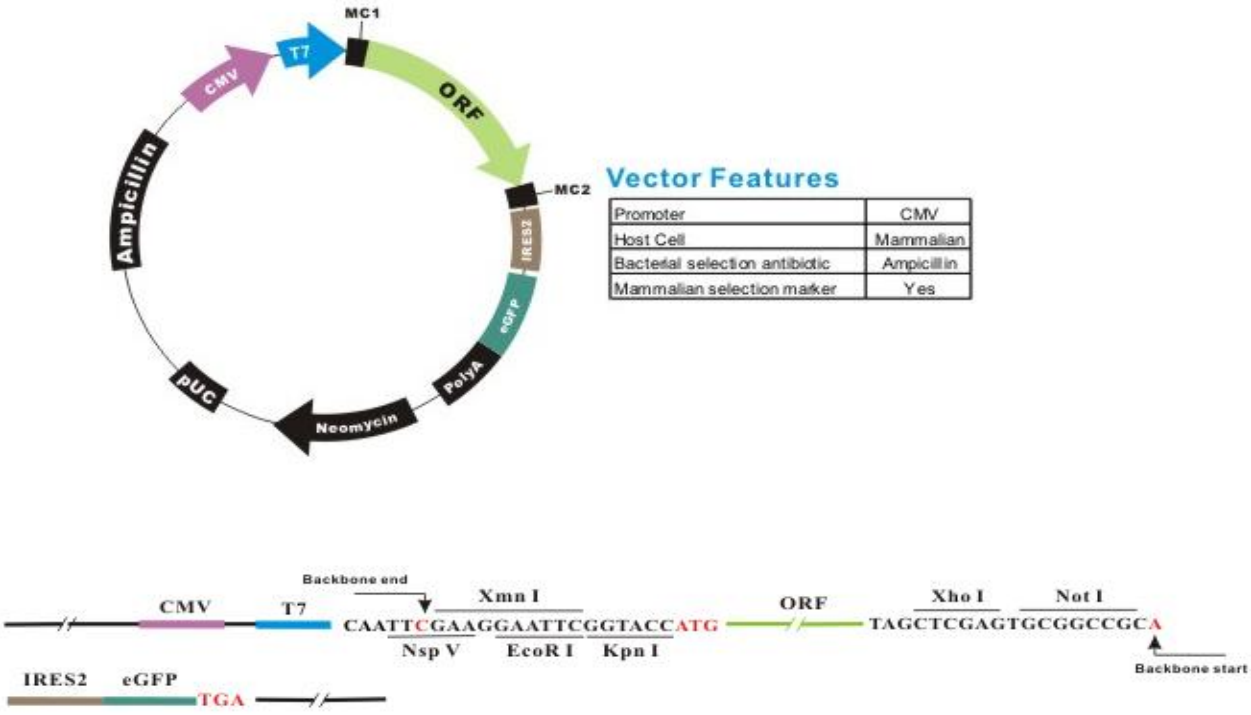

Figure 40: Vector map of the bicistronic IRES-eGFP vector (EX-T0150-M61) obtained from Genecopoeia. The vector backbone along with restriction sites flanking the ORF can also be seen.

3.3.2.2. Generation of IRES-eGFP negative control

In order to generate an IRES-eGFP negative control, two attempts were made.

Initially, the start codon was made to mutate from ATG to GGG, therefore transcription of ADM would not take place. KOD PCR was done using the following primers:

Forward : 5’ TTC GGT ACC GGG AAG CTG GTT TCC 3’
Reverse : 5’ GGA AAC CAG CTT CCC GGT ACC GAA 3’

The PCR cycle conditions were:

95°C – 2mins
95°C – 20secs
60°C – 20 secs
72°C – 1:10mins
} 35 cycles
72°C – 5mins

Next attempt was made to mutate a stop codon after the generation of four amino acids, as IRES-eGFP vector requires transcription to take place in order for the ribosome to re-enter and transcribe GFP. Therefore after the generation of the first four amino acids – M, K, L, V, two stop codons would end transcription. The TCCGTC codons that code for Serine and Valine were made to mutate into TAGTGA, which code for amber and opal stop codons respectively. The primers used for this KOD PCR are:

Forward : 5' G AAG CTG GTTTAG TGA GCC CTG ATGTA C 3'
Reverse : 5' GTACATCAGGGCTCACTAAACCAGCTTC 3'

The PCR conditions were:

95°C – 2mins
95°C – 30secs
61°C – 30 secs
72°C – 4mins
} 40 cycles
72°C – 5mins

Since the mutations were not being incorporated, commercially available IRES-eGFP negative control was purchased. The negative control for IRES-eGFP vector contains a random sequence in place of ADM cDNA.

3.3.2.3. Fluorescent Activated Cell Sorting (FACS)

MDA-MB-231 cells transfected with ADM-IRES-GFP and negative control vector was sorted for varying GFP intensities using FACSAria flow cytometry. Cells cultured under standard cell culture conditions in presence of antibiotics were trypsinised and sorted. Non-GFP MDA-MB-231 cells were used to optimise for background fluorescence. In a log10 scale of intensity, cells with less than 10^2 was sorted as very low group, cells with 10^2-10^3 intensity was sorted as low group, cells with 10^3-10^4 were sorted into medium intensity group and cells with $>10^4$ were sorted into high intensity group. Two days post sorting, pictures were taken of cells for GFP in 90% confluent T75 flasks in Leica DM4000B microscope.

3.3.2.4. Measuring GFP intensity

Cells sorted for varying intensities for GFP were cultured under antibiotic selection in standard cell culture conditions. $1x10^6$ cells/well cells were cultured in a six well plate overnight. GFP intensity was measured using a fluorescent micro plate reader at 485nm excitation and 480nm emission.

3.3.2.5. RNase Treatment

In order to remove any contaminating RNA in the cDNA sample, RNase treatment was carried out.

If 1µg of RNA was used for initial cDNA synthesis, then it was considered that 1µg of cDNA was synthesised. In a 60µl reaction, 1µg cDNA was treated with buffers and 20 units* of RibonucleaseH for 20mins at 37°C. 0.5M EDTA was added to stop the reaction. The cDNA was precipitated as described in section 3.3.6. was used for RT-PCR.

**One Unit of Ribonuclease H is the amount of enzyme required to increase fluorescence 1.5RFUs per sec at 37°C using 20pmol of RNaseAlert probe coupled to 1000pmol of a complementary oliogonucleotide as substrate.Taken from Applied Biosystems.*

3.3.2.6. Reverse Transcription – PCR

mRNA expression of ADM and GFP was quantified by RT-PCR using the KapaPCR kit. HPRT1 was used as an endogenous control.

The primers used to amplify ADM, GFP and HPRT1 are:

ADM Forward : 5′ AAG CTG GTT TCC GTC GCC C 3′
ADM Reverse : 5′ C TGG GGC CGA ATA AGG GTC 3′

GFP Forward : 5′ TAA TAA GCT TGC CAC CAT GGT GAG CAA GG 3′
GFP Reverse : 5′ AAT TGG TAC CCT TGT ACA GCT CGT CCA TGC 3′

HPRT1 Forward : 5′ TGT AAT GAC CAG TCA ACA GGG 3′
HPRT1 Reverse : 5′ TGG CTT ATA TCC AAC ACT TCG 3′

The PCR conditions used to amplify ADM are:

95°C – 3mins
95°C – 20secs
56°C – 30 secs
72°C – 30mins
} 35 cycles
72°C – 2mins

Data Analysis

Quantification of the bands was similar to that of quantifying western blotting bands as described in 2.3.9. The band intensities were measured in pixels and normalised to HPRT1 endogenous control.

3.3.2.7. Bone metastases in immunodeficient mice

All animals and experiments were carried out in accordance with the local guidelines and with Home Office approval under project license number 40/2972 held by Prof. Nicola J Brown, University of Sheffield, United Kingdom.

Female Balb/C nude/nude mice that were 5 weeks old were ordered from Harlan, United Kingdom. Mice were allowed to acclimatize for a week before the commencement of the experiment. Experiments were carried out with the test group containing 16 animals and control groups contained 15 animals each.

General anaesthesia was induced by 100mg/kg Ketamine and 15mg/kg Xylazine. $1x10^5$ cells/mice in 100µl PBS was injected into the left ventricle of the heart using a 25Gx$^5/_8$" needle. Mice were monitored twice weekly by measuring body weights and detecting tumours in hind legs using a Light Tools GFP imaging system. Tumours were detectable in most animals two weeks post injection. Mice were sacrificed humanely and blood was drawn through inter-cardiac punctures to obtain serum for further analyses. Hind legs were removed and stripped off excess muscle. Legs were viewed under GFP imaging system and pictures were taken. The right legs were fixed in 4% PFA for micro CT analysis. Left legs were used for RNA analysis and saved in RNAlater solution.

Counting Tumours

Tumours were counted as 1, if present in one of the four positions – proximal femur, distal femur, proximal tibia and distal tibia as shown in figure 41. Counts were made from both inside and outside images and are combined in the analysis. Intensity of GFP was not taken into account because a) imaging position was variable between bones and b) intensity of GFP expression may vary between animal groups.

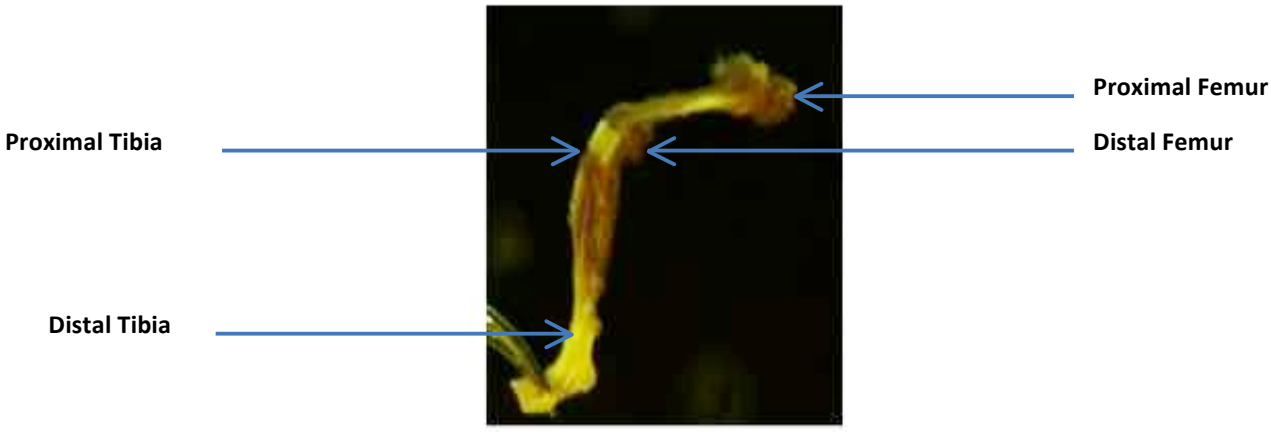

Figure 41: Mouse hind limb. Tumours were counted only if present in any of these four postions.

3.3.2.8. Statistical Analysis

For proliferation assay, scratch test, invasion assay analyses and weights of mice *in vivo*, One Way Analysis of Variance (ANOVA) was done to gain statistical analysis. Tukey post hoc test was done to compare between groups. Data are expressed as mean±SEM, and p value <0.05 was considered to be statistically significant.

3.4. Results

3.4.1. Over-Expression of Adrenomedullin

ADM cDNA in pOTB7 vector was obtained from Genecopoeia. The vector after transforming into E.Coli was cultured and plasmid DNA was extracted. As described previously, KOD gradient PCR was done to incorporate the two restriction sites (section 3.3.1.5).

Figure 42 shows the product of gradient PCR for ADM with temperatures from 50°C, 50.2°C, 50.7°C, 51.6°C, 52.7°C, 54°C, 55.4°C, 56.8°C, 58.1°C, 59.2°C, 60°C and 60.4°C. The PCR products were around 1500bp long, ADM cDNA is ~1488bp long. The higher band is >10,000kb, belongs to pOTB7 vector.

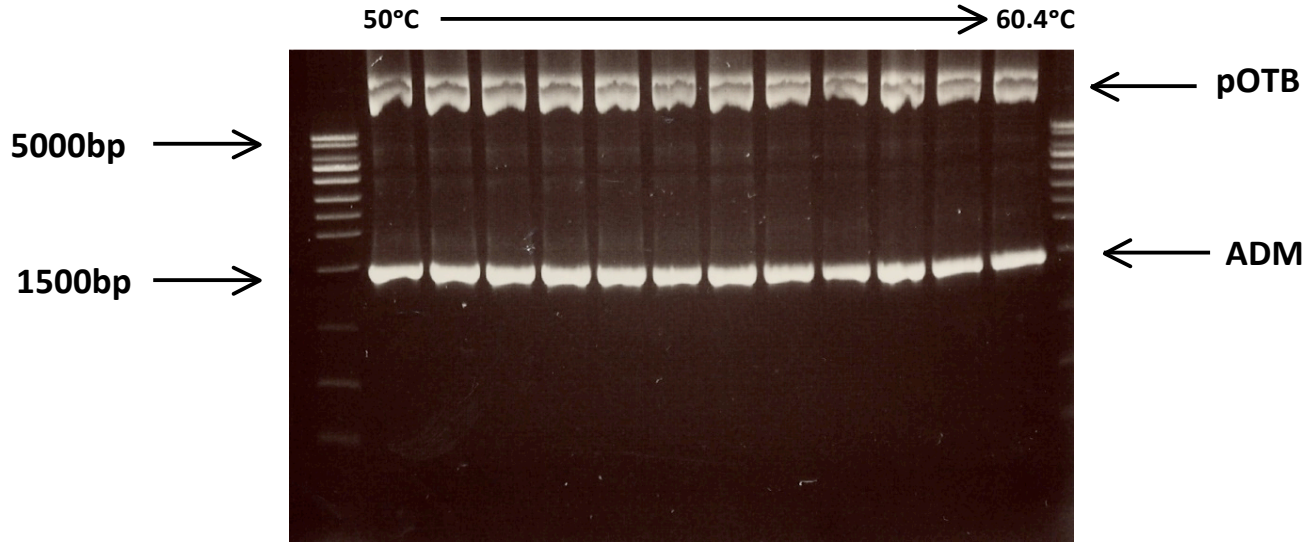

Figure 42: Gel electrophoresis of ADM amplified by gradient PCR. The amplified ADM cDNA belongs to ~1500bp. The higher band belongs to pOTB7 vector.

ADM amplified from the pOTB7 vector was cloned into pcDNA3.1 vector as previously described and the E.Coli clones were cultured and restricted using XhoI and HindIII enzymes. The products of restriction were separated by gel electrophoresis. Figure 43 shows the ADM bands in all three clones run in duplicates belonging to 1500bp and the pcDNA3.1 vector bands belonging to 5400bp.

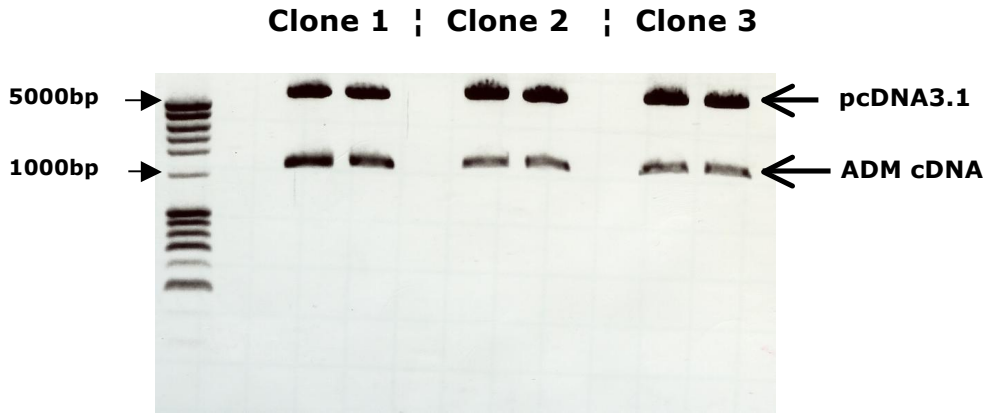

Figure 43: Restriction digestion after cloning ADM cDNA into pcDNA3.1 vector. The three colonies of E.Coli contained the pcDNA3.1 vector containing ADM gene.

The plasmid DNA from all three clones was sequenced in University of Sheffield Core Facilities Unit. The sequencing result was run in BLAST. Figure 106 shows the screen shot of BLAST output in appendix section. BLAST returned with 97% match to the Human Adrenomedullin mRNA sequence (NM_001124). This result confirms that ADM had been cloned into the pcDNA3.1 vector.

3.4.1.1. Confirmation of ADM over-expression in cell lines

Three cell lines were transfected with pcDNA3.1 vector containing ADM with the protocol that is previously described. After antibiotic selection, the cells were screened to confirm ADM over-expression in these cell lines when compared to non-transfected (native) and vector control transfected cells.

A fold change in ADM expression as quantified in qPCR was observed in prostate cancer (PC3), glioblastoma (U87) and breast cancer (MDA-MB-231) cells. Figure 44 shows the quantified qPCR, confirming ADM over-expression. PC3 transfected with ADM produced 8 times and 13.2 times more ADM than native and pcDNA3.1 vector transfected cells respectively.

U87 transfected with ADM produced 8.5 and 15.8 times more ADM than native and pcDNA3.1 vector transfected cells respectively.

MDA-MB-231 cells transfected with ADM produced 14.5 and 13.6 times more ADM than native and pcDNA3.1 vector transfected cells respectively.

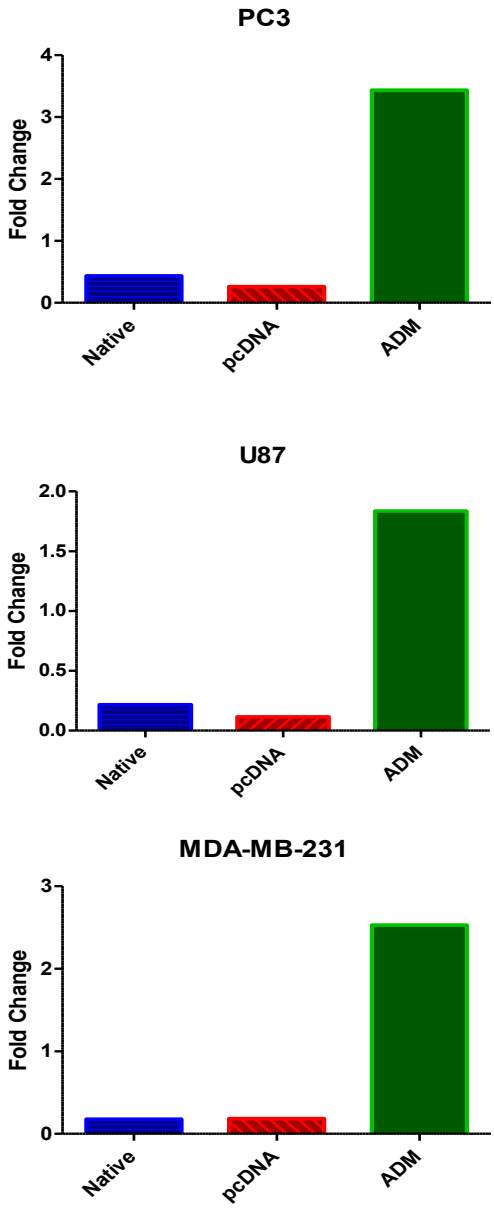

Figure 44: Confirmation of over-expression of ADM mRNA prostate cancer (PC3), glioblastoma (U87) and breast cancer (MDA-MB-231) cell lines. The graphs confirm that cells transfected with vector containing ADM gene expressed more ADM than native (non-transfected) and control transfected cells. Bars show the fold change in ADM mRNA expression normalised to β-actin. n=1

3.4.1.2. Effect of ADM Over-Expression on Cell Proliferation

The effect of over-expressing ADM was tested on cell proliferation in MDA-MB-231 and PC3 cells.

MDA-MB-231 Cells

Proliferation analysis was carried out on MDA-MB-231, breast cancer native cells and cells transfected with pcDNA3.1 vector containing ADM cDNA, vector control. The mean absorbance for days 0, 2, 4, 6 and 8 are shown in table 5. Figure 45 shows the assessment of the mean absorbances. It was observed that there was no significant difference between native cells, vector control and cells transfected with ADM cDNA.

	Native	**pcDNA3.1**	**ADM**
Day 0	0.17±0.01	0.18±0.07	0.17±0.02
Day 2	0.23±0.09	0.23±0.05	0.33±0.20
Day 4	0.56±0.04	0.56±0.10	0.58±0.04
Day 6	0.64±0.16	0.71±0.25	0.69±0.29
Day 8	1.30±0.9	1.06±0.77	1.15±0.61

Table 5: Mean absorbances (OD) of proliferation of native, vector control and ADM over-expressing MDA-MB-231 cells. Proliferation was assessed using MTT assay. OD values were measured at 570nm. The values are mean from three replicate experiments.

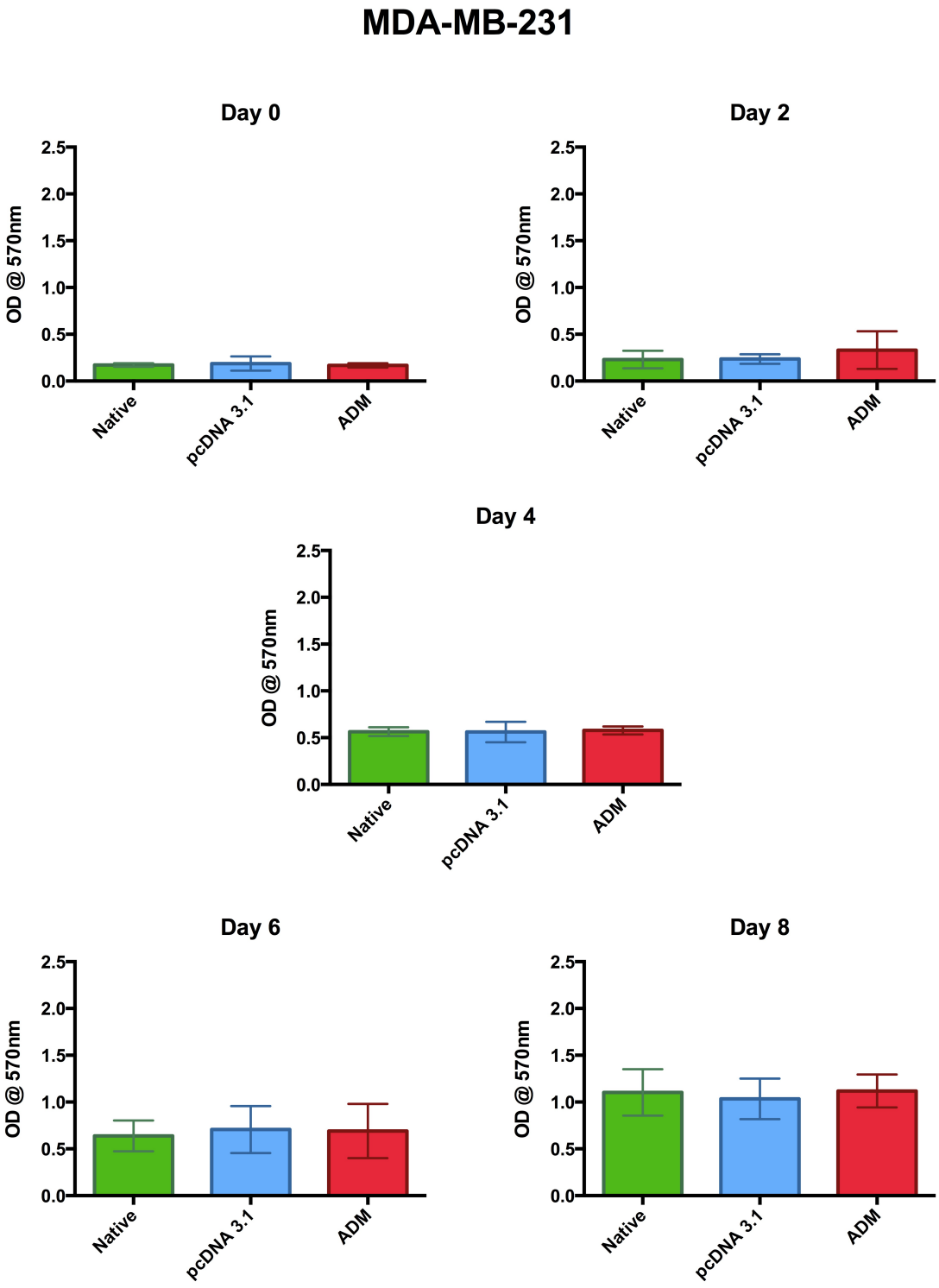

Figure 45: Proliferation of native (non-trasfected), vector control and cells transfected with ADM in breast cancer (MDA-MB-231) cells assessed by MTT over eight days. The bar shows the OD at 570nm. The bars represent mean absorbance ± SEM (error bars). ANOVA and Tukey post hoc test was done to gain statistical significance. n=3, $p<0.05$

PC3 Cells

Proliferation analysis on PC3 cells were tested over a period of 10 days. the mean absorbances (OD) of native, vector control and ADM transfected cells are shown in table 6.

	Native	**pcDNA3.1**	**ADM**
Day 0	0.31±0.06	0.30±0.05	0.30±0.08
Day 2	0.30±0.09	0.26±0.05	0.27±0.09
Day 4	0.39±0.18	0.61±0.30	0.50±0.19
Day 6	0.42±0.28	0.39±0.10	0.46±0.10
Day 8	0.49±0.38	0.54±0.29	0.50±0.13
Day 10	0.44±0.20	0.31±0.10	0.42±0.09

Table 6: Mean absorbances (OD) of proliferation of native, vector control and ADM over-expressing PC3 cells. Proliferation was assessed using MTT assay. OD values were measured at 570nm. The values are mean from three replicate experiments.

Figure 46 shows the assessment of the mean absorbances. At days 0, 2, 6 and 8 there were no significant differences between the groups. At day 4, the OD of vector control cells was 1.6 times significantly more than native cells. At day 10, the OD of native cells were 1.4 times significantly more than vector control cells.

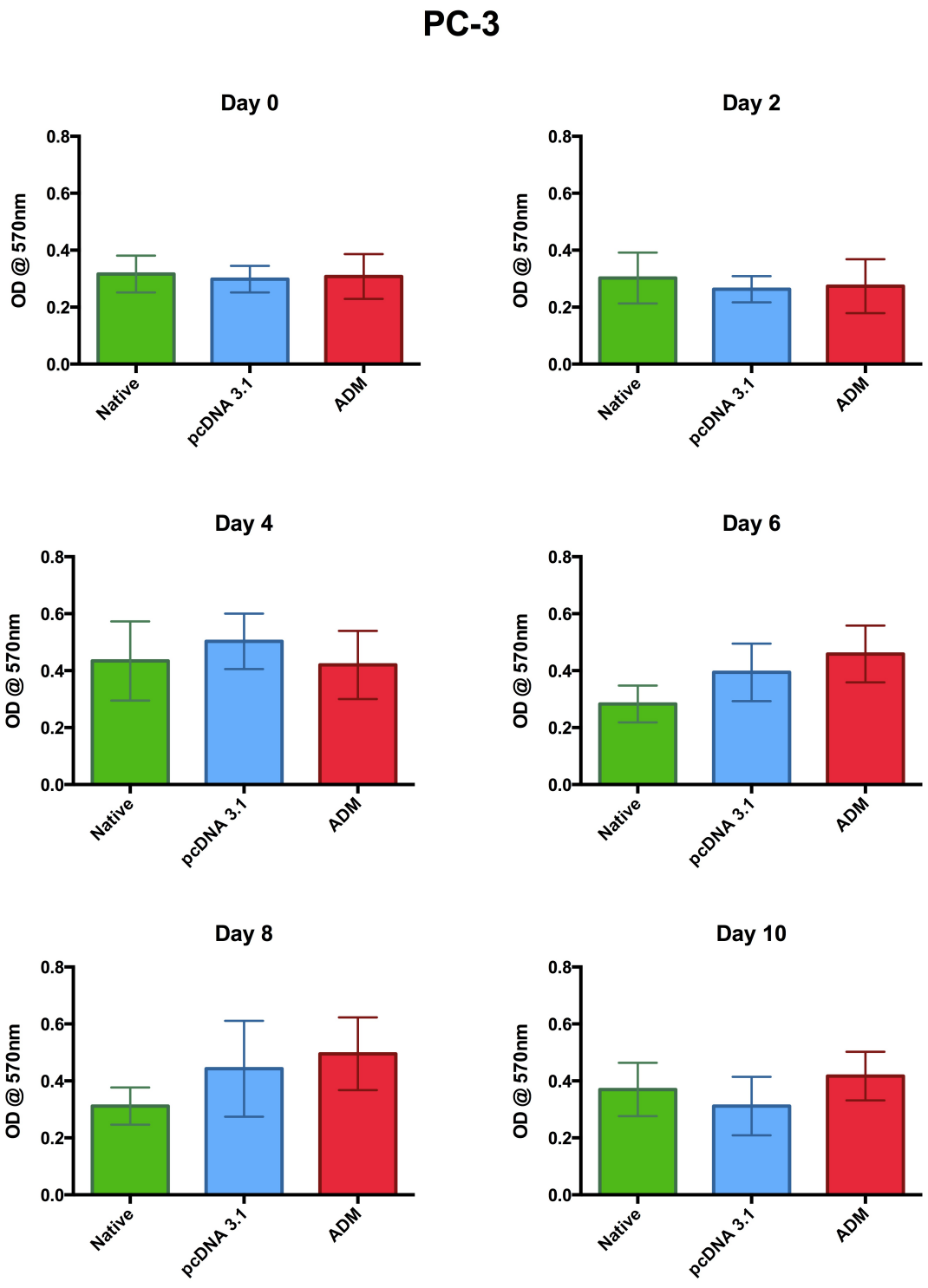

Figure 46: Proliferation of native, vector control and ADM transfected prostate cancer (PC3) cells assessed by MTT assay over 10 days. The bars show OD at 570nm. The error bars represent mean ± SEM. ANOVA and Tukey post hoc test was done to gain statistical significance. n=5, $p<0.05$.

3.4.1.3. Effect of ADM Over-Expression on Cell Migration

The effect of over-expressing ADM was next tested on cell migration assessed by wound healing assay/scratch test. Scratch test was done in PC3 cells and MDA-MB-231 cells. Migration was assessed by distance between scratch edges or area of scratch as previously described in Methods section 4.3.1.12.

PC3 Cells

Table 7 shows the distance between the two edges of the scratch test at different time points.

	Native	pcDNA3.1	ADM
0hrs	584.66±8.63	589.20±31.35	576.55±19.09
24hrs	446.58±31.67	545.48±11.03	554.68±16.05
48hrs	269.64±54.22	483.91±22.7	210.70±5.04
72hrs	277.22±25.37	402.28±36.97	150.06±57.51

Table 7: Mean distances between the two edges of the scratch in native, vector control and ADM transfected PC3 cells. The distances were measured in μm using ImageJ. The values are mean of 5 replicate experiments.

Figure 47 shows the migration of PC3 cells transfected with vector control and ADM.

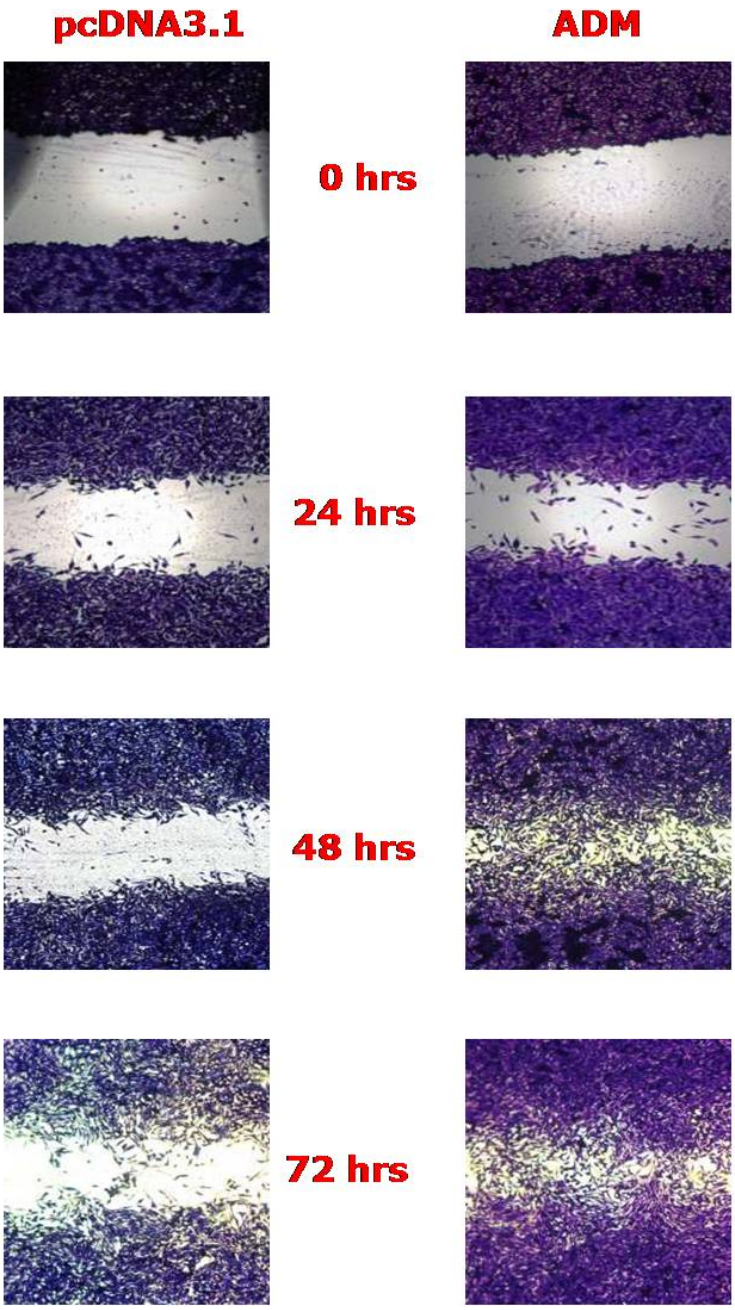

Figure 47: *In vitro* wound healing assay / migration assay to determine the migration of prostate cancer (PC3) cells transfected with pcDNA3.1 vector control and ADM. The biggest effect in ADM transfected cells is observed between 24hrs and 48hrs. The Images were taken in LeicaDMI4000B microscope.

Figure 48 contains histograms of the quantified scratch test. At 0hrs, there was no significant diference between the distances. At 24hrs, native cells migrated 1.2 times faster than vector control and ADM transfected cells. At 48 hrs, cells transfected with ADM migrated 4 times faster than vector control cells. Native cells migrated 1.8 times faster than vector control cells. At 72 hrs, ADM transfected cells migrated 2.3 times and 3.5 times than native and vector control cells respectively.

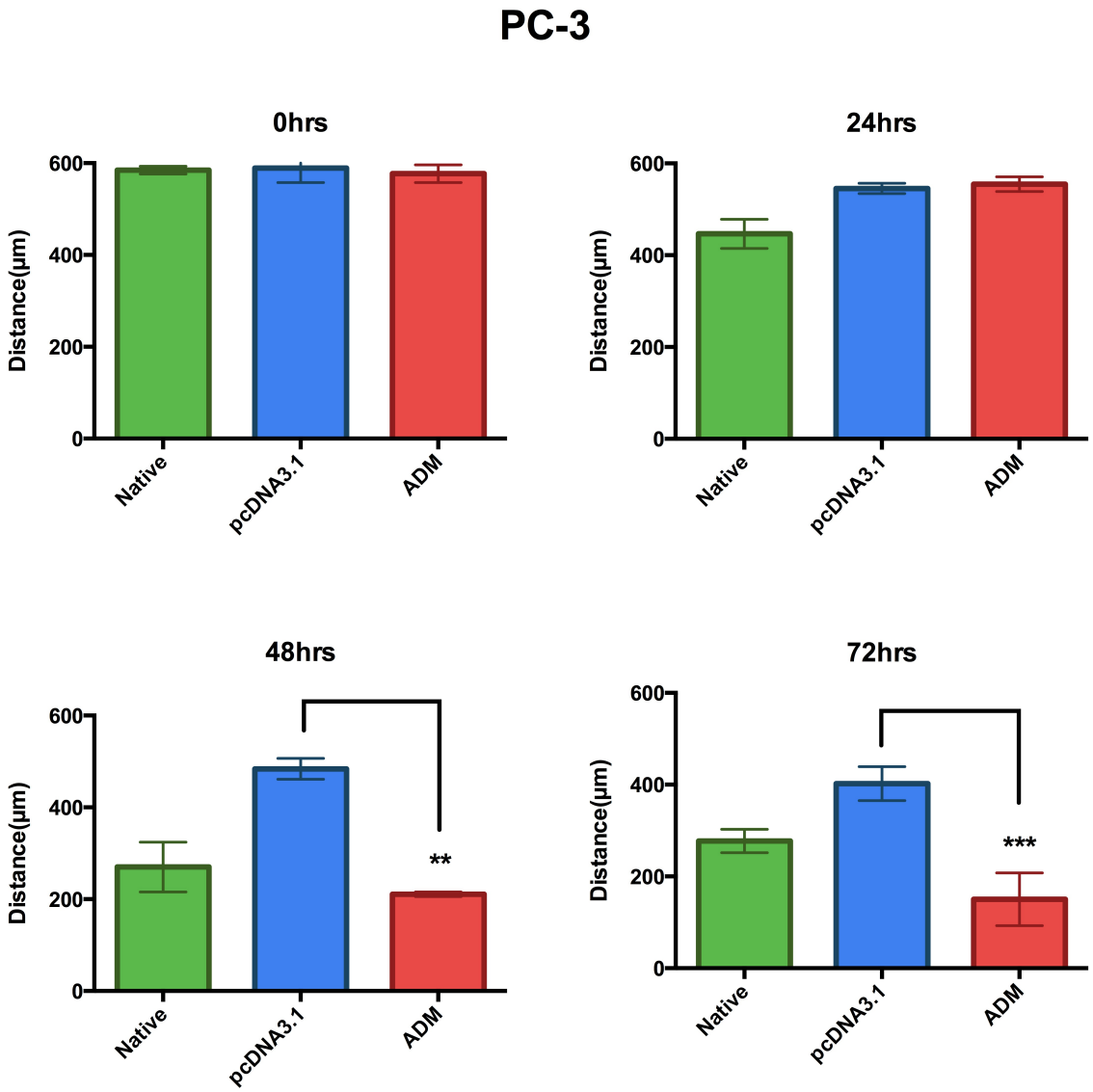

Figure 48: Migration of transfected PC3 cells in *in vitro* wound healing assay. Graph shows the distance covered by PC3 cells transfected with ADM, control vector (pcDNA3.1) and non-transfected cells, in wound healing assay. The bars represent mean ± SEM (error bars). ANOVA and Tukey post hoc test was done to gain statistical significance. n=5, $p<0.001$.

MDA-MB-231 Cells

The effect of ADM over-expression was tested on the migration of MDA-MB-231 cells over a period of 24hrs. Table 8 shows the mean areas of scratch in native, vector control and ADM transfected cells.

	Native	pcDNA3.1	ADM
0hrs	28.21±10.83	28.89±11.98	27.43±9.68
12hrs	19.81±4.51	20.00±6.88	13.32±3.57
24hrs	11.23±1.88	12.20±3.36	3.33±4.04

Table 8: Mean areas of the scratch in native, vector control and ADM transfected MDA-MB-231 cells. The areas are a mean from three replicate experiments.

Figure 49 shows the migration of MDA-MB-231 cells transfected with vector control and ADM at different time points.

Figure 50 contains histograms of the quantified scratch test. At 0hrs, there was no significant difference between the areas. At 12 hrs, ADM transfected cells migrated 1.5 times more than native and vector control cells. At 24hrs, ADM transfected cells migrated 3.6 times and 4 times faster than native and vector control cells respectively.

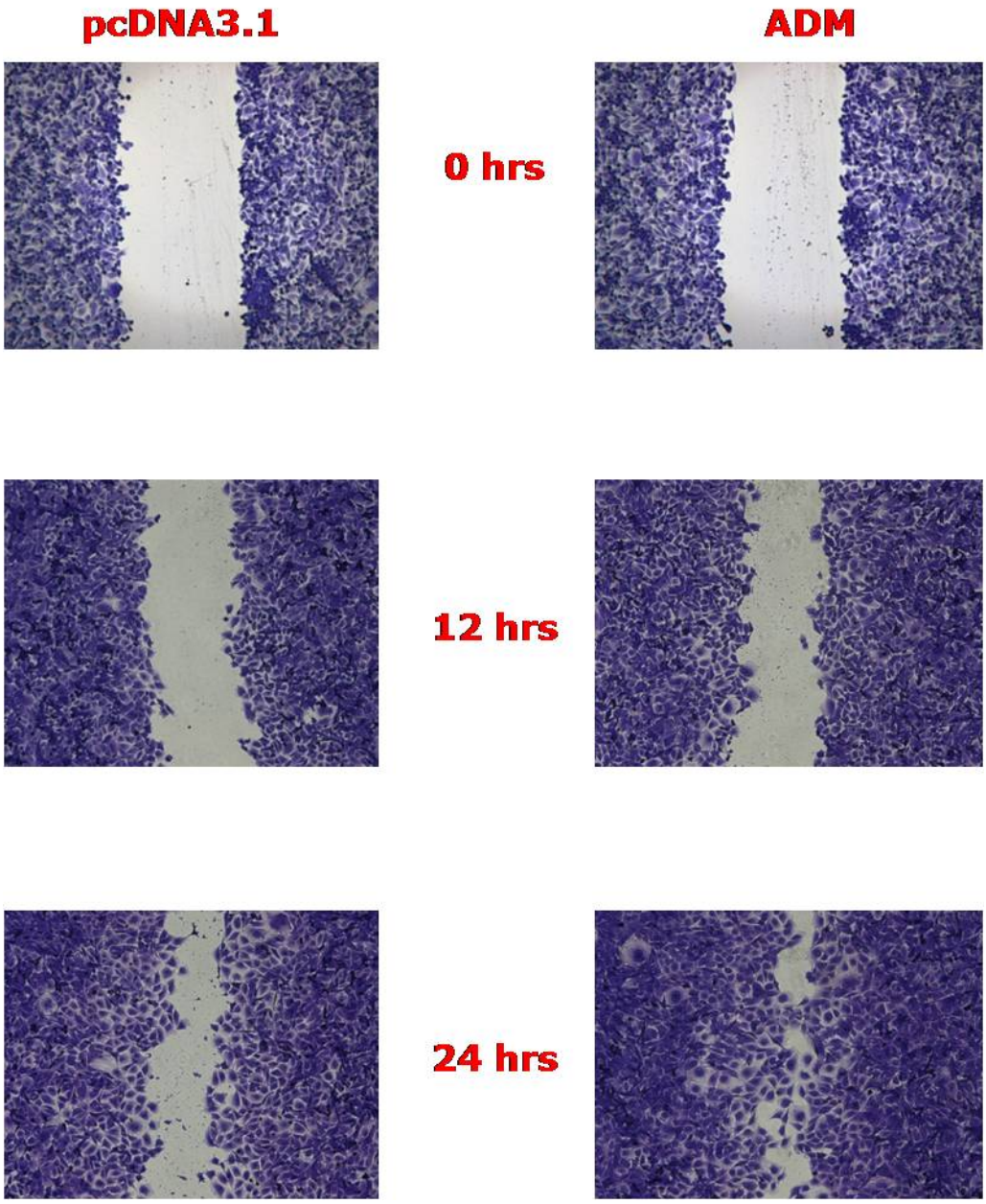

Figure 49: *In vitro* wound healing assay / migration assay to determine the migration of breast cancer (MDA-MB-231) cells transfected with pcDNA3.1 vector control and ADM. Cells transfected with ADM migrated faster in closing the wound than pcDNA3.1 transfected cells. Images were taken in LeicaDMI4000B microscope.

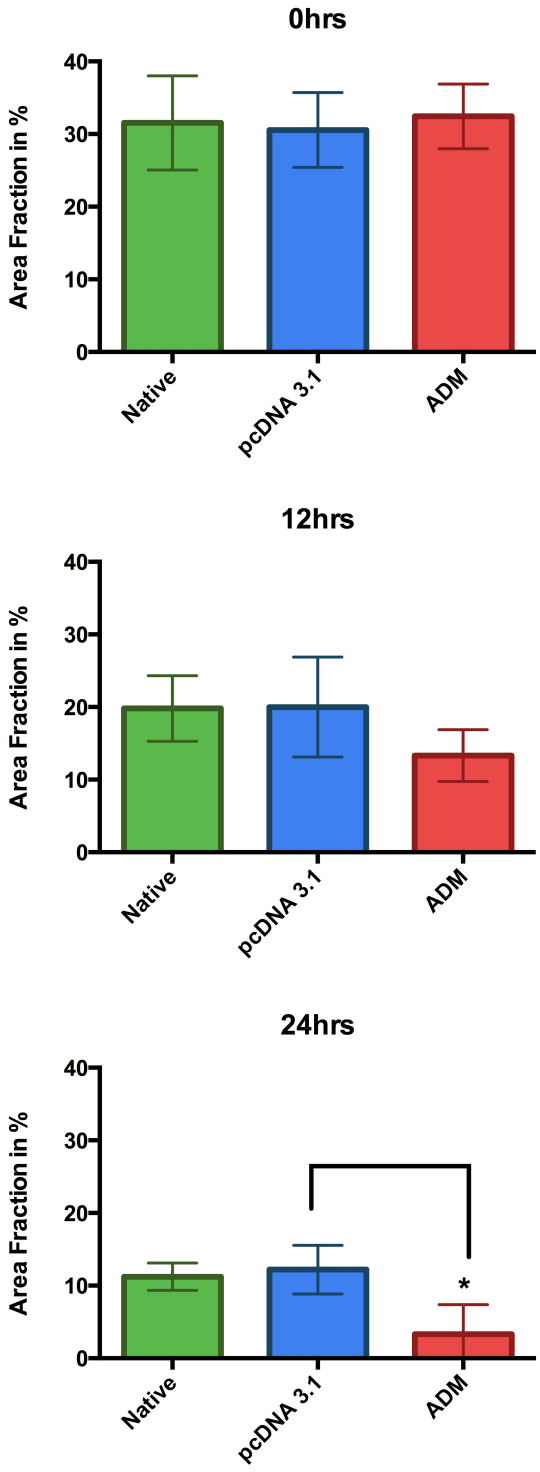

Figure 50: Migration of breast cancer cells in wound healing assay. Graph shows the area of the wound in cells transfected with ADM, control vector (pcDNA3.1) and non-transfected cells. The error bars represent mean ± SEM. ANOVA and Tukey post hoc test was done to gain statistical significance. n=3, $p<0.001$.

3.4.1.4. Effect of ADM Over-Expression on Cell Invasion

The invasive potential of cells when over-expressing cells were determined by Cell Invasion Assay as described in Methods section 4.3.1.13. MDA-MB-231 and U87 cells were tested for their invasive potential.

Figure 51 shows the graphs of the number of cells that have invaded through the matrigel coated membrane of a Boyden chamber.

ADM transfected MDA-MB-231 cells invaded more than pcDNA3.1 transfected and native cells. The mean number of cells that invaded was 13.67±1.94, 11.17±1.64 and 60.67±8.12 for native pcDNA3.1 and ADM transfected cells respectively. 3.3 times significantly more ADM transfected cells invaded through matrigel than native and pcDNA3.1 transfected cells.

Preliminary analysis of invasion potential of U87 cells was done, n=1. There were more ADM transfected cells that invaded through the matrigel coated membrane than native and pcDNA3.1 transfected cells.

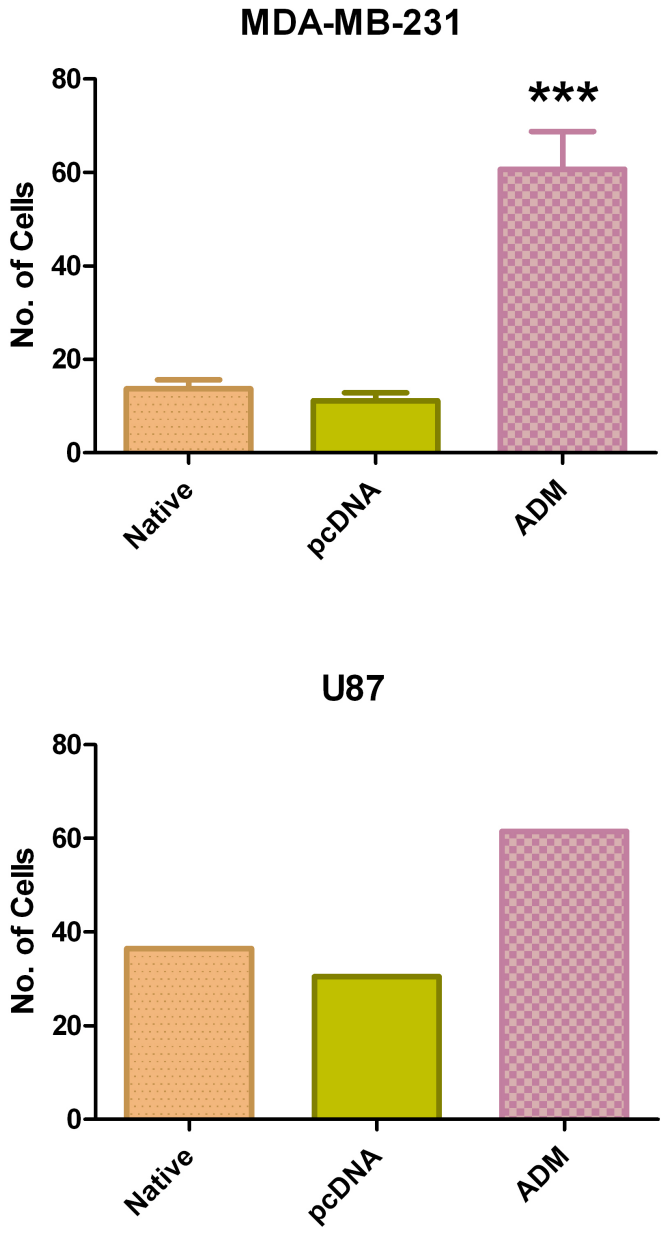

Figure 51*:* *In vitro* matrigel invasion assay in ADM and vector control (pcDNA3.1) transfected and non-tranfected breast cancer (MDA-MB-231) and glioblastoma (U87) cells. The error bars represent mean ± SEM. ANOVA and Tukey post hoc test was done to gain statistical significance. MDA-MB-231, n=3, $p<0.001$; U87, n=1.

3.4.1.5. Effect of ADM over-expression on Receptor Regulation

The effect of ADM over-expression on the regulation of RAMPs and CLR was done using Flow Cytometry. Histograms are shown in figures 101 to 103 under appendix section.

Table 9 shows the percentage of cell surface and total protein expression in MDA-MB-231 cells analysed by flow cytometry. The receptor expression analysis was carried out after normalising for any isotype background. Figure 52 contains graphs showing the percentage of cells positive for receptors in both total and cell surface. These analysis was carried out one time and due to technical difficulties discussed later, only n=1 was carried out.

Total Protein Expression in % of cell population			
	RAMP2	**RAMP3**	**CLR**
Native	25.5%	46.8%	25.2%
pcDNA3.1	20.1%	60.7%	27%
ADM	45.5%	72.8%	59.4%
Cell surface Protein Expression in % of cell population			
Native	1.29%	20.6%	4.7%
pcDNA3.1	4.6%	4%	1.7%
ADM	17.6%	29%	12.7%

Table 9: Percentage of cell surface and total protein expression in native, vector control and ADM transfected MDA-MB-231 cells. Protein expression analysis was carried out using flow cytometry. The expression analysis was normalised for any isotype background.

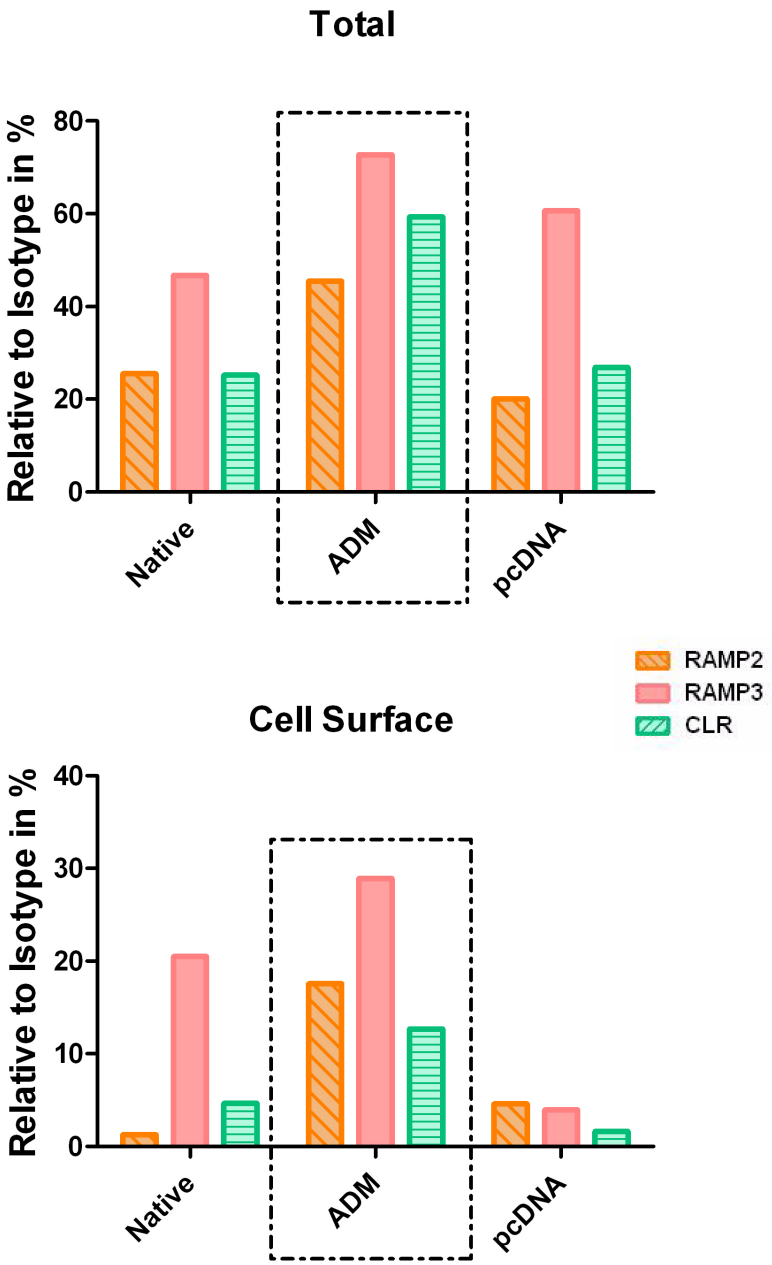

Figure 52: Flow Cytometric analysis of the expression of RAMP2, RAMP3 and CLR in breast cancer (MDA-MB-231) cells transfected with ADM, pcDNA3.1 and native cells. Bars show the protein expression at both total and cell surface normalised to isotype control. The quantified values are a result of 10,000 cells. n=1

3.4.1.6. Effect of ADM Over-Expression on bone homing *in vivo*

3.4.1.6.1. Generation of ADM over-expressing cells

Please Note: This section contains supplementary figure that was included here at the request of the examiners.

The effect of over-expressing ADM was tested on the bone homing potential of breast cancer cells (MDA-MB-231) *in vivo.* MDA-MB-231 cells transfected with GFP is the parental control. The bicistronic IRES-eGFP vector containing ADM cDNA was transfected into MDA-MB-231 cells. Flow cytometry was used to sort levels of GFP expression, as GFP expression is directly proportional to ADM expression in these cells. The cells after flow cytometry sorting were cultured to quantify the ADM expression. The images of these cells can be seen in figure Supplementary figure 3.4.1.6.1.1.

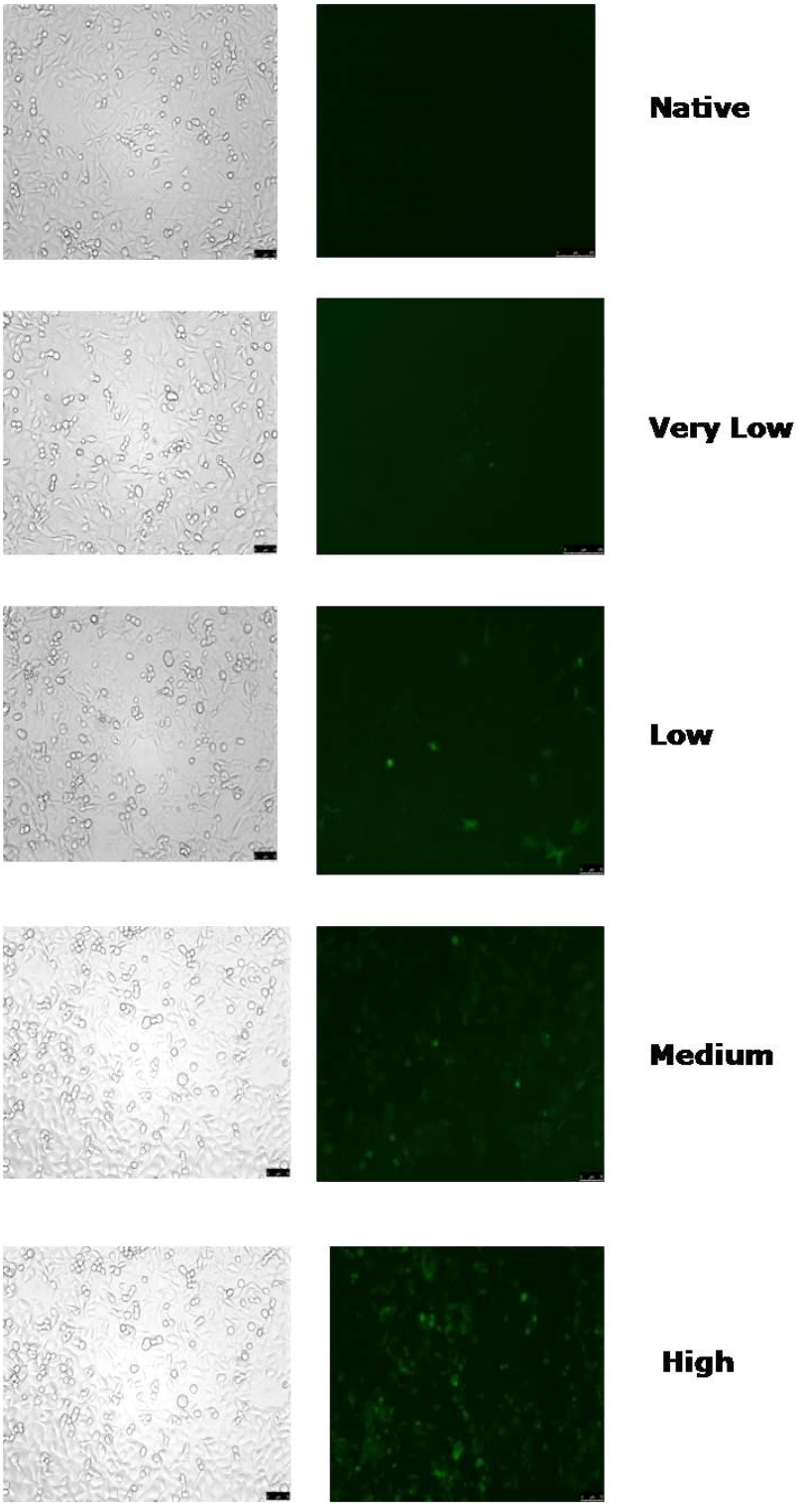

Supplementary Figure 3.4.1.6.1.1 : Images of breast cancer cells (MDA-MB-231) sorted by flow cytometry for different fluorescent intensities into very low, low, medium and high. Native cells do not have auto fluorescence. Pictures are taken of cells that are 90% confluent in T75 flasks. Bar = 250µm.

3.4.1.6.2. Quantification of GFP and ADM

Since GFP expression is directly proportional to ADM expression in the IRES-eGFP vector, I measured fluorescence to determine ADM expression. From figure 53, it can be seen that the GFP intensity was increasing from very low to high intensity group. Native cells show fluorescence to the level of the very low group; this is due to auto fluorescence of cells.

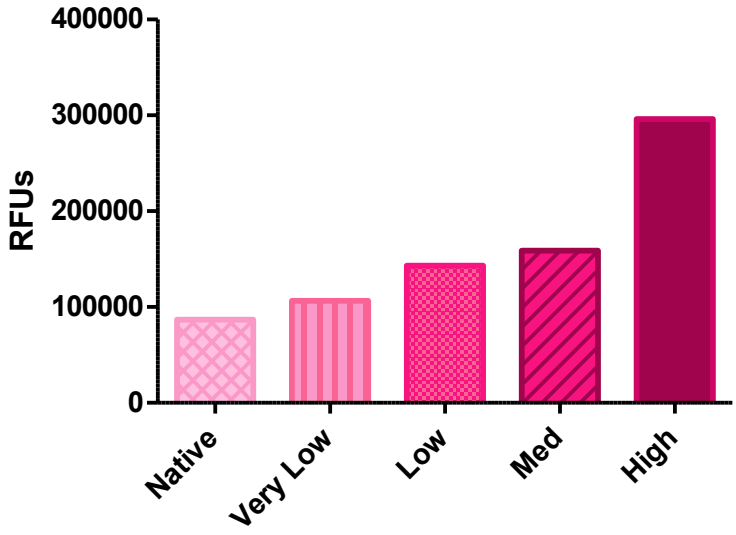

Figure 53: GFP fluorescent intensity of breast cancer cells (MDA-MB-231) sorted for varying fluorescent intensities. The GFP intensity was measured using a plate reader at 480nm excitation and 500nm emission.

Since Native cells showed auto fluorescence, in order to be 100% certain that MDA-MB-231 cells do not have GFP, RT-PCR was done for GFP expression. As it can be seen from figure 54, native cells do not express GFP (700bp). HPRT1 is expressed by all cell lines (210bp).

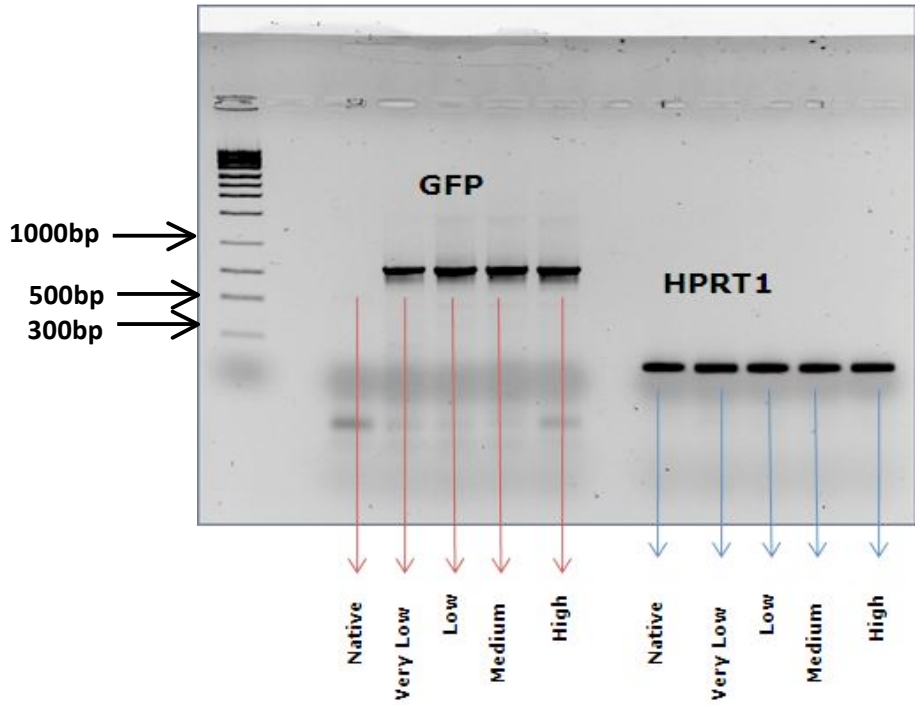

Figure 54: Gel electrophoresis of GFP and HPRT1 RT-PCR in MDA-MB-231 cells transfected with IRES negative control vector. For both GFP and HPRT1 bands, from left, the products belong to native, very low, low, medium and high groups.

The gel electrophoresis image was quantified in ImageJ by measuring the pixels in the bands. From figure 55, it can be seen that the native cells expressed no GFP, whereas the GFP expression was less in the very low group when compared to the other groups.

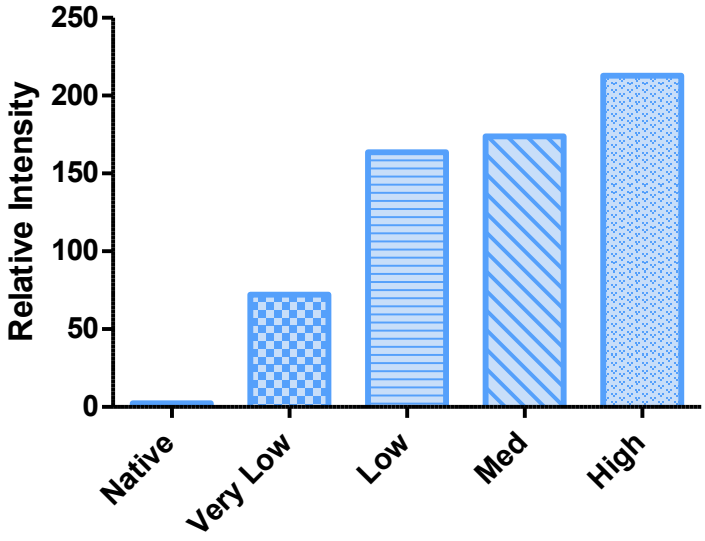

Figure 55: GFP mRNA expression by MDA-MB-231 cells correlated with the performed intensity of fluorescence of the sorted groups.

In order to confirm the over-expression of ADM in transfected cells, RT-PCR was done for ADM and HPRT1. Figure 56, shows the gel electrophoresis image of ADM and HPRT1. The product sizes of both ADM and HPRT1 were 210bp.

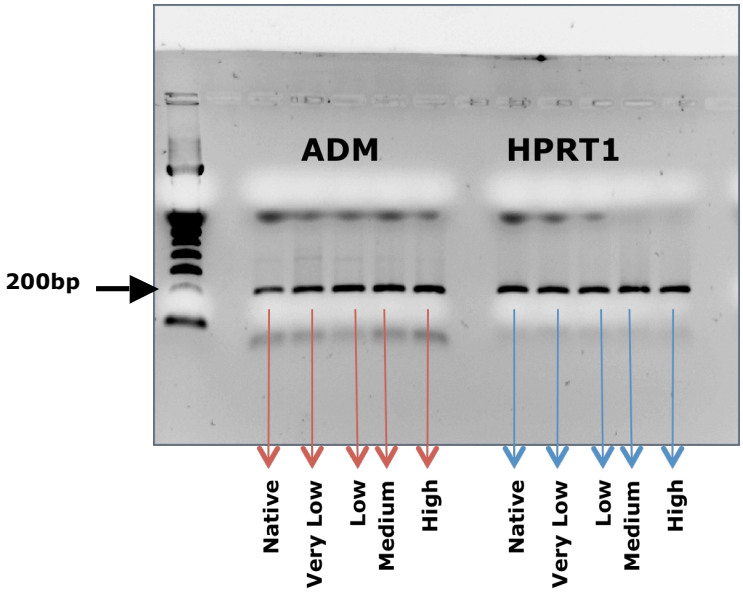

Figure 56: RT-PCR gel electrophoresis for ADM and HPRT1 as endogenous control in ADM transfected breast cancer cells (MDA-MB-231) sorted for different GFP intensities.

The intensities of the bands were measured as pixels in Image J and the relative intensity was calculated from the expression of HPRT1 in each sample. From figure 57, it can be seen that ADM expression was more in transfected cells when compared to native cells. There was 1.2 times more ADM in transfected cells (from low to high) than non-transfected cells.

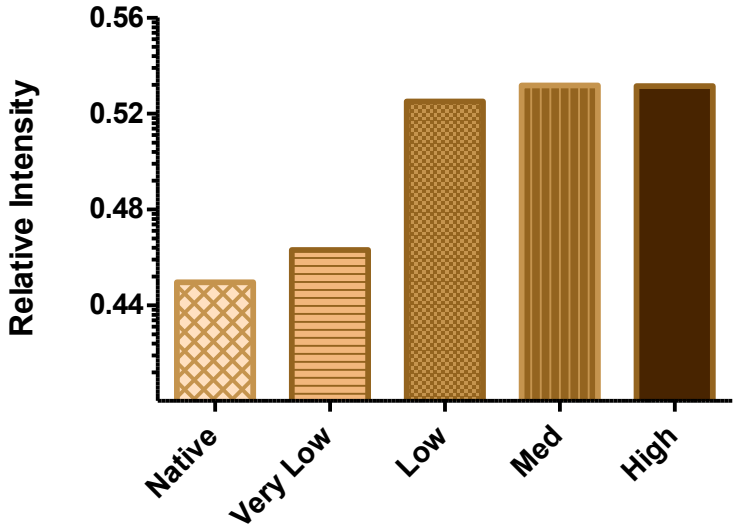

Figure 57: Relative intensity of ADM mRNA expression normalised to HPRT1 mRNA expression.

3.4.1.6.3. IRES-eGFP Negative Control

The IRES negative control vector for ADM was transfected into MDA-MB-231 cells. Cells were sorted according to fluorescent intensities into very low, low, medium and high, as previously described. Sorted cells were cultured in a six wells plate and fluorescent intensity was measured using a plate reader at 485nm excitation and 480nm emission. From figure 58 it can be seen that the GFP intensity increased from very low to high intensity groups. Native cells had low levels of auto fluorescence.

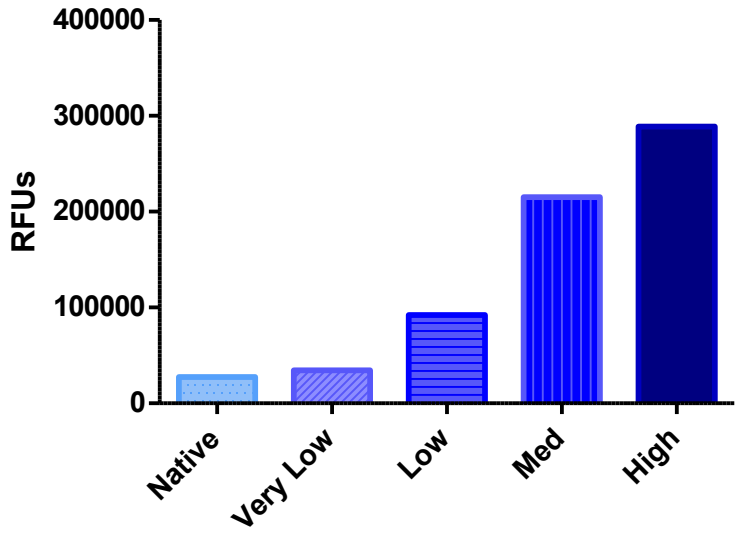

Figure 58: GFP fluorescent intensity in MDA-MB-231 cells transfected with IRES negative control vector. The intensity was measured using a plate reader at 485nm excitation and 480nm emission.

Since the IRES negative control vector expresses high amounts of GFP, ADM protein expression was measured from the cells after reading the fluorescent intensities in the six wells plate. Figure 59 shows the gel electrophoresis from native and four different GFP intensity groups. HPRT1 was used as a control. The product sizes for ADM and HPRT1 is 210bp.

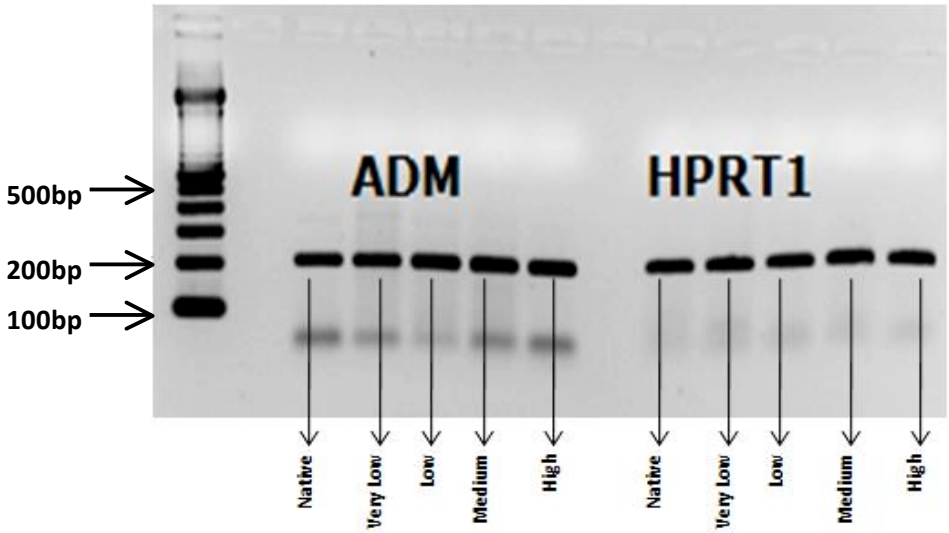

Figure 59: Gel electrophoresis of ADM and HPRT1 RT-PCR in MDA-MB-231 cells transfected with IRES negative control vector. The product sizes for both ADM and HPRT1 are 210bp.

The intensity of ADM and HPRT1 gel electrophoresis was measured in pixels and quantified in ImageJ. Figure 60 shows the relative intensity of ADM expression to HPRT1 as endogenous control. ADM expression remained same across all groups, showing that the cells transfected with IRES negative control vector expressed same amount of ADM as that of native cells.

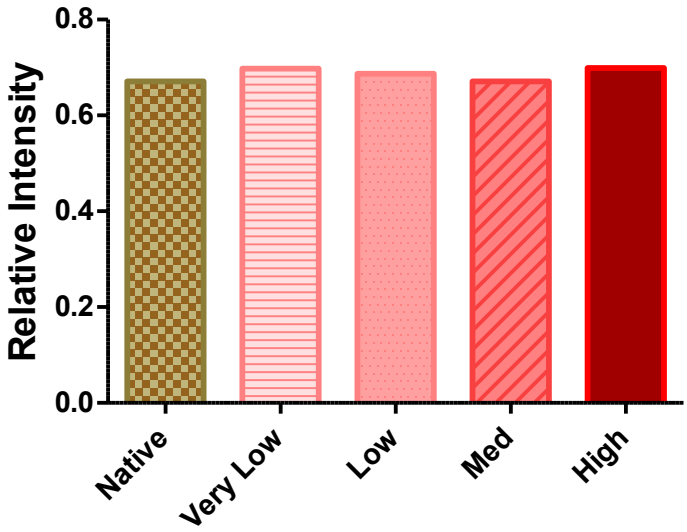

Figure 60: ADM mRNA expression quantified as relative intensity to HPRT1 in RT-PCR. The intensity of the bands were measured in pixels and quantified. The expression of IRES negative control transfected cells are uniform.

MDA-MB-231 cells containing ADM-IRES vector, IRES negative control vector (Scrambled) along with cells (parental) containing just GFP and no GFP were cultured in T25 flasks. The cells were sorted for GFP using flow cytometry. The flow cytometric histograms of these cells can be seen in figure 61. Upon quantifying for high intensity GFP for 500,000 cells, both parental and scrambled cells showed ~100% of cells in high intensity region. Only 56% of ADM transfected cells were present in the high intensity region.

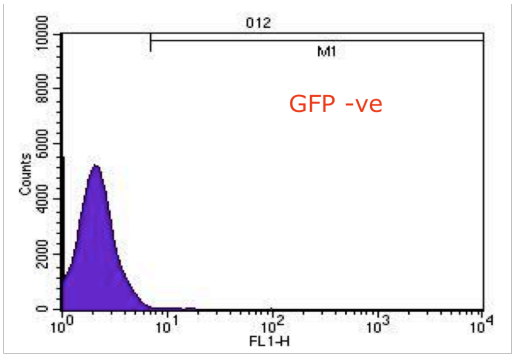

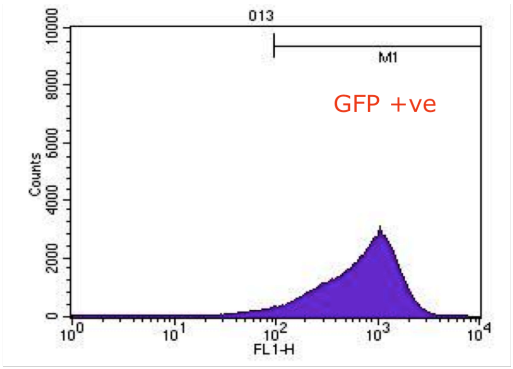

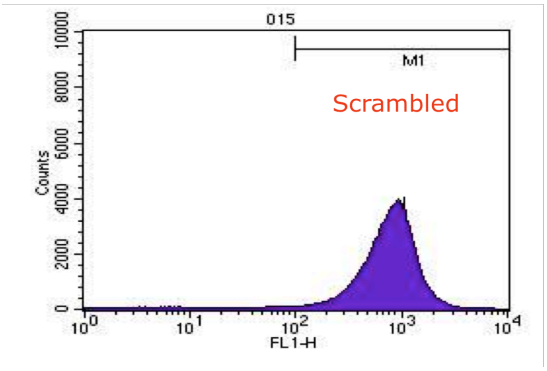

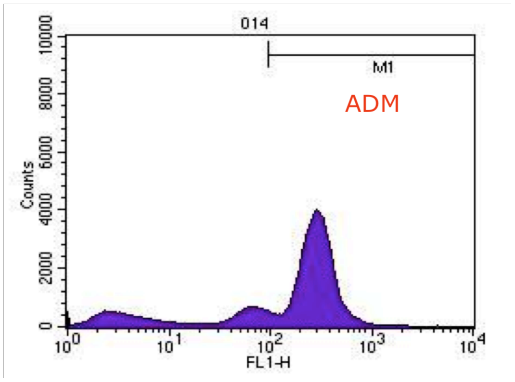

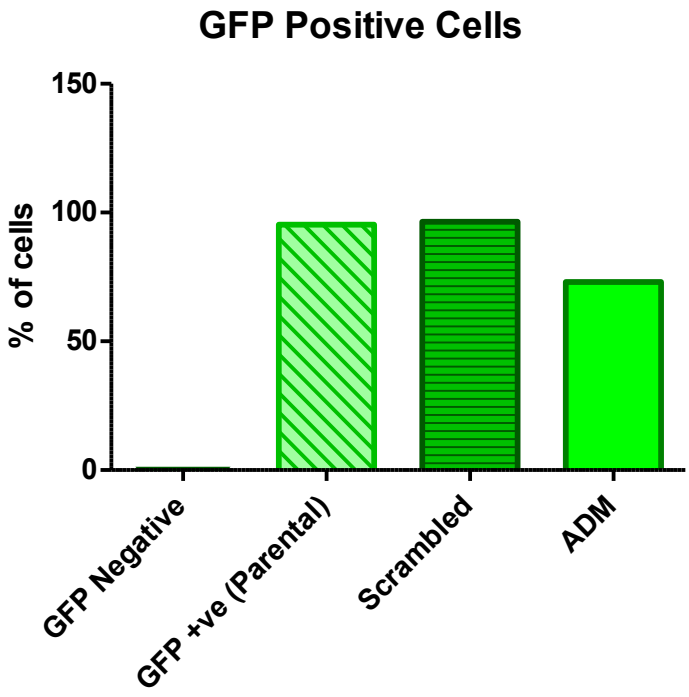

Figure 61: The histograms show the GFP positive cells in MDA-MB-231 parental both positive and negative for GFP, scrambled and ADM IRES transfected cells. The graph shows the quantified flow cytometric analysis of GFP positive for high intensity GFP out of 500,000 cells that were counted.

3.4.1.6.4. *In Vivo*

$1x10^5$ cells/mice were injected into into the left ventricle of the heart of Female Balb/ C nude/ nude mice. Body weights were measured twice weekly. The body weights of mice from the three groups are shown in figure 62. There was no statistically significant difference in body weights between three groups of mice.

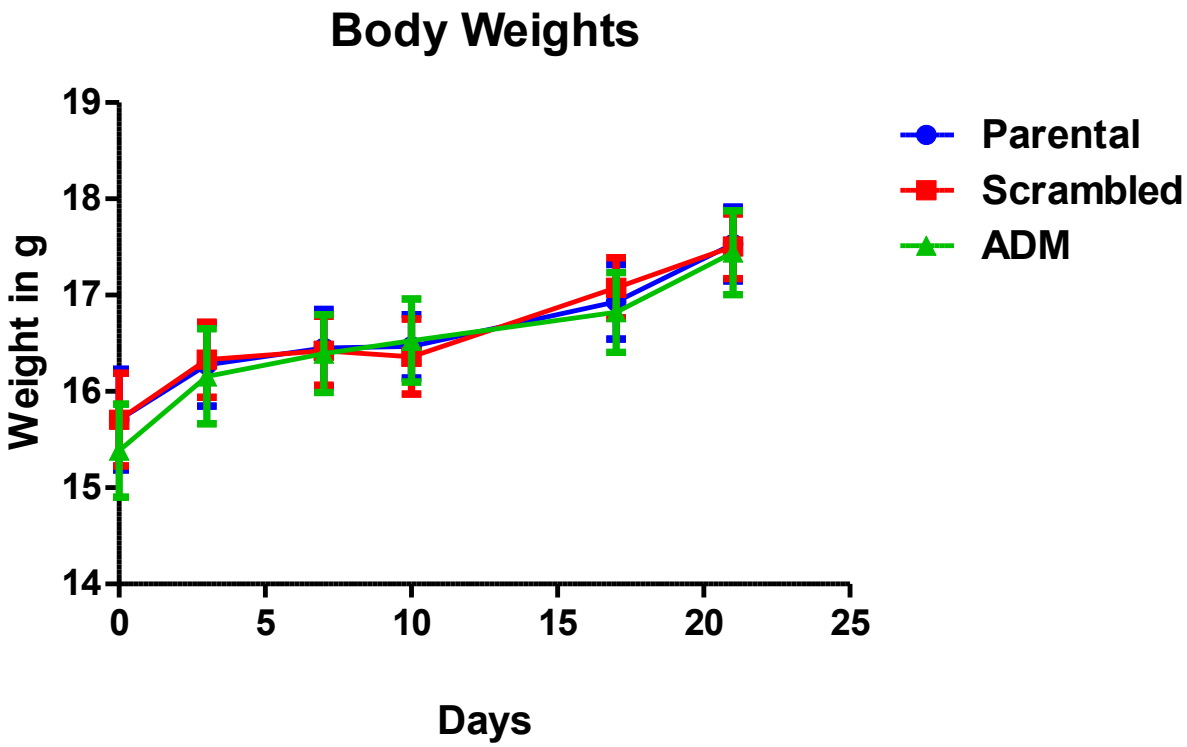

Figure 62: Body weights of mice injected with MDA-MB-231 cells, over 20 days from the start of injection, measured weekly. There was no significant difference in body weights between groups. ANOVA and Tukey post hoc test was performed to gain statistical significance.

Parental, n=13; Scrambled, n=13; ADM, n=14;

Two weeks after inter-cardiac injections of cells, animals were culled and hind legs were stripped of muscle and tumours were viewed under Light Tools. Figure 63 shows representative pictures of left and right legs from the three groups of mice. Bright green spots in the proximal femur, distal femur, proximal tibia and distal tibia of the bone show presence of tumours. It can be seen that both the parental and scrambled have tumour in the bone while mice injected with ADM transfected cells did not have any tumour in the legs.

Images of all the mice can be seen in figures 114, 115 and 116 in appendix section.

Parental

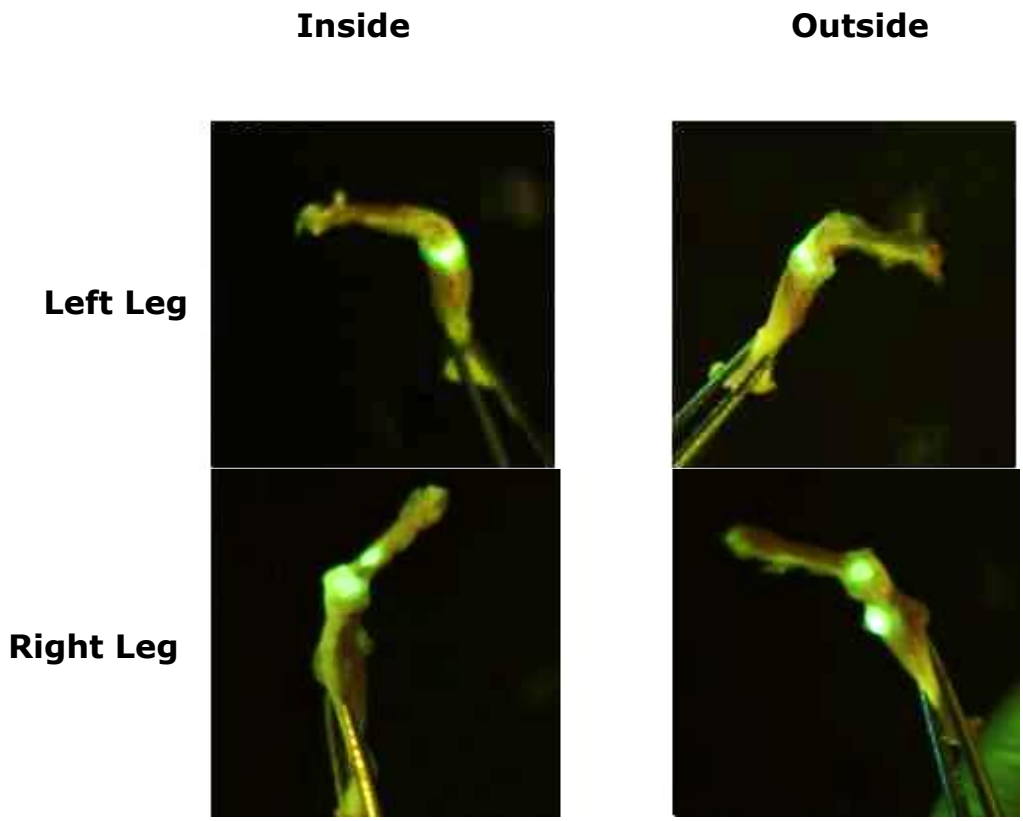

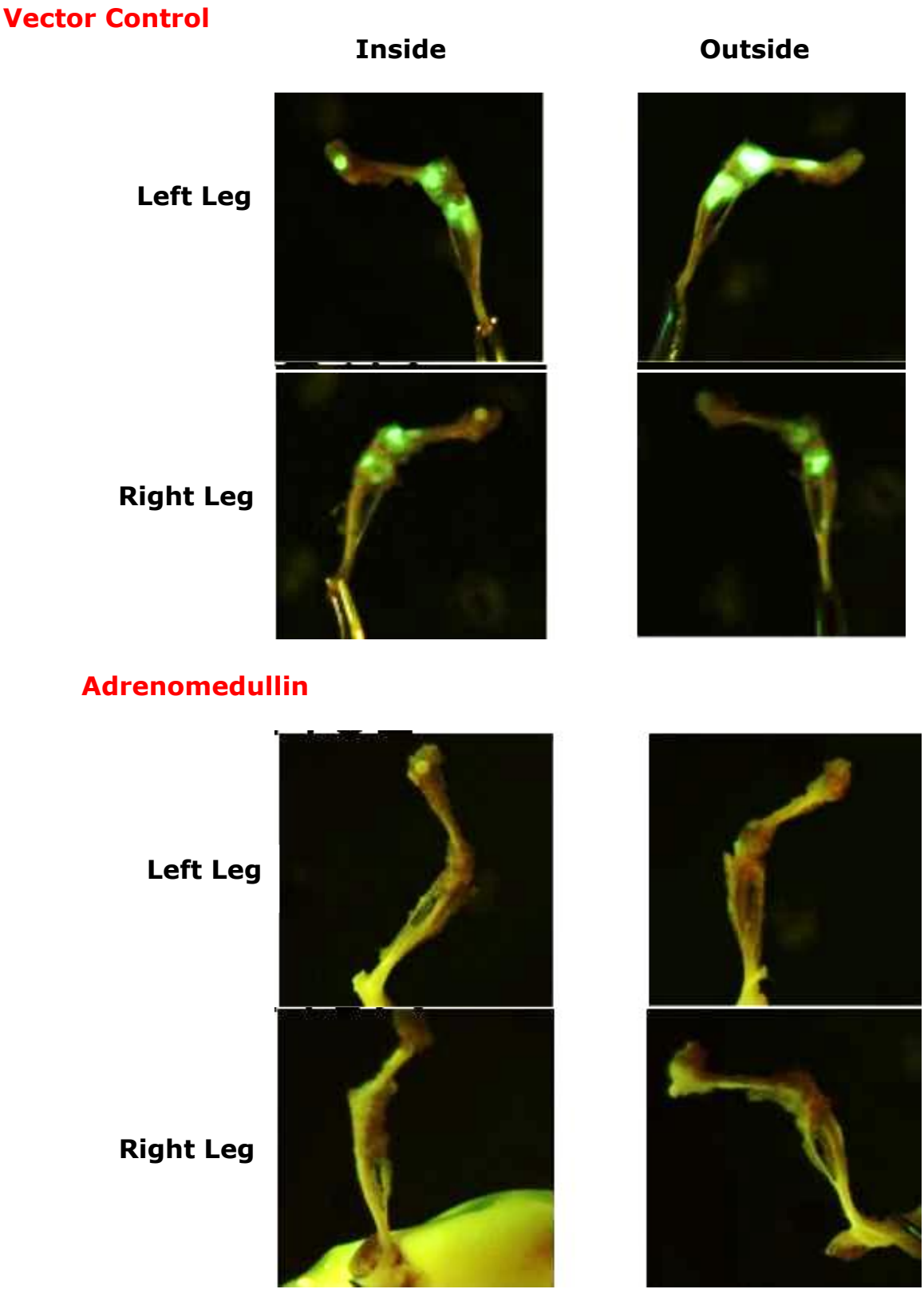

Figure 63: Representative pictures of left and right legs of mice injected with MDA-MB-231 cells with three different backgrounds. Tumours in bone can be seen as bright green spots due to GFP.

Table 10 shows the number of tumours counted in hind legs of each of the three groups of mice. Tumours were counted as described in section 3.3.2.7. Fluorescent tumours were visible in the parental and scrambled legs (3 and 5 respectively) but none were visible in the legs from mice injected with ADM over-expressing cells.

	No. of Mice	Tumour Count	Average Tumour Count
Parental	13	39	3
Scrambled	13	67	5.1
ADM	14	0	0

Table 10: Number of tumours present in each group of mice. Both legs were used to count the number of tumours and groups A and B are pooled together for analysis.

3.4.1.6.5. Over-Expression of ADM Receptors

In order to investigate the effect of over-expression of ADM receptors (RAMP2 + CLR and RAMP3 + CLR), cell proliferation and migration were measured.

Cell Proliferation

The cell Proliferation of PC3 cells transfected with ADM receptors were assessed using MTT assay over a period of 10 days and six independent experimental replicates were performed for each time point. The mean absorbances of native, pBUDCE4.1, RAMP2+CLR, and RAMP3+CLR transfected

cells are shown in table 11. Figure 64 shows the consolidated result of the proliferation of PC3 cells.

	Native	pBUDCE4.1	RAMP2	RAMP3
Day 0	0.29±0.02	0.32±0.04	0.30±0.02	0.34±0.30
Day 2	0.29±0.04	0.35±0.06	0.29±0.05	0.29±0.07
Day 4	0.43±0.14	0.26±0.04	0.36±0.07	0.39±0.11
Day 6	0.66±0.49	0.48±0.17	0.40±0.16	0.41±0.16
Day 8	0.77±0.55	0.45±0.20	0.46±0.28	0.52±0.40
Day 10	0.50±0.22	0.35±0.11	0.36±0.21	0.40±0.29

Table 11: Mean absorbances (OD) of proliferation of native, vector control and RAMP2/3+CLR transfected PC3 cells. Proliferation was assessed by MTT assay. OD values were measured at 570nm. The values are mean from 6 independent experiments.

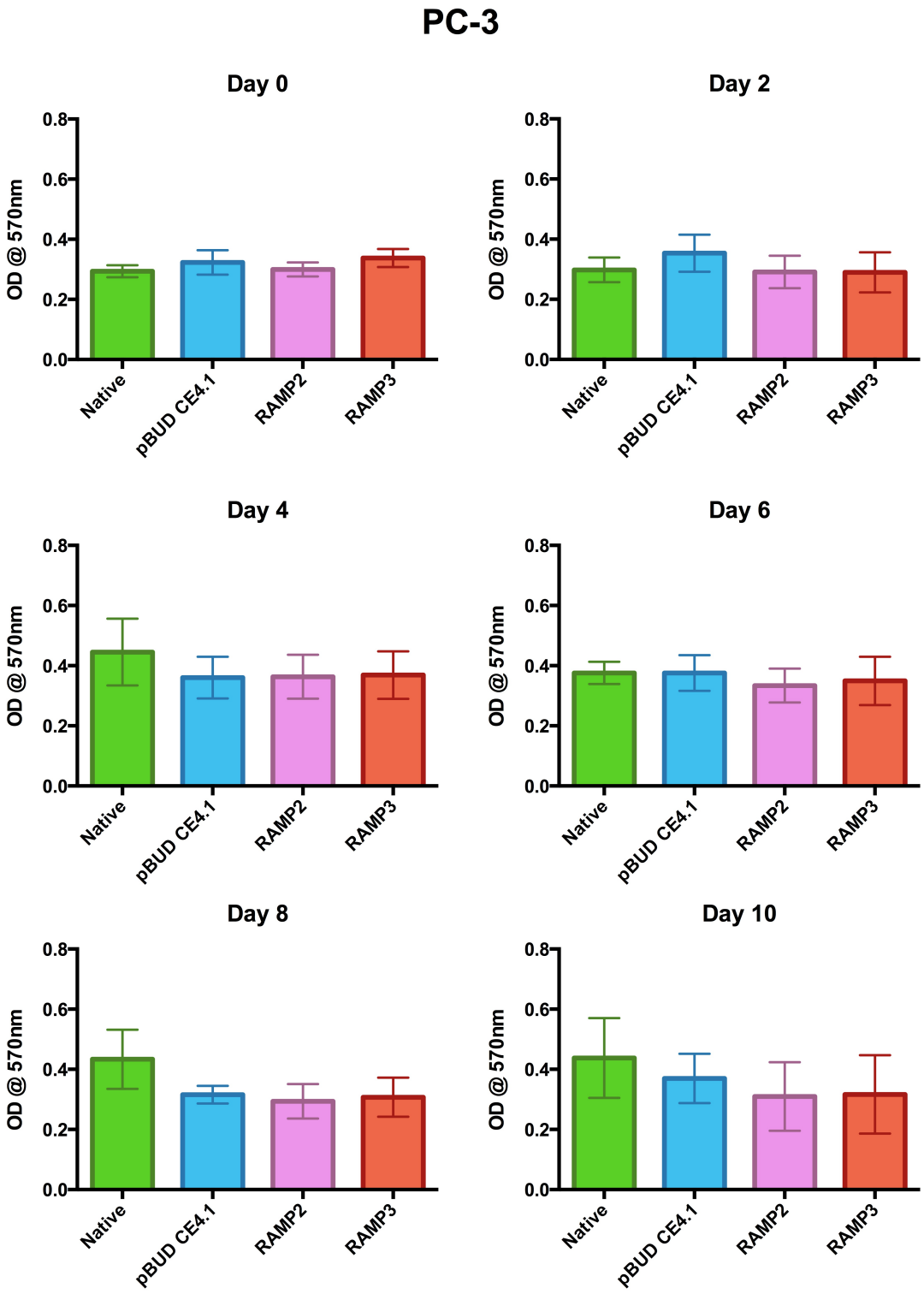

Figure 64: Proliferation of PC3 cells transfected with RAMP2+CLR, RAMP3+CLR, and vector (pBUD.CE.4.1) as determined by the MTT assay. OD values are plotted as mean± SEM and statistical significance was determined by a one way ANOVA and Tukey's multiple comparison post hoc test. n=6; $p<0.05$

Cell Migration

Would healing assay / Scratch test was perfored to assess PC3 cells migration. Figure 65 shows the migration of native and PC3 cells transfected with RAMP2+CLR and RAMP3+CLR, stained at various time points of the assay. The distance between the scratch was measured using ImageJ.

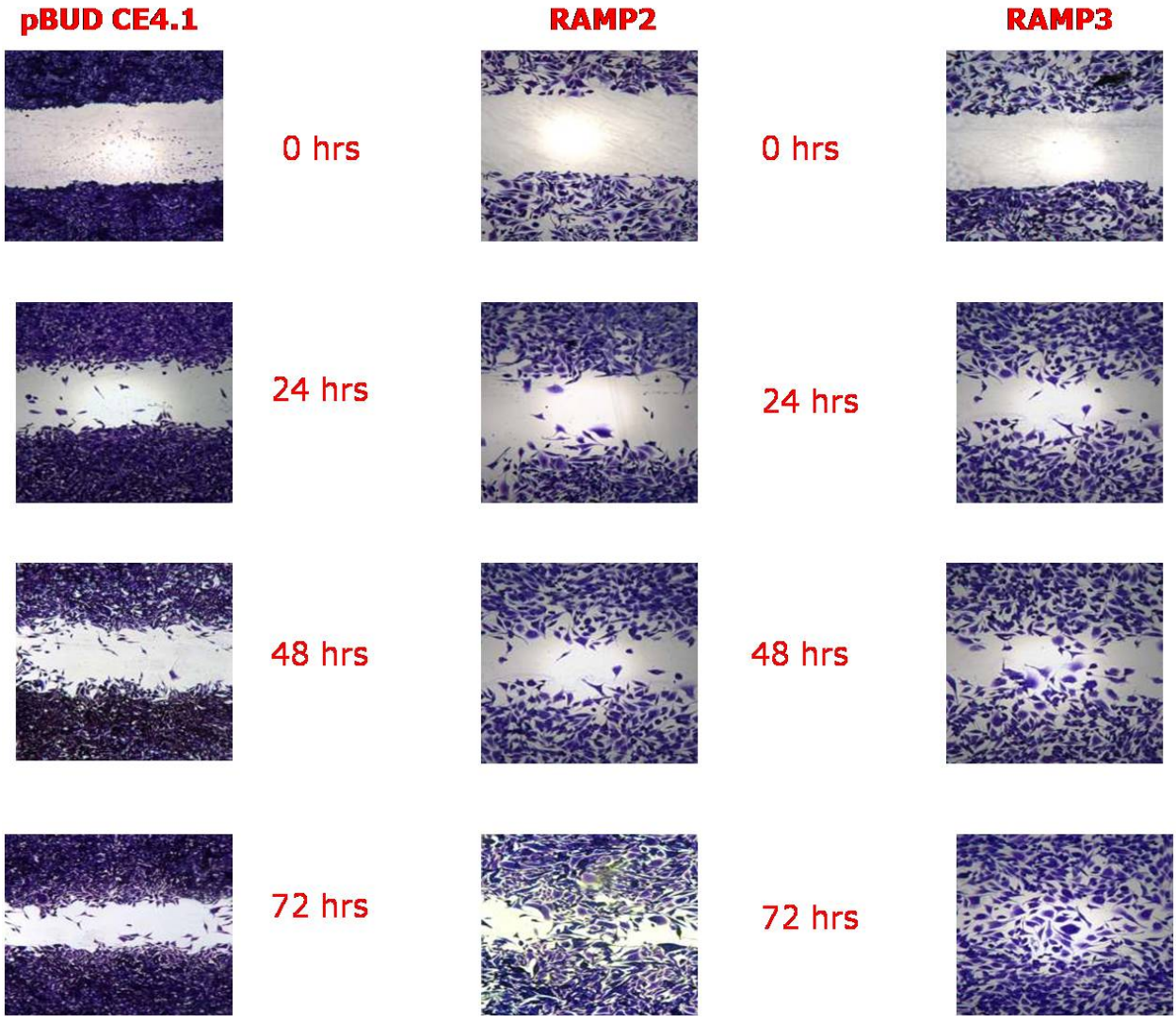

Figure 65: *In vitro* wound healing assay / migration assay to determine the migration of prostate cancer (PC3) cells transfected with pBUDCE4.1 vector control, RAMP2+CLR and RAMP3+CLR in wound healing assay. Cells were fixed in methanol and stained with crystal violet at appropriate time points. Images were taken in 10X magnification in LeicaDMI4000B microscope.

The mean distances of Native, pBUDCE4.1, RAMP2 and RAMP3 are shown in table 12. Figure 66 shows the consolidated results of the migration assay of three independent experimental repeats.

At 0hrs, 24hrs and 48hrs, there was no significant difference between RAMP2/3 over-expressed cells and control cells. Although native cells migrated faster from 24hrs.

At 72hrs, RAMP2+CLR transfected cells migrated 109% to 143% faster than control cells. RAMP3+CLR transfected cells migrated 120% to 148% faster than control cells.

	Native	**pBUDCE4.1**	**RAMP2**	**RAMP3**
0hrs	589.70±11.0	577.35±20.90	582.45±32.13	589.98±3.53
24hrs	440.59±20.53	563.02±63.0	549.22±16.60	535.28±5.80
48hrs	307.20±50.68	512.40±20.19	519.95±36.78	460.04±46.50
72hrs	277.22±25.37	529.26±17.45	424.78±42.11	396.70±27.76

Table 12: Mean distances between the two edges of the scratch in native, vector control and RAMP2/3+CLR transfected PC3 cells. The distances were measured in μm using ImageJ. The values are a mean of 3 independent experiments.

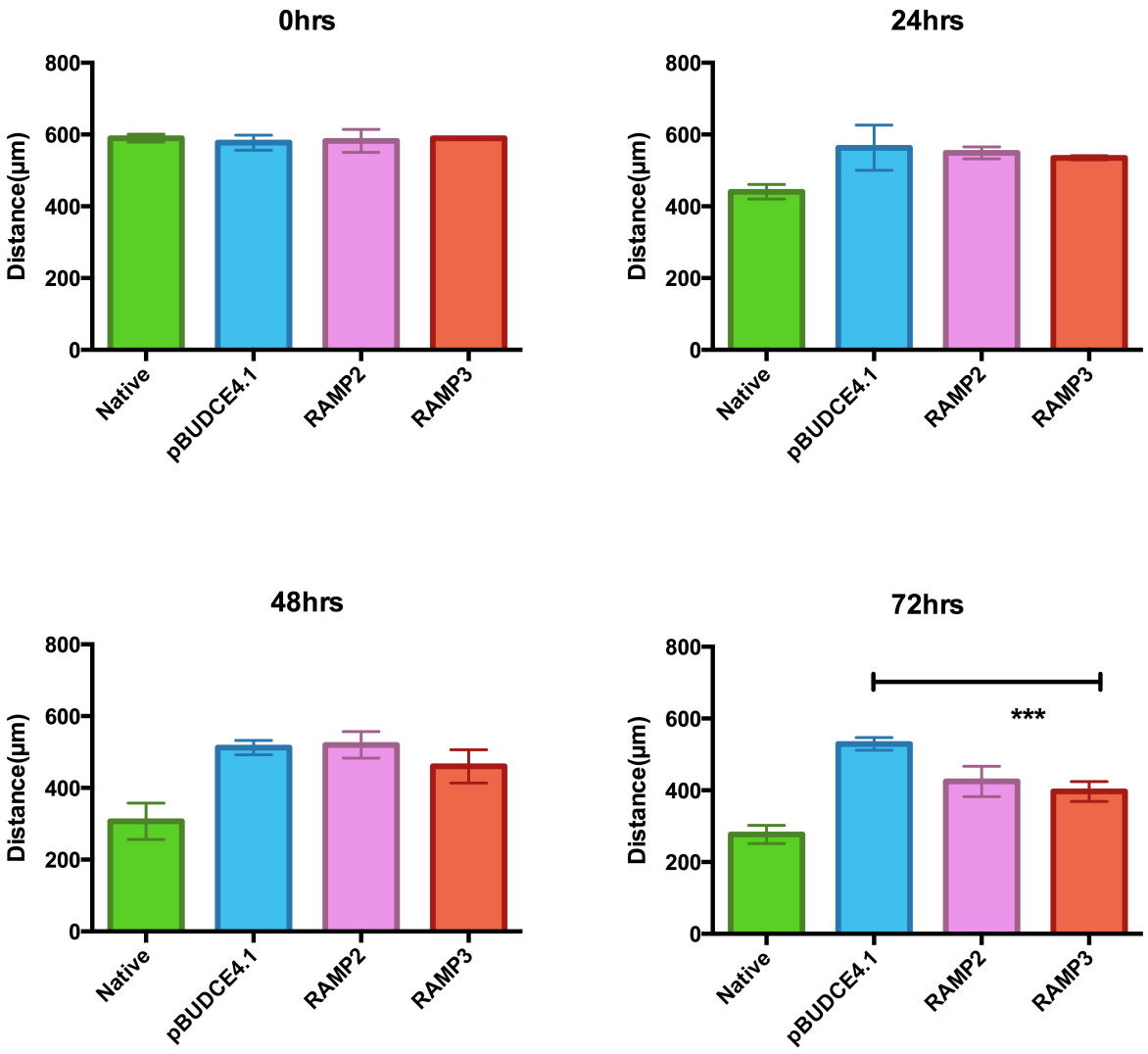

Figure 66: Quantification of *in vitro* wound healing assay / migration assay in PC-3 cells transfected with RAMP2+CLR, RAMP3+CLR, pBUDCE4.1 (vector control) and non-transfected cells. Bars represent the distance cells migrated toward the centre of scratch from the scratch edge. Data is shown as mean ± SEM and statistical analysis was performed by using ANOVA and Tukey's multiple comparison test. n=3; $p<0.05$.

3.5. Technical Discussion

This part of the project was aimed at determining the effect of ADM over-expression on cells and their ability to metastasize to bone.

3.5.1. Effect of ADM on Cell proliferation

The effects for over-expression of ADM were observed in both the cell lines for breast cancer (MDA-MB-231) and prostate cancer (PC-3). No significant proliferation was observed in MDA-MB-231 cell lines transfected with pcDNA3.1, ADM, and native cells. Similar results were recognized by Martinez *et al*, 2002 while working on breast cancer cells (T47D). The study identified that effect of ADM over-expression on enhanced proliferation can be observed only in the presence of serum otherwise ADM over-expression can also work as non-proliferative factor (Martinez et al. 2002). Since the observations in the present study by us were in the presence of serum, no proliferation was noted this could be due to the cells achieving their maximum proliferative potential.

No significant proliferation for prostate cancer line (PC3) transfected with pcDNA3.1, ADM and native cells was observed. Similarly study by Rocchi *et al*, 2001 recognized that cell lines transfected with ADM has no significant proliferation as compared to other cell lines. The study also revealed that cell lines transfected with ADM and vector control has no significant difference in cell proliferation over 10 days (Rocchi et al. 2001). However, in the present study significant difference in proliferation in native cell line was seen as compared to pcDNA3.1 on 10th day. The proliferation in native cell line was 1.4 times more than vector control transfected cells. This finding is in the accordance to the evaluation of Rocchi *et al*, 2001 which confirms that ADM over-expression can also act as non-proliferative factor. Since the PC3 native and ADM over-expressing cells have achieved maximum levels of ADM, the cells might have stopped ADM transcription. The reduced levels of ADM thus hold the proliferation process as a negative feedback system. Another plausible explanation why ADM over-expressing cells do not have an effect on cell proliferation is that cells would have already attained their maximal proliferative potential using endogenous factors.

3.5.2. Effect of ADM over-expression on Cell migration

Cancer cells need to detach from the basement membrane and migrate in order to cause metastasis. An immune-histochemical study by Harper *et al*, in 1996 identified expression of VEGF in prostate cancer cell lines PC3 and DU-145. VEGF in the cytoplasm of neuroendocrine cells is capable of producing response by activating its receptors VEGFR1 and VEGFR2 (Harper et al. 1996). Activation of these tyrosin kinase receptors can activate PIP3 which in turn activates actin polymerization. Continuous activation and deactivation of actin leads to cell movement and migration (Cantley 2002). Over-expression of ADM in this project was observed to enhance migration in both breast cancer and prostate cancer cell lines. This might be due to transactivation of VEGFR and enhanced downstream signalling pathway. Correlating this information, it can be suggested that over-expression of ADM enhances cell migration in neuroendocrine cells like prostate and breast by enhancing the downstream signalling pathway of VEGF receptors.

3.5.3. Effect of ADM over-expression on Cell invasion

Effect of ADM over-expression on invasive property of cancer cells were observed on breast cancer cell line (MDA-MB-231) and Glioblastoma cell line (U87). Enhanced invasion in MDA-MB-231 cells was observed under over-expression of ADM. Since experimental repeats could not be carried out for U-87 cells, it is not possible to conclude if there was an increase in cell invasion. The mechanism of enhanced invasion due to over-expression of ADM was explained by Martinez *et al* in 2002. ADM over-expression causes certain morphological changes in cells. ADM leads to elevation of gelsolin protein which is responsible for cytoskeletal restructuring of cells. Cells develop projections and the plasma membrane become more dynamic along with reducing cell adhesion. All these factors together enhance cell migration and thus the cells over-expressing ADM become more invasive and thus become more involved in metastasis (Martinez et al. 2002).

3.5.4. Effect of ADM over-expression in Receptor Regulation

A possible up-regulation of ADM receptor components - RAMP2, RAMP3, and CLR in presence of ADM over-expression was observed in MDA-MB-231 cells when compared to native and vector control cells in preliminary analysis. It cannot be concluded that there was a significant change is receptor regulation since the results are obtained from a single experiment. Although, upon reviewing the results from this single experiment, RAMP3 (29% cell surface and 73% total) expression was more when compared to RAMP2 (17% cell surface and 45% total) in ADM over-expressing MDA-MB-231 cells. Similar results were observed by Schwarz *et al* in 2006 while observing the effect of ADM over-expression on microvascular endothelial cells. The results showed that within 5-45 minutes of ADM treatment, cAMP levels increased in the cells followed by increased extracellular signal-regulated kinase 1/2 phosphorylation. The entire cascade leads to up-regulation of peptide and mRNA expression for VEGF, RAP2 and CLR, thus increasing receptor up-regulation (Schwarz et al. 2006). The flow cytometric histogram analysis of receptors on ADM over-expressing cells are shown in figures 101 to 103 in appendix section.

3.5.5. Effect of ADM over-expression on Bone Homing

Effect of ADM on bone homing was assessed *in vivo*. Only 56% of 500,000 MDA-MB-231 cells produced ADM as observed from flow cytometric analysis (figure 61). 90% of 500,000 GFP positive parental and scrambled (IRES-eGFP Negative control) produced ADM. The fluorescence from ADM-GFP positive cells had less intensity when compared to parental and scrambled controls. Since ADM-GFP positive cells were already less in number, it is plausible to conclude that either there were not enough ADM-GFP positive cells for successful bone homing or since cancer cells already produce high levels of ADM, after injecting these cells into mice, production of ADM would have been rendered to a stop. The failure of mice to produce ADM made the experiment a failure as the effect of these invasive cancer cell lines on bone homing was not observed. Similar results were observed by Calvo *et al* in 2002, while studying the effects of ADM

on PC3 cell lines. The study explained that the hormone refractory prostate carcinoma line is growth inhibited mainly by cAMP. It has been suggested that over-expression of ADM causes cAMP elevation which in turn inhibits growth of PC3 cell lines. The study also revealed that growth inhibition by the ADM over-expression is due to the G0/G1 cell cycle arrest. The elevated levels of ADM increase the number of cells in G0/G1 phase and thus reduce the percentage of cells in S/G2/M phase. The entire cascade finally results in reduced mitosis and thus reduced bone homing and tumour formation (Calvo et al. 2002). The same effect might have reduced bone homing in MDA-MB-231 cell line transfected with ADM in the present study.

3.5.6. Effect of ADM receptor over-expression

To understand the effect of ADM receptor over-expression on cell proliferation and cell migration, PC3 cell lines were transfected with ADM receptors RAMP2 + CLR and RAMP3 + CLR. Interesting cell proliferation patterns were observed. It was found that difference in cell proliferation of lines transfected with ADM receptor and the control line was not significant on day 0, 6, 8, and 10; but significant proliferation in receptor transfected cell lines was seen on day 2 and 4. This finding suggests that over-expression of ADM receptor initially increased ADM action and thus proliferation increased but after that elevated levels of ADM was sensed by the cells and cells stopped ADM transcription. Increased ADM levels thus acted as negative feedback mechanism and over-expression of ADM mediated by over-expression of ADM receptors acted as a non-proliferative factor. This finding was in accordance to the negative feedback hypothesis for ADM for cell proliferation as suggested by Rocchi *et al,* 2001. It also concludes that ADM can act as both proliferative and non-proliferative factor for cancer development.

It was observed that significant increase in cell migration of cell lines transfected with ADM receptors RAMP2 + CLR and RAMP3 + CLR started after 48 hours and cell migration continued to increase significantly upto 48 hours and 72 hours. This observation suggests that due to the over-expression of ADM

receptors, over-expression of ADM occurred. Over-expression of ADM in the cells could have caused transactivation of VEGFR and enhanced downstream signalling pathway. The downstream signalling pathway would have caused activation PIP3 that in turn activates actin polymerization. Continuous activation and deactivation of actin thus leads to cell movement and migration (Cantley 2002). It is also possible that over-expression of ADM receptors increased ADM production, resulting in morphological changes such as increased projection on cell membrane, increased dynamicity of plasma membrane, and reduced cell adhesion contributing to increased cell migration (Martinez et al. 2002).

3.5.7. Optimisation and Validation

ADM cloning

ADM cDNA in pOTB7 vector was cloned into pcDNA3.1 vector and sequenced. The sequencing result was run in BLAST and it showed a 97% match to ADM confirming that ADM was cloned into pcDNA3.1 vector (figure 100 in Appendix).

Various attempts were made to generate a negative control for ADM cDNA. Firstly the start codon was mutated from ATG to GGG so that ADM would not be generated. But sequencing results after site directed mutagenesis showed that the mutation did not take place (figure 104 in Appendix). Next a premature stop codon was made to incorporate after transcription of the first four amino acids. The sequence TCCGTCG was to be made to TAGTGAG, but again the mutation did not take place (figure 105 in Appendix). Since site directed mutagenesis was unsuccessful, commercially available negative control for the IRES-eGFP vector was bought and sequenced. BLAST result of the sequenced product showed 99% identity to a part of the Eukaryotic Translation Initiation Factor 4 gamma (figure 106 in Appendix).

Assessment of Migration

Migration of cells was assessed at set time points as described. There are two ways of assessing cell migration, one is by measuring the distance between the margins of the wound (scratch) and the other is by measuring the area of the wound (scratch). It was not possible to monitor cell migration on a single well over time, as it was very difficult to deduce the wound margin in a phase contrast microscope. Therefore fixing and staining cells at appropriate time points and either measuring distance or area would give a good measure of cell migration. The distance measured in the scratch was not very accurate as the scratch was not in a straight line and the linings of scratch were haphazard. Problems were also observed while measuring surface area as the wounded area gets converted to non-wounded area due to scratches and dust on the surface of the plate.

Monitoring ADM-IRES-eGFP over-expression in cells

MDA-MB-231 cells were transfected with GFP (parental), ADM-IRES-eGFP and IRES-GFP (scrambled or negative control). After transfection, cells were sorted by fluorescent intensities into very low, low, medium and high. Since the GFP expression is directly proportional to ADM expression in IRES-eGFP vector, the GFP intensity and corresponding ADM and GFP expression was measured. The results showed that higher the GFP expression, higher was the ADM expression. On the other hand, endogenous control HPRT1 remained the same in all groups. In the scrambled control, level of ADM did not vary with different GFP intensities. Therefore the cells with highest GFP intensity were chosen for *in vivo* experiment.

3.5.8. Conclusion

It can be concluded that ADM acts as both proliferative and non-proliferative factor for the development of both prostatic and breast cancer. ADM over-expression reduces proliferation in the cancerous cells as elevated levels of ADM acts as negative feedback (Mazzocchi et al. 1996). ADM over-expression could cause transactivation of VEGFR and enhances downstream signalling which leads to increased cell migration of cancerous cells. Studies have shown that morphological changes in plasma membrane of cells caused by over-expression of ADM leads to reduced cell adhesion and thus increased cell migration as well as cell invasion. Ability of ADM to increase the number of cells in G0/G1 phase and thus reduce the percentage of cells in S/G2/M phase could have led to reduction in cell mitosis and thus ADM over-expression reduces bone homing and tumour formation in cancer. The flow cytometry for screening GFP positive cells showed less fluorescence in ADM transfected cells when compared to parental and scrambled controls; this suggests that inside the animal system the vector switched off the production of ADM. This could be due to the presence of high levels of ADM within the tumour containing mice.

Over-expression of ADM receptors provides similar results for cell proliferation and cell migration as that of ADM over-expression. Study of over-expression of ADM receptor provides best support to the hypothesis that ADM can act as both proliferative and non-proliferative factor. Observations of cell migration pattern for ADM receptor over-expression concludes that the cell migration in cancer cells also increase with increase in number of ADM receptors.

Collectively, it is plausible to conclude that ADM acts as an important player for cancer progression and metastasis.

CHAPTER IV: NEUTRALISATION OF ADM ACTIVITY USING ANTI-RAMP3 ANTIBODY

4.1. HYPOTHESIS

Hypothesis

Neutralising RAMP3 significantly reduces cell growth in vitro and tumour growth in vivo

The aim is to determine the effects of the in-house generated anti-RAMP3 antibody (JF2) on cell proliferation *in vitro* and tumour growth *in vivo.*

4.2. INTRODUCTION

4.2.1. Treatment options for cancer

With better understanding of cancer pathophysiology along with development in diagnostic and treatment interventions, cancer can be diagnosed and treated in its early stages. The growing research in the field of cancer treatment has opened multimodality management and treatment plans for cancer patients. The research and development in the field of cancer is helping to develop and modify the present treatment options, hence to be more effective, precise, and lifesaving. The traditional treatment options for cancer include surgery, chemotherapy, and radiation therapy. Treatment options like immunotherapy and monoclonal antibody therapy are under rapid development phase. The cancer physician decides the treatment plan for any patient in accordance to the location and grade of the tumour as well as cancer stage and general state of patient. Goal of any cancer treatment is to completely remove the disease with minimal damage to rest of the body (Franklin 2007). This section discusses the presently available treatment options for breast, prostate, glioblastoma and pancreatic cancers.

Surgery

Surgery is normally considered as first line of treatment for cancers of breast, prostate, glioblastoma and pancreas. Although theoretically a surgery can entirely remove the cancer from the patient, it is practically not always possible due to the tendency of cancer cells to metastasize and affect the adjacent normal tissue or distant organs (Mayoclinic, 2011). Different studies over the years have shown that precisely performed surgical procedure can increase patient survival rate and reduce the chances of metastasis. The extremely malignant and fatal pancreatic cancer requires initial treatment with surgical process known as Whipple's procedure. Another study found that 10-20% patients treated with surgery followed by adjuvant therapy with Gemcitabin have higher chances of survival above five years as compared to non-operated patients (Oettle and Neuhaus 2007). A twenty year follow up study suggested that both radical mastectomy and breast conservative surgery of breast cancer

increases survival rate in almost 59% patients (Veronesi et al. 2002). Similar beneficial effects of oncosurgery are also observed by glioblastoma patients. Although glioblastoma is extremely fatal, complete resection along with lobectomy extends the survival time by 12.6-12.9 months (Hollerhage et al. 1991).

Chemotherapy

Since surgery do not provide guarantee for complete cure of cancer, the patients are always treated with multimodality approach. Chemotherapy with cytotoxic drugs is a treatment approach following surgery. The anti-cancer drugs interfere with cell division in various ways, e.g. with the duplication of DNA or the separation of newly formed chromosomes. Although chemotherapy presents certain adverse effects like compromised immunity, fatigue, alopecia and gastrointestinal distress; it is known to enhance overall life quality in many cancers (Balducci and Beghe 2001). A 17 year observatory study of breast cancer patients identified that induction chemotherapy followed to breast surgery not only increases disease free survival rate but also causes tumour regression and thus benefits in controlling breast cancer metastasis (Schwartz et al. 1993). Guidelines indicate surgery, hormone treatment and radiation as management for prostate cancer. Reviews suggest that advanced adenocarcinoma of the prostate after hormonal manipulation becomes relatively chemotherapeutic nonresponsive tumour and only 8.7% of such patients respond to any chemotherapy (Yagoda and Petrylak 1993). However, another study suggested that chemotherapy with mitoxantrone plus prednisone or prednisone alone for symptomatic hormone-resistant prostate cancer provides palliation by reducing pain and improving life quality. Similar palliative use of chemotherapeutic agents is done for the treatment of pancreatic cancer (Tannock 1996). Another study suggests that erlotinib (Tarceva) in combination with gemcitabine as a palliative regimen for pancreatic cancer can exhibit improved survival rates, improved tumour response and improved progression-free survival rates. On the other hand FDA (1998) approved gemcitabin only as palliative treatment for pancreatic cancer as it is known to improve survival rate by 5 weeks along with providing

symptomatic relief (Moore et al. 2007). Study by Stupp *et al* in 2005 observed no significant enhancement in survival rates of Glioblastoma patients treated with surgery plus radiation alone (12.1 months) as compared to Glioblastoma patients treated with surgery plus radiation plus Temozolomide (14.2 months) (Stupp et al. 2005).

Radiotherapy

Radiotherapy is another adjuvant therapy to surgery. If the cancer is localized to one area of the body, ionizing radiations can act as a curative therapy. The therapy can also be used to prevent tumour recurrence after surgery and to remove remnants of original malignant tumours after surgery. Radiation therapy is synergistic with chemotherapy, and has been used before, during, and after chemotherapy in susceptible cancers. Although radiations affect normal tissue, the fractionated treatment procedure allows the normal cells to repair themselves. The high effectiveness of radiation in reducing recurrences nullifies its minor side effects like gastrointestinal disturbances, mouth sores, edema, fibrosis, cognitive decline, and possibility for development of secondary cancer (Bomford *et al*, 2005, pg, 311). Radiotherapy is widely applied for treatment of breast cancer and prostate cancer. For women with localized ductal breast carcinoma in situ, radiation along with surgery reduces the recurrence chances by 10.4% to 7.5% for non-invasive cancers and from 10.5% to 2.9% for invasive cancers as compared to surgery alone approach (Fisher et al. 1993). Similarly for clinically localized prostate cancer, radiation therapy following surgery can increase 5 year survival rate of patients by 81-85% (Shipley et al. 1999). Radiation therapy in addition to surgery or surgery combined with chemotherapy has been reported to extend survival in Glioblastoma Multiforme (GBM) patients as compared to surgery alone. The adjuvant therapy increases survival from 3-4 months to 7-12 months (Stupp et al. 2005). However, the responsiveness of Glioblastoma Multiforme to radiotherapy varies and may even induce phase of remission. Regrettably, any type of response is transitory as the tumour typically recurs within 1 year, thus leading to further clinical deterioration and the emergence of a region of contrast enhancement (Stupp et

al. 2006). Due to the systemic nature of pancreatic cancer, use of radiation as adjuvant therapy is still debated. Considering the short survival span of such patients, radiation therapy is normally not applied to them (National Comprehensive Cancer Network, NCCN, 2011).

Recent advancements in cancer management include immunotherapy, targeted therapy, hormonal therapy, and angiogenesis inhibitor. Hormonal therapy's main principle involves the management of the endocrine system by administering certain hormones (eg.steroid hormones) or drugs which interferes with production or activity of these hormones. Since steroid hormones are responsible for gene expression in various cancers, manipulating levels or activity of these hormones lead to cancer growth cessation. Hormonal therapy is now used in treatment of prostate and breast cancer (Souhami et al. 2009). Researchers are also trying to develop angiogenesis inhibitor drugs which can prevent blood vessel formation and reducing cancer progression. In spite of problems like route of administration, maintenance of stability and activity and targeting at the tumour vasculature, angiogenesis inhibitor Bevacizumab is now officially used in treatment of breast cancer and glioblastoma (Kleinman and Liau 2001). Reports suggest that Bevacizumab is not very effective in treatment of breast cancer (Couzin-Frankel and Ogale 2011) but it provides significant improvement in cases of Glioblastoma (Burkhardt et al. 2012). Research and development for immunotherapy treatment is in a nascent stage. Cancer immunotherapy refers to an assorted set of curative strategies proposed to stimulate the patient's own immune system to fight the tumour. Trials are researching a vaccine-like immunotherapy strategy for prostate cancer namely Sipuleucel-T in which dendritic cells from the patient are stacked with prostatic acid phosphatase peptides to stimulate a specific immune response against prostate-derived cells. The targeted antibody treatment for cancer is discussed in detail in the next section.

4.2.1.1. Antibody treatment in cancer

Antibodies are crucial components of human immune system. Antibodies or immunoglobulin are huge heterodimeric molecules (150 KDa) and possess two different polypeptide chains. These chains are called heavy (~50kDa) and the light chain (~25kDa). The antibody recognizes a unique part of the foreign target, called an antigen. Figure 67 shows the diagrammatic representation of antibody. The main functions of these antibodies are to identify and neutralize any foreign material in the body like microbes. Structurally immunoglobulins G are Y-shaped proteins which are produced by B-cells. The structure of immunoglobulin has two main parts namely Fab (fragment-antigen binding) and Fc (fragment constant). The tip of Y shaped antibody (Fab) carries a portion called paratope composed of three hypervariable amino acid domain. These specific amino acids provide specificity to each antibody. Paratop acts by lock & key mechanism and thus binds to specific epitope. By this binding technique, an antibody tags the foreign material like microbes or abnormal cell and easily displays the target to the further immune cascade. The antibody can also directly neutralize the target by binding in this manner with the antigen, e.g. by blocking essential part of microbe, which is crucial for invasion and survival (Janeway, 2001).

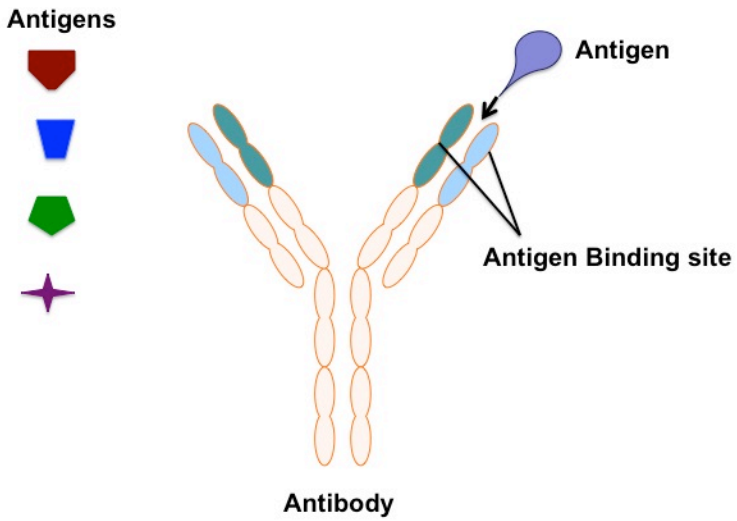

Figure 67: Structure of antibody showing the light chain and heavy chain. The antigen binding site is shown where the antigen binds to. Figure drawn by self.

There are five known antibody subclasses all of which are involved in Antibody-dependent cellular cytotoxicity. The IgA subtype is found in areas consisting mucous like gut and respiratory track and is mainly responsible for preventing colonization of antigen. Immunoglobulin IgD acts as antigen receptor on B-cell and initiates basophil and mast cell activity after antigen-antibody binding. IgE is mainly involved in allergic reaction and triggers histamine secretion from basophils and mast cells after binding with allergens. The majority of antibody-mediated immunity to fight the invading pathogens is provided by four subclasses of immunoglobulin IgG. The other advantage of IgG over others is its capacity to pass placenta and provide fetal immunity. The immunoglobulins IgM is expressed on the surface of B-cells and are responsible for killing pathogens in very preliminary stage, before the action of IgG, via B-cell mediated immunity (Roux 1999).

4.2.1.2. Monoclonal Antibody Therapy for Cancer

Monoclonal antibody therapy for cancer utilizes monoclonal antibodies to specifically bind to a particular target like cancer cells or receptors present on cells. Monoclonal antibodies (mAb or moAb) are specific antibodies which are developed by sophisticated techniques and are identical to each other as they are clones of unique parental immune cell. Monoclonal antibodies differ from polyclonal antibodies, which are composed of different types of immune cells. This property of monoclonal antibody provides it monovalent affinity where unwanted immune response to other non-target cells can be prevented (Rang & Dale, 2003).

This specific activity of mAbs is now getting utilized in the treatment of cancer. Monoclonal antibodies like Bevacizumab, Cetuximab, Panitumumab, and Trastuzumab bind only to the specific antigens present on cancer cells only. Such binding of mAb to cell specific-antigen induces immunological cascade and ultimately vanishes the target cancer cell (Hudis 2007). Recent research in field of monoclonal antibody therapy is trying to develop mAb which can deliver

toxins, radioisotope, cytokine or other active conjugate to the target cell by binding to its cell-specific antigen (NCCN, 2011). Three main variances of modified mAb used in cancer treatment are radioimmunotherapy, antibody-directed enzyme prodrug therapy, and antibody-conjugated liposomes (immunoliposome) (Carter 2001).

US FDA approval of the anti-VEGF antibody for the treatment of metastatic colorectal cancer was based on the *in vivo* testing results of the treatment. It was found that the anti-VEGF antibody reduced the tumour growth in the mice implanted with grafts of colorectal tumour. The detailed analysis of related factors and histological samples of the tumour showed that the anti-VEGF antibody reduced the angiogenesis process mediated by VEGF (Ferrara 2004).

Presently, the human IgG1 isotype antibody is most widely used in cancer treatment due to its ability to induce human complement and get NK cells employed for ADCC (antibody-dependent cellular cytotoxicity). Also IgG1 has extended plasma half-life, which allows it to provide extended pharmacological action. Human IgG2 isotypes are used in conditions where mAb is expected to act only via its antigen binding property, e.g. anti-epidermal growth factor receptor antibody (Adams and Weiner 2005). However, another work identified that the most effective cytotoxic human cell, the neutrophills, are more effectively recruited by IgA as compared to IgG. Furthermore, IgA antibodies provide additional advantages like capacity to form dimmers naturally, improve tumour cell signaling for immunological response, and characteristic for active transportation into mucosal secretion. Thus IgA can prove to be better mAb for cancer of luminal surface as compared to IgG (Dechant and Valerius 2001). Research by Karagiannis *et al* in 2007 highlighted that antibody isotype IgE is more effective in treating ovarian cancer lines in mice as compared to the conventional IgG. The ability of IgE to engage cell surface IgE receptors on ovarian tumour cells and initiating phagocytic and cytotoxic mechanism helps it to reduce ovarian cancer cells more rapidly as that of IgG (Karagiannis 2007).

It was believed that IgM istoype cannot be utilized as monoclonal antibody due to its big size and limited capacity to move around and inside the target cell (Roux 1999). However, recent studies have suggested that IgM would have a slower penetration rate and would reach their tumour targets. Their slower penetration and accumulation would be advantageous if their role is to induce apoptosis (Vollmers and Brandlein 2006). For example, an IgM mAb – PAT-SM6 that binds to GRP78, a member of heat shock protein 70 family, is a potential anti-cancer drug. This drug has been cleared as a potential treatment for melanoma in phase I clinical trials (Rosenes et al. 2012).

4.2.1.2.1. Mechanism of tumour cell killing by Monoclonal Antibody

mAbs for cancer treatment acts by three main mechanisms namely direct tumour cell killing, immune mediated cell killing, and vascular and stromal cell ablation.

Direct tumour cell killing by mAb can be either achieved by receptor agonist activity or receptor antagonist activity. Acting as an agonist, the mAb bind to tumour cell surface receptor and initiates apoptosis as a normal physiological process to eliminate abnormal cells. mAbs can also act as antagonist and may cease crucial physiological functions of receptor and target cell like dimerisation, kinase activation, and downstream signalling. Inhibition of such important function may thus lead to reduced cell proliferation and even cell apoptosis. Many antibodies can also bind to important enzymes and cause enzyme neutralization and signal abrogation, ultimately leading to cell death.
For immune mediated tumour cell killing, mAbs induce immune response after binding to the cell-specific antigen. Such tumour killing can be achieved by various properties of mAb like induction of phagocytosis; ability for complement activation; and activation of antibody dependent cellular cytotoxicity. Certain mAbs also act on T-cells to provide immune mediated cell killing. Single chain variable fragment (scFv) of antibody targets genetically modified T-cells to the tumours. T-cells are also activated by antibody-mediated cross-presentation of antigen to dendritic cells. Many mAbs block the T-cell inhibitory receptors like

CTLA4 (cytotoxic T-lymphocyte-associated antigen) and allows the progression of T-cell mediated immune cascade (Scott et al. 2012).

As an additional mode of action, some mAbs induce vascular and stromal cell ablation by different methods such as vasculature receptor antagonism, ligand trapping, inhibition of stromal cells, direct delivery of toxins to stromal cells or vasculature (Scott et al. 2012). These mechanisms of action of mAbs are diagramatically represented below:

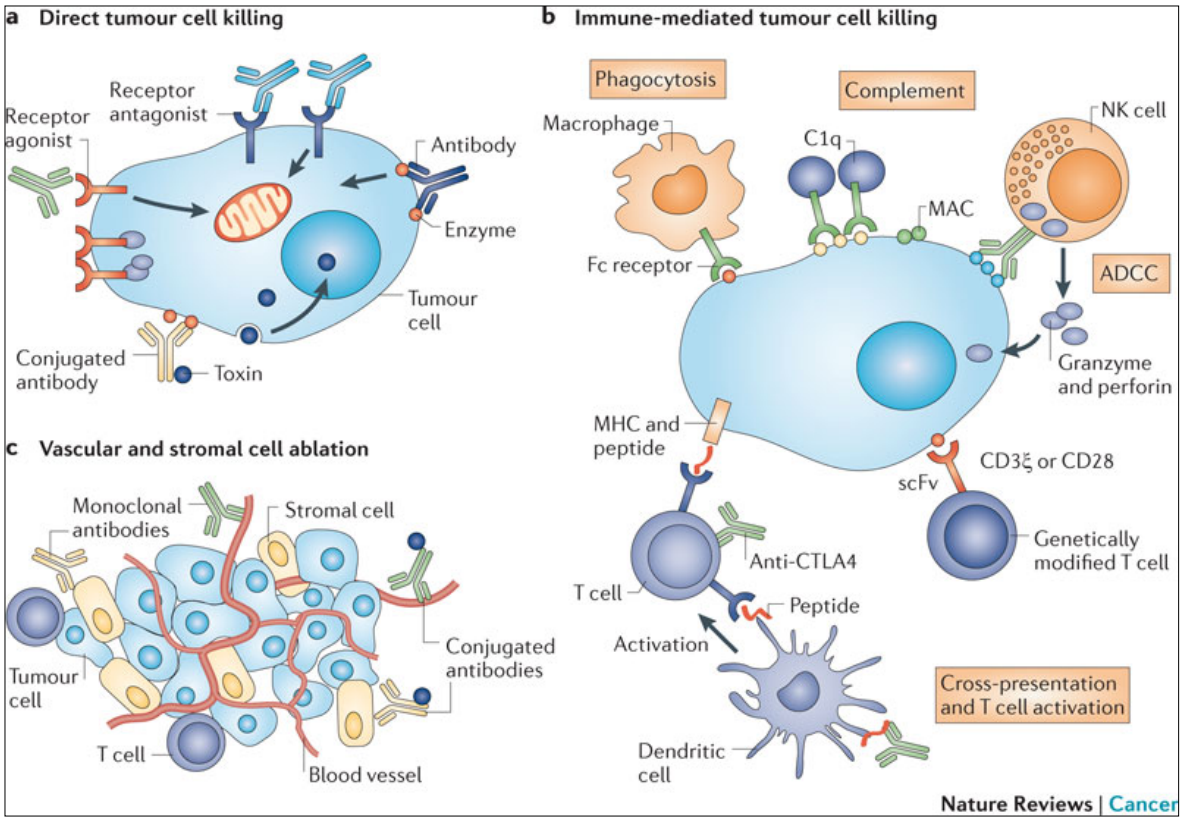

Figure 68: Mechanism of action of monoclonal antibody on tumour cells. **A)** shows the direct tumour killing in mitochondria, mediated by antibody binding to cell surface receptor **B)** immune mediated tumour killing in phagocytosis, complement activation, antibody-dependent cellular cytotovicity (ADCC), genetically modified T cells by single-chain variable fragment (ScFv, antibody mediated T cell activation in dendritic cells and inhibition of cytotoxic T lymphocyte-associated antigen 4 (CTLA4) **C)** shows the vascular and stromal cell ablation by antagonist binding to vasculature receptor and delivering toxins to stromal cells and vaculature. MAC – Membrane Attack Complex; MHC – Major Histocompatibility Complex; NK – Natural Killer. Picture taken from Scott *et al,* 2012.

4.2.1.3. Anti-Adrenomedullin Therapy

ADM plays an important role in the progression of cancer and metastasis. Over-expression of ADM in different tumours aggravates the molecular and physiological features of malignant cells. Different studies have identified that blocking the action of ADM by ADM antagonist (ADM_{22-52}) destabilizes tumour vascularisation and inhibit the growth of xenografted pancreatic cancer cells and glial tumour cells (Ishikawa et al. 2003; Ouafik et al. 2002). The role of ADM in cancer progression and characteristics of CLR and RAMPs make them important targets for research in monoclonal antibody therapy.

Anti-ADM monoclonal antibody have been observed to neutralize ADM activity in different tumours like breast cancer (Martinez et al. 2002), glioblastoma cell lines (Ouafik et al. 2002), ovarian cancer cell lines (Giacalone et al. 2003), and in patients with primary hyperparathyroidism (Letizia et al. 2004). It has been suggested that mixture of anti-CLR/anti-RAMP2 antibodies as well as anti-CLR/anti-RAMP3 antibodies can specifically inhibit ADM binding to its receptors on tumour cell and induce apoptosis, reduce cell proliferation and block the formation of vascular tubes (Fernandez-Sauze et al. 2004). An international application numbered WO/2007/045927 (patentscope, 2007) has displayed that anti-RAMP2 or anti-RAMP3 antibodies can inhibit angiogenesis and proliferation of cancer cells and thus can be used for treating cancers.

The project investigates the effect of anti-RAMP3 antibody on cell proliferation in cancer cell lines of the previously described cancers. *In vivo* investigation of anti-RAMP3 on tumour growth was carried out using pancreatic cancer cells. Thus the aim of the present study is to identify the effect of anti-RAMP3 antibody in neutralizing ADM mediated cell proliferation and tumour growth *in vitro* and *in vivo*.

4.3. METHODS

Materials and Recipes for solutions used are given in Chapter 6, Appendix.

4.3.1. Optimal Cell Count

In order to determine the right cell concentration and incubation period for proliferation assay for each cell line, an optimal cell count experiment was done. Cells were cultured and counted as previously described. Serial dilutions of cells from $1x10^3$ cells/well to $1x10^5$ cells/well were seeded in a 96 well plate, in triplicates. MTT assay as previously described was carried out and absorbance was measured at 570nm. Cell numbers belonging to the linear portion of the optimal cell count curve was used for proliferation assay.

4.3.2. Proliferation Assay

Proliferation of cells was assessed by MTT assay. Anti-RAMP3 antibody named as JF2 was developed in the Antibody Resource Unit, University of Sheffield, United Kingdom.

Antibody Doses

An antibody dose response was done for varying concentrations of JF2 antibody. The dilutions were done in PBS and the concentrations were 1ng, 10ng, 100ng, 1µg, 10µg and 20µg. Antibody control was accomplished by using an IgG isotype control for the highest dose of JF2 concentration. PBS was used as a vehicle control and a no treatment control was used to assess the general proliferation of cells.

4.3.3. Xenograft Modelling

A. Mice

All animals and experiments were carried out in accordance with the local guidelines and with Home Office approval under project license number 40/2972 held by Prof. Nicola J Brown, University of Sheffield, United Kingdom.

Six weeks old NOD-SCID male mice were obtained from Harlan, United Kingdom. Mice were allowed to acclimatize for a week before start of the experiment. Pancreatic Cancer Cells (Panc-2.3) was used for xenograft modelling to test the effect of JF2 on tumour growth.

B. Injection of tumour cells

Panc-2.3 cells were cultured under standard cell culture conditions. Cells were counted and $4x10^7$ cells were resuspended in 4ml matrigel diluted in 4ml PBS. Cell suspension in matrigel was maintained in ice until injection to prevent solidification.

General anaesthesia was induced using Isofluorane in a glass chamber. Six mice were used as no tumour control and $1x10^6$ cells/mice in 200µl matrigel/PBS of Panc2.3 was injected into twenty four mice subcutaneously using 23G needle.

C. Treatment

Tumours were palpable ten days post-injection. Upon initial observation, mice were divided into small, medium and large tumour groups. Each treatment group contained four mice from small group, and two from medium and large groups. Therefore, the treatment groups contained eight mice each.

The dose of JF2 and Isotype antibody used in this experiment was 200µg in 100µl volume. This dose was based on extrapolation of the maximum dose used

in proliferation assay. Mice were treated twice weekly; tumour size was measured using digital vernier callipers and body weight measured. No tumour control, received 100µl of PBS.

D. End of Treatment

Mice were sacrificed in a humane way after six weeks post injection. Treatment had to be terminated at six weeks since control mice developed large tumours which could affect the well-being of mice. Inter-cardiac punctures were done to withdraw blood. Blood was centrifuged at 10,000xg for 10mins and serum was stored at -80°C.

Tumours were excised, weighed and cut longitudinally, where one half was stored in 75% ethanol for histology and the other half was snap frozen using liquid nitrogen for protein extraction.

E. Analysis

i. Tumour volume was calculated using the formula:

$$\text{Tumour Volume, TV } (mm^3) = \frac{(\text{width}^2 \times \text{length})}{2}$$

ii. Tumour volume at day "n" is expressed as,

$$\text{Relative Tumour Volume (RTV)} = \frac{TV_n}{TV_0}$$

Where, TV_n = Tumour volume at day n

TV_0 = Tumour volume at day 0

iii. The tumour growth inhibition rate (IR) is calculated as

$$IR\% = \frac{1- TWt}{TWc} \times 100$$

Where, TWt = mean tumour weight of treated (JF2)

TWc = mean tumour weight of control (Isotype)

4.3.4. Histology

Tumours stored in 75% ethanol were processed for paraffin embedding. Tissues were embedded in paraffin and serial sections of 5µm thickness were cut in the Histology Unit of University of Sheffield, United Kingdom.

A. Haemotoxylin and Eosin (H&E) Staining

Sectioned tissues were prepared for H&E staining as follows:

i. Dewaxing

Sections were dewaxed in two washes of xylene each lasting for 5mins each. Sections were hydrated from 99% IMS through till 70% IMS each step lasting 5mins.

ii. Staining

Rehydrated sections were briefly washed in tap water and stained with Gill's haemotoxylin to stain nucleus for 90-120 secs. The slides were washed with tap water for 3mins to turn the stain blue in order to give better contrast with cytoplasm. Sections were next stained with 1% aqueous eosin with 1% calcium carbonate in order to stain the cytoplasm for 5mins.

iii. Dehyrating and Mount

Sections were dehydrated quickly through 70% IMS to xylene. Sections were dehydrated quickly since eosin would wash out easily. Sections were mounted in glass coverslips using DPX mountant. Sections were air dried and used for analysis.

B. Evaluation for Necrosis

Sections were evaluated for necrosis kindly by Dr. Steve Shynder from University of Bradford.

At 5X objective magnification, ten whole fields per slide was evaluated (or less if smaller samples) for tumour necrosis using 96-point grid overlay. The number of points overlying necrotic areas was counted and the percentage necrosis for each section was evaluated.

4.3.5. Statistical Analysis

For Proliferation assay, tumour volume, tumour weight and necrosis evaluation, One Way Analysis of Variance (ANOVA) was done to gain statistical analysis. Tukey post hoc test was done to compare between groups. Data are expressed as mean±SEM and p value <0.05 was considered to be statistically significant. Statistical analyses were carried out in GraphPad Prism 5 software.

4.4. RESULTS

4.4.1. Optimal Cell count

Please Note: This section contains supplementary figure that were been included here at the request of the examiners.

In order to determine the optimal cell count and the incubation period for each cell type to determine cell proliferation using MTT assay, an optimal cell count assay was carried out. Supplementary figure 4.4.1.1 shows the optimal cell count for Panc2.3, MDA-MB-231 and U87 cells.

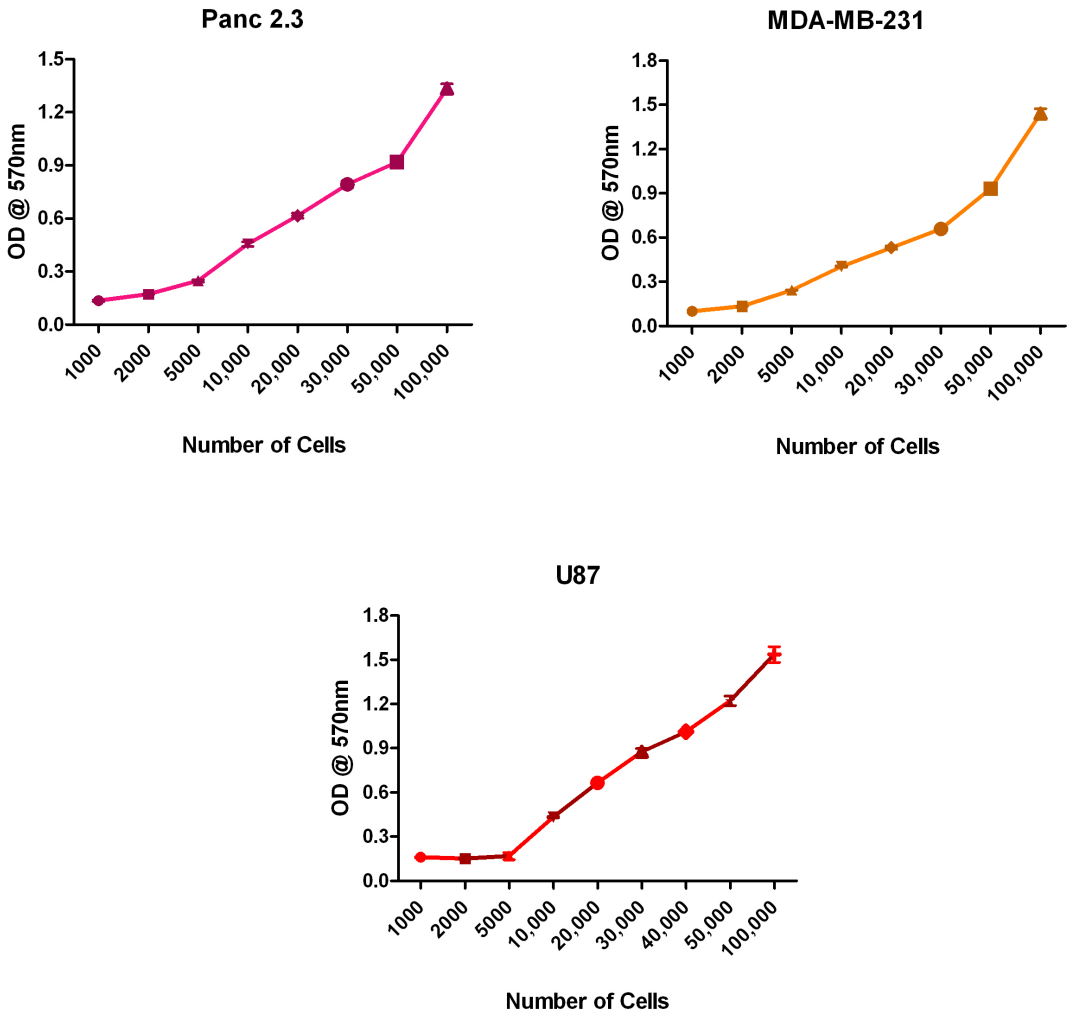

Supplementary Figure 4.4.1.1 : Optimal Cell Count measured by MTT assay in Panc2.3 pancreatic cells, MDA-MB-231 breast cancer cells and U87 glioblastoma cells.

The effect of JF2, anti-RAMP3 antibody on cell proliferation was tested in MDA-MB-231, Panc 2.3, MDA-MB-436 and U87 cells.

4.4.2. Effect of JF2 on MDA-MB-231 cells

Proliferation of MDA-MB-231 cells assessed by MTT assay is shown in figure 69. At Day 0, the average absorbance of all groups was 0.24± 0.00. There was no significant difference between groups.

At day 2, there was no significant difference in OD between groups. The mean absorbances were 0.55±0.01, 0.56±0.01, 0.46±0.00, 0.54±0.00, 0.55±0.00, 0.52±0.01, 0.46±0.00 and 0.42±0.02 for blank, PBS, Isotype, 10ng JF2, 100ng JF2, 1µg JF2, 10µg JF2 and 20µg JF2 treated cells respectively.

At day 4, there was no significant difference in OD between groups. The mean absorbances were 0.33±0.02, 0.39±0.02, 0.37±0.01, 0.44±0.04, 0.37±0.00, 0.36±0.02, 0.33±0.00 and 0.38±0.02 for blank, PBS, Isotype, 10ng JF2, 100ng JF2, 1µg JF2, 10µg JF2 and 20µg JF2 treated cells respectively.

At day 6, there was no significant difference in OD between groups. The mean absorbances were 0.79±0.02, 0.86±0.03, 0.80±0.02, 0.83±0.02, 0.80±0.01, 0.77±0.04, 0.75±0.03 and 0.82±0.06 for blank, PBS, isotype, 10ng JF2, 100ng JF2, 1µg JF2, 10µg JF2 and 20µg JF2 treated cells respectively.

At day 8, there was a significant reduction in proliferation between isotype and antibody treated cells, except for 20µg JF2 dose. The mean absorbances were 1.11±0.04, 1.06±0.01, 1.28±0.04, 1.06±0.01, 1.16±0.02, 1.02±0.03, 1.06±0.05 and 1.12±0.04 for blank, PBS, isotype, 10ng JF2, 100ng JF2, 1µg JF2, 10µg JF2 and 20µg JF2 respectively. The percentage reduction in proliferation were, 17% for 1ng JF2, 9.4% for 10ng, 20.3% for 100ng JF2 and 17.2% for 1µg JF2.

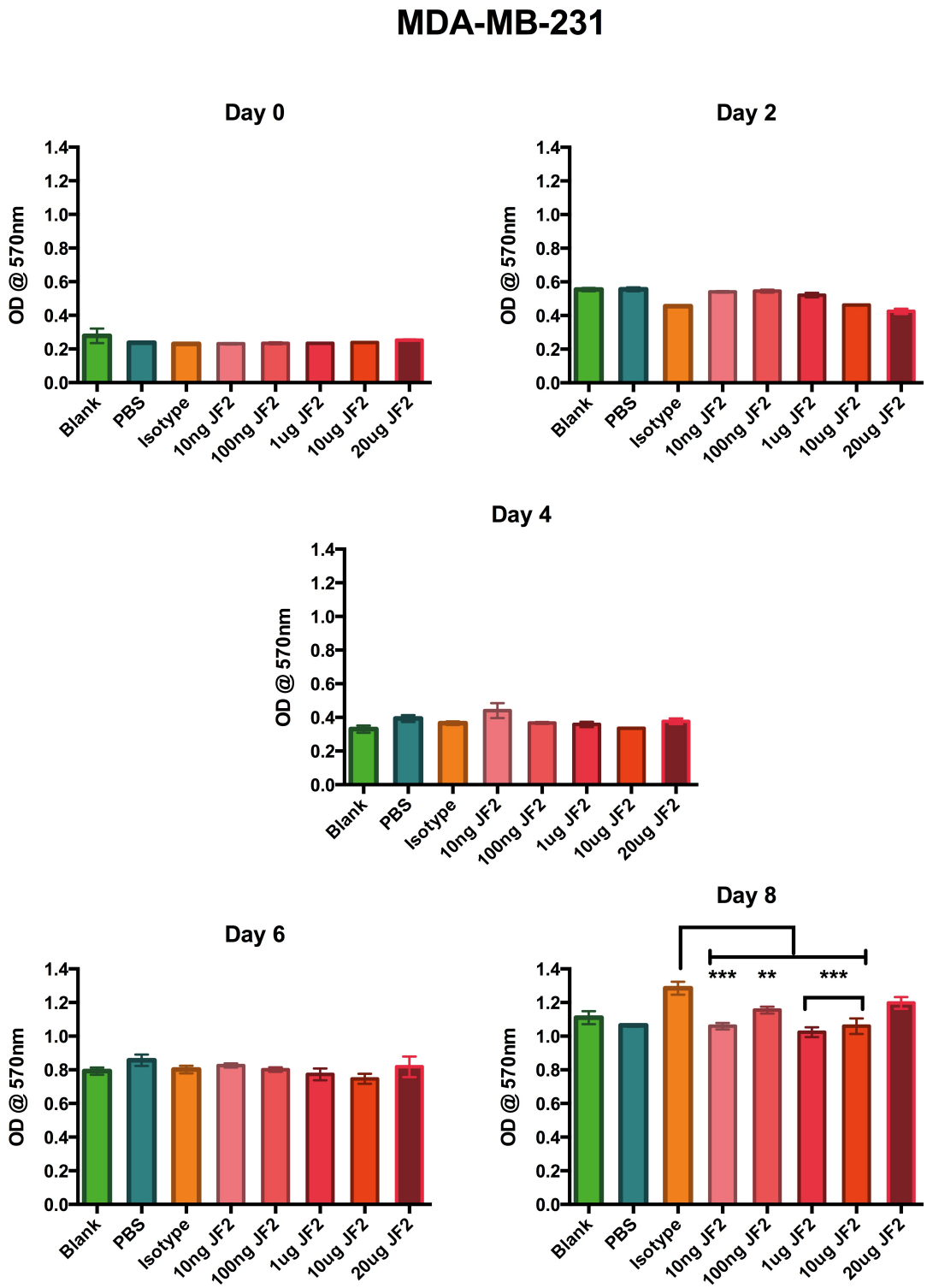

Figure 69: Proliferation of breast cancer cells treated with 20µg isotype, PBS and different doses for JF2 antibody. Proliferation was assessed by MTT assay for 8 days. The OD was measured at 570nm and data is shown as mean ± SEM. ANOVA and Tukey post hoc test was done to gain statistical significance. n=3; $p<0.05$

4.4.3. Effect of JF2 on Panc2.3 cells

Proliferation of pancreatic cells assessed by MTT is shown in figure 70.

At day 0, there was no statisticaly significant difference in OD between the groups. The mean of absorbances for all groups were 0.19±0.02.

At day 2, there was no statistically significant difference in OD between the groups. The mean absorbances were, 0.41±0.02, 0.36±0.01, 0.35±0.02, 0.36±0.01, 0.36±0.01, 0.37±0.02, 0.35±0.01 for blank, PBS, isotype, 10ng JF2, 100ng JF2, 1µg JF2, 10µg JF2 and 20µg JF2 treated cells respectively.

At day 4, there was significant reduction in 20µg JF2 treated cells when compared to isotype control. There was a 21.4% reduction in proliferation with mean absorbances of 0.42±0.03 and 0.33±0.01 for isotype and 20µg JF2 treated cells.

At day 6, there was a significant reduction in 20µg JF2 treated cells when compared to isotype control. There was a 24% reduction in proliferation with mean absorbances of 0.46±0.01 and 0.35±0.01 for isotype and 20µg JF2 treated cells.

At day 8, there was a significant reduction in cells treated with 10ng JF2 to 20µg JF2 treated cells when compared to isotype control. There was 28.6%, 23%, 28.6%, 28.6% and 25.7% reduction in proliferation for 10ng JF2, 100ng JF2, 1µg JF2, 10µg JF2 and 20µg JF2 treated cells.

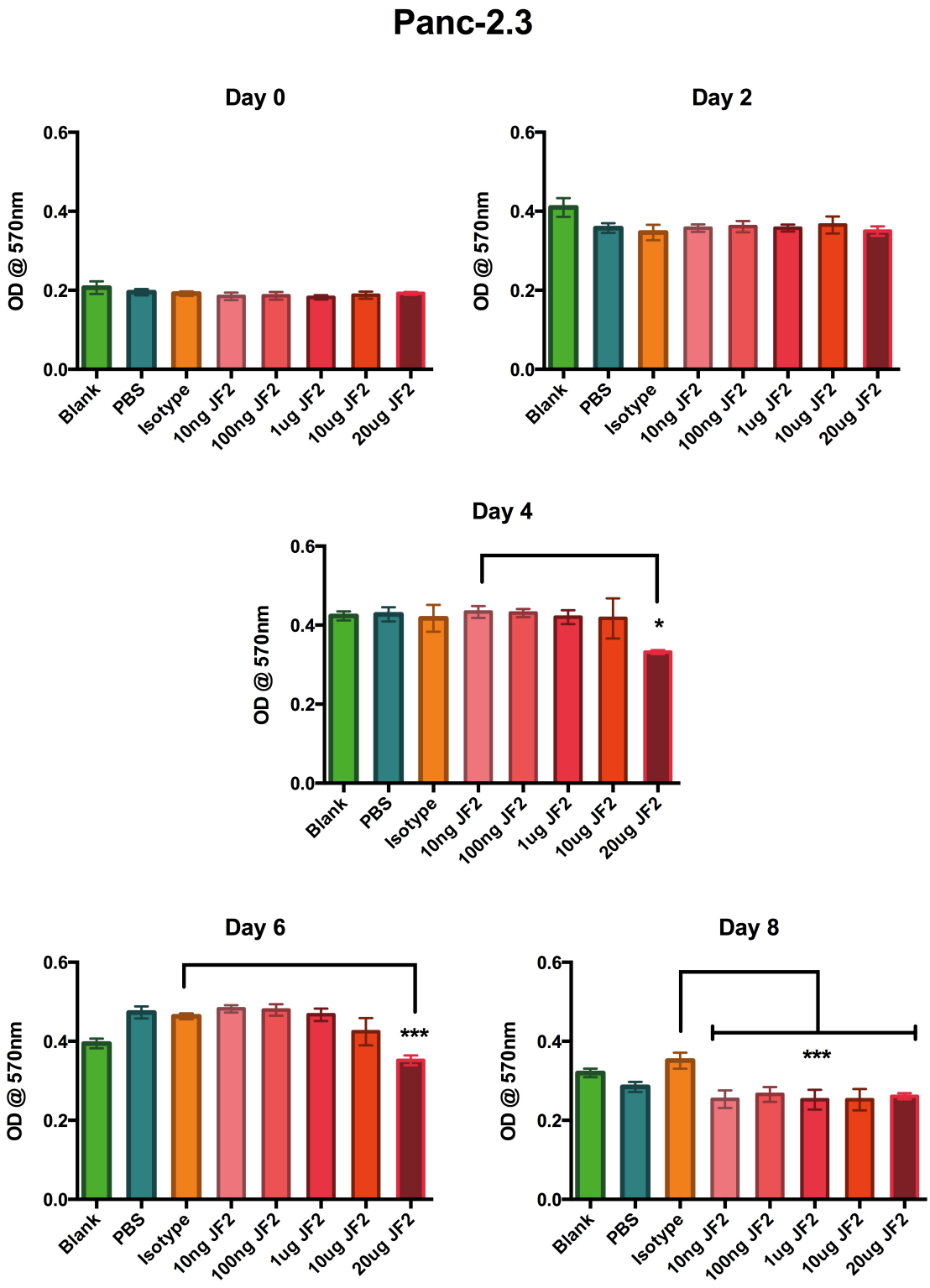

Figure 70: Proliferation of pancreatic cancer cells treated with 20µg isotype, PBS and different doses for JF2 antibody. Proliferation was assessed by MTT assay for 8 days. The OD was measured at 570nm and data is shown as mean ± SEM. ANOVA and Tukey post hoc test was done to gain statistical significance. n=3; $p<0.05$

4.4.4. Effect of JF2 on MDA-MB-436 cells

Proliferation of breast cancer cells assessed by MTT is shown in figure 71.

At day 0, there was no significant difference in OD between groups. The mean OD of all groups were 0.23±0.00.

At day 2, there was no significant difference in OD between groups. The mean absorbances were 0.55±0.01, 0.56±0.01, 0.46±0.00, 0.54±0.00, 0.55±0.00, 0.52±0.01, 0.46±0.00, 0.42±0.02 for blank, PBS, isotype, 10ng JF2, 100ng JF2, 1µg JF2, 10µg JF2 and 20µg JF2 treated cells respectively.

At day 4, there was no significant difference in OD between groups. The mean absorbances were 0.33±0.02, 0.39±0.02, 0.37±0.01, 0.44±0.04, 0.37±0.00, 0.36±0.02, 0.33±0.00, 0.38±0.02 for blank, PBS, isotype, 10ng JF2, 100ng JF2, 1µg JF2, 10µg JF2 and 20µg JF2 treated cells respectively.

At day 6, there was no significant difference in OD between groups. The mean absorbances were 0.79±0.02, 0.86±0.03, 0.80±0.02, 0.83±0.01, 0.80±0.01, 0.77±0.04, 0.75±0.03, 0.82±0.06 for blank, PBS, isotype, 10ng JF2, 100ng JF2, 1µg JF2, 10µg JF2 and 20µg JF2 treated cells respectively.

At day 8, there was a significant reduction in proliferation for 10ng JF2, 100ng JF2, 1µg JF2 and 10µg JF2 when compared to isotype control. Percentage reduction compared to isotype were 15.6%, 11.5%, 15.6%, 11.5% for 10ng JF2, 100ng JF2, 1µg JF2 and 10µg JF2 treated cells respectively.

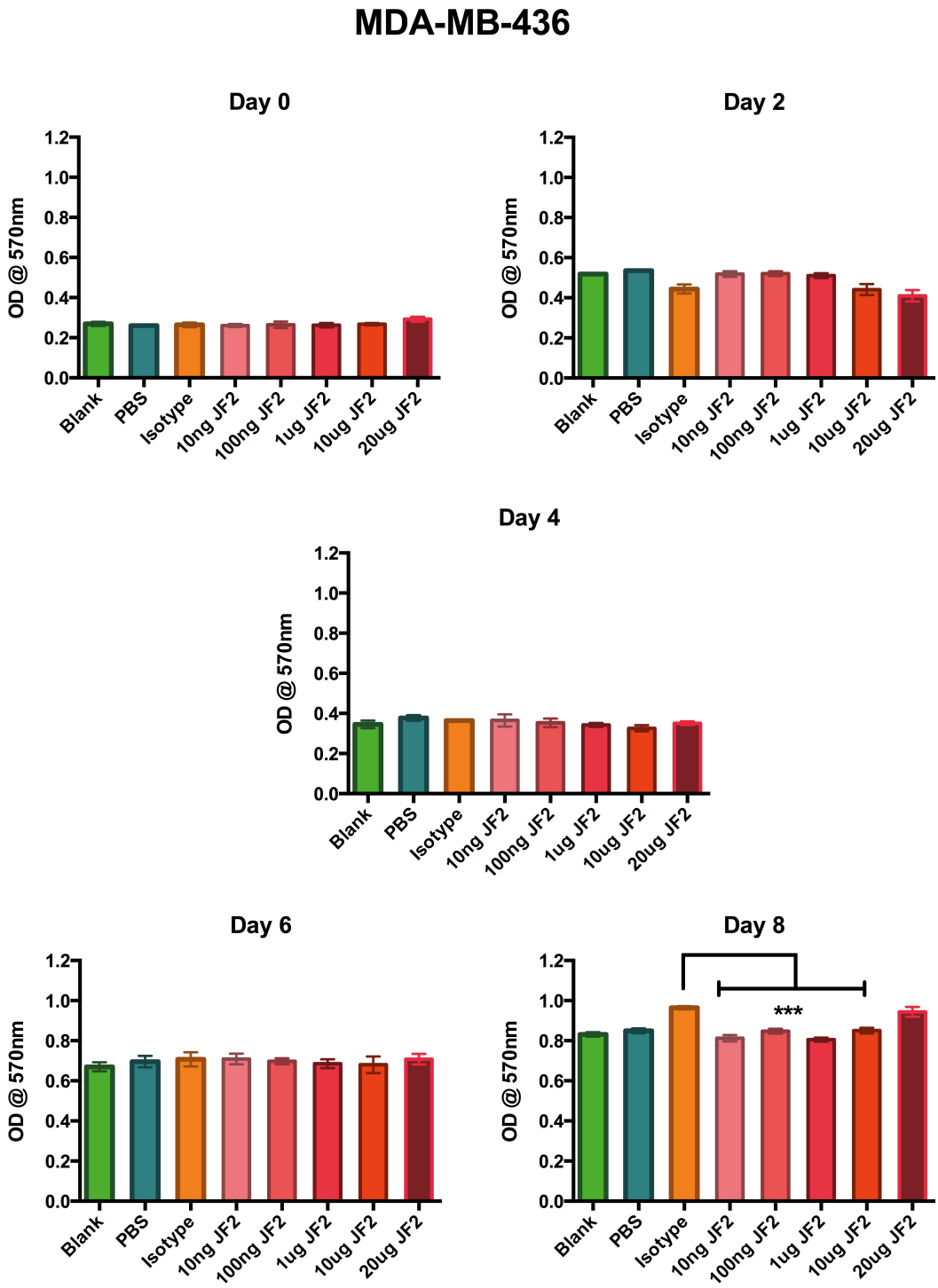

Figure 71: Proliferation of breast cancer cells (MDA-MB-436) treated with 20µg isotype, PBS and different doses for JF2 antibody. Proliferation was assessed by MTT assay for 8 days. The OD was measured at 570nm and data is shown as mean ± SEM. ANOVA and Tukey post hoc test was done to gain statistical significance. n=3; $p<0.05$

4.4.5. Effect of JF2 on U87 cells

Proliferation of U87 cells assessed by MTT assay is shown in figure 72.

At day 0, there was no significant difference between groups. The average of their means was 0.14±0.01.

At day 2, there was no significanct difference in OD between groups. The mean absorbances were 0.22±0.02, 0.21±0.02, 0.21±0.01, 0.20±0.02, 0.20±0.01, 0.19±0.01, 0.20±0.01, 0.19±0.01 for blank, PBS, isotype, 1ng JF2, 10ng JF2, 100ng JF2, 1µg JF2 and 10µg JF2 treated cells respectively.

At day 4, there was a significant reduction for 1µg JF2 treated cells when compared to isotye control. The percentage reduction in proliferation was 10.3%.

At day 6, there was a significant reduction for 10ng JF2, 100ng JF2, 1µg JF2, 10µg JF2 when compared to isotype control. The percentage reduction in proliferation was 14%, 25%, 11%, 32.8% for 10ng JF2, 100ng JF2, 1µg JF2, 10µg JF2 treated cells respectively.

At day 8, there was a significant reduction for 10ng JF2, 100ng JF2, 1µg JF2, 10µg JF2 treated cells when compared to isotype control. The percentage reduction in proliferation was 22.5%, 26.8%, 39.4%, 50.7% for 10ng JF2, 100ng JF2, 1µg JF2, 10µg JF2 treated cells respectively.

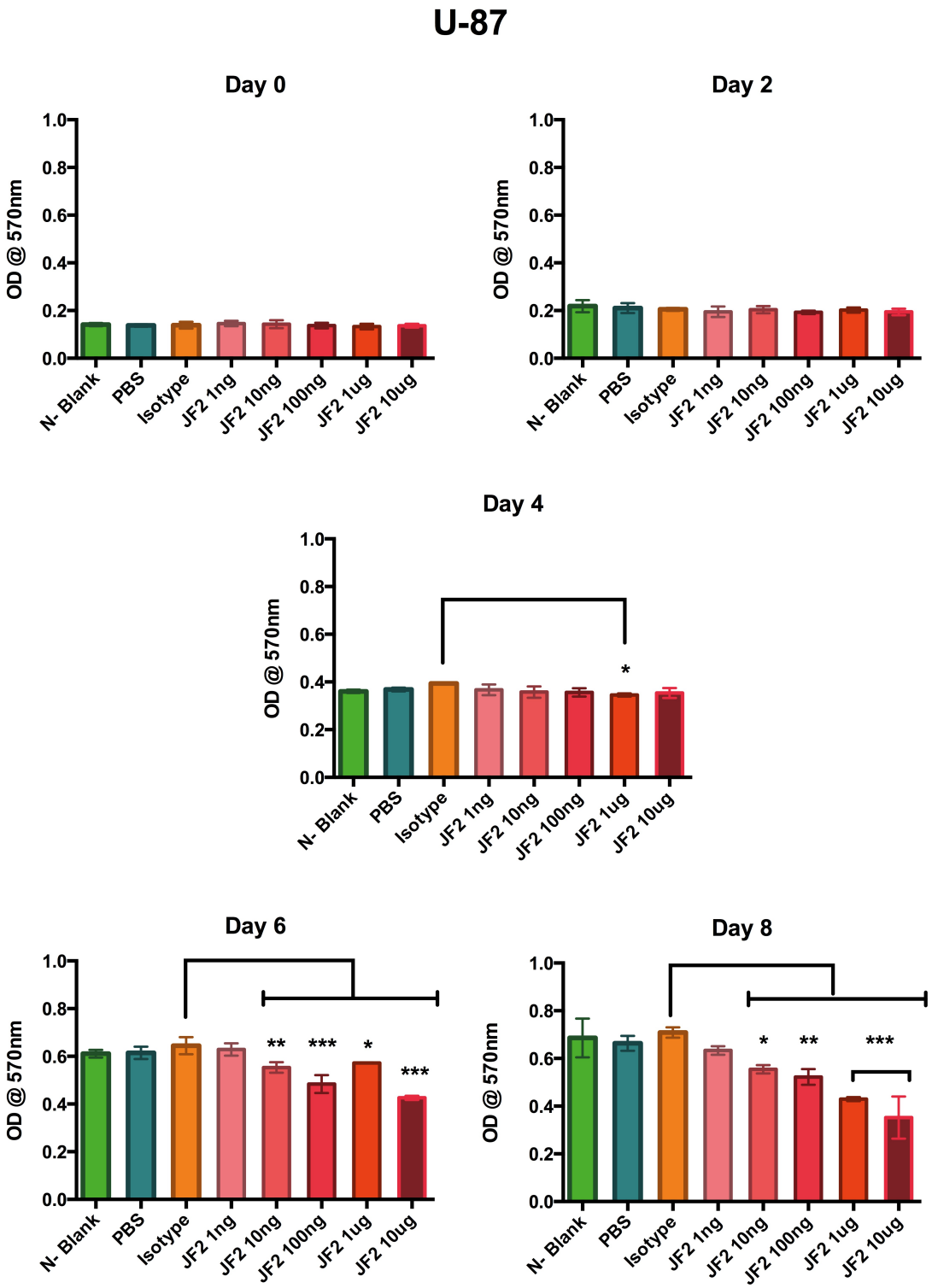

Figure 72: Proliferation of Glioblastoma cells treated with 10µg isotype, PBS and different doses for JF2 antibody. Proliferation was assessed by MTT assay for 8 days. The OD was measured at 570nm and data is shown as mean ± SEM. ANOVA and Tukey post hoc test was done to gain statistical significance. n=3; $p<0.05$

4.4.6. Effect of JF2 *in vivo*

The effect of JF2 antibody was tested *in vivo* using Panc2.3 cells. Over the six week period of the *in vivo* experiment, the general health of mice was monitored by measuring body weights. Figure 73 shows body weights of NOD SCID mice injected with pancreatic cancer. There was no significant difference in mice under treatment and no tumour control group. The average body weights were 29.13g, 28.66g, 28.76g and 26.39g for no tumour control, JF2, PBS and isotype control groups respectively.

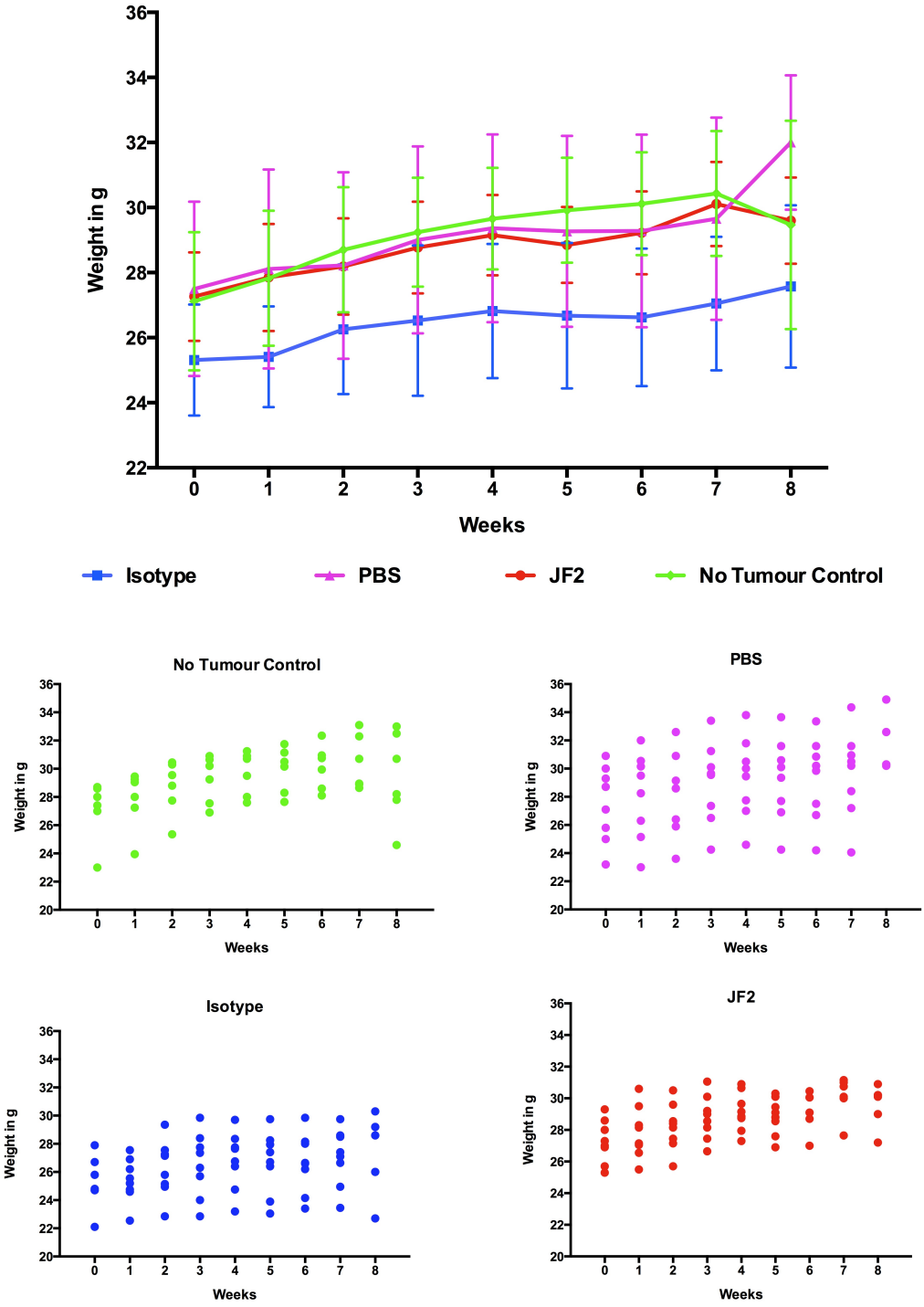

Figure 73: Body weights of NOD-SCID mice injected with pancreatic cancer cells. There was no significant difference in mice under treatment and no tumour control group. The mice in isotype group however had lower body weights from Day 0 of injection, but their body weights seemed to be as normal as that of the other groups. n=6 for no tumour group and n=8 for others.

Figure 74 shows the tumour volumes from mice injected with pancreatic cancer. Week 0 is the start of treatment post tumour cell injection. The average tumour volumes were 603.73mm^3, 530.62mm^3, 323mm^3 for isotype control, PBS control and JF2 injected cells. There was significant difference between tumour volumes between isotype control and JF2 treated cells. By the end of the experiment, the tumour volumes were 1145.44mm^3 for isotype control, 1060.29mm^3 for PBS control and 616.3mm^3 for JF2 treated cells. The relative tumour volumes at the end of the experiment were 5.15, 3.84 and 2.69 for isotype, PBS and JF2 treated mice.

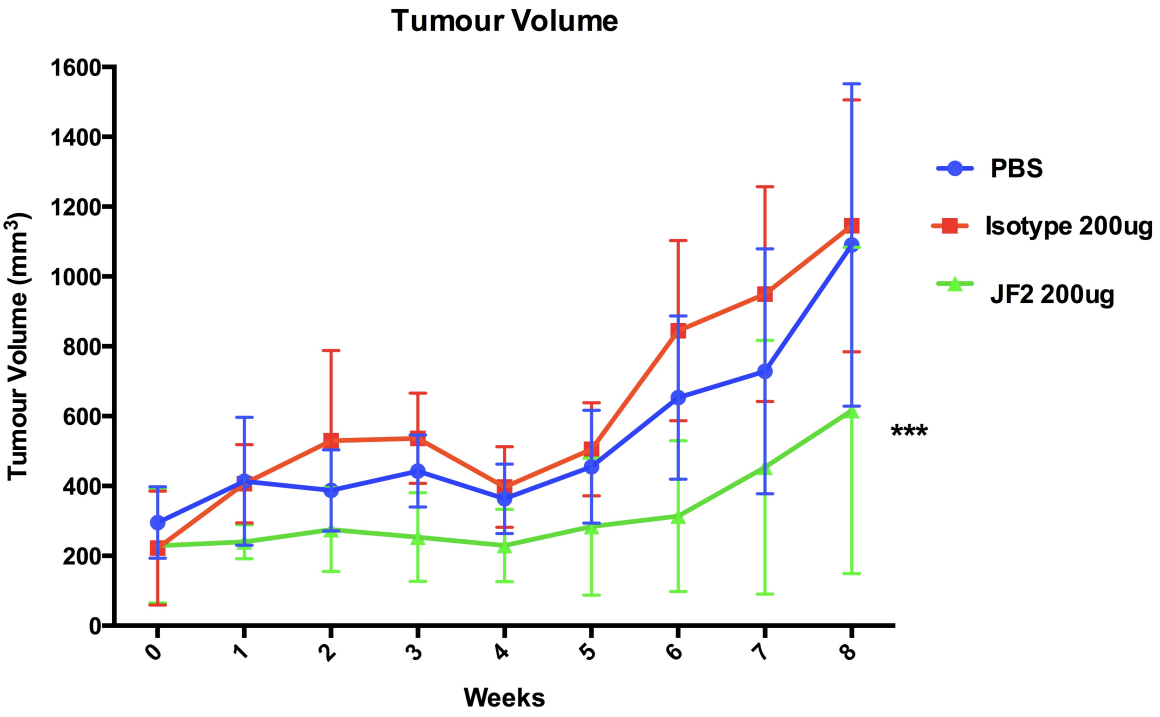

Figure 74: Tumour Volumes from mice injected with pancreatic cancer cells. Tumour volumes were measured twice weekly during treatment using digital vernier callipers. There was a statistically significant difference in tumour volumes between JF2 treatment and controls. ANOVA and Tukey post hoc test was done to gain statistical significance. n=8 ; $p<0.001$

After six weeks of treatment, the tumours were excised and weighed immediately. Figure 75 shows the tumour weights of mice from three groups. There was no statistically significant difference between isotype control, PBS control and JF2 treated mice. The average tumour weights were 0.578g for JF2, 1.023g for isotype control and 0.819g for PBS control. Although the tumour weights were not statistically significant, the growth inhibition at the end of the experiment was 43% reduction of tumour weight in JF2 treated mice when compared to isotype controls.

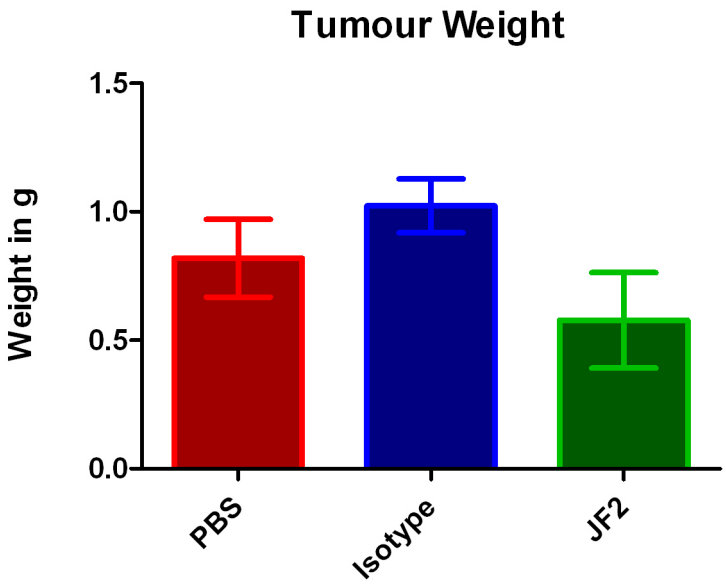

Figure 75: Tumour Weights from mice injected with pancreatic cancer cells. Tumours were excised after 6 weeks of treatment and weighed immediately. There was no significant difference between tumour weights in all three groups. ANOVA and Tukey multiple comparison test was done to gain statistical significance.

n=6 for JF2 and n=8 for PBS/isotype;

The excised tumours were fixed and processed as mentioned under section 4.3.4. The processed sections were stained with haemotoxylin and eosin and analysed and evaluated for necrosis – figure 76. There was no significant difference between the groups. The mean necrosis was 36%, 37% and 36% for PBS, Isotype and JF2 respectively.

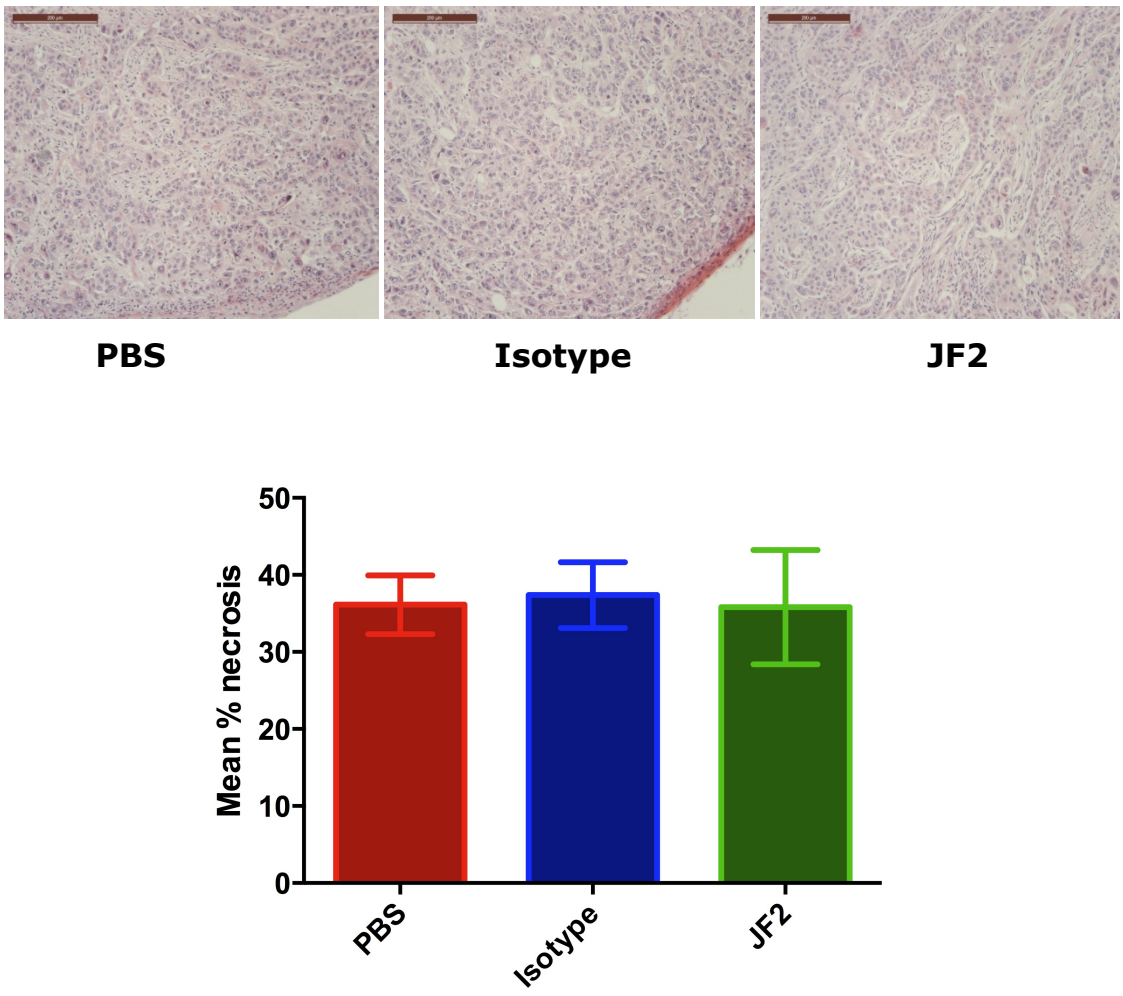

Figure 76: H&E sections from pancreatic xenografts mice after six weeks of treatment with PBS/isotype/JF2. Necrosis evaluation was done at 5X magnification. 10 whole fields per sample were evaluated for necrosis using a 96-point grid overlay. No significant difference in amounts of necrosis for the 3 groups. ANOVA and Tukey multiple comparison test was done to gain statistical significance. n=5 for JF2 and n=8 for PBS/Isotype; $p<0.05$.
Bars = 200µm.

4.5. Technical Discussion

4.5.1. Blocking RAMP3

RAMPs are crucial for action of various transmembrane receptors. RAMPs have key role in executing physiological effect of ADM and other receptors. Research has proved that ADM presents significant mitogenic stimulating activity in several cancers and also encourages more severe tumour phenotype. ADM is also known to get up-regulated in the hypoxic proximity of solid tumours (Zudaire et al. 2003).

A hypothesis by Martinez *et al* in 2002 explained that over-expression of ADM under various circumstances result in over-expression of ADM receptors - CLR+RAMP2 and CLR+RAMP3. Over activity of ADM receptors may in turn increase the activity of ADM at the cellular level. Excessive action of ADM on cancer cells causes morphological changes like increased projection on cell membrane, increased dynamicity of plasma membrane, and reduced cell adhesion contributing to increased cell migration and cancer metastasis. (Martinez et al. 2002). Considering this background, it can be hypothesized that blocking of RAMP3 can reduce the over activity of excessive ADM and thus may help in reducing or stopping cancer cell metastasis

Continuous research is going on for identifying the ways to block RAMP3 inorder to inhibit ADM activity in cancer cells. One study identified that N-Glycosylation and conserved cysteine residues in RAMP3 can play an important role for the functional expression of CLR/RAMP3 ADM receptor. When CLR and RAMP3 assemble they form a heterodimeric receptor which acts as high affinity ADM receptor. Since RAMP3 carries an extracellular N-terminus which contains six highly conserved cysteine residue and four N-glycolysation consensus sites, it helps in ADM binding with receptor. Thus removal of all N-glycans in RAMP3 leads to a noteworthy inhibition of receptor and thus reduced ADM binding. Removal of N-glycan also increases the EC50 value for ADM. On the other hand, removal of all cysteine eliminates ADM binding and leads to a complete loss of receptor function (Flahaut et al. 2003).

The role of RAMP2 and RAMP3 were studied in gene knockout studies by Dackor *et al* in 2007 as mentioned previously. Their results showed that the RAMP2 knockout mice were embryonically lethal, while RAMP3 knockout mice survived until adulthood with the only repercussion being loss in body weight during oldage (R. Dackor et al. 2007). These studies show that RAMP2 is important for physiology while RAMP3 knockout could be up-regulated under a physiological stress or under a pathological condition. Therefore we hypothesise that neutralising ADM activity by blocking RAMP3 would not result in adverse effects.

4.5.2. Effect of JF2 on MDA-MB-231 cells

MDA-MB-231 cell line represents breast cancer and is widely used to identify the effect of various drugs on the improvement of breast cancer. A study by Brekhman *et al* in 2011 explained the action of RAMP3 on MDA-MB-231 cell line. Researchers compared the action of RAMP3 with LOXL2. LOXL2 (Lysyl oxidase-like protein 2) is responsible for inducing epithelial to mesenchymal transition and in turn promote invasiveness. It was found that LOXL-2 also up-regulated the expression of RAMP3 on MDA-MB-231 cell line. However, if the LOXL2 expression was inhibited in any cell line, RAMP3 expression restored the cellular actions like vimentin expression, invasiveness, and tumour development. The study also found that inhibition of RAMP3 has the similar effects as that of LOXL2 inhibition along with p38 phosphorylation. These findings suggested that RAMP3 is strongly co-expressed in breast cancer. Besides functioning as transducer for mediating autocrine signals by ADM, RAMP3 also mediates pro-tumorigenic effect of LOXL2 in MDA-MB-231 cell line. Thus inhibition of RAMP3 can help in reducing tumourogenic activity in breast cancer (Brekhman et al. 2010).

We observed that there was no significant percentage reduction in cell viability until day 6 in both JF2 antibody treated cells or isotype control cells. This data suggests that though RAMP3 is widely distributed over MDA-MB-231

cell line (Brekhman et al. 2010), anti-RAMP3 antibody is not very effective in preventing cell proliferation in it. This conclusion is again strengthened by the fact that varied doses of JF2 were also not showing any significant difference in cell proliferation until day 6. However, on day 8 a small significant difference in cell proliferation was observed between isotype control and 20µg JF2 treated cells. This suggests that initiation of complement activation and antibody-dependent cell cytotoxicity by JF2 antibody takes longer duration in MBA-MD-231 cell line or treatment of the particular cell line require higher or repeated dosing of JF2. The motility of JF2 could be cell type specific; therefore, testing the effects of JF2 on cell proliferation for longer periods in these cells should be investigated.

4.5.3. Effect of JF2 on Panc 2.3 cells

Panc2.3 cells treated with JF2, 18-23% reduction in proliferation was observed in 20µg JF2 treated Panc 2.3 cells when compared to isotype control on day 4. On day 6, 20-27% reduction in proliferation was observed. On day 8, all doses of JF2 produced a reduction in proliferation ranging from 18% to 34%, although it was not a dose response. This suggests that JF2 antibody is effective in reducing cell survival and cell growth in the pancreatic cancer cell line. Our findings concur with previous studies where anti-ADM therapies have significantly reduced tumour cell growth both *in vitro* and *in vivo*. Intra-tumoural injection of ADM antagonist (AMA) peptide for 10 days suppresses *in vivo* growth of human pancreatic cancer cells in SCID mice by suppressing angiogenesis and large blood vessel formation (Ishikawa et al. 2003). Another study found that single intra-tumoural or intra-muscular injection of naked DNA encoding AMA was extremely efficient in suppressing the growth of pancreatic cancer cell lines in SCID mice. A complete regression of blood vessel formation was observed in the tumours treated with naked DNA encoding AMA. These findings suggest that there is strong correlation between ADM activity and tumour progression in pancreatic cancer (Miseki et al. 2007).

Although JF2 showed a significant effect on the Panc 2.3; a study found that pancreatic adenocarcinoma cells (PAC) of BxPC-3 cell line do not express RAMP3. The study found that mRNA levels of both ADM and CLR are very high in PAC and they expressed RAMP1 and RAMP2 but not RAMP3. The study also stated that RAMP3 is only expressed in 1 out of 5 cancer cells (Keleg et al. 2007). This finding is in contrast with our results, which show prominent anti-RAMP3 effect in the pancreatic cancer cell line. This contrast can be justified by the fact that BxPC-3 is a cancer cell line which was derived from a 61-year-old woman's adenocarcinoma of the body of the pancreas, while the Panc2.3 cell line was derived from a 56-year-old male with an adenocarcinoma in the head of the pancreas which invaded the duodenal wall (Deer et al. 2010). So, it can be considered that anti-RAMP3 antibody can work on pancreatic adenocarcinoma of pancreatic head but its effectiveness in treating pancreas body cancer needs to be investigated.

4.5.4. Effect of JF2 on U87 cells

Effects of JF2 were observed in this project on the U87 cell line, which had an epithelial morphology and was cultured from a stage IV cancer patient (ATCC, 2010). Therefore these U87 cells are an aggressive cell line. Treatment with JF2 started showing reduction in proliferation from day 4 at 1µg dose (9-14% reduction) when compared to isotype control. At day 6, a reduction of 11-39% was observed from doses 10ng to 10µg. On day 8, a dose response with a reduction of 15-49% for the same doses was observed. This finding suggests that as explained by previous studies that anti-RAMP3 antibody reduces cell proliferation and enhances apoptosis in glioblastoma cells *in vitro* and reduces tumour growth in *in vivo* conditions (Robinson et al. 2009) (Kaafarani et al. 2009). A significant dose response was also observed among the cells treated with different doses of JF2. Fernandez et al. (2004) demonstrated that U87 glioblastoma xenograft tumours treated with anti-ADM antibody were less vascularized than control tumours. This outcome suggested that ADM play an important role in neovascularisation and vessel stabilization in glioblastoma. The study further investigated that the action of ADM mediated via CLR/RAMP2 and

CLR/RAMP3 promoted migration and invasion in a dose dependent manner in glioblastoma. When VEGF was blocked by specific antibodies, ADM continued to promote capillary tube formation in glioblastoma. These findings concluded that ADM and its receptors can be investigated as a new potential target for anti-angiogenic therapy for glioblastoma. A precise and optimized dose for JF2 antibody must be determined for each cell line in order to use JF2 as a possible therapy.

4.5.5. Effect of JF2 on MDA-MB-436 cells

The widely used MDA-MB-231 cell lines are very aggressive, metastatic cells characterized as rapidly growing metastatic breast cancer. It represents ductal carcinoma and slow growing breast cancer. The MDA-MB-436 cells were first cultured form pleural fluid obtained from a 43-year-old breast cancer patient. MDA-MB-436 cells are pleomorphic and react intensively with anti-tubulin antibody. When the MDA-MB-436 cells are experimented *in vitro* they show abundant activity in both the Boyden chamber chemoinvasion and chemotaxis assay. The other advantages of MDA-MB-436 cell line over other breast cancer cell lines are that it is able to grow on agarose which can precisely indicate transformation and tumourigenicity. Additionally, this cell line displays a relatively high colony forming efficiency and forms mammary fat pad tumours in nude mice (Burdall et al. 2003; Holliday and Speirs 2011).

Published data suggest that slow growing but tumorigenic MDA-MB-436 breast cancer cells were very useful in understanding the role of extracellular matrix metalloproteinase inducer (EMMPRIN) in the tumour progression. When the MDA-MB-436 cells were transfected with EMMPRIN cDNA and injected orthotopically into mammary tissue of female NCr nu/nu mice, increase in expression of matrix metalloproteinase (MMPs) was observed which lead to increased gelatinase A and gelatinase B expression along with elevated stromal or inflammatory cell reaction ultimately leading to tumor progression. Thus the experiment on MDA-MB-436 cell lines helped to conclude that EMMPRIN plays an important role in cancer progression (Zucker et al. 2001).

A patent application by Ouafik *et al* in 2011 claimed that a mixture of antibodies against CLR, RAMP2 and RAMP3 was able to cause 30% reduction in cell proliferation in the treated MDA-MB-436 cell line as compared to the isotype antibody treated cell cultures. The study also showed that mice xenografted with MDA-MB-436 cell line and treated with mixture of anti-ADM receptor antibodies showed suppression in tumour growth as compared to mice treated with pre-immune serum. These findings suggested that mixture of anti-ADM receptor antibodies could be developed as a possible treatment for slow growing ductal breast carcinoma. (Ouafik et al. 2002; Ouafik et al. 2009). The MDA-MB-436 cells treated with JF2 showed significant reduction in proliferation on day 8 when compared with isotype control. Doses from 10ng upto 10µg showed a decrease in cell proliferation. However non similar to the previous published work, the MDA-MB-436 cell line did not exhibit dose dependent cell reduction when treated with JF2.

4.5.6. Effect of JF2 *in vivo*

Several murine models have been made available by researchers to study and investigate human cancer. These models helps to identify the factors involved in malignant transformation, invasive property of cancer cells, metastasis of cancer cells, and also to quantify the response of therapy.

Researchers investigating the effect of CTGF-specific monoclonal antibody (FG-3019) in mouse model injected with Panc-1 cells, observed that administration of FG-3019 decreased tumour growth and metastasis and attenuated tumour angiogenesis and cancer cell proliferation (Aikawa et al. 2006). Recently a dual combination therapy of anti- EMMPRIN (extracellular matrix metalloprotease inducer) antibody and anti-DR5 antibody were investigated for pancreatic adenocarcinoma in orthotopic mouse models. It was observed that tumour growth was significantly restrained by the combined antibody therapy in both MIA PaCa-2 and PANC-1 tumour models of pancreatic cancer (H. Kim et al. 2011).

In this project six weeks old NOD-SCID with xenograft of pancreatic cancer cells Panc 2.3 were used to examine the *in vivo* effect of JF2. It was observed that by the sixth week of experiment, the mice treated with 200µg JF2 showed suppression in tumour growth when compared to mice treated with isotype antibody. Suppression in tumour growth was established by both the reduction in tumour weight and tumour volume. These findings justify that blocking ADM action by anti-RAMP3 antibody increased apoptosis of cancer cells and suppressed angiogenesis as well as cell proliferation. While the apoptosis of cancer cell was responsible for reduction in tumour weight, suppression of angiogenesis and cell proliferation reduced the tumour growth and thus reduced the tumour volume. Although there is no significant difference in tumour weights and IHC analysis, the tumours excised from JF2 treated mice had considerably lower weights. The non-statistical significance could be due to loss of two mice in the JF2 group during the course of the experiment due to an overdose of anesthesia during treatment. Out of the six mice that were alive, one mouse had a very small tumour, which looked like a pustule. This tumour could not be processed; therefore the total number of tumours from JF2 treated mice was five. Therefore the less numbers could be the reason why there was no significance in tumour necrosis profile.

Somehow the random allocation of mice in different groups caused allotment of comparatively low weight mice to the isotype group but all the mice were healthy. No drastic changes in weights of mice in any groups were observed, especially JF2 treated mice, which indicates that although the treatment with the anti-RAMP3 antibody JF2 is effective as anti-cancerous it is also non-toxic.

Since the changes in tumour volume and tumour size suggest anti-cancerous effect of JF2 antibody, the histopathological findings can be considered false. Although hematoxylin and eosin staining is widely used for histopathological examination of tumours, in the present case analysis of necrosis lead to contradictory results. ADM is well known for its property to stop apoptosis and initiate angiogenesis. Since mast cells play a huge role in

apoptosis, toluidine blue dye can be used to stain mast cells present in the tumours. Presence of mast cells in tumour treated with JF2 may suggest its effectiveness in stopping ADM induced prevention of apoptosis. Since anti-RAMP3 antibody inhibits ADM mediated angiogenesis and neovascularisation in the tumour grafts, staining with anti-CD31 and F VIII RAg IHC can be helpful in differentiating effects of control and JF2 on cancerous tumours (D. Wang et al. 2008).

4.5.7. Optimization of cell count in MTT assay

The MTT colorimetric assay is a well-known and tested method of identifying viable cells and cytotoxicity studies. The main principal of assay is that the mitochondrial enzymes of live cancer cell cleaves the yellow tetrazolium salt MTT and converts it to a soluble blue/purple formazan. The OD of formazan thus obtained is directly proportional to the number of living cells. Although MTT assay is extremely popular for quantifying the number of viable due to rapid, convenient and economical outcome, there are various factors, which affects the precision of MTT assay. Different factors that can either affect cellular metabolism or other factors, which can modify MTT specific activity may lead in calculation of false results. Thus it is extremely crucial to optimize assay conditions by establishing strict assay parameters. These parameters must include determining correct cell densities, culture medium, optimal concentrations and exposure times for MTT, fresh culture medium at the time of assay to avoid nutrient depletion, and controlling for drug treatment effects that may influence cellular metabolism. By controlling these important parameters, the MTT colorimetric assay provides accurate and reliable quantification of viable cell number (Sylvester 2011).

In figures 45, 46, 64 and 70, the OD values were either the same as it was two days ago or it reduced. This could be due to cell death since these are rapidly proliferating cells and are getting pushed through the cell cycle. Another plausible conclusion is that the 10% serum in the media is enabling the cells to reach their maximum proliferative potential that they are unaffected by

treatment/experimental conditions. Therefore these cells would not be in the linear phase of cell growth and must have attained plateau phase.

4.5.8. Conclusion

The *in vitro* and *in vivo* findings of this project suggest that anti-RAMP3 is effective in reducing tumour growth in both slow and fast growing breast cancer cells, glioblastoma cells, prostate cancer cells and adenocarcinoma in the head of the pancreas. Furthermore, the absence of drastic weight changes in mice models treated with JF2 suggests that it a safe option for treatment. However, safety profile of JF2 as a drug must be investigated on a larger profile.

CHAPTER V: DISCUSSION

5.1. Discussion

Adrenomedullin (ADM) is a pluripotent peptide secreted by various malignant cells like breast, lung, pancreas and prostate. ADM is known to display its physiological effects by paracrine, autocrine or endocrine mechanism. Along with mediating pathological conditions like cardiovascular disorders, renal problems, sepsis and inflammation; ADM plays an important role in the progression of cancer and metastasis (Zudaire et al. 2003). Results from different range of studies which used many different models have strongly implied that ADM has an important role in tumour growth and metastasis. Clinical data gathered over years of research confirms that ADM is over-expressed in cancer patients like colon and lung cancer (Ehlenz et al. 1997), ovarian cancer (Hata et al. 2000), prostate cancer (Rocchi et al. 2001), intraocular and orbital tumour (Udono et al. 2000), leiomyomas (Hague et al. 2000), and pituitary tumour (Letizia et al. 2004). Based on these, it was hypothesized that inhibiting ADM would be a viable therapy for cancer. Therefore the project was divided into three sections, namely

1. Effect of hypoxia, which is a classical feature of tumour cells, on ADM and its receptors
2. Determine the role of ADM in cell proliferation, migration and invasion by enabling cells to over-express ADM
3. Neutralise ADM activity by targeting its receptor component, namely RAMP3, using an anti-RAMP3 antibody (JF2) both *in vitro* and *in vivo*.

5.1.1. Effect of hypoxia on Cancer, ADM and Receptors

As an important physiological effect, HIF (hypoxia inducible factors) signalling cascade gets mediated in the state of low oxygen. Since hypoxia often controls cell differentiation, role of HIF cascade becomes important for normal cell differentiation and survival. The stabilized HIF-1 causes up-regulation of several genes coding for glycolysis enzymes and vascular endothelial growth

factor (VEGF) and thus promotes cell survival in low-oxygen conditions. While the glycolysis enzymes allow ATP synthesis, VEGF promotes angiogenesis. However, chronic effect of HIF is self-perpetuating and is responsible for distorting cell microenvironment by inducing aberrantly active transcription factors. The changes in levels of growth factors, chemokines, cytokines and ROS in response to chronic activity of HIF provide the environment for proliferation and survival required for development of cancer and metastasis (Benizri et al. 2008). Hypoxia is also referred as "Janus face" in tumour biology because it is associated with controlled proliferation, differentiation, necrosis, apoptosis and can initiate or enhance the development of an aggressive phenotype.

5.1.1.1. HIF-1 and ADM levels

Hypoxia induced ADM gene expression is governed by HIF-1 transcription factor. The transcription factor binds with HIF-1 responsive element localized on ADM promoter region and therefore enhances ADM gene expression. Since ADM has cancer proliferative and anti-apototic mechanism of action, over-expression of ADM under chronic hypoxia worsens the cancerous status of the cells (Nguyen and Claycomb 1999).

This project evaluated the implications of hypoxia in different cancer cell lines. When glioblastoma cells were exposed to hypoxia, a significant elevation in the levels of HIF-1 was observed after 24 and 48 hours. Similar elevation in the levels of HIF-1 within 24 hours following hypoxia in glioblastoma has been previously reported (Damert et al. 1997). The study found that increased HIF-1 levels also caused increased levels of VEGF and caused tumour angiogenesis. Therefore it is concluded that VEGF mediated by HIF-1 in glioblastoma cells following hypoxia has a major role in progression of cancer. Impact of HIF-1 elevation following hypoxia in glioblastoma was also observed in another study. The study reported that different glioblastoma models with complete knock-down of HIF-1 complement showed impairment in cell migration *in vivo* and their invasion *in vivo*. All the findings together imply that hypoxia has a major role in

glioblastoma progression induced by elevated levels of HIF-1 (Mendez et al. 2010).

The U87 cell line exposed to hypoxia also showed increased levels of ADM within 48 hours and thus reflected the relationship between hypoxia, elevated HIF-1 levels and increased ADM expression. Various studies have identified ADM as a hypoxia-inducible factor. While studying the effect of hypoxia on ADM expression in glioblastoma cells, Metellus *et al* in 2011, found that hypoxic condition ($CoCl_2$, DFX) significantly increased ADM mRNA levels *in vitro* by increasing transcriptional rate of ADM gene and enhanced ADM mRNA stability mediated by HIF-1. The study also found that the GBM (Glioblastoma) specimen exposed to hypoxia presented co-localized ADM mRNA and protein particularly abundant around areas of vascular proliferation and in pallissading cells surrounding necrotic foci (Metellus et al. 2011).

The other cell lines in the present study like prostate cancer cell line (PC-3) and breast cancer cell lines (MDA-MB-436 and MDA-MB-231) also showed significant increase in ADM levels within 24-48 hours hypoxia. ADM elevation in different cell lines under hypoxic conditions is described by a strong evidence based research (Garayoa et al. 2000). The study demonstrated that reduced oxygen tension (1% O_2) or exposure to hypoxia mimetics such as desferrioxamine mesylate (DFX) or $CoCl_2$ highly induce the expression of ADM mRNA in numerous human tumour cell lines in a time-dependent manner. Such ADM expression is observed to be regulated by HIF-1, since HIF-1α and HIF-1β knockout mouse cell lines presents ablated or greatly reduced hypoxia mediated ADM mRNA induction. Similarly blocking or enhancing the HIF-1 activity in human tumour cells shows an analogous modulation of ADM mRNA. ADM mRNA stabilization has been shown to be partially responsible for the hypoxic up-regulated expression of ADM in the study. Furthermore, the study also reflects the fact that enhanced ADM gene expression followed by hypoxia is also because of the several putative hypoxia response element (HREs) in the human ADM gene. Therefore the transient co-expression of HIF-1α results in an augmented transactivation of the reporter gene after DFX treatment and increase ADM

levels. Since most solid human tumours have focal hypoxic areas and that ADM functions as a mitogen, angiogenic factor, and apoptosis-survival factor, all these published data along with our findings implicate the HIF-1/ADM link as a possible promotion mechanism of carcinogenesis (Garayoa et al. 2000).

Although all the cancer cell lines in the present study showed elevated levels of ADM after 48 hours of hypoxia, pancreatic cancer cell line showed reduction in ADM levels. This unexpected result may have developed due to cell death in the culture. Pancreatic cancer cell lines are known to be very sensitive to change in culture media or exposure to any disrupting element (M. Kato et al. 1999). Therefore a regular cell viability testing for pancreatic cell line must be performed at regular intervals.

Since ADM is an angiogenic factor, its up-regulation under hypoxia elicits angiogenic response resulting in tumour survival. Therefore it is suggested that blocking ADM would also be beneficial in blocking hypoxia induced angiogenesis.

5.1.1.2. Down-regulation of ADM receptors

A significant down-regulation of ADM receptors CLR, RAMP2, and RAMP3 under 48 hour hypoxia was observed in both breast cancer cell line and glioblastoma cell line. Similar results were obtained by Kitamuro *et al* in 2001 while studying the effect of hypoxia on human neuroblastoma cells (Kitamuro et al. 2001). While another group observed no changes in ADM levels in human chondrocyte cells under hypoxia while CLR remained undetectable, RAMP1 and RAMP2 were down-regulated and RAMP3 expression was up-regulated. Both the researchers concluded that this non-uniform behaviour of ADM receptor expression in different types of cells is not yet clear and may be constituted due to any possible adaptation mechanism in response to hypoxic stress (Velard, 2012, Rheumatology conference). Cromier-Regard in 1998 explains the underlying mechanism to this issue. It was found that ADM expression during hypoxia is controlled by ADM promoter. During hypoxia, ADM promoter expression increases by 1.8 fold during initial 6 hours and then gradually decline

(Cormier-Regard et al. 1998). Based on these findings, it can be suggested that ADM and ADM receptor expression initially increase under hypoxia and then decline due to adaptation mechanism.

5.1.1.3. Hypoxia and PAM

ADM is expressed as an immature peptide and in order to render it active, the C terminal of ADM has to be amidated by an enzyme called PAM, as previously described. PAM expression was measured under hypoxia to test our hypothesis that the up-regulated ADM under hypoxia is mature and fully active.

In our study, PAM levels were possibly elevated at 24hrs hypoxia and the levels dropped at 48hrs. Previous studies showed that PAM expression was down-regulated at the end of 48 hour hypoxia (Cormier-Regard et al. 1998). Similar to ADM, pro-ADM expression is also controlled by cellular adaptation mechanism, which may be regulated by ADM promoter expression. Assessment of PAM under continuous hypoxia (CH) and intermittent hypoxia (IH) in brain stem of rats suggest that IH, not CH, caused production of reactive oxygen species (ROS) which in turn elevated PAM levels by increasing activity and levels of O2-sensitive peptidylglycine α-hydroxylating monooxygenase (PHM) (Sharma et al. 2009).

These findings suggest that frequent and intermittent hypoxia conditions can increase PAM levels in tumours and thus increase mature ADM levels. Since continuous hypoxia was presented to the experimental cell lines, a down-regulation in levels of PAM at 48hours was observed in this project. Although PAM levels were not high, it cannot be concluded that the up-regulated ADM is not fully active/mature. Levels of PAM required rendering ADM mature/active and/or quantifying the amidated ADM in culture media could convey that the up-regulated ADM under hypoxia is active and that it would act as a tumour promoting factor.

5.1.1.4. Hypoxia and AKT signalling

It was observed that there was a strong AKT signalling from 6 hour to 24 hour of hypoxia and then it declined. The result is in association with the results of a study that analysed the effect on PC12 cells (pheochromocytoma). Hypoxia dramatically increased phosphorylation of Akt (Ser^{473}) in the study. The AKT signalling effect peaked at 6 hours after hypoxia and remained persistent till 24 hours. The effect of hypoxia on phosphorylation of Akt was completely blocked by pretreatment of the cells with wortmannin (100 nM), indicating that this effect is mediated by phosphatidylinositol 3-kinase (P13K) (Beitner-Johnson et al. 2001). A study by Kim *et al* in 2003 identified the relationship between ADM and AKT. The study found that ADM (10^{-7} mol/L)) induced by any conditions (like hypoxia) increased phosphorylatin of AKT within 10 minutes which reached its peak value within 30 minutes. The study also demonstrated that ADM has dose dependent action on phosphorylation of AKT and it can be inhibited by ADM antagonist ADM_{22-52} (W. Kim et al. 2003a). Since the consequences of ADM action causes enhanced AKT signalling, blocking the action of ADM using anti-RAMP3 can be helpful in reducing AKT signalling and thus inducing apoptosis in the cancerous cells.

5.1.1.5. ADM and the vicious cycle

Adrenomedullin is a HIF-1 mediated factor which mainly helps cell survival and proliferation by virtue of its angiogenic action. Furthermore, ADM also plays a major role in regulating blood flow to the tumour cells by the modulation of vascular tone and thus help it to proliferate. Features of ADM like anti-apoptosis action, mediation of cell migration, and up-regulation of ADM receptors acts as additional supporters for malignant cell proliferation and tumour growth. In majority cases, the rate of tumour growth exceeds the rate of new blood vessel formation and thus the newly formed patches of tumour faces hypoxia and thus the vicious cycle of hypoxia followed by ADM elevation again followed by hypoxia continues (Ryan et al. 2000). Research also highlights that the newly formed tumour cell, in response to hypoxia, eventually becomes the dominant tumour

cell type and also become chemoresistant. In this project, hypoxia up-regulated the expression of ADM by several folds in all of the cell lines tested. Therefore it can be concluded that ADM is up-regulated under a potentially lethal microenvironment and increase other tumour promoting factors resulting in an aggressive tumour phenotype.

5.1.2. ADM over-expression and cancer

Over-expression of ADM in different tumours aggravates the molecular and physiological features of malignant cells (Zudaire et al. 2003).

Morphologic changes like increased projections, more dynamic plasma membrane and increased migration in response to ADM over-expression have been previously reported (Weisberg et al. 1997). The projection on the cancerous cells are hub for ADM over-expression and also responsible for more dynamic plasma membrane and elevated levels of gelsolin due to ADM over-expression (Martinez et al. 2002). Gelsolin protein vigorously participates in cytoskeletal restructuring that underlies morphological changes and lead to reduction in cell adhesion by reducing the cell adhesion molecules like Fak (Deng et al. 2012). All of these data, together with the fact that ADM increases tumour cell motility, suggest that tumour cells that express high levels of ADM may be more likely to be involved in metastasis.

Figure 77 shows the morphological changes observed in PC3 cells when transfected with vector control (pBUD CE 4.1), RAMP2+CLR and RAMP3+CLR. This study was done in our group by an M.Sc student Nasim Eskandari, while studying the effects of ADM receptor over-expression in PC3 cells. The PC3 cells contained a mixture of phenotypes, although majority of them are more spindle shaped than an epithelial like morphology. Besides spinde shaped and epithelial like, some cells were giant multipolar with flattened appearance. Spindle shaped morphology suggests an early stage of invasiveness (Ding et al. 2010). Cells transfected with vector control contained a mixture of spindle shaped and epithelial morphology. RAMP3+CLR transfected cells contained longer projections

with spindle shaped morphology. RAMP2+CLR transfected cells were large and contained irregular surface when compared to native PC3 cells and vector control. These results show that the neuroendocrine phenotype in prostate cancer correlates with an aggressive phenotype (Abrahamsson 1999). Our findings show that RAMP3+CLR transfected cells are more aggressive looking than RAMP2+CLR transfected cells.

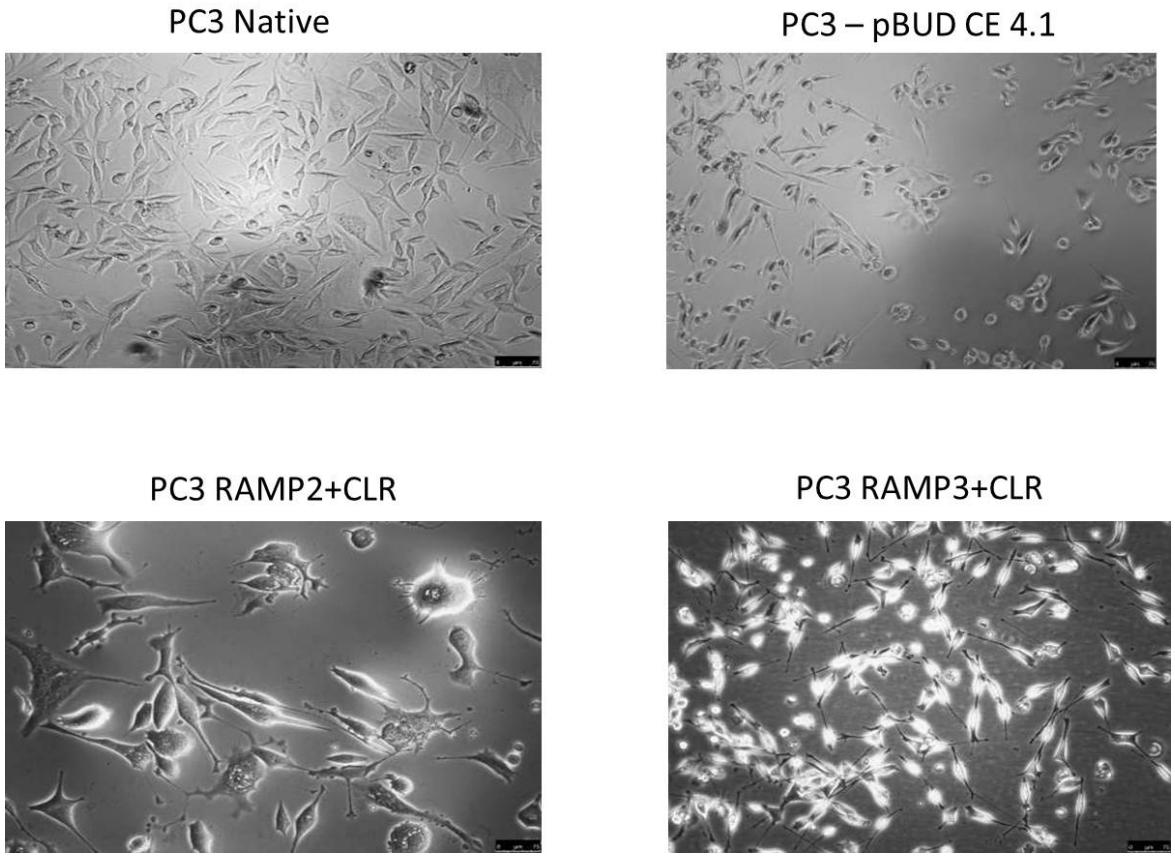

Figure 77: Morphological assessment of PC3 cells transfected with pBUDCE4.1 vector control, RAMP2+CLR and RAMP3+CLR. Cells were viewed under phase contrast microscope. The bar represents 75µm.
Image Courtesy: Over-expression of ADM and its receptors affect cancer cell invasiveness by Nasim Eskandari, 2010.

5.1.2.1. Implication of ADM over-expression in cancer

5.1.2.1.1. Cell proliferation

No proliferation was observed in the breast cancer (MDA-MB-231) and prostate cancer (PC3) cell lines in the present study. Previous studies on breast cancer cells (T47D) identified that effect of ADM over-expression on enhanced proliferation can be observed only in the presence of serum otherwise ADM over-expression can also work as a non-proliferative factor (Martinez et al. 2002). Growth promoting effect of ADM is based on Tyrosin kinase/Mitogen activated protein kinase (TK/MAPK) mechanism. Insulin like growth factor 1 receptor (IGFR) and protein kinase p42/44 MAPK are the main players of tumour progression by ADM. Prototypic signalling by MAPK induces cyclin D mediated cell cycle transition G0 to G1 and G2 to M and thus promotes cell proliferation (Andreis et al. 2000). Even though the present study was done in presence of serum, no proliferation was noted which contrasted with the earlier findings by other researchers. It is plausible that the cells already contained elvated levels of ADM and have reached their full proliferative potential where ADM over-expression would not enhance the proliferation of cells. ADM induced proliferative and non-proliferative effect could be cell type dependent, which needs to be elucidated.

5.1.2.1.2. Cell migration

Cancer cell needs to detach from the basement membrane and migrate in order to cause metastasis. An immune-histochemical study identified the activation of tyrosin kinase receptors can activate PIP3 which in turn activates actin polymerization (Harper et al. 1996). Continuous activation and deactivation of actin leads to cell movement and migration (Cantley 2002). Changes in local microenvironment such as over-expression of ADM can increase migratory characteristic of cancer cells which in turn invade the surrounding tissue and the vasculature (H. Yamaguchi et al. 2005). Over-expression of ADM in this project was observed to enhance migration in both breast cancer and prostate cancer

cell lines. Molecular mechanisms downstream of ADM over-expression resulting in increased cell migration needs to be studied.

5.1.2.1.3. Cell invasion

Enhanced invasion as an effect of ADM over-expression on invasive property of cancer cells were observed on breast cancer cell line (MDA-MB-231) and glioblastoma cell line (U87). One study explains that ADM over-expression causes certain morphological changes in cells. ADM leads to elevation of gelsolin protein which is responsible for cytoskeletal restructuring of cells that enhance cell migration and thus the cells over-expressing ADM become more invasive and more involved in metastasis (Martinez et al. 2002). Another study supports the present outcomes that ADM is strongly induced by hypoxia in pancreatic cancer cell lines and treatment with anti-ADM drugs and anti-CLR antibodies reduces cell invasiveness. However, the study reports that anti-RAMP3 drug cannot be used to treat adenocarcinoma of pancreas as such types of tumour lacks RAMP3 (Keleg et al. 2007). Therefore it is crucial to identify the presence of RAMP3 receptors in any solid tumour before treating it with anti-RAMP3 drugs.

5.1.2.1.4. Receptor regulation

An up-regulation of ADM receptors RAMP2, RAMP3, and CLR was observed in MDA-MB-231 cells over-expressing ADM. An overall increase of ADM receptors in ADM over-expressing cells when compared to native and vector control cells was observed. Similar findings were observed in a study, which noticed that within 5-45 minutes of ADM treatment, cAMP levels increased followed by increased extracellular signal-regulated kinase 1/2 phosphorylation. The entire cascade leads to up-regulation of peptide and mRNA expression for VEGF, RAMP2 and CLR, thus increasing receptor up-regulation (Schwarz et al. 2006). The findings suggest that blocking ADM involvement in proliferation, angiogenesis and inhibition of apoptosis can be effectively achieved by blocking ADM receptors.

5.1.2.1.5. ADM and Bone Homing

Bone homing of breast cancer cells transfected with ADM-GFP could not be determined as the cells stopped producing GFP post inter-cardiac injections. Therefore upon analysing the hind legs of mice, animals injected with cells transfected with ADM-GFP did not produce any tumours on the bone. μCt bone analysis can be carried out to determine if there is any tumour growth on bone. μCt analysis would reveal small niches where tumour cells would lodge and proliferate. Histological analysis of the bone sections would be beneficial as it is possible to determine any abnormality in cell morphology.

5.1.3. Effect of blocking ADM activity in cancer

The role of ADM in cancer progression and characteristics of CLR and RAMP2/3 make them important targets for research in monoclonal antibody therapy. Anti-ADM inhibitor GRP77427 (Gastrin releasing peptide) treated mice resulted in a significant reduction in tumour growth (Martinez et al. 2005). This is one example of how blocking ADM activity can be beneficial in treatment. Published data suggests that mixture of anti-CLR/anti-RAMP2 antibodies as well as anti-CLR/anti-RAMP3 antibodies can specifically inhibit ADM binding to its receptors on tumour cell and thus can induce apoptosis, reduce cell proliferation and block the formation of vascular tubes (Ouafik et al. 2002). An international application numbered WO/2007/045927 (patentscope, 2007) has displayed that pharmaceutical composition consisting of anti-RAMP2 or anti-RAMP3 antibodies can inhibit angiogenesis and proliferation of cancer cells and thus can be used for treating cancers. Different anti-ADM therapies like ADM antagonist, anti-ADM monoclonal antibody, and anti-ADM receptor antibodies are being investigated.

In the current project, *in vitro* studies using JF2, an anti-RAMP3 antibody resulted in reduction in cell proliferation measured by MTT assay. There was 18% reduction in proliferation for MDA-MB-231 cells, 25% reduction in Panc2.3 cells, 11% reduction in MDA-MB-436 cells and 42% reduction in U87 cells.

For the highest dose of 10µg JF2, at day 8 of treatment, MDA-MB-231 cells showed a reduction in proliferation ranging from 4.3% to 9.2%, Pan2.3 cells showed 22.5% to 33.5% reduction, MDA-MB-436 cells showed 10% to 14% reduction and U87 cells showed 35.9% to 49.4% reduction in proliferation. During evisceration, of heart, lungs, liver, spleen and kidneys were analysed for any secondary tumours. Although histologial assessments will have to be carried out to confirm the absence of secondary tumours.

5.1.3.1. ADM receptors and implications of blocking them

G-protein coupled receptors have been found to play important role in different biological and pathological processes and thus are most desirable targets for drug development. GPCRs like endothelin receptors, chemokine receptors, protease-activated receptors and lysophosphatidic acid receptors are known to have action in tumourigenesis and metastasis of multiple human cancers like non-small cell lung cancer, breast cancer, prostate cancer, melanoma, gastric cancer, and diffused large B cell lymphoma. Prominent up-regulation of GPCRs has been observed in these primary and metastatic cancer cells (S. Li et al. 2005).

Two different studies identified that blocking the action of ADM by antagonist (ADM22-52) destabilizes tumour vascularisation and thus inhibit the growth of xenografted pancreatic cancer cells and glial tumour cells (Ishikawa et al. 2003; Ouafik et al. 2002). The role of ADM in cancer progression and characteristics of CLR and RAMPs make them important targets for research in monoclonal antibody therapy. Anti-ADM monoclonal antibody has been observed to neutralize ADM activity in different tumours like breast cancer (Martinez et al. 2002), human glioblastoma (Ouafik et al. 2002) and ovarian cancer cell lines (Giacalone et al. 2003). Figure 78 shows the regulation of ADM and targeting ADM2 receptor would be a viable option for cancer treatment.

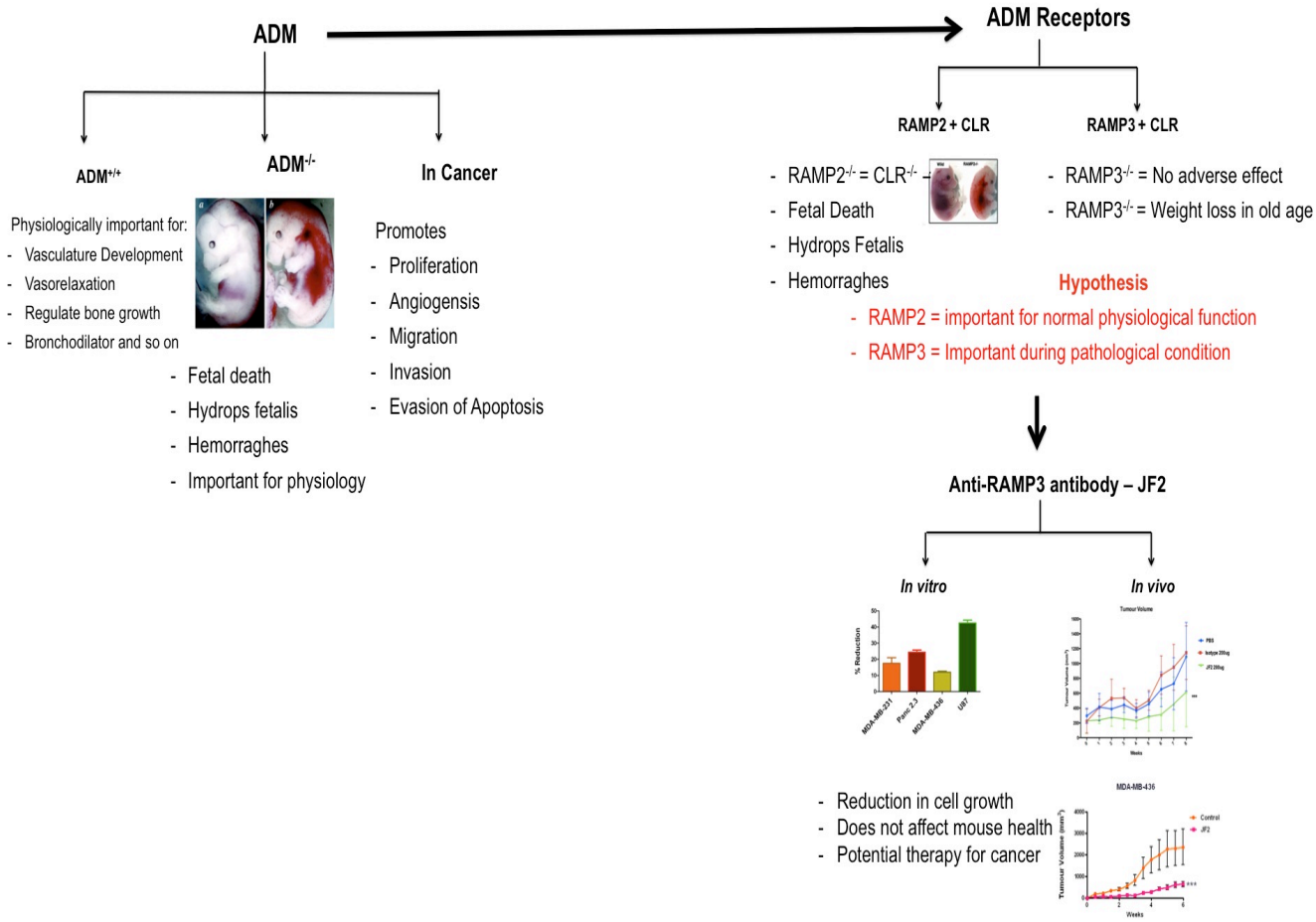

Figure 78: ADM regulates tumour progression and is important for physiology. Two receptors for ADM mediate its functions. It is hypothesized that ADM1 receptor is essential for the basal activity of receptor while ADM2 receptor is important in a pathological conditions. Anti-RAMP3 antibody (JF2) reduces cell proliferation *in vitro* and *in vivo.* Anti-RAMP3 antibody could be a potential therapy for cancer.

5.1.3.2. Targetting RAMP3

There are three important features of RAMP3 that makes it a better target for cancer therapy when compared to RAMP2.

1. CLR/RAMP3 can be recycled to the cell surface for resensitization after the internalization process while the CLR/RAMP2 complex does not get recycled.

Thus prolonged effect can be observed for RAMP3 antagonist than RAMP2 antagonist.

2. Although RAMP3 exhibits three different types of polymorphism, it is resistant to any alterations in coding sequence. This suggests that RAMP3 is less prone to mutation and thus it cannot develop resistance to anti-RAMP3 drug soon.

3. Lysyl oxidase (LOX) produced during hypoxic stress inside tumour up-regulates RAMP3 expression and thus RAMP3 can be targeted for the treatment of solid tumours (Brekhman et al. 2010).

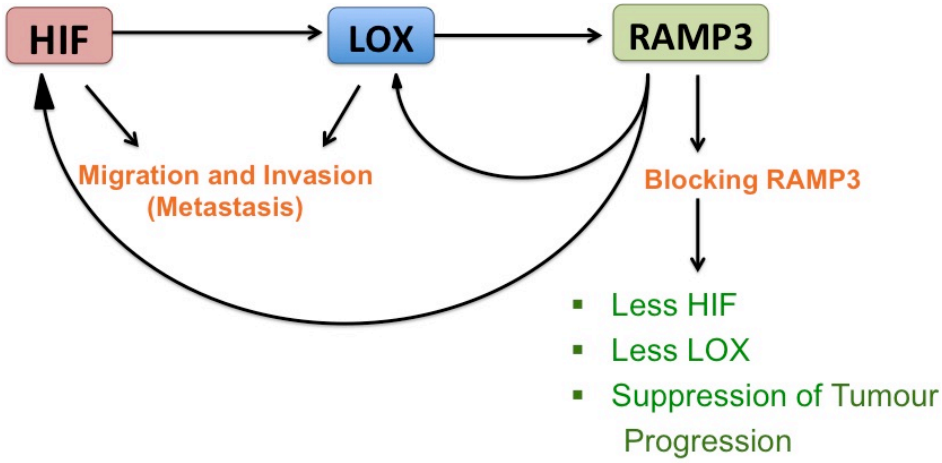

Figure 79: Hypothetical repercussion of blocking RAMP3. The effect of hypoxia on inducing LOX, which in turn activates RAMP3 resulting in migration and invasion of tumour cells. Therefore the hypothesis is to block RAMP3, which results in less HIF, LOX and eventual suppression of tumour progression. Figure drawn by self.

The two facts that

1. RAMP3 gets up-regulated during hypoxia by LOX and
2. Hypoxia can be correlated with poor prognosis in cancer patients;

provides a combined conclusion that RAMP3 has a strong potential to be developed as an anti-cancer drug target. LOX-2 levels elevated during hypoxia gets bound to the RAMP3 and affect signalling, transcription and translation (both directly and indirectly), leading to changes in cell adhesion, motility and proliferation (Barker et al. 2012). Figure 79, shows the hypothetical model put forth by this research.

5.3. Limitations of study

Results obtained this far are not a conclusive evidence for what has been discussed. The discussion merely suggests the possible outcomes of the results obtained. Limitations of the study have been discussed below:

1. It was unable to quantify the amount of ADM that was being secreted by the cells. This would have enabled a better understanding of the actual protein levels as mRNA levels does not correlate with protein levels.

2. Accurate quantification of ADM receptors is one of the biggest limitation to this study. As discussed under validation studies, RAMP2 and RAMP3 could not be determined using western blotting. Whether it is the specificity of the antibodies or protein extraction methods is unclear. Since the antibodies produce non-specific bands in western blotting, FACS data seem to show otherwise.

3. Flow cytometry results although is shown as 10,000 cells per experiment, experimental repeats resulted in high control IgG binding. This control IgG binding could not be hindered despite several attempts such as blocking for non-specific epitopes using serum, different concentrations of antibodies and different cell numbers.

4. The time points taken for hypoxia experiment (24hrs and 48hrs) are not ideal to determine intracellular signalling and receptor expression. Although this time point would be sufficient to determine changes in ADM and other secretory peroteins. Since shorter time points are not possible using the current incubator that we have. Determining the right concentration of $CoCl_2$ that elicits HIF-1α protein could be used to mimic hypoxia. This could then be used to determine intracellular changes at very short time points.

5. The unavailability of stable ADM over-expressing vector was a major disadvantage. Unfortunately, the ADM-IRES-GFP vector inserted in the experimental mice stopped producing ADM. The failure of mice to produce ADM made the experiment a failure as the effect of these invasive cancer cell lines on bone homing was not observed.

6. Result assessment for migration assay was also cumbersome. The distance measured in the scratch was not very accurate as the scratch was not in a straight line and the linings of scratch were haphazard. Problems were also observed while measuring surface area as the wounded area gets converted to non wounded area due to scratches and dust on the surface of the plate.

7. The binding of JF2 to RAMP3 was not confirmed by western blot or by FACS. Despite using high JF2 concentrations, it was not possible to get a RAMP3 blot in both cell membrane and whole cell lysate samples. Although this was not possible by me, this has been done previously by Dr. Gareth Richards in our Lab while optimising and validating JF2 antibody (unpublished data).

8. Although cell proliferation is a good measure of determing the activity of JF2, apoptosis assay to measure the rate of cell death, functional assays such as cAMP, cell migration, cell invasion assays in presence of JF2 would have been a stronger advocate of its activity.

9. Measuring circulating ADM levels during *in vivo* experiments would have been a good marker for the role of ADM in cancer. It would have been interesting to know if circulating ADM levels were reduced in JF2 treated mice.

10. IHC for angiogenesis, apoptosis, CLR, RAMP2 and RAMP3 for *in vivo* samples would have provided information on receptor expression levels in treatment and control groups in *in vivo* studies.

11. In some experiments, n = 1 makes statistical analysis impossible and therefore no real conclusions could be determined.

5.4. Future Work

Since the mechanism of action of ADM1 and ADM2 receptors are unclear, hene knock down studies of RAMP2 or RAMP3 or both can be established in cancer cell lines. Microarray analysis of these gene knockdown models would provide information on the differential signalling mechanism between RAMP2 and RAMP3. These knockdown models can also be assessed for cell migration and invasion.

Although the findings of the study suggested anti-RAMP3 antibody as an efficient treatment for pancreatic, glioblastoma and breast cancers, there was no dose response. Functional studies using anti-RAMP3 antibody such as migration assay, apoptosis assay, invasion assay, cAMP assay would be beneficial. Information on the toxicity, stability and potency of the antibody would establish it as a potential therapeutic agent. It would be beneficial to compare the effects of RAMP3+CLR complex antibody with that of RAMP3 antibody, as this would be specifically neutralise the ADM2 receptor.

5.5. Conclusion

In conclusion, the present study has shown that ADM is up-regulated in a malignant setting, concurring with previously published data. Hypoxia was used as a measure of an aggressive tumour characteristic. ADM expression in response to hypoxia was increased by several folds in glioblastoma, pancreatic, breast and prostate cancer cells. Effect of ADM up-regulation resulted in no difference in cell proliferation since ADM is known to be pro-proliferative. Despite no significant difference in cell proliferation, there was an increase in cell migration, invasion and receptor up-regulation, specifically RAMP3 receptor under ADM over-expression. This led to hypothesize that RAMP3 component is crucial for ADM activity in cancer. Our in-house generated anti-RAMP3 antibody – JF2 was used to neutralise/inhibit ADM mediated cell proliferation in various cancer cells and tumour growth in xenograft model. Our preliminary results show that JF2 is efficient in blocking ADM mediated proliferation at ng and µg levels in glioblastoma, pancreatic, breast and prostate cancer cell lines. *In vivo* studies using pancreatic cancer cells resulted in significant reduction in tumour size and volume. Tumour regression in xenograft models suggested the the tumour was responding to anti-RAMP3 treatment. No physiological abnormalities were observed in all vital organs in mice receiving JF2 treatment. This suggests that targeting RAMP3 using JF2 antibody does not result adverse side effects. Further research into the toxicity, reactivity, pharmacokinetics and pharmacodynamics of JF2 is required in order to establish it as a potential anti-cancer therapeutic agent.

CHAPTER VI: APPENDIX

6.1. Recipes and Materials

6.1.1. Hypoxic Regulation of Adrenomedullin and its Receptors

6.1.1.1. Western Blotting

A. Resolving gel

	7% **(HIF-1α, PAM)**	**12%** **(RAMP2, RAMP3, CLR, Actin, Akt)**	**15%** **(ADM)**
ddH_2O	5ml	3.3ml	2.3ml
30% Acrylamide	2.33ml	4ml	5ml
1.5M Tris pH8.8	2.5ml		
10% SDS	100µl		
10% APS	100ul		
TEMED	10ul		
Total	10ml		

B. Stacking gel

	4%
ddH_2O	3ml
30% Acrylamide	670µl
0.5M Tris pH6.8	1.25ml
10% SDS	50µl
10% APS	50µl
TEMED	5µl
Total	5ml

C. NP-40 Cell lysis Buffer

1% NP40	2ml
50mM Tris pH8	1.21g
150mM NaCl	1.5g
2mM EDTA	148.88mg

Make upto 200ml in ddH_2O.
+ Protease inhibitors added during cell lysis.

D. 10x Protein Loading Buffer

DTT	500mg
20% SDS	3.33ml
1M Tris HCl pH 6.8	800µl
Glycerol	6.65ml
2% Bromophenol blue	665µl

Aliquot and freeze at -20°C.

E. 5x Running Buffer

Glycine	72g	1M
Tris Base	15.5g	130mM
20% SDS	25ml	
ddH_2O	975ml	

F. Transfer Buffer

Tris Base	3g	25mM
Glycine	14.4g	200mM
Methanol	200ml	20% (v/v)
ddH_2O	800ml	

G. 10X TBS

NaCl	80g
KCl	2g
Tris Base	30g
ddH_2O	800ml

Adjust pH to 7.4 and make upto 1L.

H. Blocking Buffer

Non-fat powdered milk	5g	5% (w/v)
TBS	100ml	

I. Washing Buffer

Tween 20	500µl
TBS	1L

2. Flow Cytometry

A. 4% PFA

Add 8g paraformaldehyde to 100ml water and heat to 60°C in a fume hood. Add few drops of 1M NaoH to help dissolve. When the solid had completely dissolved, allow the solution to cool to room temperature and add 100ml 2X PBS. Aliquot and freeze at -20°C.

B. Permeabilisation solution

Tween	250µl	0.5% (v/v)
PBS	50ml	

C. Wash Buffer

BSA	2.5g	0.5%(w/v)
PBS	500ml	

Materials

Cell Culture

Media	GIBCO
PBS	
Trypsin EDTA	Sigma Aldrich
Pencillin/Streptomycin	
Fetal Calf Serum	Invitrogen
Haemocytometer	Hawksleys

Hypoxia

Cobalt Chloride	Sigma Aldrich

RNA Isolation

Tri Reagent	Sigma
Chloroform	
DEPC treated water	
Isopropyl Alcohol	Fisher Scientific
DNase treatment	
TURBO DNA-free kit	Applied Biosystems
cDNA Synthesis	
High Capacity RNA-cDNA Kit	Applied Biosystems

Real Time PCR

Taqman Gene Expression Master Mix	Applied Biosystems
DEPC treated water	Sigma

Hoechst Staining

Hoechst stain	Sigma
Ethanol	Fisher Scientific
Acetic Acid	VWR – Prolabo
Mowiol	Polysciences
Phenylenediamine	Sigma

Western Blotting

NP-40	Fluka
Protease Inhibitors	CalBioChem
Protein Quantification	
BCA Assay Kit	Sigma
BSA	
Poly Acrylamide Gel Electrophoresis	
Glass sides	BioRad
30% Acrylamide	National Diagnostics
SDS	Sigma
APS	agtcBioproducts

TEMED	Sigma
Tween	Fisher Scientific
Biotinylated protein ladder	Fisher Scientific
Kaleidoscope ladder	
PVDF- Amersham Hybond-P	GE Healthcare
Milk Powder	Marvel
Protein Detection	
ECL – Super Signal West Dura Extended Duration Substrate	Thermo Scientific
Amersham Hyperfilms	GE Healthcare

Flow Cytometry

PFA	Fisher Scientific
Normal Rabbit Serum	Vector Laboratories
IgG Control	

Antibodies for Western Blotting and Flow Cytometry

Primary Antibodies	
RAMP2	SantaCruz/ Catalogue no: sc-8852
RAMP3	SantaCruz/ Catalogue no: sc-8854
CLR	SantaCruz/ Catalogue no: sc-18007
ADM	SantaCruz/ Catalogue no: sc-33187
HIF-1α	SantaCruz/ Catalogue no: sc-8711
Akt	Cell Signalling/ Catalogue no: 4691

Phospho-Akt	Cell Signalling/ Catalogue no: 4060
PAM	Abcam/ Catalogue no: ab77592
β-actin	Abcam/ Catalogue no: ab16039
Western Blotting Secondary Antibodies	
Anti-goat HRP	Sigma/Catalogue no: A5420-1ML
Anti-rabbit HRP	Sigma/ Catalogue no: A9169-2ML
Anti-biotin HRP	Cell Signalling
Flow Cytometry Secondary Antibodies	
Anti-goat FITC	Dako/ Catalogue no: F0250

6.1.2. Effect of Over-Expression of ADM and its Receptors

6.1.2.1. Transfection

Electroporation Buffer

Water	5ml	
KCl	50.3mg	135mM
$MgCl_2$	952.1µg	2mM
HEPES	23.83mg	20mM
Ficoll 400	25µl	0.5%

Adjust pH to 7.6. Filter Sterlise and add ATP and Glutathione fresh during transfection.

Xylene DNA Loading Buffer

Xylene Cyanol	25mg
Sucrose	4g
Water	10ml

6.1.2.2. Kapa PCR

In a 25µl reaction volume, combine the following:

Reaction Component	Final Concentration
2X Kapa Ready mix	1X
Primer mix	0.5µM each
Template DNA	10-100ng

6.1.2.3. KOD PCR

In a 50µl reaction volume, combine the following:

Reaction Component	Final Concentration
10X Buffer	1X
25mM $MgSO_4$	1.5mM
dNTPs (2mM each)	0.2mM each
Primer mix	0.3µM each
Template DNA	100ng
KOD DNA Polymerase (1U/µl)	0.02U/µl

Materials

Bacterial Culture

LB Broth	Sigma
LB Agar	
Ampicillin	
Chloramphenicol	
Zeocin	Invivogen

Top 10 E.Coli Chemically Competent Cells	Invitrogen

Vectors

pcDNA3.1	Invitrogen
pBUDCE4.1	
EX-Receiver-M61 (IRES-eGFP)	Genecopoeia

Plasmid DNA Extraction

Plasmid DNA Extraction kit	Promega

PCR

Kapa 2G Readymix PCR Kit	KapaBiosystems
KOD PCR Kit	Novagen Toyobo
Primers	MWR

Gel Electrophoresis

Agarose	Sigma
Tris Borate EDTA	
Xylene Cyanol	
Sucrose	Fisher Scientific
DNA ladder	Promega

Gel Extraction of DNA

Zymoclean Gel DNA Recovery Kit	Zymoresearch

DNA Manipulation

Precipitation	
Ethanol	Fisher Scientific
Sodium Acetate	
Restriction Digestion	
Xho I	New England Biolabs (NEB)
Hind III	
Dephosphorylation	
Antartic Phosphatase	NEB
Ligation	
T4 DNA Ligase	NEB
Demethylation	
Dpn I	NEB
RNase Treatment	
Ribonuclease H, E.Coli	Ambion

Transfection

Linearisation	
Fsp I	NEB
Mfe I	
Electroporation	
4mM gap Cuvette	Cell Projects
ATP	
Glutathione	Sigma
Antibiotics	
G418 (Geneticin)	Sigma

Proliferation assay

MTT Cell Proliferation Assay Kit	ATCC

RT-PCR

RNase Zap	Ambion

In vivo

Mice	Harlan, UK
Ketamine	Fort Dodge Animal Health
Xylazine	Bayer Plc
25Gx$^{5}/_{8}$" Needle	BD Microlance

6.1.3. Neutralisation of ADM activity using anti-RAMP3 antibody

Materials

Proliferation Assay

MTT Assay Kit	ATCC
IgG1 Isotype	Antibody Resource Unit, University of Sheffield.
JF2	

Xenograft Modelling

Matrigel	BD Biosciences
Isoflurane	IsoFlo
23G Needle	BD Microlance
Ethanol	Fisher Scientific

Histology

Haemotoxylin	Fluka
Eosin	
Xylene	Fisher Scientific
DPX Mountant	BDH Laboratory Supplies

6.2. Results

6.2.1. Hypoxic Regulation of Adrenomedullin and its Receptors

6.2.1.1. Hypoxia using Cobalt Chloride ($CoCl_2$)

Glioblastoma (U87) cells were treated with 300μM $CoCl_2$ to induce hypoxia since it is known to mimic hypoxic environments. Cells respond to hypoxia by up-regulating the expression of HIF-1α. HIF-1α is the marker for hypoxia and is stabilised under hypoxic conditions.

Figure 80, shows the preliminary analysis of HIF-1α mRNA expression quantified by qPCR. The bars show the HIF-1α mRNA in relation to the mRNA expression of HPRT1. It is seen that HIF-1α mRNA is not up-regulated at any of the time points when compared to the respective normoxic controls.

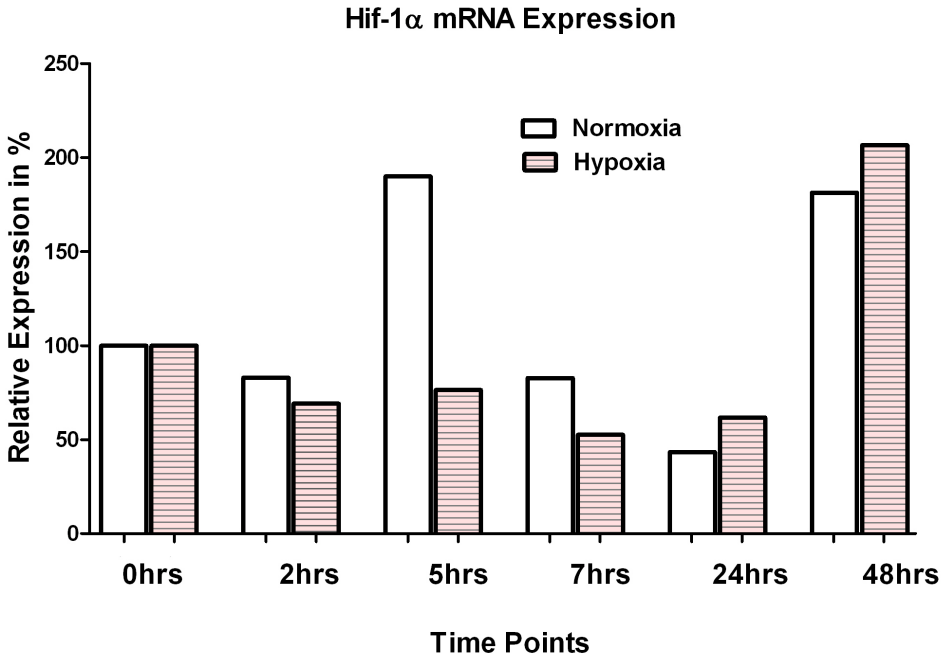

Figure 80: Preliminary analysis of HIF-1α mRNA expression in Glioblastoma cells when exposed to hypoxia and normoxia. β-Actin was used as an endogenous control to normalise the results. The bars are shown as a relative expression to HIF-1α expression at 0hrs. n=1.

6.2.1.2. Hoechst Staining

In order to test if the $CoCl_2$dose was toxic to the cells, Hoechst staining was done to morphologically assess the dead cells. Figure 81, shows the cell death index of cells belonging to both $CoCl_2$ treated and untreated groups. It can be seen that cells were undergoing apoptosis as a result of either overdose of or prolonged exposure to $CoCl_2$. Since cells in normoxa seemed less dead, it is plausible to conclude that the cells were dying as a result of $CoCl_2$.

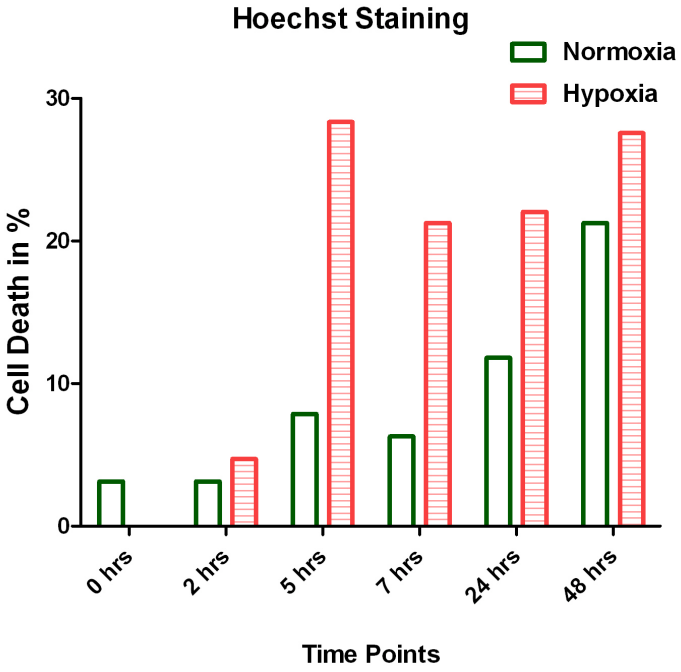

Figure 81: Cell death index of Glioblastoma cells when exposed to 300μM of $CoCl_2$. Cells were stained with Hoechst and pictures were taken at 10X magnification in Leica 4000B microscope and counted using ImageJ. Cells exposed to $CoCl_2$ seemed to be more apoptotic than cells in normoxia. n=1.

6.2.1.3. $CoCl_2$ Dose Response

In order to determine the optimal concentration of $CoCl_2$; a dose response over a 6hr period was done.

Figure 82A, shows the mRNA expression of HIF-1αin the Glioblastoma cells when treated with 50μM $CoCl_2$. The bars are drawn relative to the expression of HIF-1αat 0hrs.It can be seen that there is no time dependent increase in the mRNA expression, although there was a several fold increase at 30mins. Similar result was observed when the $CoCl_2$ dose was increased to 100μM (figure 82B).

A 150μM dose showed a time dependent decrease, but the levels were never above the base line (0hrs) as shown in figure 82C.

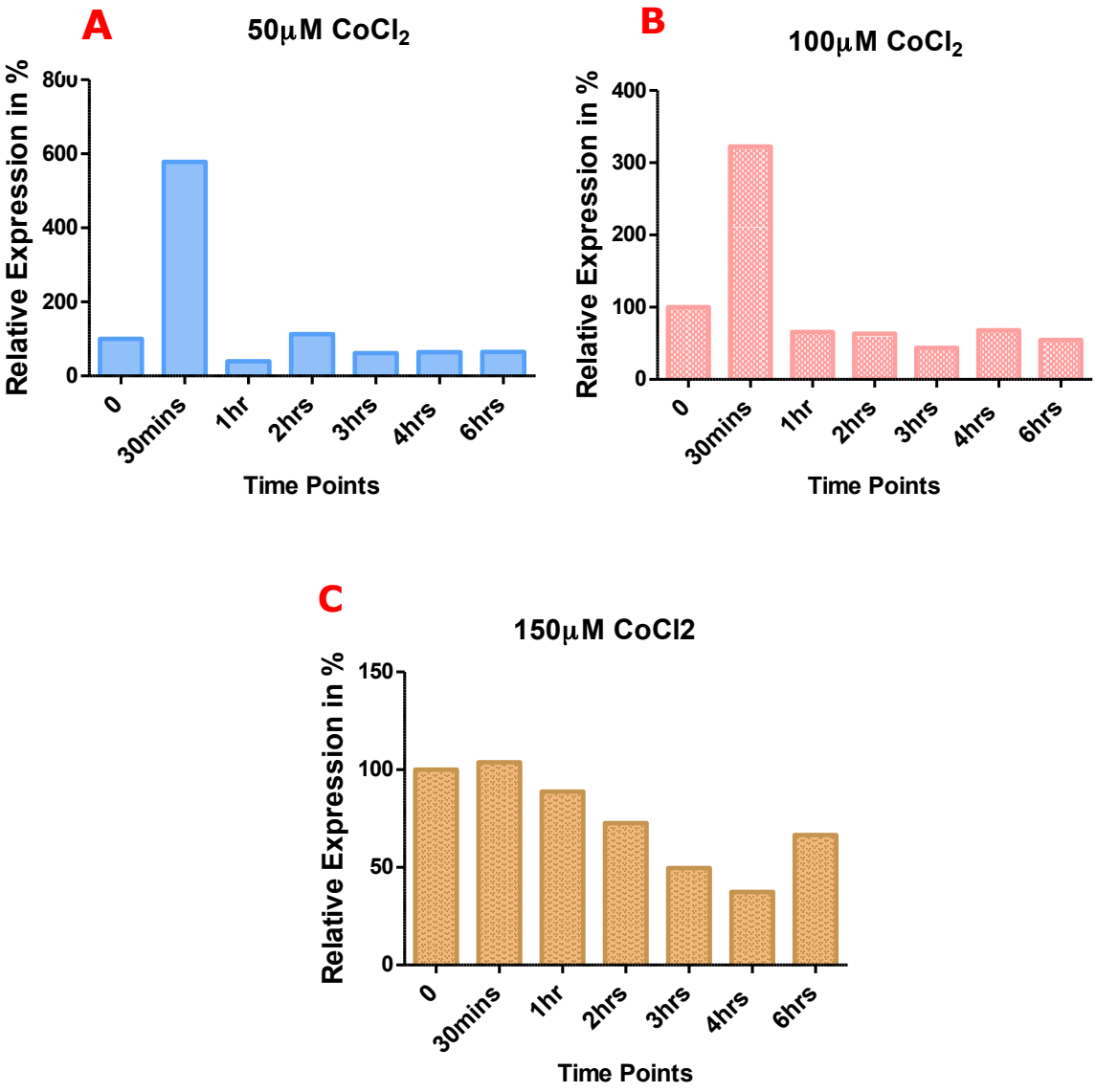

Figure 82: Graph shows the mRNA expression of HIF1-α under different time points in Glioblastoma cells when treated with 50μM (A), 100μM (B) and 150μM (C) Cobalt Chloride. The bars are shown relative to the expression at 0hrs at the respective doses. n=1.

6.2.1.4. Hypoxia using 0.1% O_2

Since HIF-1α mRNA expression was not up-regulated when treated with various doses of $CoCl_2$, hypoxia was induced using an incubator containing 0.1% O_2.

Figure 83A shows the mRNA expression of HIF-1α in Glioblastoma cells and figure 83B shows the expression in breast cancer cells (MDA-MB-436). Both these cell lines did not show an increase in the HIF-1α expression when compared to normoxic controls.

A

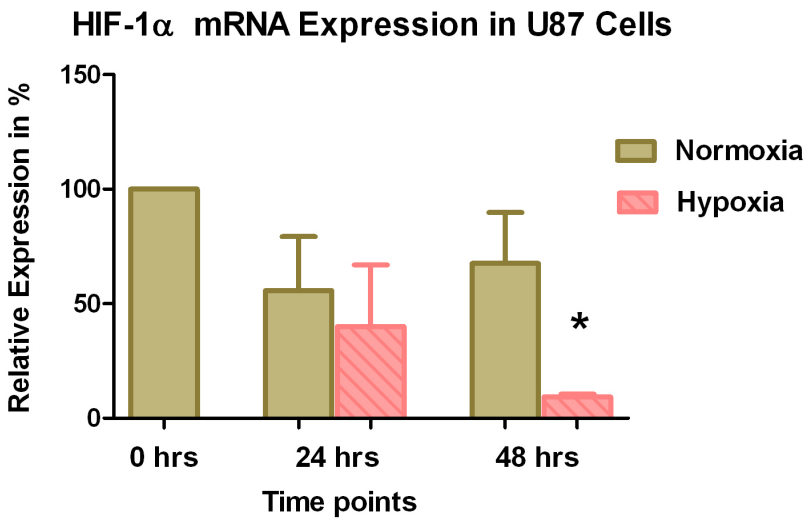

B

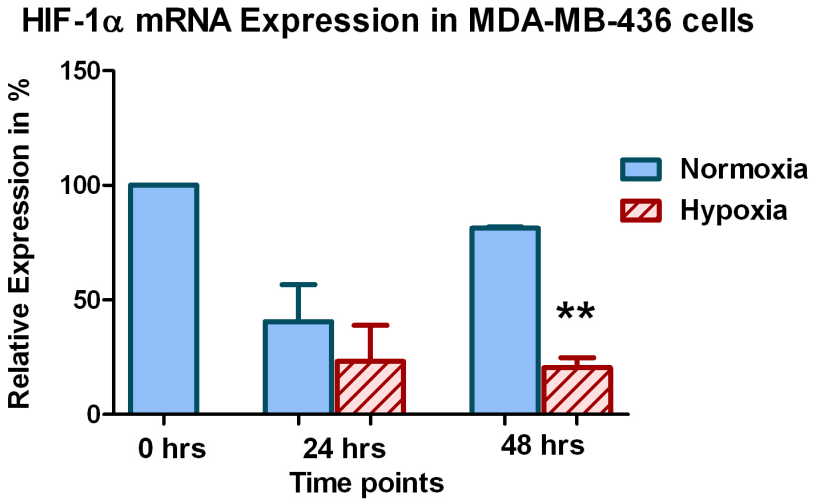

Figure 83: mRNA expression of HIF-1α under hypoxia and normoxia in glioblastoma (A) breast cancer (B) cells measured by qPCR. The bars show relative expression to the expression at 0hrs. n=4 each, $p<0.005$

Since 24hrs could be a long time point, a 2hr exposure to hypoxia was done. Figure 84 shows the HIF-1α expression at 2hrs hypoxia in the Glioblastoma and breast cancer cells.

The breast cancer cells did not show an increase in the HIF-1α expression, while the Glioblastoma cells showed an increase when compared to its normoxic

counterparts although it was not a significant increase from the expression at 0hrs.

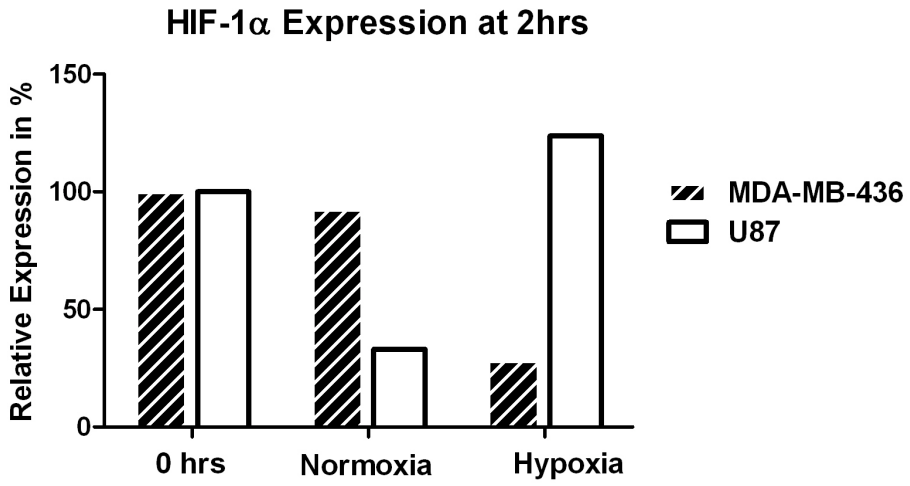

Figure 84: mRNA expression of HIF-1α in two different cell lines under 2hrs hypoxia measured by qPCR. The bars show relative expression to the expression at 0hrs for each cell line. n=1

6.2.1.5. Induction of Hypoxia using hypoxic media

Another strategy was undertaken to induce hypoxia – the media was incubated in the hypoxic incubator for 24hrs and Glioblastoma cells were treated with this media and cultured in a regular incubator.

Figure 85 shows the image of cells treated with regular and hypoxic media for an hour. It can be seen that cells treated with hypoxic media look stressed while cells cultured in regular media look normal with their usual morphology.

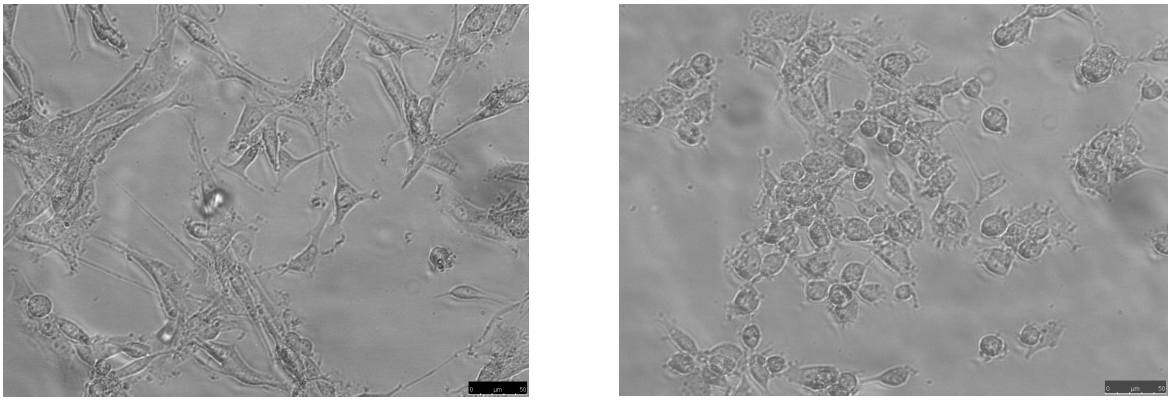

Normoxia **Hypoxia**

Figure 85: Pictures of the stress experienced by U87 cells when treated with regular and hypoxic media for 1hr. Cells treated with regular media looks healthy. Bar = 50µm.

Figure 86 shows the mRNA expression of HIF-1α in Glioblastoma cells when treated with hypoxic media. The bars are drawn in relative to the expression at 0hrs. It can be seen that the HIF-1α mRNA was not up-regulated under hypoxia when compared to normoxia.

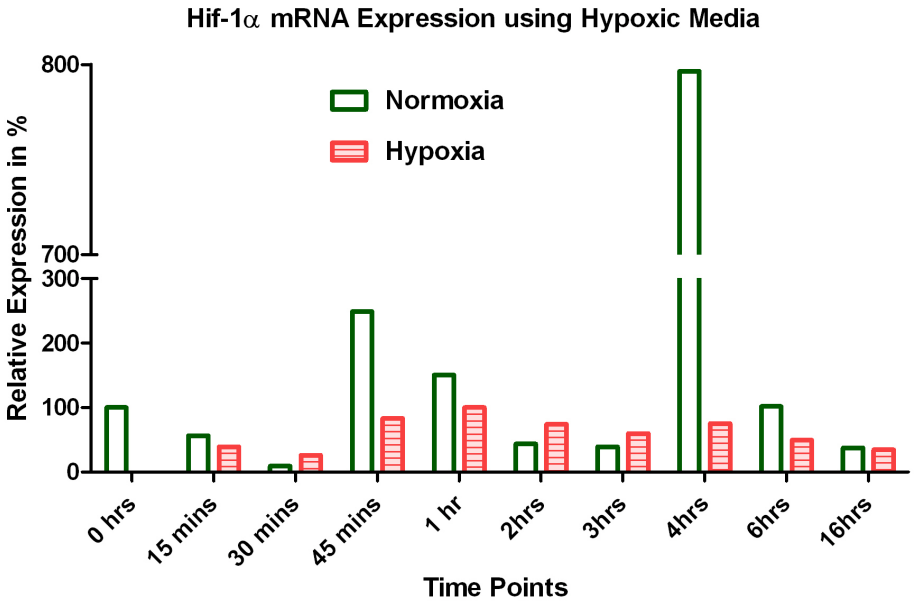

Figure 86: mRNA expression over different time points in glioblastoma cells when treated with hypoxic media measured by qPCR. The bars are represented in relative to the expression at 0hrs, which is 100%. n=1.

6.2.1.6. Validation of qPCR primers

qPCR primers obtained from applied biosystems were validated using plasmid DNA containing RAMP2, RAMP3, CLR and ADM. Concentrations of plasmid DNA ranging from 1pg to 1µg in log10 increments was done – figure 87. The goodness of fit was considered good if R^2 was $0.95 \leq R^2 < 1$. The R^2 for RAMP2 is 0.99, RAMP3 is 0.95, CLR is 0.97 and ADM is 0.98. Actin primers were validated using Human Dermal Micro Endothelial Cells (HuDMEC). RAMP2 primers was also tested in this cell line. The R^2 values for Actin and RAMP2 in HuDMEC samples were 0.98 and 0.97 respectively.

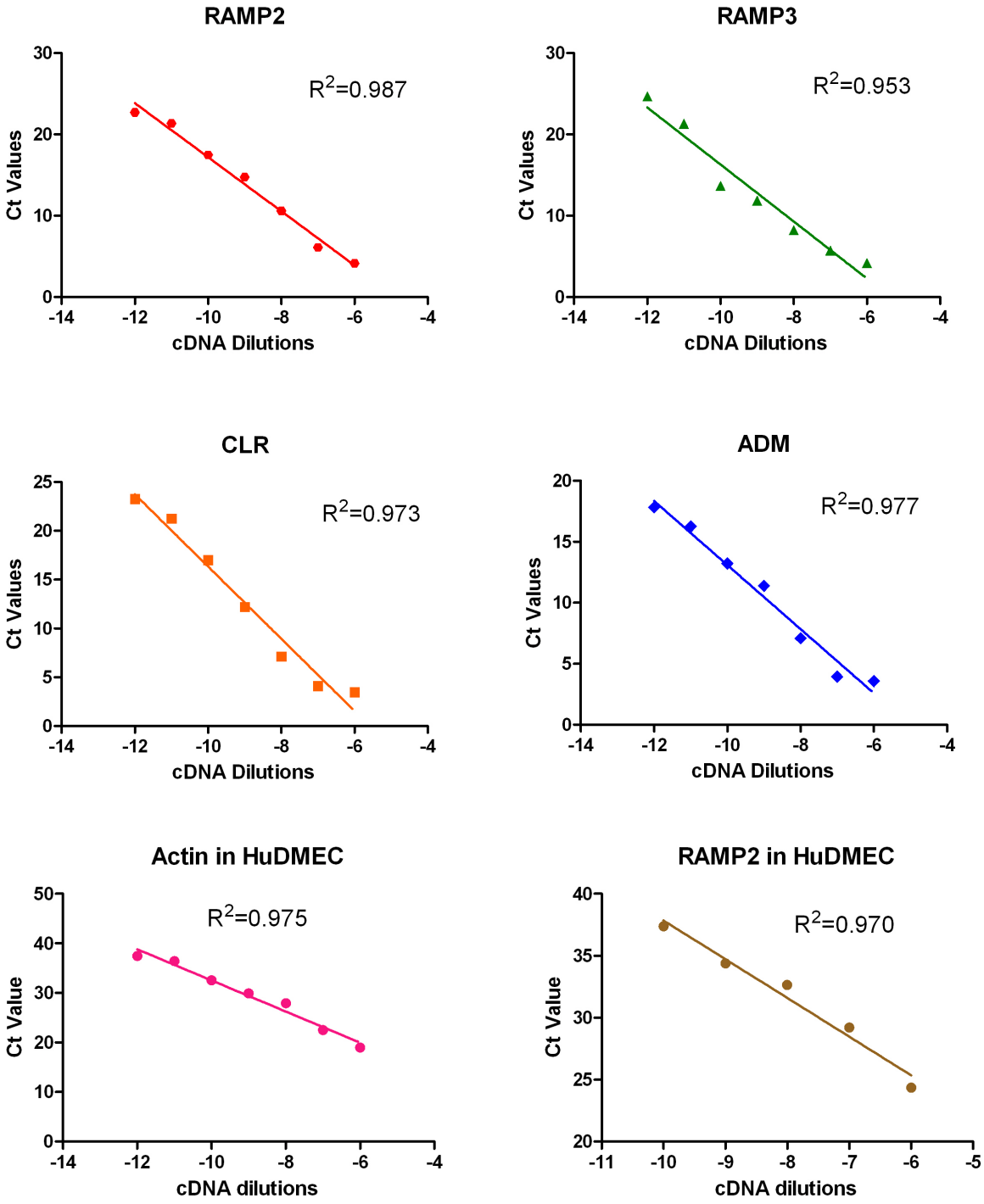

Figure 87: Linear Regression analysis of qPCR amplification of plasmid DNA for RAMP2, RAMP3, CLR and ADM in pcDNA3.1 vector. Actin and RAMP2 was amplified in HuDMEC cell line. The R^2 values for each regression analysis are shown as a goodness of fit.

ADM qPCR primers were tested on various cancer cell lines to determine the level of expression.

Preliminary analysis of the mRNA expression of ADM is shown in figure 88. The bars are drawn as a relative expression to the HPRT1 housekeeping gene. That is, the mRNA expression of HPRT1 is considered to be 100% and the expression of ADM is relative to HPRT1. ADM and the calibrator HPRT1 were normalised to β-actin.

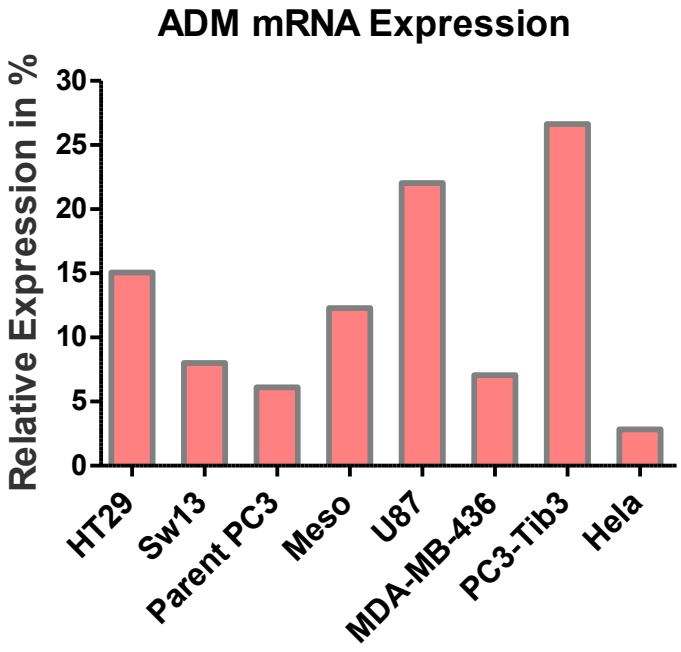

Figure 88: mRNA analysis of ADM expression in nine different cancer cells measured by qPCR. The expression is shown in relative percentage to HPRT1, the expression of which is considered 100% (not shown). qPCR data was analysed using the ΔΔCt method. n=1.

The mRNA expression of RAMP2 and RAMP3 could not be determined under both normoxic and hypoxic conditions.

6.2.1.7. ADM Protein Expression

Figure 89 shows the western blotting for ADM expression in glioblastoma cells when exposed to hypoxia and normoxia. The protein sample was 50µg of whole cell lysate of cells. The bands seen belong to 40kDa and 50kDa. A faint band at 20kDa can be seen for 24hrs hypoxia sample.

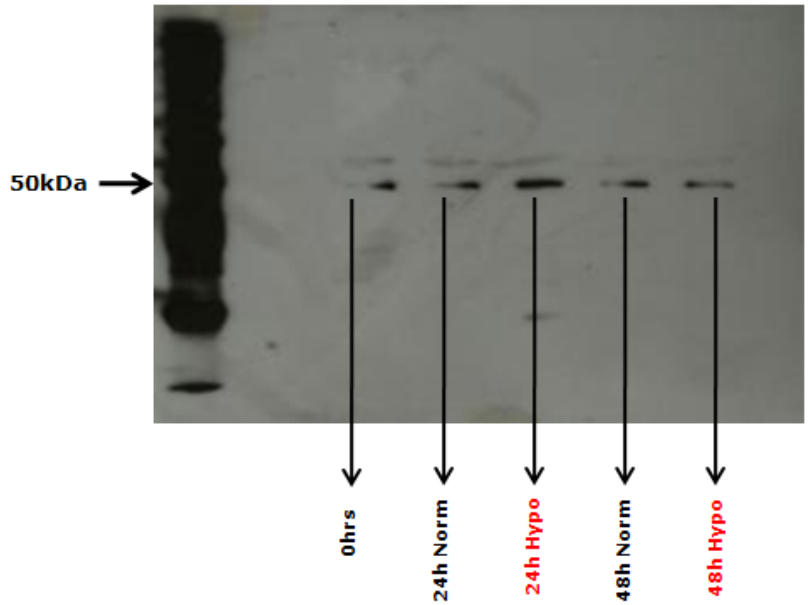

Figure 89: Western blot for ADM expression in whole cell lysate of Glioblastoma cells when exposed to hypoxia and normoxia.

Figure 90 shows the western blotting for ADM expression in Glioblastoma cultures media when exposed to hypoxia and normoxia. Multiple bands belonging to 120kDa, 50kDa, 30kDa and 7kDa were observed. The 7kDa bands could belong to ADM.

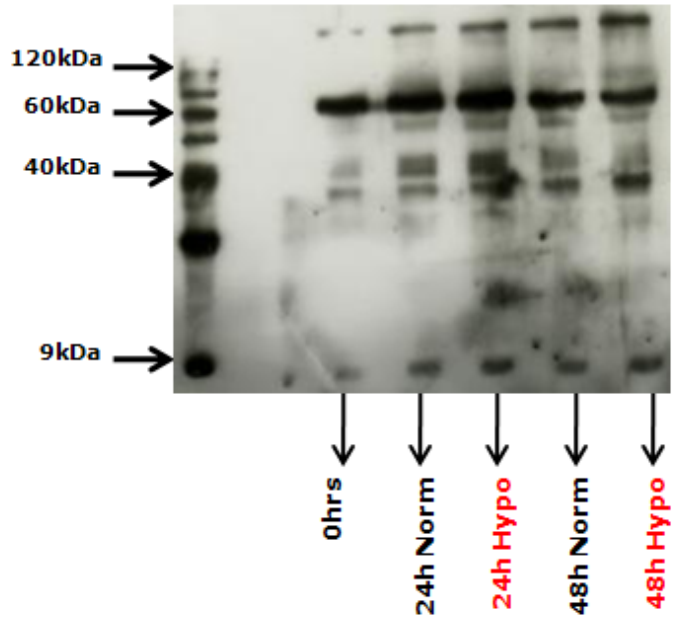

Figure 90: Western blot for ADM expression in culture media of glioblastoma cells when exposed to hypoxia and normoxia.

6.2.1.8. Quantification of RAMP2 and RAMP3

Figure 91 shows the flow cytometric analysis of receptor expression in native (non-transfected cells) cos-7 cells used as negative control. M1 is the histogram statistics after normalising for control IgG.

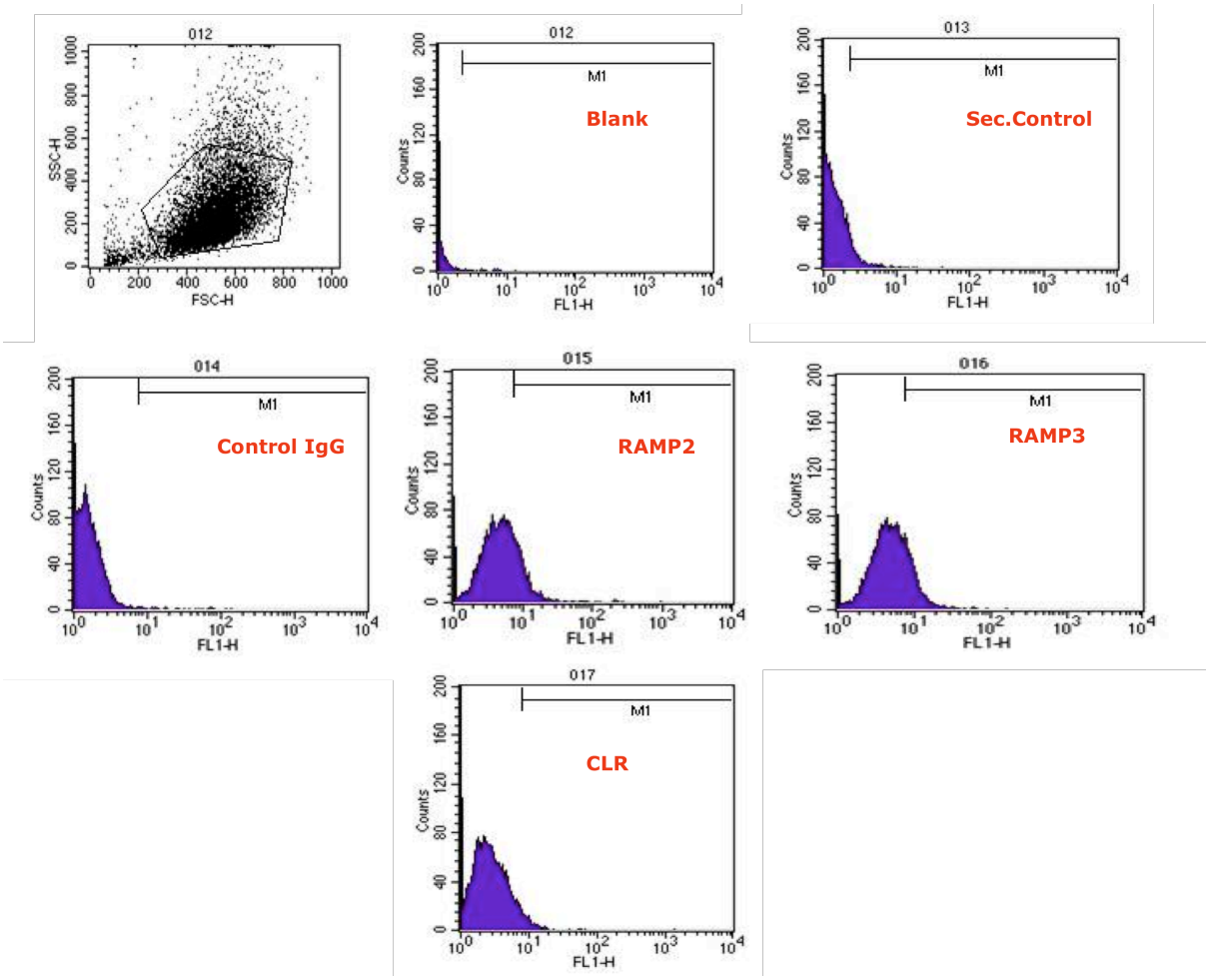

Figure 91: Histograms show the fluorescent intensities for ADM receptors, isotype control, secondary control and non-stained Cos-7 cells.

Figure 92 shows the flow cytometric analysis of receptor expression in U87-glioblastoma cells. M1 is the histogram statistics after normalising for isotype control.

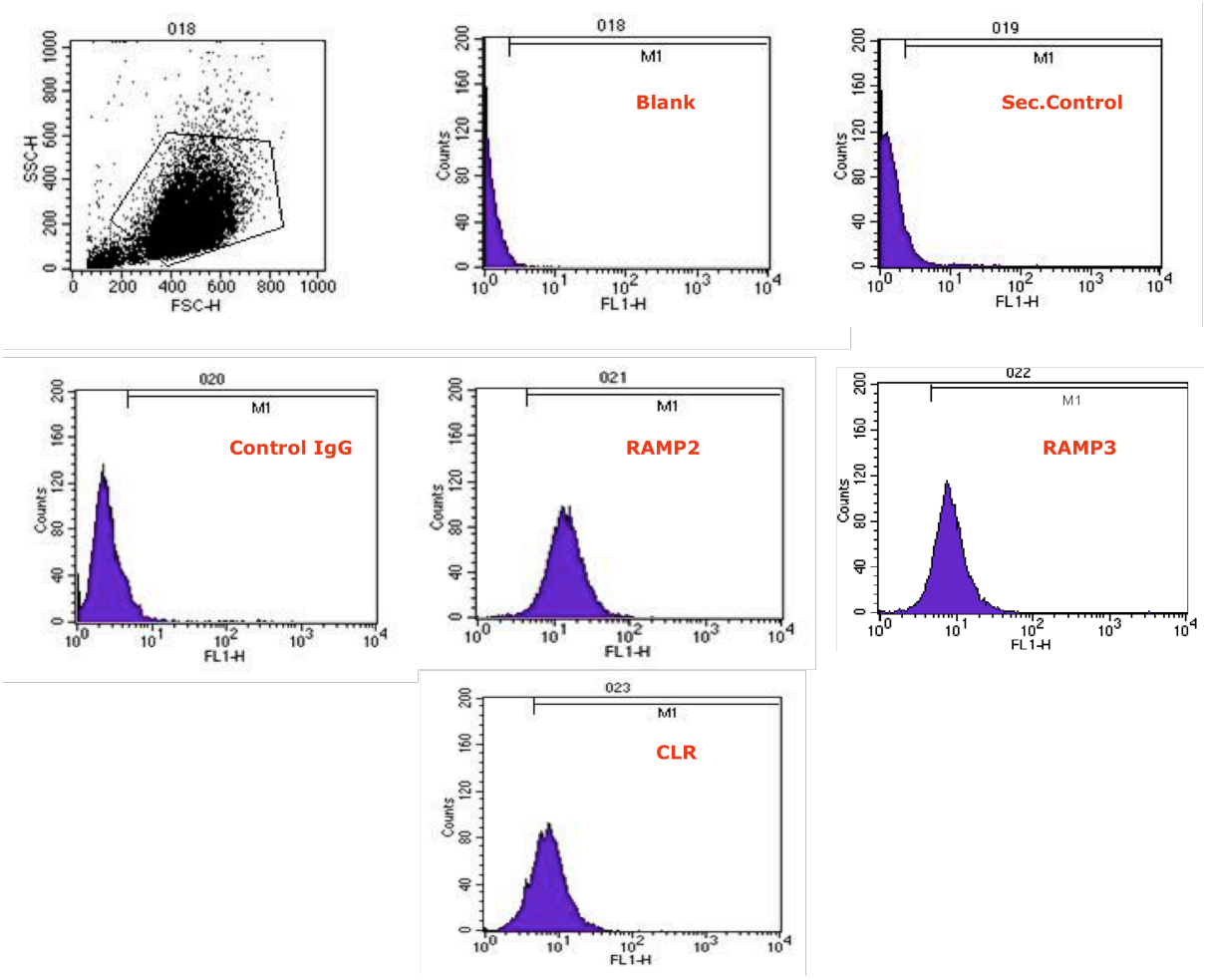

Figure 92: Histograms show the fluorescent intensities for ADM receptors, isotype control, secondary control and non-stained glioblastoma (U87) cells.

Figure 93 shows the histograms of U87 cells at 0hrs normoxia/hypoxia. Figure 93A shows the total protein expression in permeabilised U87 cells whereas figure 93B shows the cell surface protein expression in non-permeabilised U87 cells. M1 shows the histogram statistics of the region after being gated for isotype control.

A

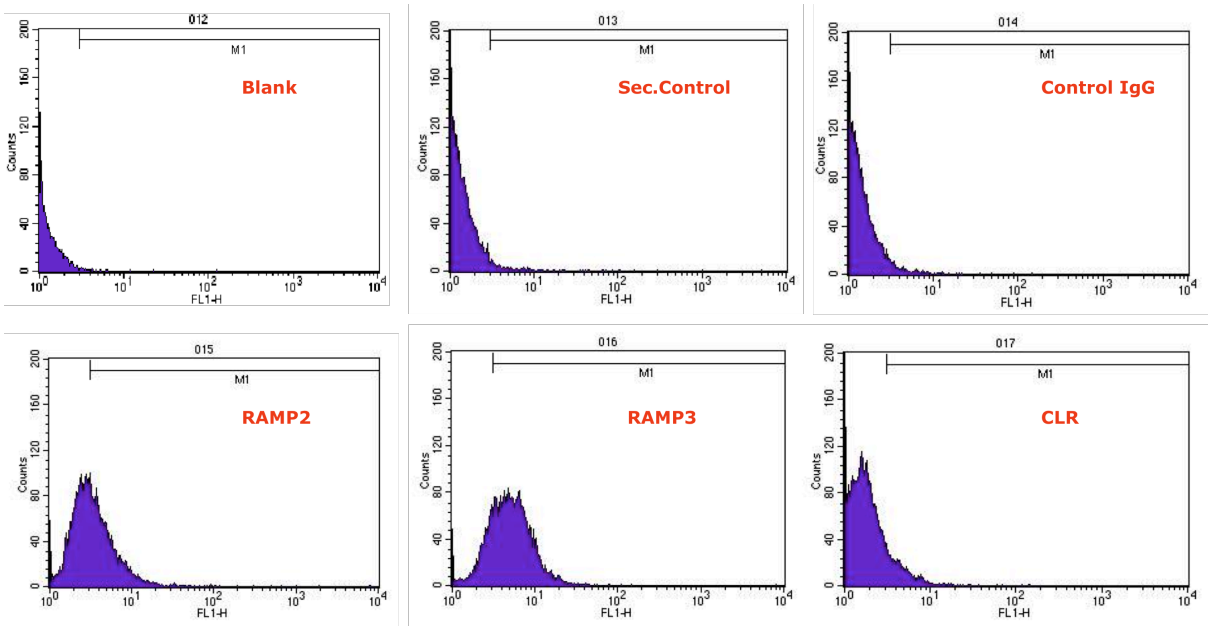

B

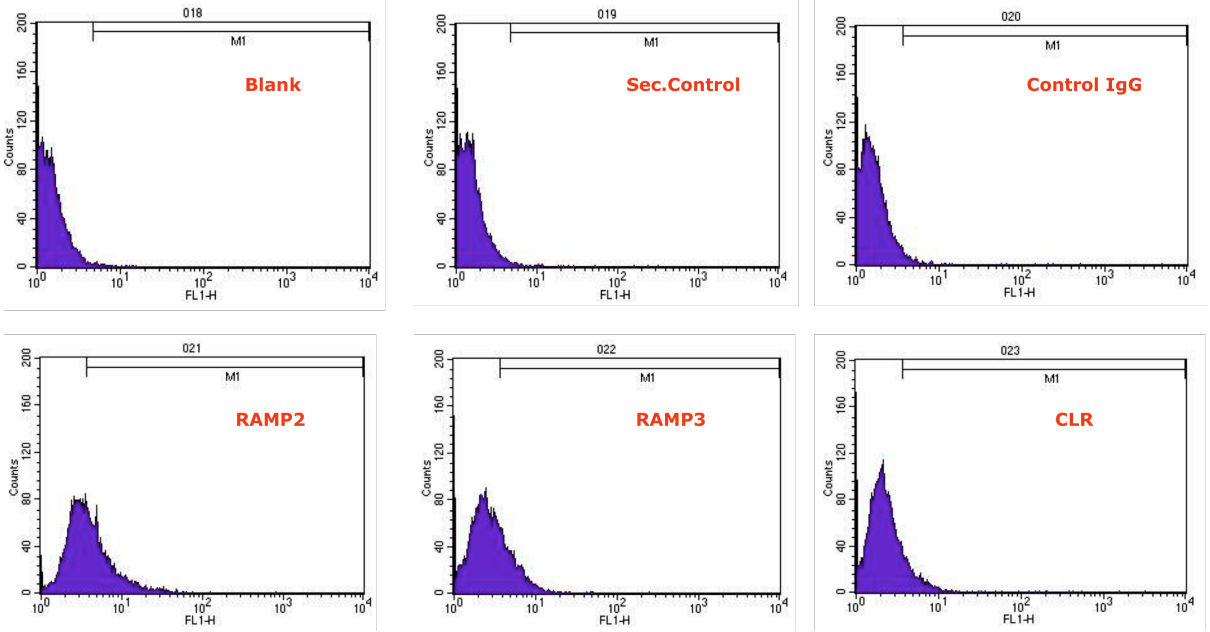

Figure 93: Flow cytometry histograms under A and B show the fluorescent intensities for ADM receptors, isotype control, secondary control and non-stained Glioblastoma (U87) cells at 0hrs. Histograms under **A** show the total protein expression and histograms under **B** show the cell surface protein expression.

Figure 94 shows the histograms of U87 cells at 24hrs normoxia. Figure 94A shows the total protein expression whereas figure 94B shows the cell surface protein expression of U87 cells. M1 is the region gated for histogram statistics for normalising isotype background.

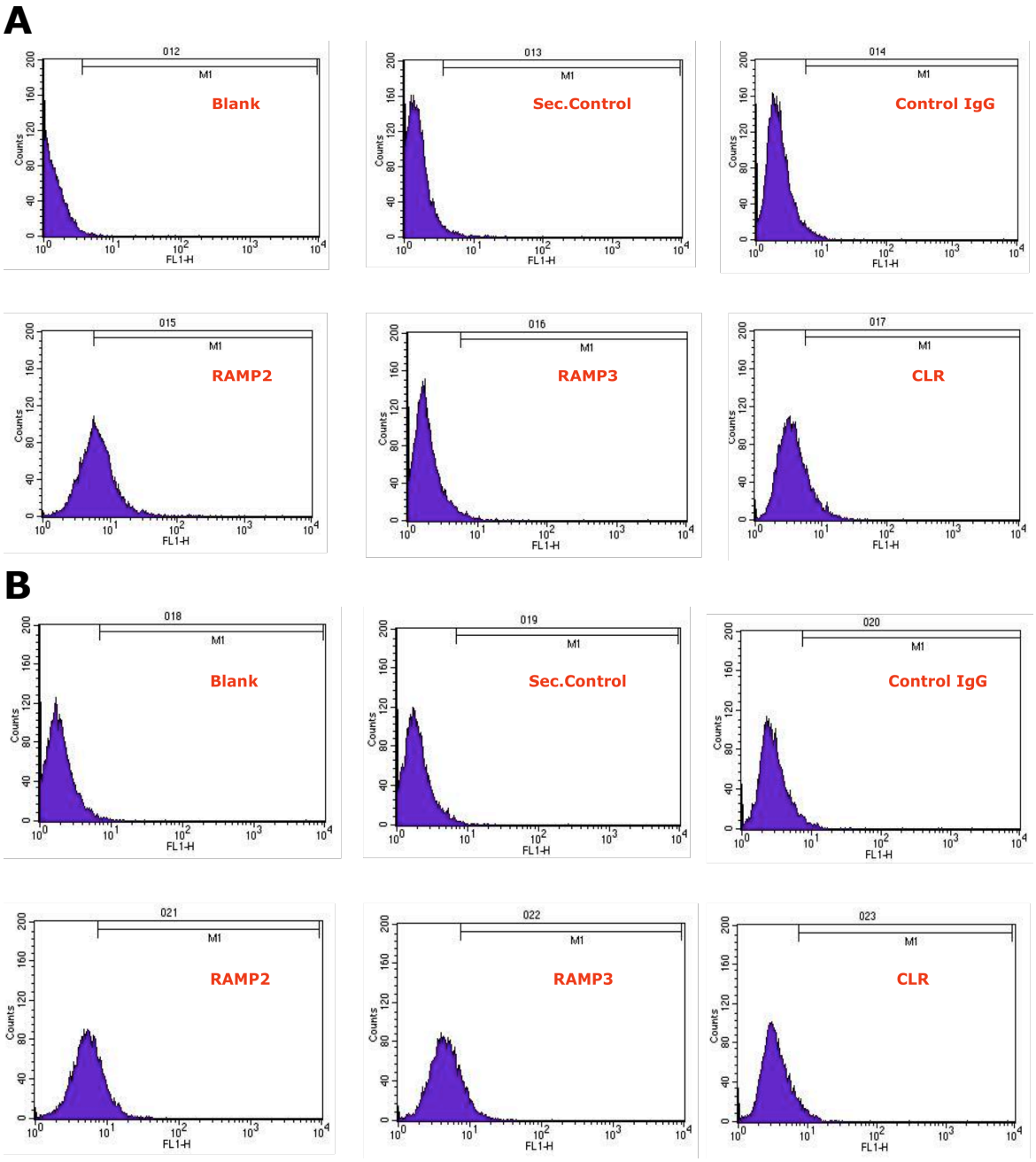

Figure 94: Flow Cytrometry histograms under A and B show the fluorescent intensities for ADM receptors, isotype control, secondary control and non-stained glioblastoma (U87) cells at 24hrs normoxia. Histograms under **A** show the total protein expression and histograms under **B** show the cell surface protein expression.

Figure 95 shows the histograms of U87 cells at 24hrs hypoxia. Figure 95A shows the total protein expression whereas figure 95B shows the cell surface protein expression of U87 cells. M1 is the region gated for histogram statistics for normalising isotype background.

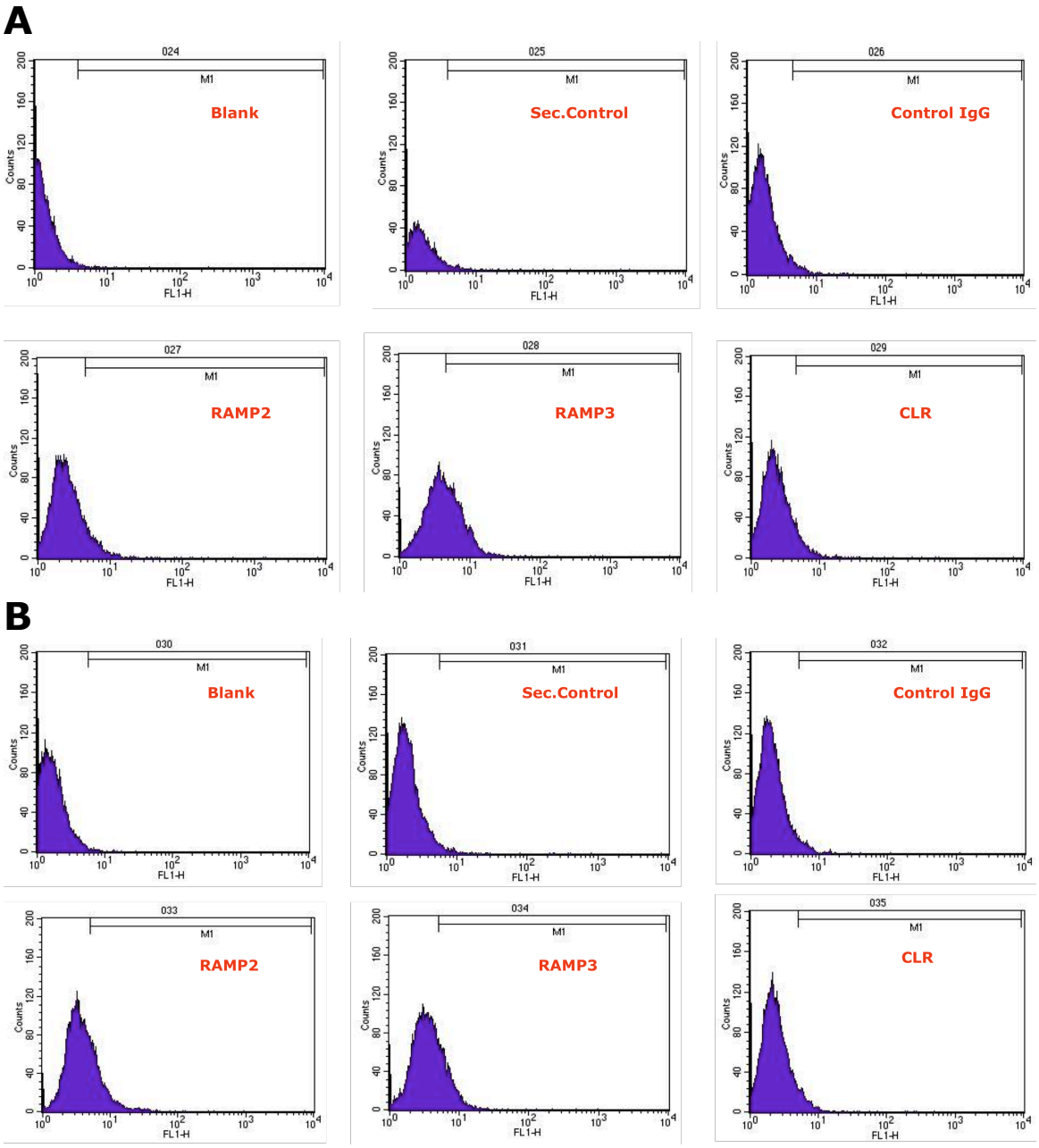

Figure 95: Flow Cytometry histograms under A and B show the fluorescent intensities for ADM receptors, isotype control, secondary control and non-stained Glioblastoma (U87) cells at 24hrs hypoxia. Histograms under **A** show the total protein expression and histograms under **B** show the cell surface protein expression.

Figure 96 shows the histograms of U87 cells at 48hrs normoxia. Figure 96A shows the total protein expression whereas figure 96B shows the cell surface protein expression of U87 cells. M1 is the region gated for histogram statistics for normalising isotype background.

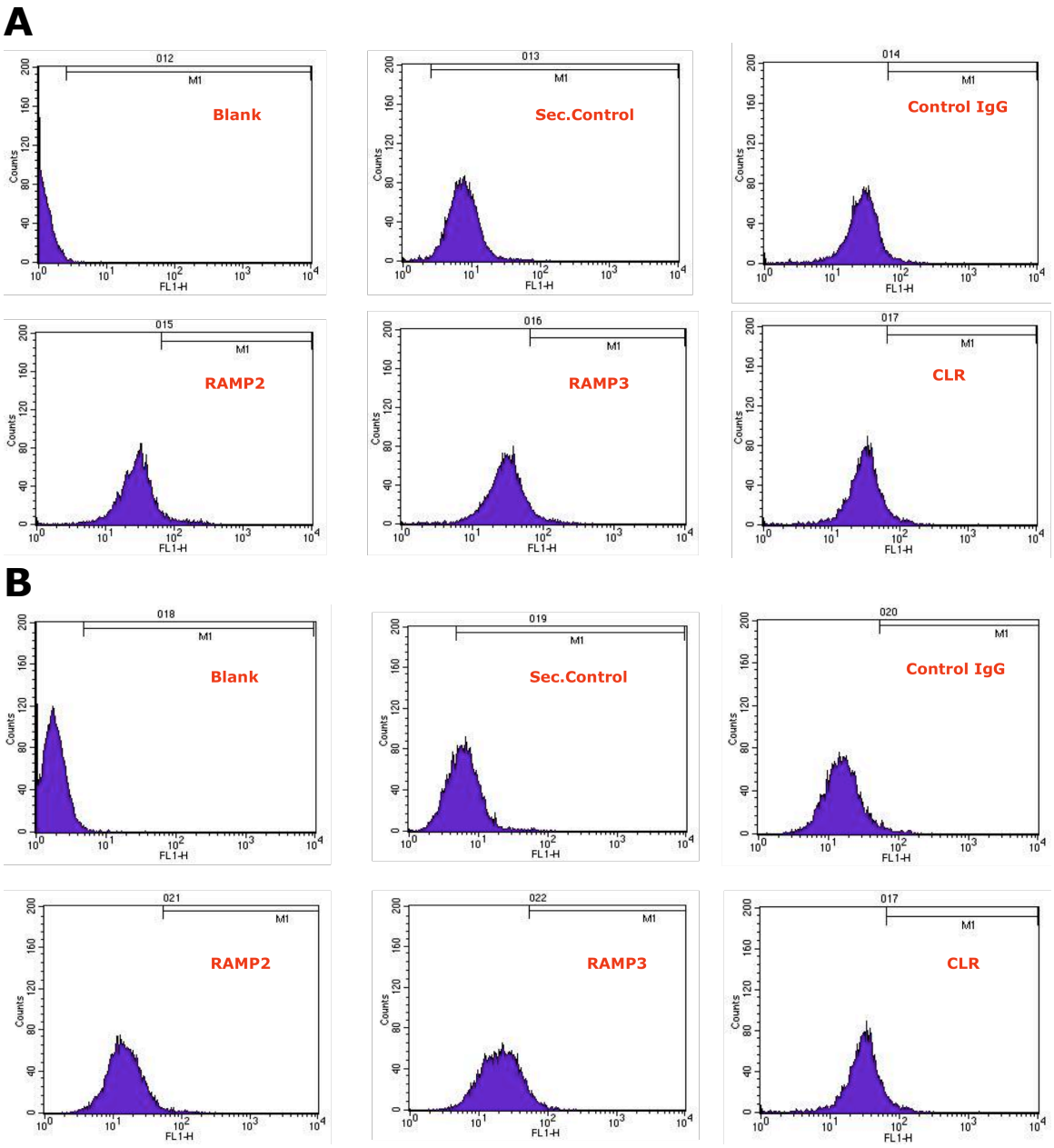

Figure 96 : Flow Cytometry histograms under A and B show the fluorescent intensities for ADM receptors, isotype control, secondary control and non-stained Glioblastoma (U87) cells at 48hrs normoxia. Histograms under **A** show the total protein expression and histograms under **B** show the cell surface protein expression.

Figure 97 shows the histograms of U87 cells at 48hrs hypoxia. Figure 97A shows the total protein expression whereas figure 97B shows the cell surface protein expression of U87 cells. M1 is the region gated for histogram statistics for normalising isotype background.

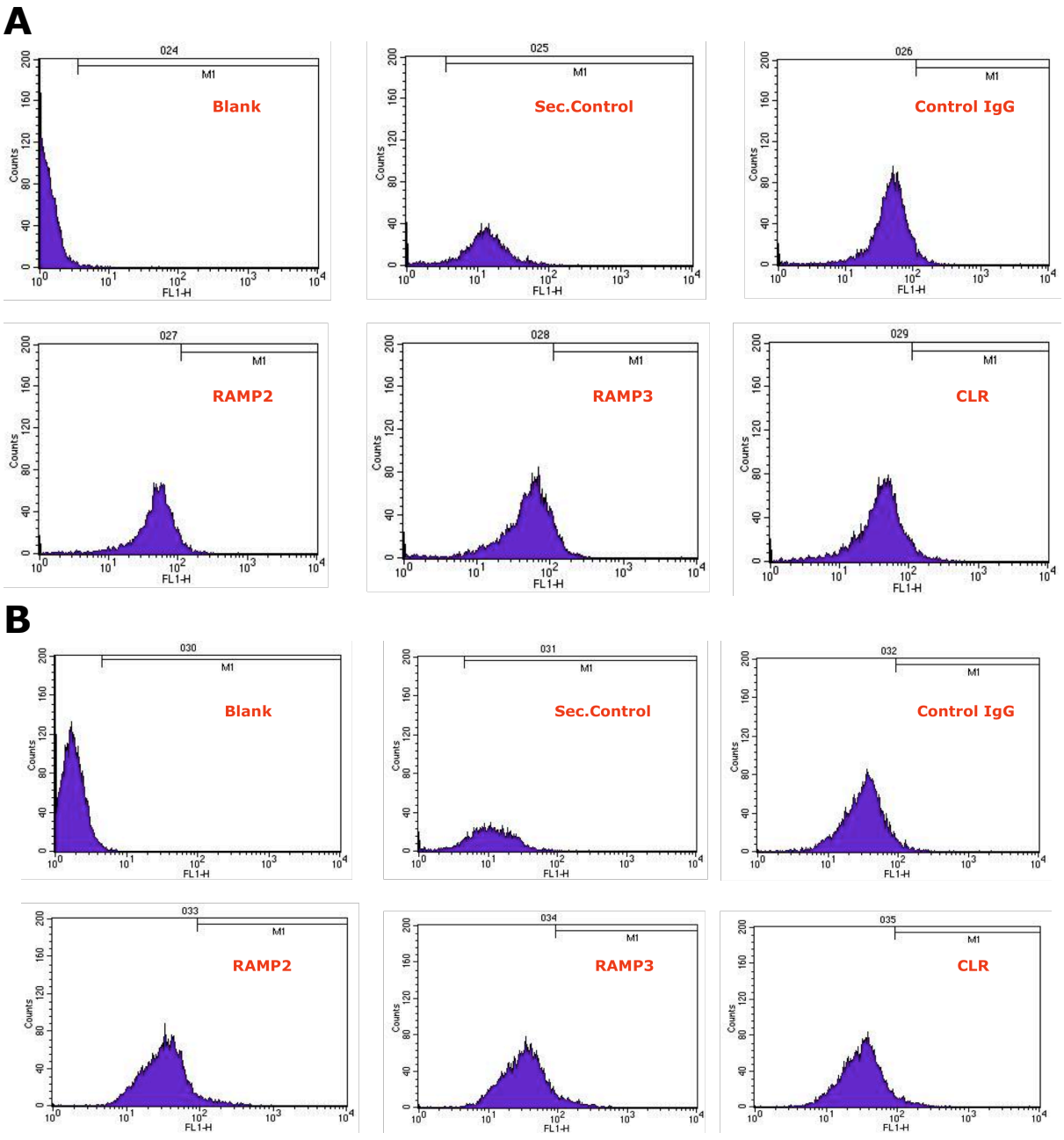

Figure 97 : Flow Cytometry histograms under A and B show the fluorescent intensities for ADM receptors, isotype control, secondary control and non-stained Glioblastoma cells at 48hrs hypoxia. Histograms under **A** show the total protein expression and histograms under **B** show the cell surface protein expression.

Figure 98, shows the histograms of the total protein expression of receptors and controls under normoxia and hypoxia. Each histogram contains "blank" or non-stained cells shaded in grey and the controls and receptor histograms are overlaid onto it. The secondary control is shown in green, isotype control in pink, RAMP2 in blue, RAMP3 in orange and CLR in yellow.

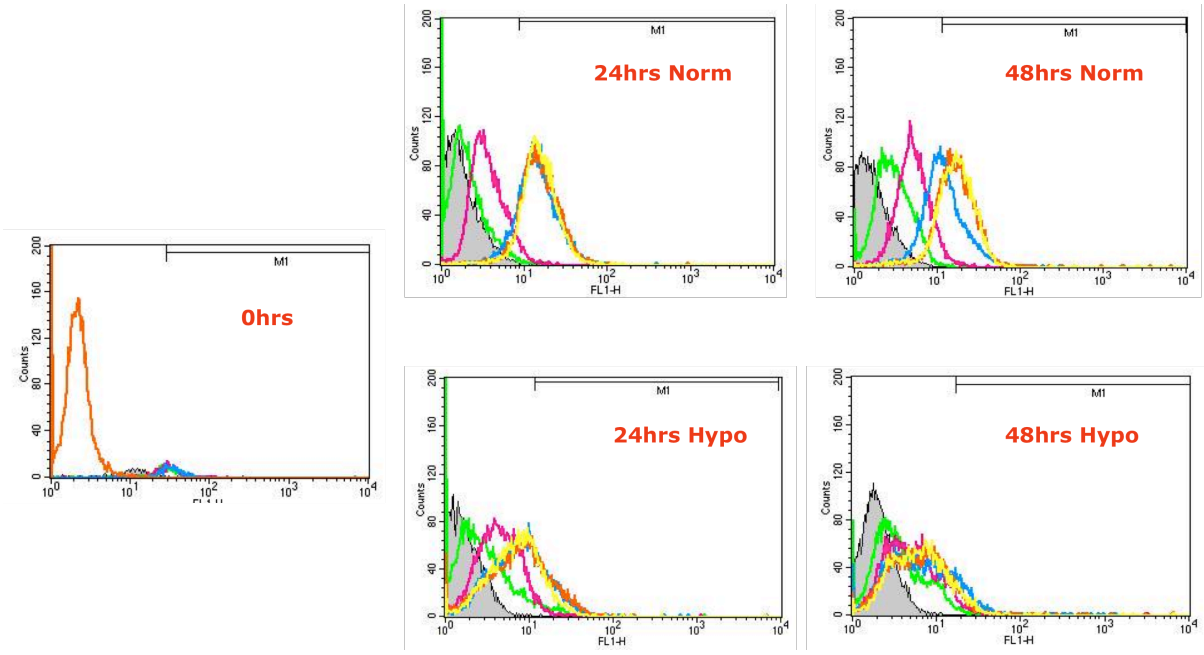

Figure 98: Flow Cytometry histogram for secondary control (green), isotype control (pink), RAMP2 (blue), RAMP3 (orange) and CLR (yellow) in breast cancer (MDA-MB-231) cells when exposed to hypoxia. The histograms represent the total protein expression in 10,000 cells.

Figure 99 shows the histograms of the cell surface protein expression of receptors and controls under normoxia and hypoxia. The colours are similar to that of figure 98, except the shaded brown region in this case belongs to the unstained cells.

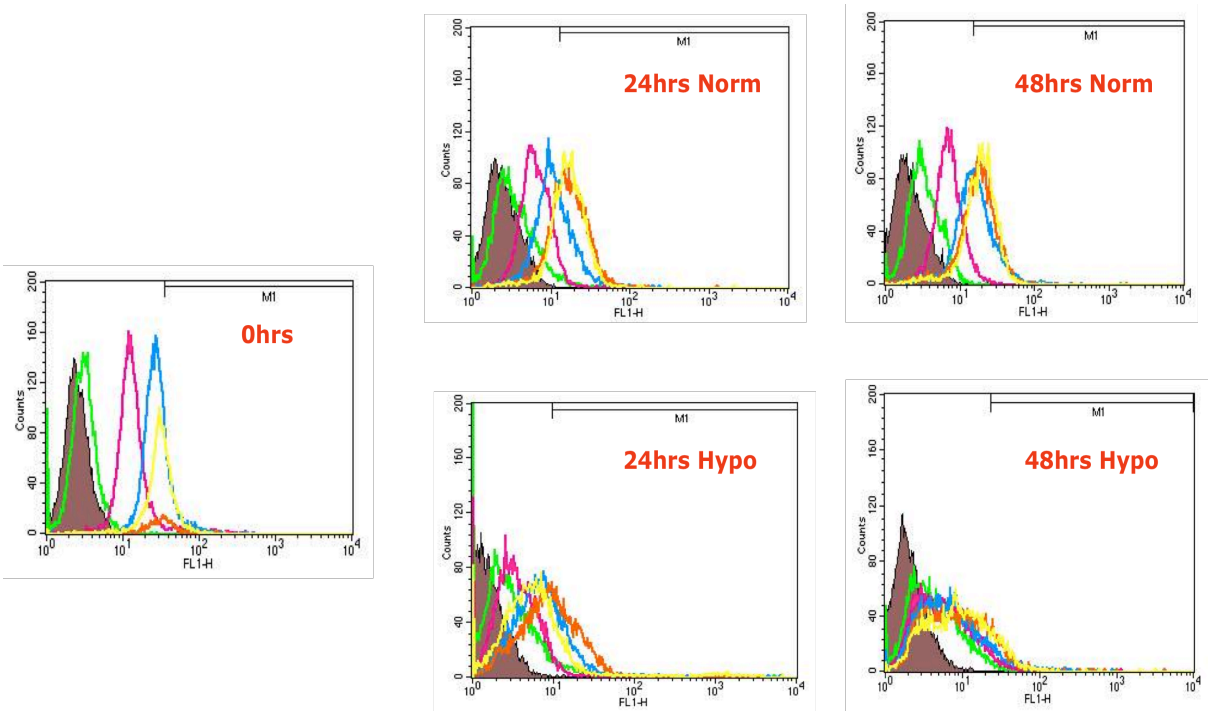

Figure 99 : Flow Cytometry histograms for secondary control (green), isotype control (pink), RAMP2 (blue), RAMP3 (orange) and CLR (yellow) in breast cancer (MDA-MB-231) cells when exposed to hypoxia. The histograms represent the cell surface protein expression in 10,000 cells.

6.2.2. Effect of Over-Expression of ADM and its receptors

6.2.2.1. ADM cloning

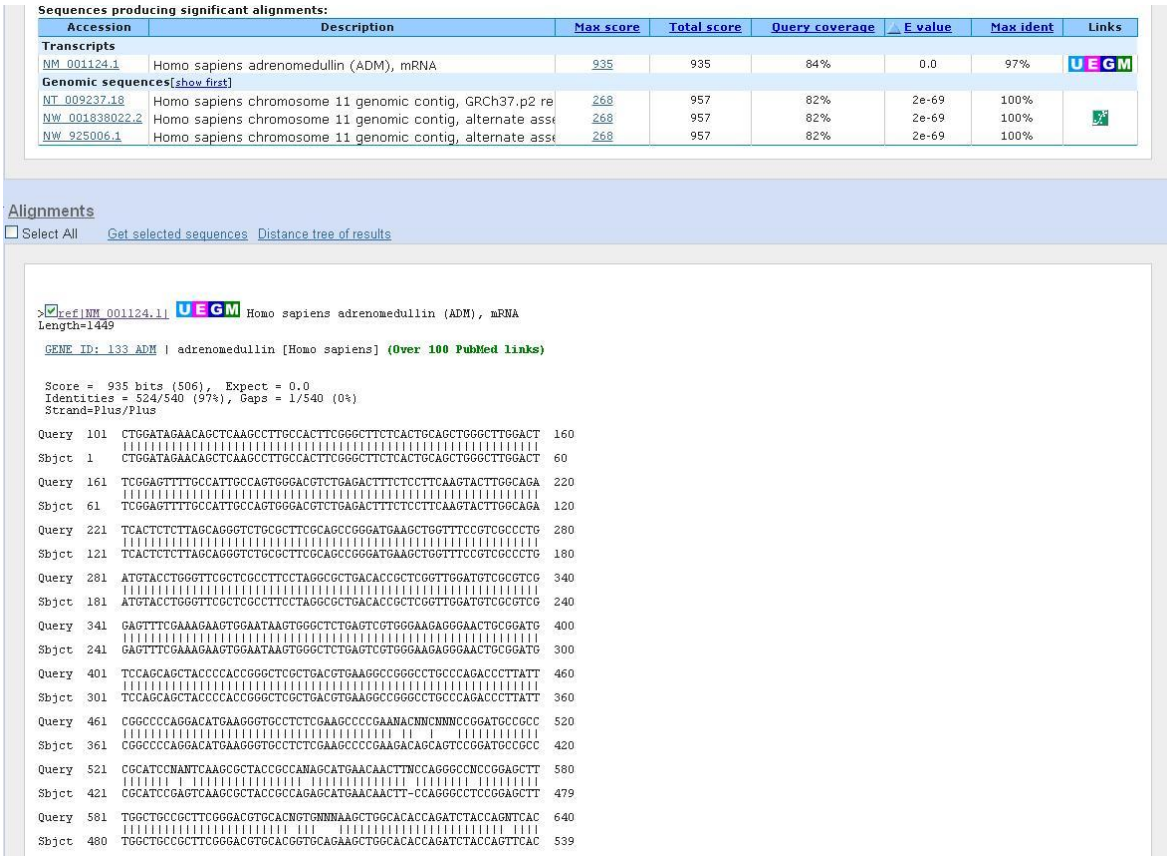

Sequences producing significant alignments:

Accession	Description	Max score	Total score	Query coverage	E value	Max ident	Links
Transcripts							
NM_001124.1	Homo sapiens adrenomedullin (ADM), mRNA	935	935	84%	0.0	97%	UEGM
Genomic sequences [show first]							
NT_009237.18	Homo sapiens chromosome 11 genomic contig, GRCh37.p2 re	268	957	82%	2e-69	100%	
NW_001838022.2	Homo sapiens chromosome 11 genomic contig, alternate ass	268	957	82%	2e-69	100%	
NW_925006.1	Homo sapiens chromosome 11 genomic contig, alternate ass	268	957	82%	2e-69	100%	

Alignments

Select All Get selected sequences Distance tree of results

>ref|NM_001124.1| UEGM Homo sapiens adrenomedullin (ADM), mRNA
Length=1449

GENE ID: 133 ADM | adrenomedullin [Homo sapiens] (Over 100 PubMed links)

Score = 935 bits (506), Expect = 0.0
Identities = 524/540 (97%), Gaps = 1/540 (0%)
Strand=Plus/Plus

```
Query  101  CTGGATAGAACAGCTCAAGCCTTGCCACTTCGGGCTTCTCACTGCAGCTGGGCTTGGACT  160
Sbjct  1    CTGGATAGAACAGCTCAAGCCTTGCCACTTCGGGCTTCTCACTGCAGCTGGGCTTGGACT  60

Query  161  TCGGAGTTTTGCCATTGCCAGTGGGACGTCTGAGACTTTCTCCTTCAAGTACTTGGCAGA  220
Sbjct  61   TCGGAGTTTTGCCATTGCCAGTGGGACGTCTGAGACTTTCTCCTTCAAGTACTTGGCAGA  120

Query  221  TCACTCTCTTAGCAGGGTCTGCGCTTCGCAGCCGGGATGAAGCTGGTTTCCGTCGCCCTG  280
Sbjct  121  TCACTCTCTTAGCAGGGTCTGCGCTTCGCAGCCGGGATGAAGCTGGTTTCCGTCGCCCTG  180

Query  281  ATGTACCTGGGTTCGCTCGCCTTCCTAGGCGCTGACACCGCTCGGTTGGATGTCGCGTCG  340
Sbjct  181  ATGTACCTGGGTTCGCTCGCCTTCCTAGGCGCTGACACCGCTCGGTTGGATGTCGCGTCG  240

Query  341  GAGTTTCGAAAGAAGTGGAATAAGTGGGCTCTGAGTCGTGGGAAGAGGGAACTGCGGATG  400
Sbjct  241  GAGTTTCGAAAGAAGTGGAATAAGTGGGCTCTGAGTCGTGGGAAGAGGGAACTGCGGATG  300

Query  401  TCCAGCAGCTACCCCACCGGGCTCGCTGACGTGAAGGCCGGGCCTGCCCAGACCCTTATT  460
Sbjct  301  TCCAGCAGCTACCCCACCGGGCTCGCTGACGTGAAGGCCGGGCCTGCCCAGACCCTTATT  360

Query  461  CGGCCCCAGGACATGAAGGGTGCCTCTCGAAGCCCCGAANACNNCNNNCCGGATGCCGCC  520
Sbjct  361  CGGCCCCAGGACATGAAGGGTGCCTCTCGAAGCCCCGAAGACAGCAGTCCGGATGCCGCC  420

Query  521  CGCATCCNANTCAAGCGCTACCGCCANAGCATGAACAACTTNCCAGGGCCNCCGGAGCTT  580
Sbjct  421  CGCATCCGAGTCAAGCGCTACCGCCAGAGCATGAACAACTT-CCAGGGCCTCCGGAGCTT  479

Query  581  TGGCTGCCGCTTCGGGACGTGCACNGTGNNNAAGCTGGCACACCAGATCTACCAGNTCAC  640
Sbjct  480  TGGCTGCCGCTTCGGGACGTGCACGGTGCAGAAGCTGGCACACCAGATCTACCAGTTCAC  539
```

Figure 100 : BLAST result showing 97% match between ADM mRNA and the sequenced product after cloning. This confirms that ADM is cloned into pcDNA3.1 vector.

Figure 100 shows BLAST result on comparing the sequencing result after cloning ADM into pcDNA3.1 vector. BLAST resulted in 97% match between human ADM mRNA and the sequenced product.

Figures 101 to 103 contain histograms for native (non-transfected), pcDNA3.1 and ADM transfected cells probed for Isotype control, RAMP2, RAMP3 and CLR. Histograms under A belong to permeabilised cells which show the total protein expression and histograms under B belong to non-permeabilised cells which show the cell surface protein expression.

6.2.2.2. ADM receptor expression in cells over-expressing ADM

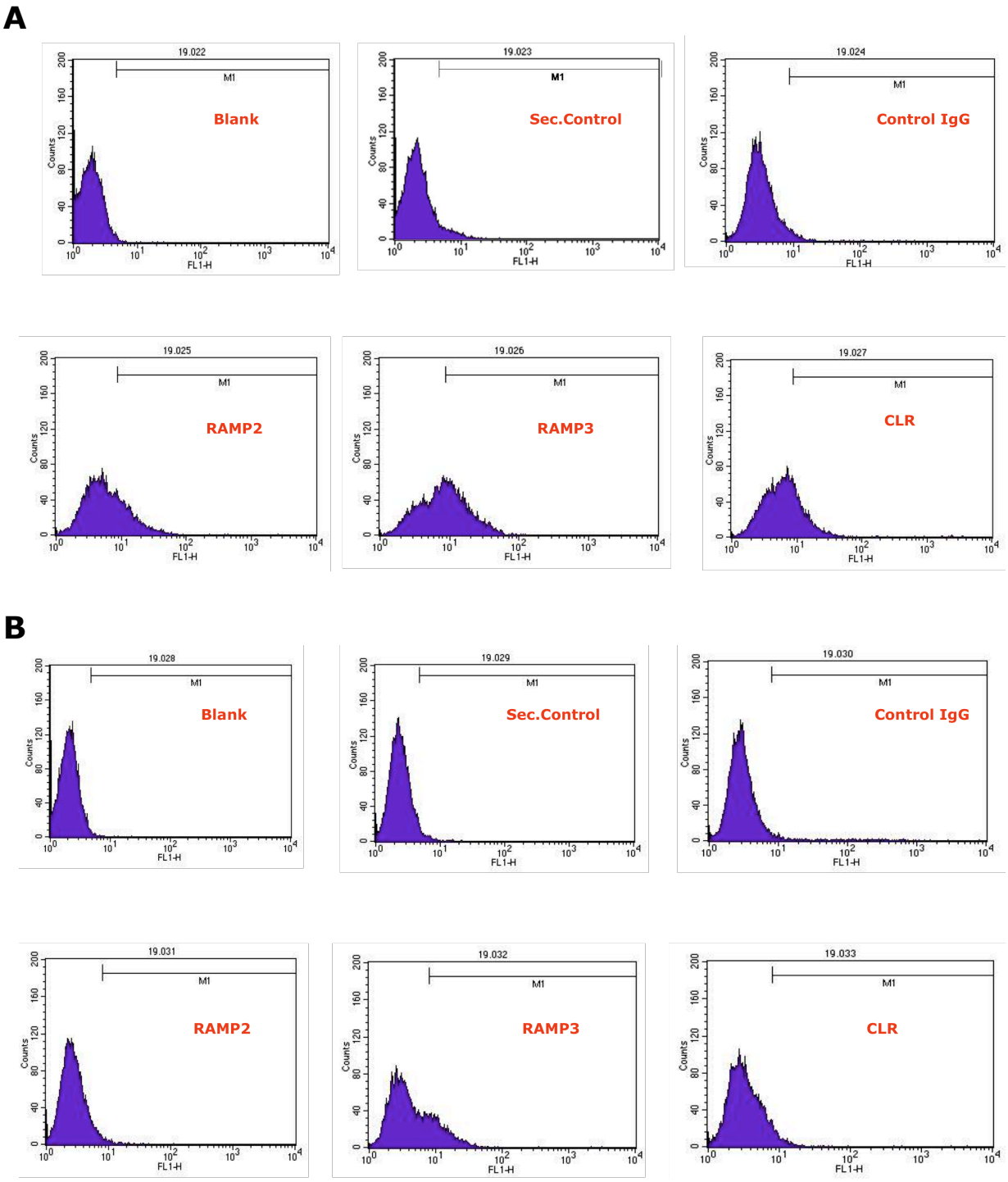

Figure 101 : Flow Cytometry histograms under A and B show the fluorescent intensities for ADM receptors, isotype control, non-stained cells and secondary control in breast cancer (MDA-MB-231) cells. Histograms under A show the total protein expression and histograms under B show the cell surface protein expression for native MDA-MB-231 cells.

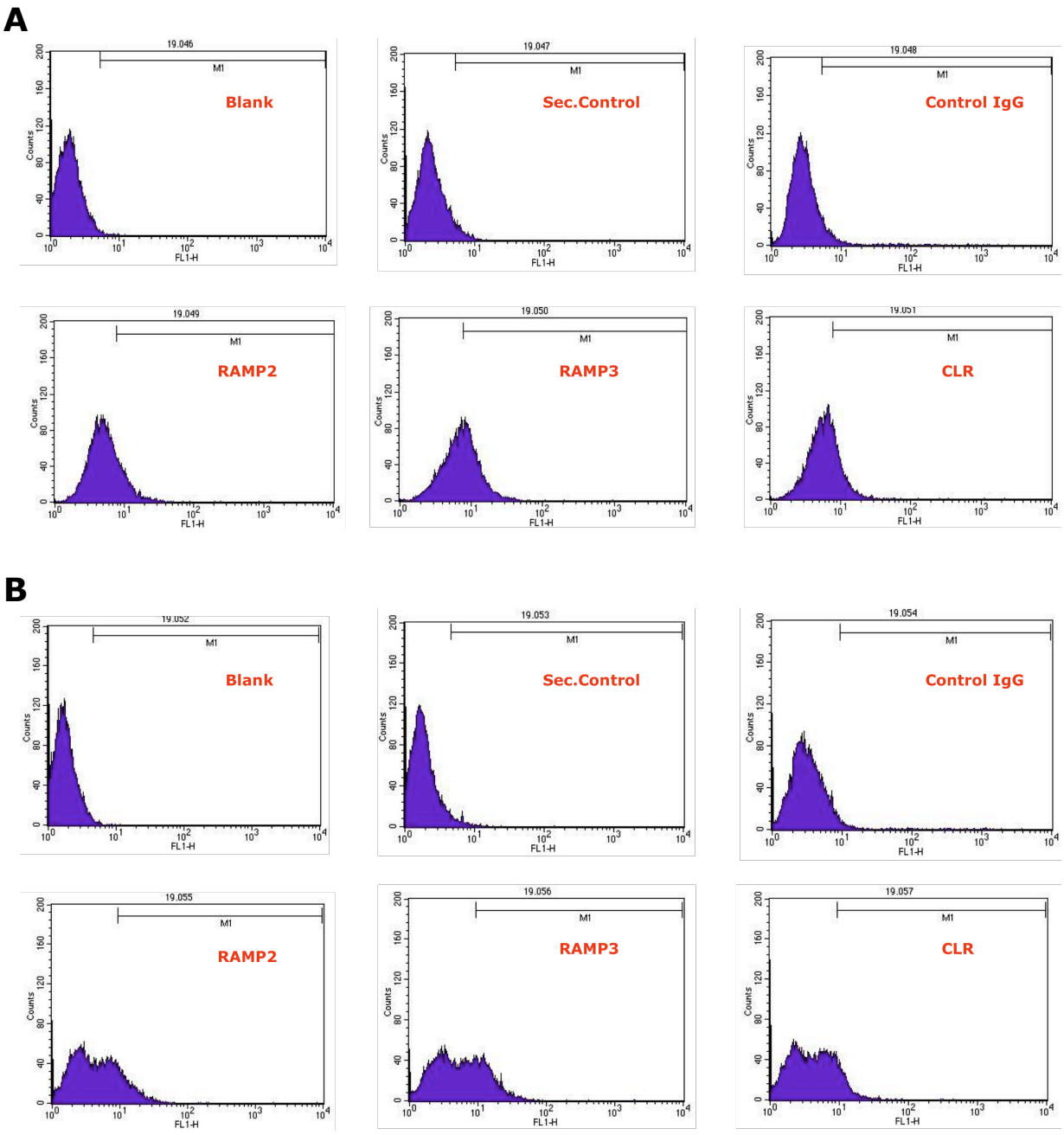

Figure 102 : Flow Cytometry histograms under A and B show the fluorescent intensities for ADM receptors, isotype control, non-stained cells and secondary control in breast cancer (MDA-MB-231) cells. Histograms under A show the total protein expression and histograms under B show the cell surface protein expression for control vector (pcDNA3.1) transfected MDA-MB-231 cells.

A

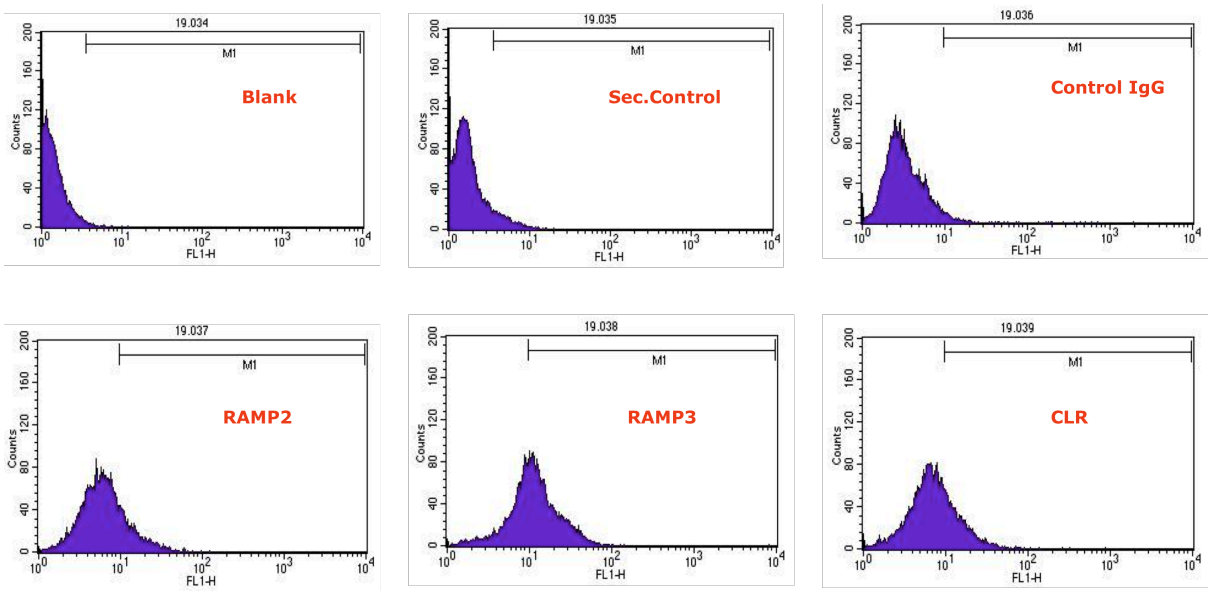

B

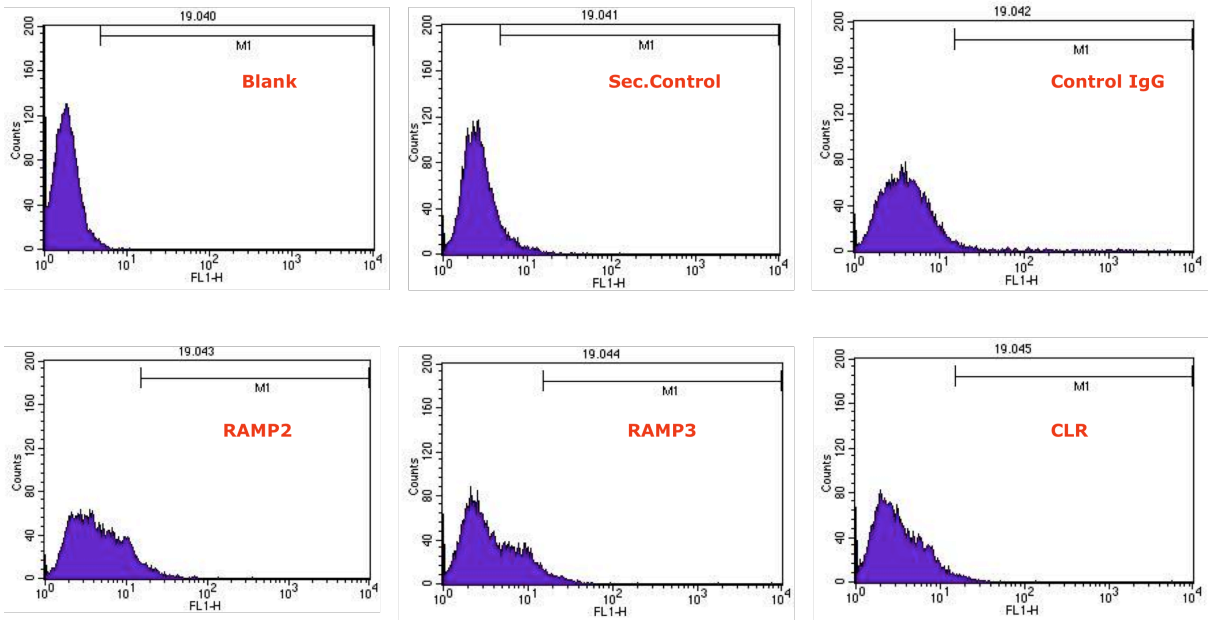

Figure 103 : Flow Cytometry histograms under A and B show the fluorescent intensities for ADM receptors, isotype control, non-stained cells and secondary control in breast cancer (MDA-MB-231) cells. Histograms under A show the total protein expression and histograms under B show the cell surface protein expression for ADM transfected MDA-MB-231 cells.

6.2.2.3. Site Directed Mutagenesis

Figure 104 contains the sequencing result after site directed mutagenesis of the start codon. As it can be seen clearly, ATG was not mutated into GGG, instead the sequencing result showed NTG, the N clearly belongs to A as it can be clearly seen that the peaks in finch TV was clearly green indicating it belongs to A.

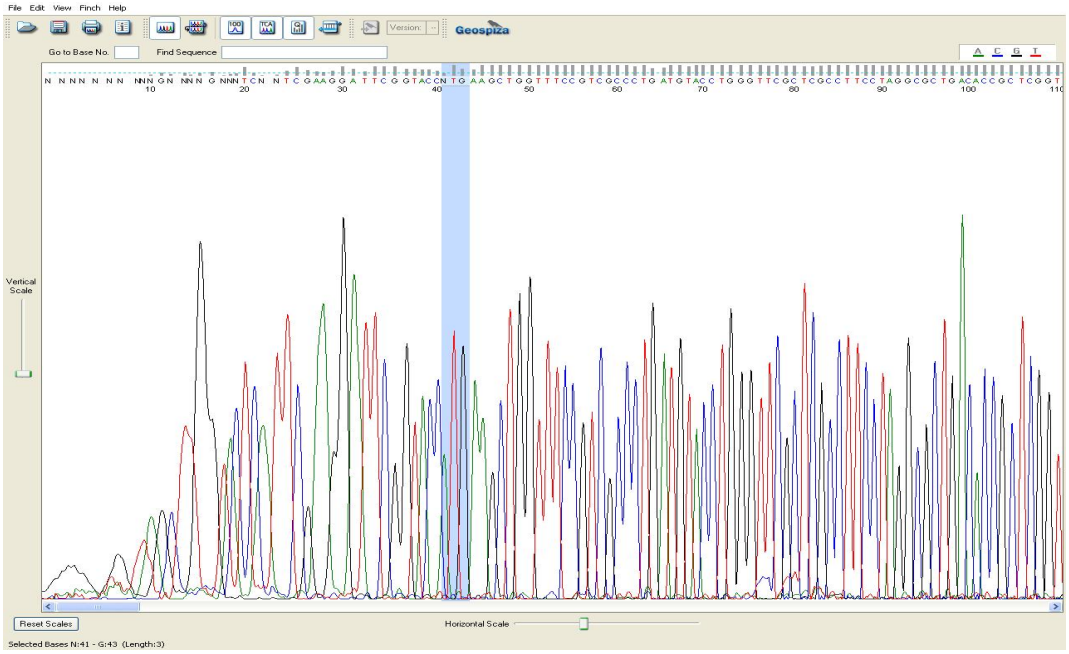

NNNNNGNNNNGNNNTCNNTCGAAGGATTCGGTACC**NTG**AAGCTGGTTTCCGTCGCCCTGATGT
ACCTGGGTTCGCTCGCCTTCCTAGGCGCTGACACCGCTCGGTTGGATGTCGCGTCGGAGTTTCG
AAAGAAGTGGAATAAGTGGGCTCTGAGTCGTGGGAAGAGGGAACTGCGGATGTCCAGCAGCTAC
CCCACCGGGCTCGCTGACGTGAAGGCCGGGCCTGCCCAGACCCTTATTCGGCCCCAGGACATGA
AGGGTGCCTCTCGAAGCCCCGAAGACAGCAGTCCGGATGCCGCCCGCATCCGAGTCAAGCGCTA
CCGCCAGAGCATGAACAACTTCCAGGGCCTCCGGAGCTTTGGCTGCCGCTTCGGGACGTGCACG
GTGCAGAAGCTGGCACACCAGATCTACCAGTTCACAGATAAGGACAAGGACAACGTCGCCCCCA
GGAGCAAGATCAGCCCCCAGGGCTACGGCCGCCGGCGCCGGCGCTCCCTGCCCGAGGCCGGCC
CGGGTCGGACTCTGGTGTCTTCTAAGCCACAAGCACACGGGGCTCCAGCCCCCCCGAGTGGAAG
TGCTCCCCACTTTCTTTAGCTCGAGTGCGGCCGCAACCCAGCTTTCTTGTACAAAGTGGTTCGATC
TAGAATGGCTAGCGAGCAGAAACTCATCTCTGAAGAGGATCTGTAGTGATCAGCCTCGACTGTGC
CTTCACGTAGTGAGATGGGGGTCCTGGGCCCCAGGGTGTGCAGCCACTGACTTNNGGACTGCTG
GTGGGGTAGGGATGAGGGANGGAGGGGCATTGTGATGTACAGGGCTGCTCTGTGAGATCNANG
GGTCTCTTANNGGTGGGANCTGGGGCANGGNCTACNANAGCAGCCNGANGGGCTGAAAGNGG
NANNTCNNGGGGTTTCTGGNACCTACCTACCTGCTTNCCNCNGGGGGGGNGGGGGNNNTNGNC
CCNNANTNNTNTGGGGNNNNAGNNGGGNNCNTCNGCTAGCTTTTTTCCC

Figure 104 : Sequencing result after site directed mutagenesis PCR. The start codon was made to mutate from ATG to GGG. The sequencing result shows that ATG was not mutated, the N clearly belonged to A as it can be seen from the image from finch TV.

The sequencing result from figure 105 shows that the mutation did not occur during site directed mutagenesis PCR.

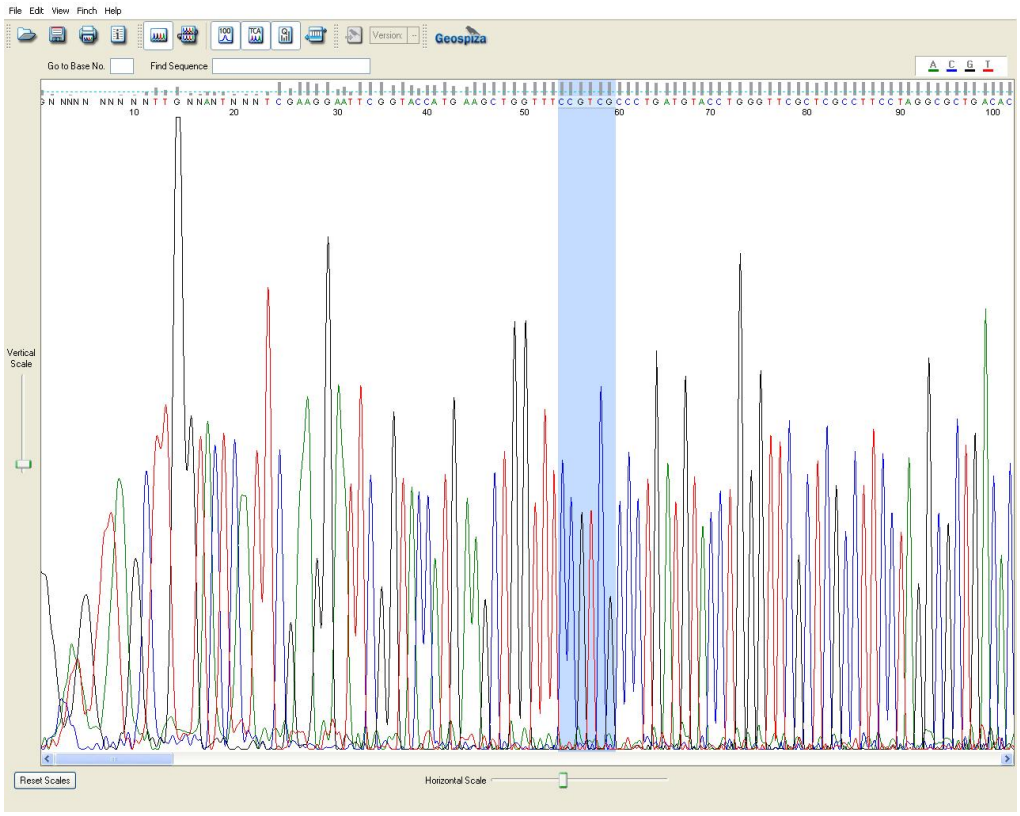

GNNNNNNNNNNTTGNNANTNNNTCGAAGGAATTCGGTACCATGAAGCTGGTTT**CCGTCG**CCCT
GATGTACCTGGGTTCGCTCGCCTTCCTAGGCGCTGACACCGCTCGGTTGGATGTCGCGTCGGAG
TTTCGAAAGAAGTGGAATAAGTGGGCTCTGAGTCGTGGGAAGAGGGAACTGCGGATGTCCAGCA
GCTACCCCACCGGGCTCGCTGACGTGAAGGCCGGGCCTGCCCAGACCCTTATTCGGCCCCAGGA
CATGAAGGGTGCCTCTCGAAGCCCCGAAGACAGCAGTCCGGATGCCGCCCGCATCCGAGTCAAG
CGCTACCGCCAGAGCATGAACAACTTCCAGGGCCTCCGGAGCTTTGGCTGCCGCTTCGGGACGT
GCACGGTGCAGAAGCTGGCACACCAGATCTACCAGTTCACAGATAAGGACAAGGACAACGTCGC
CCCCAGGAGCAAGATCAGCCCCCAGGGCTACGGCCGCCGGCGCCGGCGCTCCCTGCCCGAGGC
CGGCCCGGGTCGGACTCTGGTGTCTTCTAAGCCACAAGCACACGGGGCTCCAGCCCCCCCGAGT
GGAAGTGCTCCCCACTTTCTTTAGCTCGAGTGCGGCCGCAACCCAGCTTTCTTGTACAAAGTGGT
TCGATCTAGAATGGCTAGCGAGCAGAAACTCATCTCTGAAGANGNNCTGTAGTGATCAGCCTCGA
CTGTGCCTTCACGTANTGAGATGGGGGTCCTGGGCCCCAGGGNGTGCAGCCNCTGACNTGGGG
ACTGCTGGNGGGGT

Figure 105: Sequencing result after site directed mutagenesis PCR. Stop codons were made to incorporate after transcription of four amino acids. The TCCGTCG sequence (highlighted in yellow) was supposed to have been mutated into TAGTGAG, but as it can be seen it was not mutated.

6.2.2.5. Sequencing Result fot IRES-eGFP Negative control

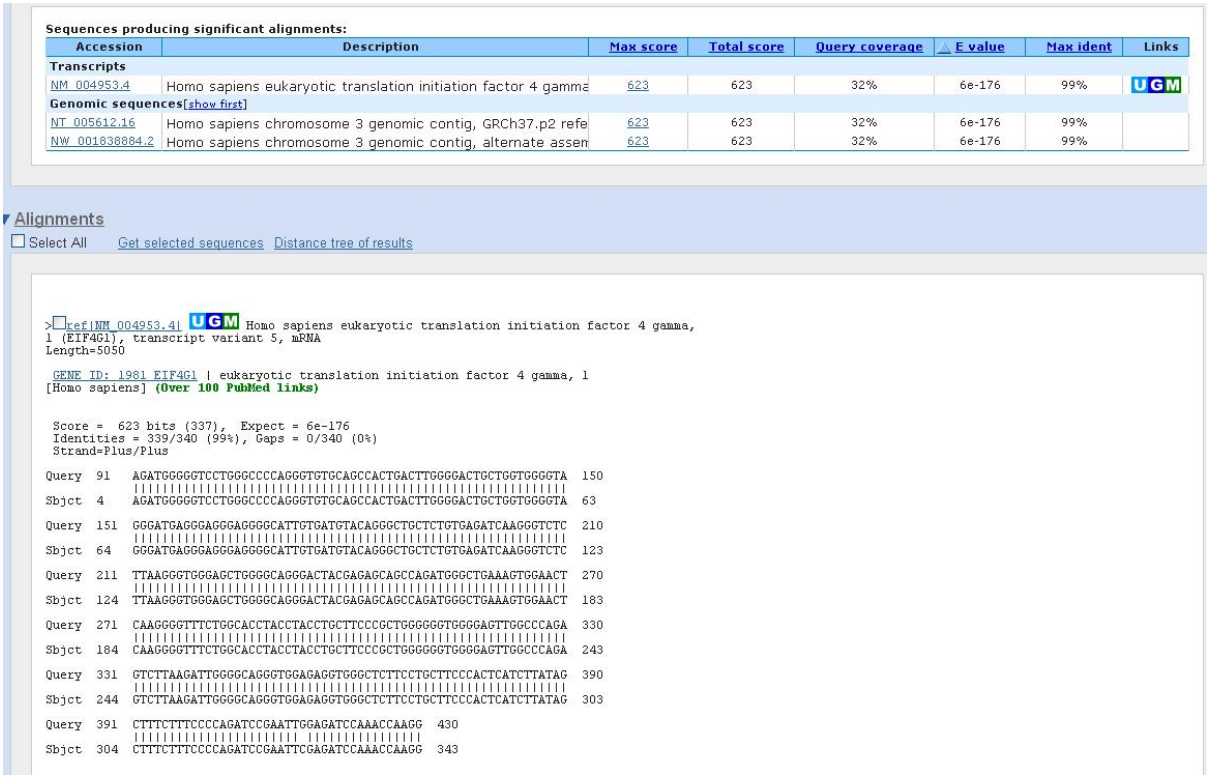

Sequences producing significant alignments:

Accession	Description	Max score	Total score	Query coverage	E value	Max ident	Links
Transcripts							
NM_004953.4	Homo sapiens eukaryotic translation initiation factor 4 gamma	623	623	32%	6e-176	99%	UGM
Genomic sequences [show first]							
NT_005612.16	Homo sapiens chromosome 3 genomic contig, GRCh37.p2 refe	623	623	32%	6e-176	99%	
NW_001838884.2	Homo sapiens chromosome 3 genomic contig, alternate assem	623	623	32%	6e-176	99%	

Alignments

Select All Get selected sequences Distance tree of results

>ref|NM_004953.4| UGM Homo sapiens eukaryotic translation initiation factor 4 gamma, 1 (EIF4G1), transcript variant 5, mRNA
Length=5050

GENE ID: 1981 EIF4G1 | eukaryotic translation initiation factor 4 gamma, 1 [Homo sapiens] **(Over 100 PubMed links)**

Score = 623 bits (337), Expect = 6e-176
Identities = 339/340 (99%), Gaps = 0/340 (0%)
Strand=Plus/Plus

```
Query  91   AGATGGGGGTCCTGGGCCCCAGGGTGTGCAGCCACTGACTTGGGGACTGCTGGTGGGGTA  150
            ||||||||||||||||||||||||||||||||||||||||||||||||||||||||||||
Sbjct  4    AGATGGGGGTCCTGGGCCCCAGGGTGTGCAGCCACTGACTTGGGGACTGCTGGTGGGGTA  63

Query  151  GGGATGAGGGAGGGAGGGGCATTGTGATGTACAGGGCTGCTCTGTGAGATCAAGGGTCTC  210
            ||||||||||||||||||||||||||||||||||||||||||||||||||||||||||||
Sbjct  64   GGGATGAGGGAGGGAGGGGCATTGTGATGTACAGGGCTGCTCTGTGAGATCAAGGGTCTC  123

Query  211  TTAAGGGTGGGAGCTGGGGCAGGGACTACGAGAGCAGCCAGATGGGCTGAAAGTGGAACT  270
            ||||||||||||||||||||||||||||||||||||||||||||||||||||||||||||
Sbjct  124  TTAAGGGTGGGAGCTGGGGCAGGGACTACGAGAGCAGCCAGATGGGCTGAAAGTGGAACT  183

Query  271  CAAGGGGTTTCTGGCACCTACCTACCTGCTTCCCGCTGGGGGGTGGGGAGTTGGCCCAGA  330
            ||||||||||||||||||||||||||||||||||||||||||||||||||||||||||||
Sbjct  184  CAAGGGGTTTCTGGCACCTACCTACCTGCTTCCCGCTGGGGGGTGGGGAGTTGGCCCAGA  243

Query  331  GTCTTAAGATTGGGGCAGGGTGGAGAGGTGGGCTCTTCCTGCTTCCCACTCATCTTATAG  390
            ||||||||||||||||||||||||||||||||||||||||||||||||||||||||||||
Sbjct  244  GTCTTAAGATTGGGGCAGGGTGGAGAGGTGGGCTCTTCCTGCTTCCCACTCATCTTATAG  303

Query  391  CTTTCTTTCCCCAGATCCGAATTGGAGATCCAAACCAAGG  430
            |||||||||||||||||||| ||||||||||||||||||
Sbjct  304  CTTTCTTTCCCCAGATCCGAATTCGAGATCCAAACCAAGG  343
```

Figure 106: The commercially available negative control for the IRES-eGFP vector was sequenced and the picture shows the BLAST result of the sequenced product. BLAST resulted in 99% identity to part of the Eukaryotic Translation initiation factor 4 gamma.

6.2.2.6. Bone Metastases in Immunodeficient mice

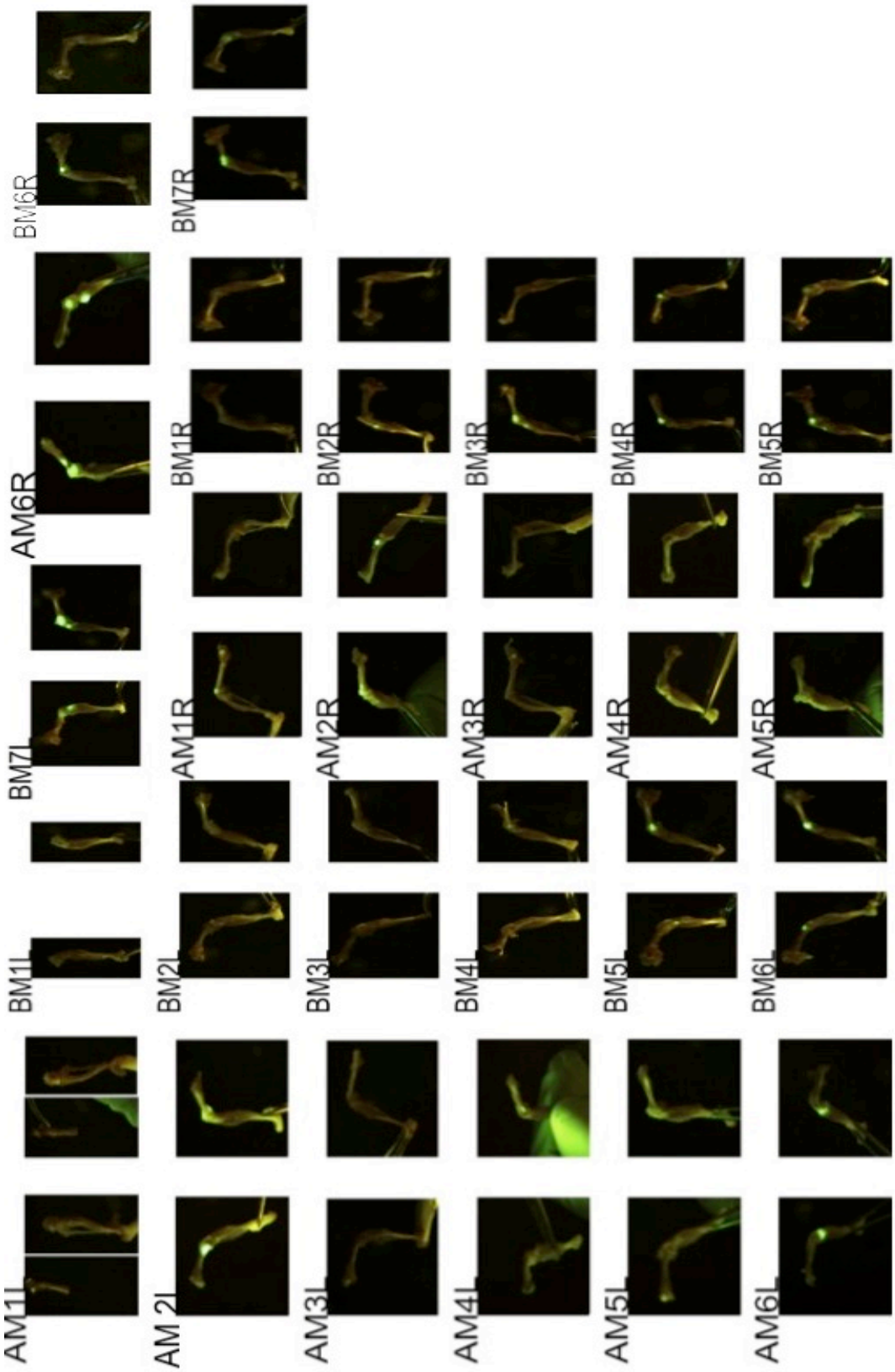

Figure 107: Pictures of left and right legs of mice injected with parental MDA-MB-231 cells. Pictures labelled with L belongs to the left legs and pictures labelled with R belongs to right legs of mice. In each picture, the left side image belongs to the inside of the legs while the right side images belong to outside of the leg.

Figure 108: Pictures of left and right legs of mice injected with IRES-eGFP negative control MDA-MB-231 cells. Pictures labelled with L belongs to the left legs and pictures labelled with R belongs to right legs of mice. In each picture, the left side image belongs to the inside of the legs while the right side images belong to outside of the leg.

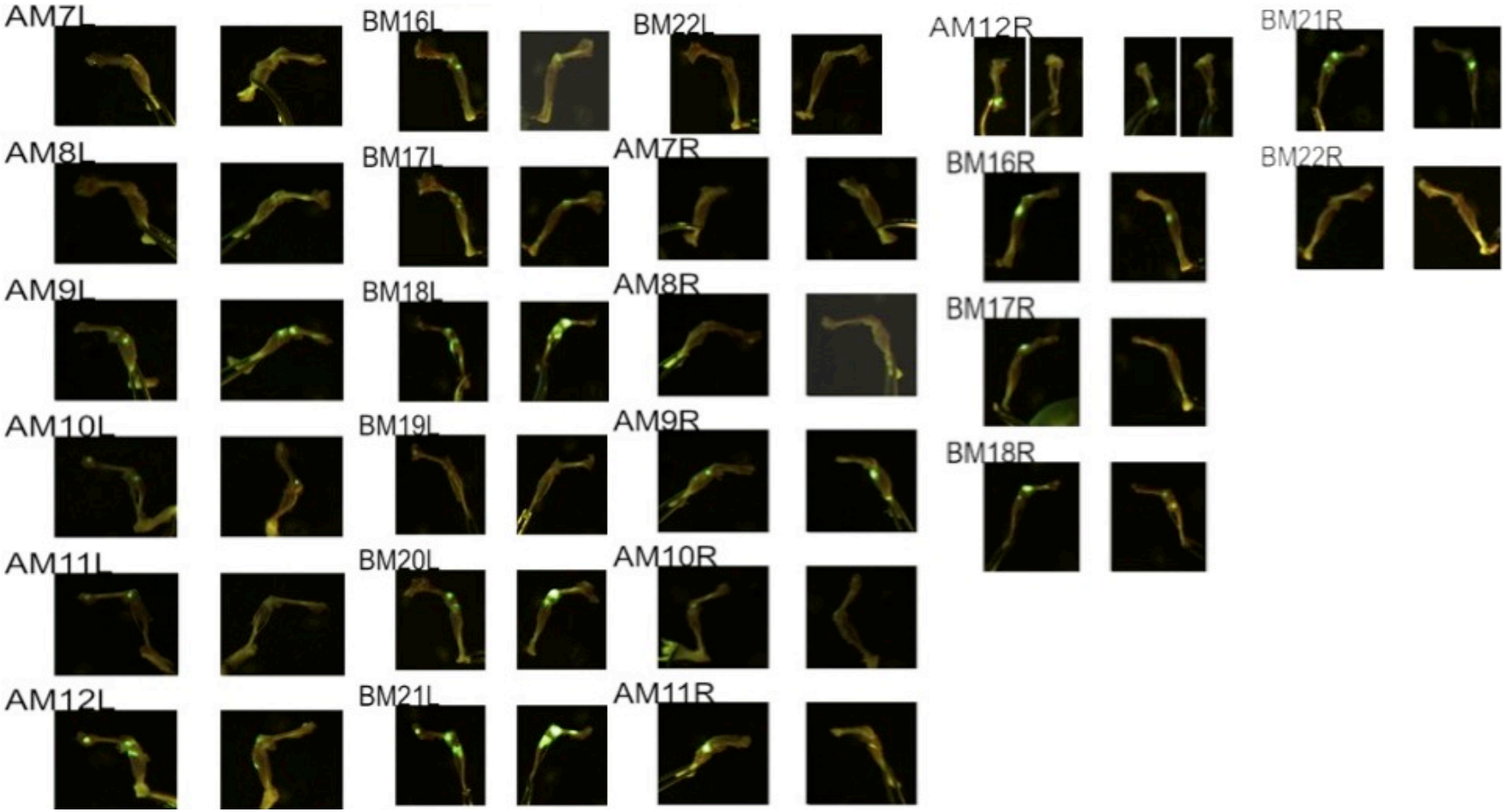

Figure 109: Pictures of left and right legs of mice injected with ADM transfected MDA-MB-231 cells. Pictures labelled with L belongs to the left legs and pictures labelled with R belongs to right legs of mice. In each picture, the left side image belongs to the inside of the legs while the right side images belong to outside of the leg.

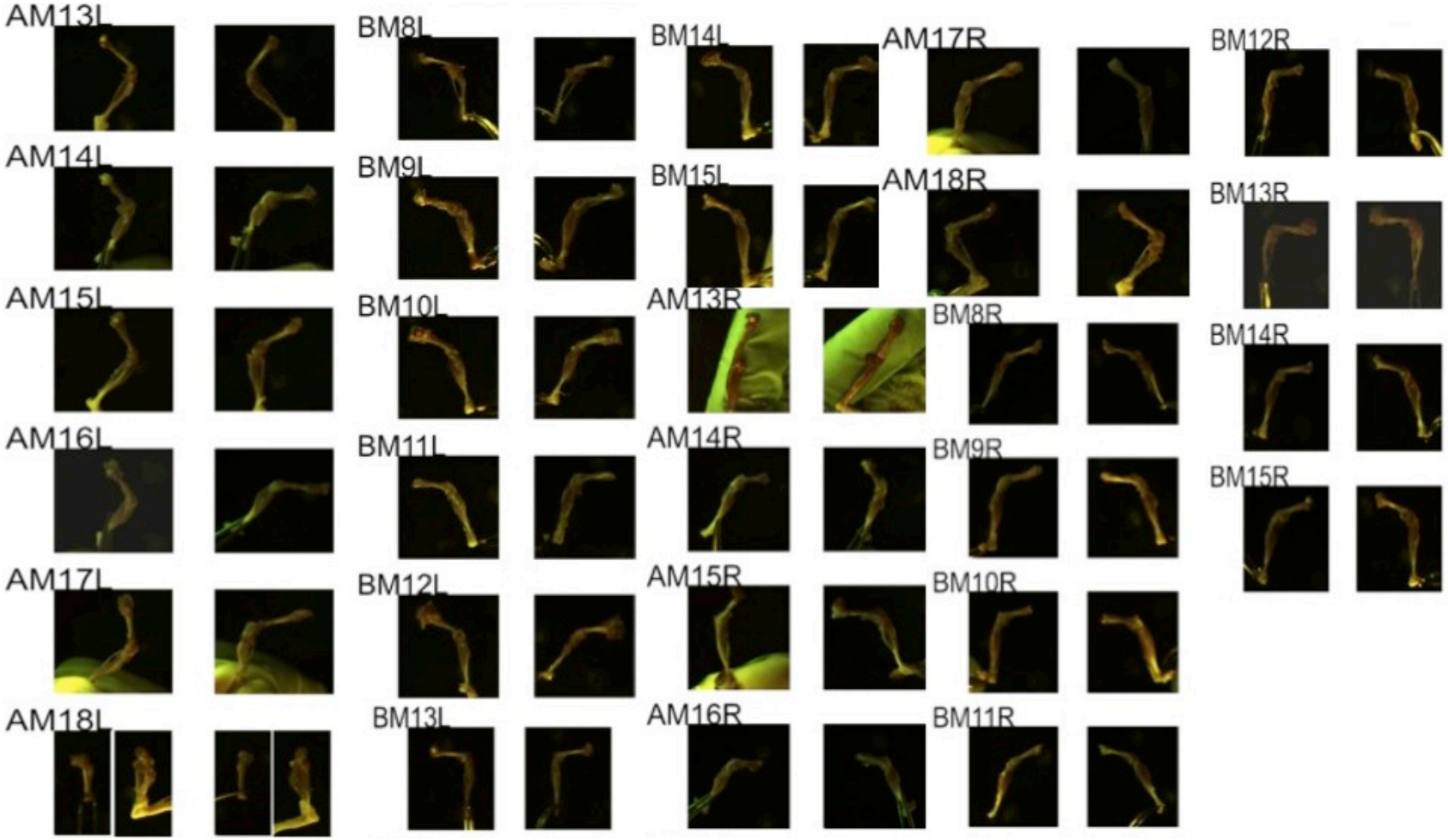

CHAPTER VII: Bibliography

Bibliography

Abasolo, I., et al. (2004), 'Adrenomedullin inhibits prostate cancer cell proliferation through a cAMP-independent autocrine mechanism', *Biochem Biophys Res Commun,* 322 (3), 878-86.

Abe, M., et al. (2003), 'Adrenomedullin augments collateral development in response to acute ischemia', *Biochem Biophys Res Commun,* 306 (1), 10-5.

Abrahamsson, P. A. (1999), 'Neuroendocrine differentiation in prostatic carcinoma', *Prostate,* 39 (2), 135-48.

Adams, G. P. and Weiner, L. M. (2005), 'Monoclonal antibody therapy of cancer', *Nat Biotechnol,* 23 (9), 1147-57.

Aikawa, T., et al. (2006), 'Connective tissue growth factor-specific antibody attenuates tumor growth, metastasis, and angiogenesis in an orthotopic mouse model of pancreatic cancer', *Mol Cancer Ther,* 5 (5), 1108-16.

Aiyar, N., et al. (1996), 'A cDNA encoding the calcitonin gene-related peptide type 1 receptor', *J Biol Chem,* 271 (19), 11325-9.

Alessi, D. R., et al. (1996), 'Mechanism of activation of protein kinase B by insulin and IGF-1', *EMBO J,* 15 (23), 6541-51.

Amati, B., et al. (1993), 'Oncogenic activity of the c-Myc protein requires dimerization with Max', *Cell,* 72 (2), 233-45.

Andreis, P. G., et al. (2000), 'Adrenomedullin enhances cell proliferation and deoxyribonucleic acid synthesis in rat adrenal zona glomerulosa: receptor subtype involved and signaling mechanism', *Endocrinology,* 141 (6), 2098-104.

Ardyanto, T. D., et al. (2006), 'CoCl2-induced HIF-1alpha expression correlates with proliferation and apoptosis in MKN-1 cells: a possible role for the PI3K/Akt pathway', *Int J Oncol,* 29 (3), 549-55.

Arrigo, A. P. (1999), 'Gene expression and the thiol redox state', *Free Radic Biol Med,* 27 (9-10), 936-44.

Balducci, L. and Beghe, C. (2001), 'Cancer and age in the USA', *Crit Rev Oncol Hematol,* 37 (2), 137-45.

Barker, H. E., Cox, T. R., and Erler, J. T. (2012), 'The rationale for targeting the LOX family in cancer', *Nat Rev Cancer,* 12 (8), 540-52.

Bates, R. C., Edwards, N. S., and Yates, J. D. (2000), 'Spheroids and cell survival', *Crit Rev Oncol Hematol,* 36 (2-3), 61-74.

Beitner-Johnson, D., et al. (2001), 'Hypoxia activates Akt and induces phosphorylation of GSK-3 in PC12 cells', *Cell Signal,* 13 (1), 23-7.

Beltowski, J. and Jamroz, A. (2004), 'Adrenomedullin--what do we know 10 years since its discovery?', *Pol J Pharmacol,* 56 (1), 5-27.

Ben-Yosef, Y., et al. (2002), 'Regulation of endothelial matrix metalloproteinase-2 by hypoxia/reoxygenation', *Circ Res,* 90 (7), 784-91.

Benizri, E., Ginouves, A., and Berra, E. (2008), 'The magic of the hypoxia-signaling cascade', *Cell Mol Life Sci,* 65 (7-8), 1133-49.

Berenguer, C., et al. (2008), 'Adrenomedullin, an autocrine/paracrine factor induced by androgen withdrawal, stimulates 'neuroendocrine phenotype' in LNCaP prostate tumor cells', *Oncogene,* 27 (4), 506-18.

Berx, G. and van Roy, F. (2009), 'Involvement of members of the cadherin superfamily in cancer', *Cold Spring Harb Perspect Biol,* 1 (6), a003129.

Betchen, S. A., et al. (2006), 'PTEN inhibits adrenomedullin expression and function in brain tumor cells', *J Neurooncol,* 79 (2), 117-23.

Bhowmick, N. A., Neilson, E. G., and Moses, H. L. (2004), 'Stromal fibroblasts in cancer initiation and progression', *Nature,* 432 (7015), 332-7.

Bindra, R. S. and Glazer, P. M. (2005), 'Genetic instability and the tumor microenvironment: towards the concept of microenvironment-induced mutagenesis', *Mutat Res,* 569 (1-2), 75-85.

Blattner, W. A. (1999), 'Human retroviruses: their role in cancer', *Proc Assoc Am Physicians,* 111 (6), 563-72.

Blume-Jensen, P. and Hunter, T. (2001), 'Oncogenic kinase signalling', *Nature,* 411 (6835), 355-65.

Bomberger, J. M., et al. (2005a), 'Receptor activity-modifying protein (RAMP) isoform-specific regulation of adrenomedullin receptor trafficking by NHERF-1', *J Biol Chem,* 280 (25), 23926-35.

Bomberger, J. M., et al. (2005b), 'Novel function for receptor activity-modifying proteins (RAMPs) in post-endocytic receptor trafficking', *J Biol Chem,* 280 (10), 9297-307.

Bos, R., et al. (2005), 'Hypoxia-inducible factor-1alpha is associated with angiogenesis, and expression of bFGF, PDGF-BB, and EGFR in invasive breast cancer', *Histopathology,* 46 (1), 31-6.

Boudouresque, F., et al. (2005), '[Role of adrenomedullin in glioblastomas growth]', *Bull Cancer,* 92 (4), 317-26.

Bourdon, J. C. (2007), 'p53 and its isoforms in cancer', *Br J Cancer,* 97 (3), 277-82.

Bouschet, T., Martin, S., and Henley, J. M. (2005), 'Receptor-activity-modifying proteins are required for forward trafficking of the calcium-sensing receptor to the plasma membrane', *J Cell Sci,* 118 (Pt 20), 4709-20.

Bradley, C. J., Given, C. W., and Roberts, C. (2002), 'Race, socioeconomic status, and breast cancer treatment and survival', *J Natl Cancer Inst,* 94 (7), 490-6.

Brahimi-Horn, M. C. and Pouyssegur, J. (2007), 'Harnessing the hypoxia-inducible factor in cancer and ischemic disease', *Biochem Pharmacol,* 73 (3), 450-7.

Brekhman, V., et al. (2010), 'Receptor activity modifying protein-3 mediates the protumorigenic activity of lysyl oxidase-like protein-2', *FASEB J,* 25 (1), 55-65.

Brown, J. M. and Giaccia, A. J. (1998), 'The unique physiology of solid tumors: opportunities (and problems) for cancer therapy', *Cancer Res,* 58 (7), 1408-16.

Bruick, R. K. and McKnight, S. L. (2001), 'A conserved family of prolyl-4-hydroxylases that modify HIF', *Science,* 294 (5545), 1337-40.

Bucher, M., et al. (1996), 'Cobalt but not hypoxia stimulates PDGF gene expression in rats', *Am J Physiol,* 271 (3 Pt 1), E451-7.

Buhlmann, N., et al. (1999), 'A receptor activity modifying protein (RAMP)2-dependent adrenomedullin receptor is a calcitonin gene-related peptide receptor when coexpressed with human RAMP1', *Endocrinology,* 140 (6), 2883-90.

Buhlmann, N., et al. (2000), 'Glycosylation of the calcitonin receptor-like receptor at Asn(60) or Asn(112) is important for cell surface expression', *FEBS Lett,* 486 (3), 320-4.

Bunn, H. F. and Poyton, R. O. (1996), 'Oxygen sensing and molecular adaptation to hypoxia', *Physiol Rev,* 76 (3), 839-85.

Bunton, D. C., et al. (2004), 'The clinical relevance of adrenomedullin: a promising profile?', *Pharmacol Ther,* 103 (3), 179-201.

Burdall, S. E., et al. (2003), 'Breast cancer cell lines: friend or foe?', *Breast Cancer Res,* 5 (2), 89-95.

Burkhardt, J. K., et al. (2012), 'Intra-arterial delivery of bevacizumab after blood-brain barrier disruption for the treatment of recurrent glioblastoma: progression-free survival and overall survival', *World Neurosurg,* 77 (1), 130-4.

Buys, S., et al. (2003), 'Adrenomedullin upregulates M2-muscarinic receptors in cardiomyocytes from P19 cell line', *Br J Pharmacol,* 139 (6), 1219-27.

Cabrera-Vera, T. M., et al. (2003), 'Insights into G protein structure, function, and regulation', *Endocr Rev,* 24 (6), 765-81.

Calvo, A., et al. (2002), 'Adrenomedullin and proadrenomedullin N-terminal 20 peptide in the normal prostate and in prostate carcinoma', *Microsc Res Tech,* 57 (2), 98-104.

Cantley, L. C. (2002), 'The phosphoinositide 3-kinase pathway', *Science,* 296 (5573), 1655-7.

Cao, Y. (2005), 'Opinion: emerging mechanisms of tumour lymphangiogenesis and lymphatic metastasis', *Nat Rev Cancer,* 5 (9), 735-43.

Carmeliet, P. (2000), 'Mechanisms of angiogenesis and arteriogenesis', *Nat Med,* 6 (4), 389-95.

Carmeliet, P. and Jain, R. K. (2000), 'Angiogenesis in cancer and other diseases', *Nature,* 407 (6801), 249-57.

Caron, K. M. and Smithies, O. (2001), 'Extreme hydrops fetalis and cardiovascular abnormalities in mice lacking a functional Adrenomedullin gene', *Proc Natl Acad Sci U S A,* 98 (2), 615-9.

Carter, P. (2001), 'Improving the efficacy of antibody-based cancer therapies', *Nat Rev Cancer,* 1 (2), 118-29.

Cases, A., et al. (2000), 'Increased plasma adrenomedullin levels in hemodialysis patients with sustained hypotension', *Kidney Int,* 57 (2), 664-70.

Cavallaro, U. and Christofori, G. (2004), 'Cell adhesion and signalling by cadherins and Ig-CAMs in cancer', *Nat Rev Cancer,* 4 (2), 118-32.

Chan, D. A., et al. (2002), 'Role of prolyl hydroxylation in oncogenically stabilized hypoxia-inducible factor-1alpha', *J Biol Chem,* 277 (42), 40112-7.

Chan, D. A., et al. (2005), 'Coordinate regulation of the oxygen-dependent degradation domains of hypoxia-inducible factor 1 alpha', *Mol Cell Biol,* 25 (15), 6415-26.

Chang, C. P., et al. (1993), 'Identification of a seven transmembrane helix receptor for corticotropin-releasing factor and sauvagine in mammalian brain', *Neuron,* 11 (6), 1187-95.

Chauhan, M., Rajarathnam, K., and Yallampalli, C. (2005), 'Role of the N-terminal domain of the calcitonin receptor-like receptor in ligand binding', *Biochemistry,* 44 (2), 782-9.

Chen, C., et al. (2001), 'Regulation of glut1 mRNA by hypoxia-inducible factor-1. Interaction between H-ras and hypoxia', *J Biol Chem,* 276 (12), 9519-25.

Cheng, N., et al. (2008), 'Transforming growth factor-beta signaling-deficient fibroblasts enhance hepatocyte growth factor signaling in mammary carcinoma cells to promote scattering and invasion', *Mol Cancer Res,* 6 (10), 1521-33.

Chini, E. N., et al. (1995), 'Adrenomedullin suppresses mitogenesis in rat mesangial cells via cAMP pathway', *Biochem Biophys Res Commun,* 215 (3), 868-73.

Christopoulos, A., et al. (2003), 'Novel receptor partners and function of receptor activity-modifying proteins', *J Biol Chem,* 278 (5), 3293-7.

Collantes, M., et al. (2003), 'Distribution of adrenomedullin and proadrenomedullin N-terminal 20 peptide immunoreactivity in the pituitary gland of the frog Rana perezi', *Gen Comp Endocrinol,* 133 (1), 50-60.

Comerford, K. M., et al. (2002), 'Hypoxia-inducible factor-1-dependent regulation of the multidrug resistance (MDR1) gene', *Cancer Res,* 62 (12), 3387-94.

Condeelis, J. and Segall, J. E. (2003), 'Intravital imaging of cell movement in tumours', *Nat Rev Cancer,* 3 (12), 921-30.

Conner, A. C. and Poyner, D. R. (2001), 'The perils of using the human genome sequence: lessons from CALCRL', *Trends Pharmacol Sci,* 22 (6), 272.

Conner, A. C., et al. (2004), 'Heterodimers and family-B GPCRs: RAMPs, CGRP and adrenomedullin', *Biochem Soc Trans,* 32 (Pt 5), 843-6.

Conway, E. M., Collen, D., and Carmeliet, P. (2001), 'Molecular mechanisms of blood vessel growth', *Cardiovasc Res,* 49 (3), 507-21.

Cormier-Regard, S., Nguyen, S. V., and Claycomb, W. C. (1998), 'Adrenomedullin gene expression is developmentally regulated and induced by hypoxia in rat ventricular cardiac myocytes', *J Biol Chem,* 273 (28), 17787-92.

Cornish, J., Naot, D., and Reid, I. R. (2003), 'Adrenomedullin--a regulator of bone formation', *Regul Pept,* 112 (1-3), 79-86.

Cornish, J., et al. (1997), 'Adrenomedullin is a potent stimulator of osteoblastic activity in vitro and in vivo', *Am J Physiol,* 273 (6 Pt 1), E1113-20.

Cornish, J., et al. (2001), 'Systemic administration of adrenomedullin(27-52) increases bone volume and strength in male mice', *J Endocrinol,* 170 (1), 251-7.

Corti, R., et al. (2001), 'Vasopeptidase inhibitors: a new therapeutic concept in cardiovascular disease?', *Circulation,* 104 (15), 1856-62.

Couzin-Frankel, J. and Ogale, Y. (2011), 'FDA. Once on 'fast track,' avastin now derailed', *Science,* 333 (6039), 143-4.

Cueille, C., et al. (2002), 'Increased myocardial expression of RAMP1 and RAMP3 in rats with chronic heart failure', *Biochem Biophys Res Commun,* 294 (2), 340-6.

Cueille, C., et al. (2005), 'Post-transcriptional regulation of CRLR expression during hypoxia', *Biochem Biophys Res Commun,* 326 (1), 23-9.

Cui, J., et al. (2006), 'c-Jun NH(2)-terminal kinase 2alpha2 promotes the tumorigenicity of human glioblastoma cells', *Cancer Res,* 66 (20), 10024-31.

Cuttitta, F., et al. (2002), 'Adrenomedullin functions as an important tumor survival factor in human carcinogenesis', *Microsc Res Tech,* 57 (2), 110-9.

Cuttitta, Frank, et al. (1999), 'The Role of Adrenomedullin as a Growth Regulatory Peptide in the Normal and Malignant Setting', *J. Anim Sci.,* 77 (suppl_3), 55-69.

Czyzyk, T. A., et al. (2005), 'Deletion of peptide amidation enzymatic activity leads to edema and embryonic lethality in the mouse', *Dev Biol,* 287 (2), 301-13.

Dackor, R., et al. (2007), 'Receptor activity-modifying proteins 2 and 3 have distinct physiological functions from embryogenesis to old age', *J Biol Chem,* 282 (25), 18094-9.

Dackor, R. T., et al. (2006), 'Hydrops fetalis, cardiovascular defects, and embryonic lethality in mice lacking the calcitonin receptor-like receptor gene', *Mol Cell Biol,* 26 (7), 2511-8.

Damert, A., et al. (1997), 'Up-regulation of vascular endothelial growth factor expression in a rat glioma is conferred by two distinct hypoxia-driven mechanisms', *Cancer Res,* 57 (17), 3860-4.

Daub, H., et al. (1996), 'Role of transactivation of the EGF receptor in signalling by G-protein-coupled receptors', *Nature,* 379 (6565), 557-60.

Davidson, B., et al. (2006), 'The mitogen-activated protein kinases (MAPK) p38 and JNK are markers of tumor progression in breast carcinoma', *Gynecol Oncol,* 102 (3), 453-61.

Debinski, W., et al. (1999), 'Receptor for interleukin 13 is a marker and therapeutic target for human high-grade gliomas', *Clin Cancer Res,* 5 (5), 985-90.

Dechant, M. and Valerius, T. (2001), 'IgA antibodies for cancer therapy', *Crit Rev Oncol Hematol,* 39 (1-2), 69-77.

Deer, E. L., et al. (2010), 'Phenotype and genotype of pancreatic cancer cell lines', *Pancreas,* 39 (4), 425-35.

Deng, B., et al. (2012), 'Adrenomedullin expression in epithelial ovarian cancers and promotes HO8910 cell migration associated with upregulating integrin alpha5beta1 and phosphorylating FAK and paxillin', *J Exp Clin Cancer Res,* 31, 19.

Dimmeler, S. and Zeiher, A. M. (2000), 'Akt takes center stage in angiogenesis signaling', *Circ Res,* 86 (1), 4-5.

Ding, W., et al. (2010), 'Epithelial-to-mesenchymal transition of murine liver tumor cells promotes invasion', *Hepatology,* 52 (3), 945-53.

Disa, J., et al. (1998), 'Interaction of adrenomedullin with calcitonin receptor in cultured human breast cancer cells, T 47D', *Peptides,* 19 (2), 247-51.

Drimal, J., Drimal, J., Jr., and Drimal, D. (2006), 'Hypoxic stress-enhanced expression and release of adrenomedullin (AM) and up-regulated AM receptors, while glucose starvation reduced AM expression and release and down-regulated AM receptors in monkey renal cells', *Physiol Res,* 55 (5), 535-42.

Eckhart, A. D., et al. (1997), 'Characterization of the alpha1B-adrenergic receptor gene promoter region and hypoxia regulatory elements in vascular smooth muscle', *Proc Natl Acad Sci U S A,* 94 (17), 9487-92.

Eguchi, S., et al. (1994), 'Structure-activity relationship of adrenomedullin, a novel vasodilatory peptide, in cultured rat vascular smooth muscle cells', *Endocrinology,* 135 (6), 2454-8.

Ehlenz, K., et al. (1997), 'High levels of circulating adrenomedullin in severe illness: correlation with C-reactive protein and evidence against the adrenal medulla as site of origin', *Exp Clin Endocrinol Diabetes,* 105 (3), 156-62.

Eipper, B. A., et al. (1992), 'Alternative splicing and endoproteolytic processing generate tissue-specific forms of pituitary peptidylglycine alpha-amidating monooxygenase (PAM)', *J Biol Chem,* 267 (6), 4008-15.

Elshourbagy, N. A., et al. (1998), 'Molecular cloning and characterization of the porcine calcitonin gene-related peptide receptor', *Endocrinology,* 139 (4), 1678-83.

Eng, C. (1999), 'RET proto-oncogene in the development of human cancer', *J Clin Oncol,* 17 (1), 380-93.

Eng, E., et al. (2005), 'Hypoxia regulates PDGF-B interactions between glomerular capillary endothelial and mesangial cells', *Kidney Int,* 68 (2), 695-703.

Evans, A. J., et al. (2007), 'VHL promotes E2 box-dependent E-cadherin transcription by HIF-mediated regulation of SIP1 and snail', *Mol Cell Biol,* 27 (1), 157-69.

Feinberg, A. P. (2007), 'Phenotypic plasticity and the epigenetics of human disease', *Nature,* 447 (7143), 433-40.

Feldser, D., et al. (1999), 'Reciprocal positive regulation of hypoxia-inducible factor 1alpha and insulin-like growth factor 2', *Cancer Res,* 59 (16), 3915-8.

Fernandez-Sauze, S., et al. (2004), 'Effects of adrenomedullin on endothelial cells in the multistep process of angiogenesis: involvement of CRLR/RAMP2 and CRLR/RAMP3 receptors', *Int J Cancer,* 108 (6), 797-804.

Ferrara, N. (2004), 'Vascular endothelial growth factor as a target for anticancer therapy', *Oncologist,* 9 Suppl 1, 2-10.

Fidler, I. J. (2003), 'The pathogenesis of cancer metastasis: the 'seed and soil' hypothesis revisited', *Nat Rev Cancer,* 3 (6), 453-8.

Fisher, B., et al. (1993), 'Lumpectomy compared with lumpectomy and radiation therapy for the treatment of intraductal breast cancer', *N Engl J Med,* 328 (22), 1581-6.

Fitzsimmons, T. J., Zhao, X., and Wank, S. A. (2003), 'The extracellular domain of receptor activity-modifying protein 1 is sufficient for calcitonin receptor-like receptor function', *J Biol Chem,* 278 (16), 14313-20.

Flahaut, M., et al. (2003), 'N-Glycosylation and conserved cysteine residues in RAMP3 play a critical role for the functional expression of CRLR/RAMP3 adrenomedullin receptor', *Biochemistry,* 42 (34), 10333-41.

Fluhmann, B., et al. (1995), 'A human orphan calcitonin receptor-like structure', *Biochem Biophys Res Commun,* 206 (1), 341-7.

Folkman, J. (1992), 'The role of angiogenesis in tumor growth', *Semin Cancer Biol,* 3 (2), 65-71.

Forsythe, J. A., et al. (1996), 'Activation of vascular endothelial growth factor gene transcription by hypoxia-inducible factor 1', *Mol Cell Biol,* 16 (9), 4604-13.

Franklin, D. J. (2007), 'Cancer rehabilitation: challenges, approaches, and new directions', *Phys Med Rehabil Clin N Am,* 18 (4), 899-924, viii.

Frazer, I. H. (2004), 'Prevention of cervical cancer through papillomavirus vaccination', *Nat Rev Immunol,* 4 (1), 46-54.

Friedl, P. and Wolf, K. (2003), 'Tumour-cell invasion and migration: diversity and escape mechanisms', *Nat Rev Cancer,* 3 (5), 362-74.

Fritz-Six, K. L., et al. (2008), 'Adrenomedullin signaling is necessary for murine lymphatic vascular development', *J Clin Invest,* 118 (1), 40-50.

Fujio, Y., et al. (2000), 'Akt promotes survival of cardiomyocytes in vitro and protects against ischemia-reperfusion injury in mouse heart', *Circulation,* 101 (6), 660-7.

Furnari, F. B., et al. (1997), 'Growth suppression of glioma cells by PTEN requires a functional phosphatase catalytic domain', *Proc Natl Acad Sci U S A,* 94 (23), 12479-84.

Futreal, P. A., et al. (2001), 'Cancer and genomics', *Nature,* 409 (6822), 850-2.

Garayoa, M., et al. (2000), 'Hypoxia-inducible factor-1 (HIF-1) up-regulates adrenomedullin expression in human tumor cell lines during oxygen deprivation: a possible promotion mechanism of carcinogenesis', *Mol Endocrinol,* 14 (6), 848-62.

Garcia-Unzueta, M. T., et al. (1998), 'Plasma adrenomedullin levels in type 1 diabetes. Relationship with clinical parameters', *Diabetes Care,* 21 (6), 999-1003.

Geiger, T. R. and Peeper, D. S. (2009), 'Metastasis mechanisms', *Biochim Biophys Acta,* 1796 (2), 293-308.

Gether, U. (2000), 'Uncovering molecular mechanisms involved in activation of G protein-coupled receptors', *Endocr Rev,* 21 (1), 90-113.

Ghosh, M., et al. (2004), 'Cofilin promotes actin polymerization and defines the direction of cell motility', *Science,* 304 (5671), 743-6.

Giacalone, P. L., et al. (2003), 'Expression of adrenomedullin in human ovaries, ovarian cysts and cancers. Correlation with estrogens receptor status', *Eur J Obstet Gynecol Reprod Biol,* 110 (2), 224-9.

Gibbons, C., et al. (2007), 'Receptor activity-modifying proteins: RAMPing up adrenomedullin signaling', *Mol Endocrinol,* 21 (4), 783-96.

Gibbs, G. W. and Berry, G. (2008), 'Mesothelioma and asbestos', *Regul Toxicol Pharmacol,* 52 (1 Suppl), S223-31.

Giordano, F. J. and Johnson, R. S. (2001), 'Angiogenesis: the role of the microenvironment in flipping the switch', *Curr Opin Genet Dev,* 11 (1), 35-40.

Gleadle, J. M., et al. (1995), 'Regulation of angiogenic growth factor expression by hypoxia, transition metals, and chelating agents', *Am J Physiol,* 268 (6 Pt 1), C1362-8.

Goel, R., et al. (2004), 'Alpha-thrombin-mediated phosphatidylinositol 3-kinase activation through release of Gbetagamma dimers from Galphaq and Galphai2', *J Biol Chem,* 279 (8), 6701-10.

Goldberg, M. A., Dunning, S. P., and Bunn, H. F. (1988), 'Regulation of the erythropoietin gene: evidence that the oxygen sensor is a heme protein', *Science,* 242 (4884), 1412-5.

Gonzalez-Moreno, O., et al. (2005), 'Gene expression profiling identifies IL-13 receptor alpha 2 chain as a therapeutic target in prostate tumor cells overexpressing adrenomedullin', *Int J Cancer,* 114 (6), 870-8.

Gorlach, A., et al. (2001), 'Thrombin activates the hypoxia-inducible factor-1 signaling pathway in vascular smooth muscle cells: Role of the p22(phox)-containing NADPH oxidase', *Circ Res,* 89 (1), 47-54.

Graeber, T. G., et al. (1996), 'Hypoxia-mediated selection of cells with diminished apoptotic potential in solid tumours', *Nature,* 379 (6560), 88-91.

Granholm, S., Lundberg, P., and Lerner, U. H. (2008), 'Expression of the calcitonin receptor, calcitonin receptor-like receptor, and receptor activity modifying proteins during osteoclast differentiation', *J Cell Biochem,* 104 (3), 920-33.

Grymer, L. F., Pallisgaard, C., and Melsen, B. (1991), 'The nasal septum in relation to the development of the nasomaxillary complex: a study in identical twins', *Laryngoscope,* 101 (8), 863-8.

Guidolin, D., et al. (2008), 'Adrenomedullin stimulates angiogenic response in cultured human vascular endothelial cells: Involvement of the vascular endothelial growth factor receptor 2', *Peptides,* 29 (11), 2013-23.

Guise, T. (2010), 'Examining the metastatic niche: targeting the microenvironment', *Semin Oncol,* 37 Suppl 2, S2-14.

Guo, P., et al. (2003), 'Platelet-derived growth factor-B enhances glioma angiogenesis by stimulating vascular endothelial growth factor expression in tumor endothelia and by promoting pericyte recruitment', *Am J Pathol,* 162 (4), 1083-93.

Guo, W. and Giancotti, F. G. (2004), 'Integrin signalling during tumour progression', *Nat Rev Mol Cell Biol,* 5 (10), 816-26.

Gupta, G. P. and Massague, J. (2006), 'Cancer metastasis: building a framework', *Cell,* 127 (4), 679-95.

Gutkind, J. S. (1998), 'The pathways connecting G protein-coupled receptors to the nucleus through divergent mitogen-activated protein kinase cascades', *J Biol Chem,* 273 (4), 1839-42.

Haddad, J. J. and Land, S. C. (2001), 'A non-hypoxic, ROS-sensitive pathway mediates TNF-alpha-dependent regulation of HIF-1alpha', *FEBS Lett,* 505 (2), 269-74.

Hague, S., et al. (2000), 'Expression of the hypoxically regulated angiogenic factor adrenomedullin correlates with uterine leiomyoma vascular density', *Clin Cancer Res,* 6 (7), 2808-14.

Hall, E. J. (1994), 'Molecular biology in radiation therapy: the potential impact of recombinant technology on clinical practice', *Int J Radiat Oncol Biol Phys,* 30 (5), 1019-28.

Hanahan, D. and Weinberg, R. A. (2000), 'The hallmarks of cancer', *Cell,* 100 (1), 57-70.

Hanahan, D. and Weinberg, R. A. (2011), 'Hallmarks of cancer: the next generation', *Cell,* 144 (5), 646-74.

Harper, M. E., et al. (1996), 'Vascular endothelial growth factor (VEGF) expression in prostatic tumours and its relationship to neuroendocrine cells', *Br J Cancer,* 74 (6), 910-6.

Harris, A. L. (2002), 'Hypoxia--a key regulatory factor in tumour growth', *Nat Rev Cancer,* 2 (1), 38-47.

Hata, K., et al. (2000), 'Expression of thymidine phosphorylase and vascular endothelial growth factor in epithelial ovarian cancer: correlation with angiogenesis and progression of the tumor', *Anticancer Res,* 20 (5C), 3941-9.

Hawtin, S. R., et al. (2006), 'Charged extracellular residues, conserved throughout a G-protein-coupled receptor family, are required for ligand binding, receptor activation, and cell-surface expression', *J Biol Chem,* 281 (50), 38478-88.

Hay, D. L., Poyner, D. R., and Sexton, P. M. (2006), 'GPCR modulation by RAMPs', *Pharmacol Ther,* 109 (1-2), 173-97.

Hay, D. L., et al. (2004), 'The pharmacology of adrenomedullin receptors and their relationship to CGRP receptors', *J Mol Neurosci,* 22 (1-2), 105-13.

Hayashi, M., et al. (1997), 'Plasma adrenomedullin in diabetes', *Lancet,* 350 (9089), 1449-50.

Hewitson, K. S., et al. (2002), 'Hypoxia-inducible factor (HIF) asparagine hydroxylase is identical to factor inhibiting HIF (FIH) and is related to the cupin structural family', *J Biol Chem,* 277 (29), 26351-5.

Hickey, M. M. and Simon, M. C. (2006), 'Regulation of angiogenesis by hypoxia and hypoxia-inducible factors', *Curr Top Dev Biol,* 76, 217-57.

Higgins, D. F., et al. (2007), 'Hypoxia promotes fibrogenesis in vivo via HIF-1 stimulation of epithelial-to-mesenchymal transition', *J Clin Invest,* 117 (12), 3810-20.

Hilairet, S., et al. (2001), 'Agonist-promoted internalization of a ternary complex between calcitonin receptor-like receptor, receptor activity-modifying protein 1 (RAMP1), and beta-arrestin', *J Biol Chem,* 276 (45), 42182-90.

Hinson, J. P., Kapas, S., and Smith, D. M. (2000), 'Adrenomedullin, a multifunctional regulatory peptide', *Endocr Rev,* 21 (2), 138-67.

Hirata, Y., et al. (1996), 'Increased circulating adrenomedullin, a novel vasodilatory peptide, in sepsis', *J Clin Endocrinol Metab,* 81 (4), 1449-53.

Hirayama, N., et al. (1999), 'Molecular forms of circulating adrenomedullin in patients with congestive heart failure', *J Endocrinol,* 160 (2), 297-303.

Ho, H. H., et al. (1999), 'Glycosylation is important for binding to human calcitonin receptors', *Biochemistry,* 38 (6), 1866-72.

Hockel, M., et al. (1991), 'Oxygenation of carcinomas of the uterine cervix: evaluation by computerized O2 tension measurements', *Cancer Res,* 51 (22), 6098-102.

Hockel, M., et al. (1993), 'Intratumoral pO2 predicts survival in advanced cancer of the uterine cervix', *Radiother Oncol,* 26 (1), 45-50.

Hofbauer, K. H., et al. (2000), 'Tissue hypoxygenation activates the adrenomedullin system in vivo', *Am J Physiol Regul Integr Comp Physiol,* 278 (2), R513-9.

Hofbauer, K. H., et al. (2002), 'Inflammatory cytokines stimulate adrenomedullin expression through nitric oxide-dependent and -independent pathways', *Hypertension,* 39 (1), 161-7.

Hollerhage, H. G., et al. (1991), 'Influence of type and extent of surgery on early results and survival time in glioblastoma multiforme', *Acta Neurochir (Wien),* 113 (1-2), 31-7.

Holliday, D. L. and Speirs, V. (2011), 'Choosing the right cell line for breast cancer research', *Breast Cancer Res,* 13 (4), 215.

Hu, J., et al. (1998), 'Hypoxia regulates expression of the endothelin-1 gene through a proximal hypoxia-inducible factor-1 binding site on the antisense strand', *Biochem Biophys Res Commun,* 245 (3), 894-9.

Huang, L. E., et al. (1996), 'Activation of hypoxia-inducible transcription factor depends primarily upon redox-sensitive stabilization of its alpha subunit', *J Biol Chem,* 271 (50), 32253-9.

Huang, L. E., et al. (1998), 'Regulation of hypoxia-inducible factor 1alpha is mediated by an O2-dependent degradation domain via the ubiquitin-proteasome pathway', *Proc Natl Acad Sci U S A,* 95 (14), 7987-92.

Huang, L. E., et al. (2007), 'Hypoxia-induced genetic instability--a calculated mechanism underlying tumor progression', *J Mol Med (Berl),* 85 (2), 139-48.

Hudis, C. A. (2007), 'Trastuzumab--mechanism of action and use in clinical practice', *N Engl J Med,* 357 (1), 39-51.

Hukovic, N., et al. (1999), 'Agonist-dependent up-regulation of human somatostatin receptor type 1 requires molecular signals in the cytoplasmic C-tail', *J Biol Chem,* 274 (35), 24550-8.

Husmann, K., et al. (2000), 'Mouse receptor-activity-modifying proteins 1, -2 and -3: amino acid sequence, expression and function', *Mol Cell Endocrinol,* 162 (1-2), 35-43.

Hwang, I. S., et al. (2007), 'Age-related changes in adrenomedullin expression and hypoxia-inducible factor-1 activity in the rat lung and their responses to hypoxia', *J Gerontol A Biol Sci Med Sci,* 62 (1), 41-9.

Ichikawa-Shindo, Y., et al. (2008), 'The GPCR modulator protein RAMP2 is essential for angiogenesis and vascular integrity', *J Clin Invest,* 118 (1), 29-39.

Iimuro, S., et al. (2004), 'Angiogenic effects of adrenomedullin in ischemia and tumor growth', *Circ Res,* 95 (4), 415-23.

Imai, T., et al. (2003), 'Hypoxia attenuates the expression of E-cadherin via up-regulation of SNAIL in ovarian carcinoma cells', *Am J Pathol,* 163 (4), 1437-47.

Inoue, D., et al. (1999), 'Calcitonin-dependent down-regulation of the mouse C1a calcitonin receptor in cells of the osteoclast lineage involves a transcriptional mechanism', *Endocrinology,* 140 (3), 1060-8.

Ishihara, T., et al. (1999), 'Increased plasma levels of mature form of adrenomedullin in patients with chronic renal failure', *Clin Nephrol,* 52 (2), 119-23.

Ishikawa, T., et al. (2003), 'Adrenomedullin antagonist suppresses in vivo growth of human pancreatic cancer cells in SCID mice by suppressing angiogenesis', *Oncogene,* 22 (8), 1238-42.

Ishimitsu, T., et al. (1994), 'Genomic structure of human adrenomedullin gene', *Biochem Biophys Res Commun,* 203 (1), 631-9.

Ivan, M., et al. (2001), 'HIFalpha targeted for VHL-mediated destruction by proline hydroxylation: implications for O2 sensing', *Science,* 292 (5516), 464-8.

Iwasaki, H., et al. (2001), 'Adrenomedullin stimulates proline-rich tyrosine kinase 2 in vascular smooth muscle cells', *Endocrinology,* 142 (2), 564-72.

Iwasaki, H., et al. (1998), 'Adrenomedullin as a novel growth-promoting factor for cultured vascular smooth muscle cells: role of tyrosine kinase-mediated mitogen-activated protein kinase activation', *Endocrinology,* 139 (8), 3432-41.

Iwase, T., et al. (2005), 'Adrenomedullin enhances angiogenic potency of bone marrow transplantation in a rat model of hindlimb ischemia', *Circulation,* 111 (3), 356-62.

Iyer, N. V., et al. (1998), 'Cellular and developmental control of O2 homeostasis by hypoxia-inducible factor 1 alpha', *Genes Dev,* 12 (2), 149-62.

Jaakkola, P., et al. (2001), 'Targeting of HIF-alpha to the von Hippel-Lindau ubiquitylation complex by O2-regulated prolyl hydroxylation', *Science,* 292 (5516), 468-72.

Jahnke, G. D., et al. (1997), 'Adrenomedullin expression in the mouse mammary gland: evidence for the mature form in milk', *J Mol Endocrinol,* 19 (3), 279-89.

Jemal, A., et al. (2010), 'Cancer statistics, 2010', *CA Cancer J Clin,* 60 (5), 277-300.

Jeong, J. W., et al. (2002), 'Regulation and destabilization of HIF-1alpha by ARD1-mediated acetylation', *Cell,* 111 (5), 709-20.

Jimenez, N., et al. (1999), 'Expression of adrenomedullin and proadrenomedullin N-terminal 20 peptide in human and rat prostate', *J Histochem Cytochem,* 47 (9), 1167-78.

Jimenez, N., et al. (2003), 'Androgen-independent expression of adrenomedullin and peptidylglycine alpha-amidating monooxygenase in human prostatic carcinoma', *Mol Carcinog,* 38 (1), 14-24.

Jogi, A., et al. (2004), 'Human neuroblastoma cells exposed to hypoxia: induction of genes associated with growth, survival, and aggressive behavior', *Exp Cell Res,* 295 (2), 469-87.

Jorgensen, K., Davidson, B., and Florenes, V. A. (2006), 'Activation of c-jun N-terminal kinase is associated with cell proliferation and shorter relapse-free period in superficial spreading malignant melanoma', *Mod Pathol,* 19 (11), 1446-55.

Joshi, B. H., Plautz, G. E., and Puri, R. K. (2000), 'Interleukin-13 receptor alpha chain: a novel tumor-associated transmembrane protein in primary explants of human malignant gliomas', *Cancer Res,* 60 (5), 1168-72.

Joshi, B. H., et al. (2008), 'Human adrenomedullin up-regulates interleukin-13 receptor alpha2 chain in prostate cancer in vitro and in vivo: a novel approach to sensitize prostate cancer to anticancer therapy', *Cancer Res,* 68 (22), 9311-7.

Josko, J., et al. (2000), 'Vascular endothelial growth factor (VEGF) and its effect on angiogenesis', *Med Sci Monit,* 6 (5), 1047-52.

Jougasaki, M., et al. (1995), 'Renal localization and actions of adrenomedullin: a natriuretic peptide', *Am J Physiol,* 268 (4 Pt 2), F657-63.

Kaafarani, I., et al. (2009), 'Targeting adrenomedullin receptors with systemic delivery of neutralizing antibodies inhibits tumor angiogenesis and suppresses growth of human tumor xenografts in mice', *FASEB J,* 23 (10), 3424-35.

Kallio, P. J., et al. (1997), 'Activation of hypoxia-inducible factor 1alpha: posttranscriptional regulation and conformational change by recruitment of the Arnt transcription factor', *Proc Natl Acad Sci U S A,* 94 (11), 5667-72.

Kallman, R. F. and Dorie, M. J. (1986), 'Tumor oxygenation and reoxygenation during radiation therapy: their importance in predicting tumor response', *Int J Radiat Oncol Biol Phys,* 12 (4), 681-5.

Kalluri, R. and Weinberg, R. A. (2009), 'The basics of epithelial-mesenchymal transition', *J Clin Invest,* 119 (6), 1420-8.

Kamitani, S. and Sakata, T. (2001), 'Glycosylation of human CRLR at Asn123 is required for ligand binding and signaling', *Biochim Biophys Acta,* 1539 (1-2), 131-9.

Kampa, M. and Castanas, E. (2008), 'Human health effects of air pollution', *Environ Pollut,* 151 (2), 362-7.

Kanazawa, H., et al. (1994), 'Adrenomedullin, a newly discovered hypotensive peptide, is a potent bronchodilator', *Biochem Biophys Res Commun,* 205 (1), 251-4.

Kapas, S., et al. (1997), 'Adrenomedullin has mitogenic effects on human oral keratinocytes: involvement of cyclic AMP', *FEBS Lett,* 418 (3), 287-90.

Karagiannis, T. C. (2007), 'Antibody-based cancer treatment with ultra-short range Auger electron-emitting radionuclides: dual receptor and DNA targeting strategies', *Hell J Nucl Med,* 10 (3), 155-9.

Kato, H., et al. (1997), 'Adrenomedullin as an autocrine/paracrine apoptosis survival factor for rat endothelial cells', *Endocrinology,* 138 (6), 2615-20.

Kato, M., et al. (1999), 'Characterization of six cell lines established from human pancreatic adenocarcinomas', *Cancer,* 85 (4), 832-40.

Ke, Q. and Costa, M. (2006), 'Hypoxia-inducible factor-1 (HIF-1)', *Mol Pharmacol,* 70 (5), 1469-80.

Keleg, S., et al. (2007), 'Adrenomedullin is induced by hypoxia and enhances pancreatic cancer cell invasion', *Int J Cancer,* 121 (1), 21-32.

Khatlani, T. S., et al. (2007), 'c-Jun N-terminal kinase is activated in non-small-cell lung cancer and promotes neoplastic transformation in human bronchial epithelial cells', *Oncogene,* 26 (18), 2658-66.

Kim, H., et al. (2011), 'Dual combination therapy targeting DR5 and EMMPRIN in pancreatic adenocarcinoma', *Mol Cancer Ther,* 11 (2), 405-15.

Kim, J. Y., et al. (2006), 'Adrenomedullin regulates cellular glutathione content via modulation of gamma-glutamate-cysteine ligase catalytic subunit expression', *Endocrinology,* 147 (3), 1357-64.

Kim, W., et al. (2003a), 'Adrenomedullin reduces VEGF-induced endothelial adhesion molecules and adhesiveness through a phosphatidylinositol 3'-kinase pathway', *Arterioscler Thromb Vasc Biol,* 23 (8), 1377-83.

Kim, W., et al. (2003b), 'Angiogenic role of adrenomedullin through activation of Akt, mitogen-activated protein kinase, and focal adhesion kinase in endothelial cells', *FASEB J,* 17 (13), 1937-9.

Kim, W., et al. (2002), 'Protective effect of adrenomedullin in mannitol-induced apoptosis', *Apoptosis,* 7 (6), 527-36.

Kinoshita, H., et al. (2000), 'Increased plasma levels of mature adrenomedullin in chronic glomerulonephritis', *Nephron,* 86 (3), 333-8.

Kitamura, K., et al. (1993), 'Adrenomedullin: a novel hypotensive peptide isolated from human pheochromocytoma', *Biochem Biophys Res Commun,* 192 (2), 553-60.

Kitamuro, T., et al. (2000), 'Induction of adrenomedullin during hypoxia in cultured human glioblastoma cells', *J Neurochem,* 75 (5), 1826-33.

Kitamuro, T., et al. (2001), 'Differential expression of adrenomedullin and its receptor component, receptor activity modifying protein (RAMP) 2 during hypoxia in cultured human neuroblastoma cells', *Peptides,* 22 (11), 1795-801.

Kleinman, H. K. and Liau, G. (2001), 'Gene therapy for antiangiogenesis', *J Natl Cancer Inst,* 93 (13), 965-7.

Kline, D. D., et al. (2002), 'Defective carotid body function and impaired ventilatory responses to chronic hypoxia in mice partially deficient for hypoxia-inducible factor 1 alpha', *Proc Natl Acad Sci U S A,* 99 (2), 821-6.

Knobbe, C. B., Merlo, A., and Reifenberger, G. (2002), 'Pten signaling in gliomas', *Neuro Oncol,* 4 (3), 196-211.

Kohno, M., et al. (1996), 'Plasma adrenomedullin concentrations in essential hypertension', *Hypertension,* 27 (1), 102-7.

Kohout, T. A. and Lefkowitz, R. J. (2003), 'Regulation of G protein-coupled receptor kinases and arrestins during receptor desensitization', *Mol Pharmacol,* 63 (1), 9-18.

Koo, D. J., et al. (2001), 'The role of adrenomedullin in producing differential hemodynamic responses during sepsis', *J Surg Res,* 95 (2), 207-18.

Kopfstein, L., et al. (2007), 'Distinct roles of vascular endothelial growth factor-D in lymphangiogenesis and metastasis', *Am J Pathol,* 170 (4), 1348-61.

Koshiji, M., et al. (2005), 'HIF-1alpha induces genetic instability by transcriptionally downregulating MutSalpha expression', *Mol Cell,* 17 (6), 793-803.

Kourembanas, S., Hannan, R. L., and Faller, D. V. (1990), 'Oxygen tension regulates the expression of the platelet-derived growth factor-B chain gene in human endothelial cells', *J Clin Invest,* 86 (2), 670-4.

Krieg, A. J., et al. 'Regulation of the histone demethylase JMJD1A by hypoxia-inducible factor 1 alpha enhances hypoxic gene expression and tumor growth', *Mol Cell Biol,* 30 (1), 344-53.

Krishnamachary, B., et al. (2006), 'Hypoxia-inducible factor-1-dependent repression of E-cadherin in von Hippel-Lindau tumor suppressor-null renal cell carcinoma mediated by TCF3, ZFHX1A, and ZFHX1B', *Cancer Res,* 66 (5), 2725-31.

Krishnamachary, B., et al. (2003), 'Regulation of colon carcinoma cell invasion by hypoxia-inducible factor 1', *Cancer Res,* 63 (5), 1138-43.

Krishnaswamy, V., et al. (2006), 'South Indian men with reduced CAG repeat length in the androgen receptor gene have an increased risk of prostate cancer', *J Hum Genet,* 51 (3), 254-7.

Kristiansen, K. (2004), 'Molecular mechanisms of ligand binding, signaling, and regulation within the superfamily of G-protein-coupled receptors: molecular modeling and mutagenesis approaches to receptor structure and function', *Pharmacol Ther,* 103 (1), 21-80.

Kroeze, W. K., Sheffler, D. J., and Roth, B. L. (2003), 'G-protein-coupled receptors at a glance', *J Cell Sci,* 116 (Pt 24), 4867-9.

Kubo, A., et al. (1998), 'Plasma and urinary levels of adrenomedullin in chronic glomerulonephritis patients with proteinuria', *Nephron,* 80 (2), 227-30.

Kureishi, Y., et al. (1995), 'Adrenomedullin decreases both cytosolic Ca2+ concentration and Ca(2+)-sensitivity in pig coronary arterial smooth muscle', *Biochem Biophys Res Commun,* 212 (2), 572-9.

Kusano, S., et al. (2011), 'Structural basis for extracellular interactions between calcitonin receptor-like receptor and receptor activity-modifying protein 2 for adrenomedullin-specific binding', *Protein Sci*.

Kuwasako, K., et al. (2009), 'Flow cytometric analysis of the calcitonin receptor-like receptor domains responsible for cell-surface translocation of receptor activity-modifying proteins', *Biochem Biophys Res Commun,* 384 (2), 249-54.

Kuwasako, K., et al. (2003a), 'Identification of the human receptor activity-modifying protein 1 domains responsible for agonist binding specificity', *J Biol Chem,* 278 (25), 22623-30.

Kuwasako, K., et al. (2004), 'Adrenomedullin receptors: pharmacological features and possible pathophysiological roles', *Peptides,* 25 (11), 2003-12.

Kuwasako, K., et al. (2010), 'Function of the cytoplasmic tail of human calcitonin receptor-like receptor in complex with receptor activity-modifying protein 2', *Biochem Biophys Res Commun,* 392 (3), 380-5.

Kuwasako, K., et al. (2003b), 'The function of extracellular cysteines in the human adrenomedullin receptor', *Hypertens Res,* 26 Suppl, S25-31.

Kuwasako, K., et al. (2006), 'Functions of the cytoplasmic tails of the human receptor activity-modifying protein components of calcitonin gene-related peptide and adrenomedullin receptors', *J Biol Chem,* 281 (11), 7205-13.

Kuwasako, K., et al. (2011a), 'The third extracellular loop of the human calcitonin receptor-like receptor is crucial for the activation of adrenomedullin signalling', *Br J Pharmacol*.

Kuwasako, K., et al. (2011b), 'Shared and separate functions of the RAMP-based adrenomedullin receptors', *Peptides,* 32 (7), 1540-50.

Kuwasako, K., et al. (2001), 'The seven amino acids of human RAMP2 (86) and RAMP3 (59) are critical for agonist binding to human adrenomedullin receptors', *J Biol Chem,* 276 (52), 49459-65.

Kuwasako, K., et al. (2000), 'Visualization of the calcitonin receptor-like receptor and its receptor activity-modifying proteins during internalization and recycling', *J Biol Chem,* 275 (38), 29602-9.

Lando, D., et al. (2002a), 'Asparagine hydroxylation of the HIF transactivation domain a hypoxic switch', *Science,* 295 (5556), 858-61.

Lando, D., et al. (2002b), 'FIH-1 is an asparaginyl hydroxylase enzyme that regulates the transcriptional activity of hypoxia-inducible factor', *Genes Dev,* 16 (12), 1466-71.

Lawson, Z. and Wheatley, M. (2004), 'The third extracellular loop of G-protein-coupled receptors: more than just a linker between two important transmembrane helices', *Biochem Soc Trans,* 32 (Pt 6), 1048-50.

Le, Y., et al. (2004), 'Silencing the formylpeptide receptor FPR by short-interfering RNA', *Mol Pharmacol,* 66 (4), 1022-8.

Lee, P. J., et al. (1997), 'Hypoxia-inducible factor-1 mediates transcriptional activation of the heme oxygenase-1 gene in response to hypoxia', *J Biol Chem,* 272 (9), 5375-81.

Lee, S. M., et al. (2006), 'Hypoxia confers protection against apoptosis via PI3K/Akt and ERK pathways in lung cancer cells', *Cancer Lett,* 242 (2), 231-8.

Leon, S. P., Folkerth, R. D., and Black, P. M. (1996), 'Microvessel density is a prognostic indicator for patients with astroglial brain tumors', *Cancer,* 77 (2), 362-72.

Letizia, C., et al. (2000), 'Circulating adrenomedullin is increased in patients with corticotropin-dependent Cushing's syndrome due to pituitary adenoma', *Metabolism,* 49 (6), 760-3.

Letizia, C., et al. (2004), 'Adrenomedullin immunoreactivity tissue distribution in parathyroids of the patients with primary hyperparathyroidism', *Horm Metab Res,* 36 (7), 480-4.

Levy, A. P., et al. (1995), 'Transcriptional regulation of the rat vascular endothelial growth factor gene by hypoxia', *J Biol Chem,* 270 (22), 13333-40.

Li, C. Y., et al. (2000), 'Initial stages of tumor cell-induced angiogenesis: evaluation via skin window chambers in rodent models', *J Natl Cancer Inst,* 92 (2), 143-7.

Li, J., et al. (2004), 'Nickel compounds act through phosphatidylinositol-3-kinase/Akt-dependent, p70(S6k)-independent pathway to induce hypoxia inducible factor transactivation and Cap43 expression in mouse epidermal Cl41 cells', *Cancer Res,* 64 (1), 94-101.

Li, S., Huang, S., and Peng, S. B. (2005), 'Overexpression of G protein-coupled receptors in cancer cells: involvement in tumor progression', *Int J Oncol,* 27 (5), 1329-39.

Lin, E. Y., et al. (2001), 'Colony-stimulating factor 1 promotes progression of mammary tumors to malignancy', *J Exp Med,* 193 (6), 727-40.

Liu, X., Davis, D., and Segaloff, D. L. (1993), 'Disruption of potential sites for N-linked glycosylation does not impair hormone binding to the lutropin/choriogonadotropin receptor if Asn-173 is left intact', *J Biol Chem,* 268 (3), 1513-6.

Logsdon, C. D., et al. (2003), 'Molecular profiling of pancreatic adenocarcinoma and chronic pancreatitis identifies multiple genes differentially regulated in pancreatic cancer', *Cancer Res,* 63 (10), 2649-57.

Lowes, V. L., Ip, N. Y., and Wong, Y. H. (2002), 'Integration of signals from receptor tyrosine kinases and g protein-coupled receptors', *Neurosignals,* 11 (1), 5-19.

Lowy, D. R. and Willumsen, B. M. (1993), 'Function and regulation of ras', *Annu Rev Biochem,* 62, 851-91.

Luttrell, L. M., Daaka, Y., and Lefkowitz, R. J. (1999), 'Regulation of tyrosine kinase cascades by G-protein-coupled receptors', *Curr Opin Cell Biol,* 11 (2), 177-83.

Majid, D. S., et al. (1996), 'Renal responses to intra-arterial administration of adrenomedullin in dogs', *Am J Physiol,* 270 (1 Pt 2), F200-5.

Mallamaci, F., et al. (1998), 'Plasma adrenomedullin during acute changes in intravascular volume in hemodialysis patients', *Kidney Int,* 54 (5), 1697-703.

Mandriota, S. J., et al. (2001), 'Vascular endothelial growth factor-C-mediated lymphangiogenesis promotes tumour metastasis', *EMBO J,* 20 (4), 672-82.

Mangiola, A., et al. (2007), 'Stem cell marker nestin and c-Jun NH2-terminal kinases in tumor and peritumor areas of glioblastoma multiforme: possible prognostic implications', *Clin Cancer Res,* 13 (23), 6970-7.

Marinissen, M. J. and Gutkind, J. S. (2001), 'G-protein-coupled receptors and signaling networks: emerging paradigms', *Trends Pharmacol Sci,* 22 (7), 368-76.

Martinez, A., Cuttitta, F., and Teitelman, G. (1998), 'Expression pattern for adrenomedullin during pancreatic development in the rat reveals a common precursor with other endocrine cell types', *Cell Tissue Res,* 293 (1), 95-100.

Martinez, A., et al. (2005), 'Gastrin-releasing peptide (GRP) induces angiogenesis and the specific GRP blocker 77427 inhibits tumor growth in vitro and in vivo', *Oncogene,* 24 (25), 4106-13.

Martinez, A., et al. (1997), 'Expression of adrenomedullin and its receptor in normal and malignant human skin: a potential pluripotent role in the integument', *Endocrinology,* 138 (12), 5597-604.

Martinez, A., et al. (1996), 'Regulation of insulin secretion and blood glucose metabolism by adrenomedullin', *Endocrinology,* 137 (6), 2626-32.

Martinez, A., et al. (2002), 'The effects of adrenomedullin overexpression in breast tumor cells', *J Natl Cancer Inst,* 94 (16), 1226-37.

Marutsuka, K., et al. (2003), 'Immunohistological localization and possible functions of adrenomedullin', *Hypertens Res,* 26 Suppl, S33-40.

Masson, N., et al. (2001), 'Independent function of two destruction domains in hypoxia-inducible factor-alpha chains activated by prolyl hydroxylation', *EMBO J,* 20 (18), 5197-206.

Mazzocchi, G., et al. (1996), 'Adrenomedullin and calcitonin gene-related peptide inhibit aldosterone secretion in rats, acting via a common receptor', *Life Sci,* 58 (10), 839-44.

McClanahan, T., et al. (2006), 'Identification of overexpression of orphan G protein-coupled receptor GPR49 in human colon and ovarian primary tumors', *Cancer Biol Ther,* 5 (4), 419-26.

McLatchie, L. M., et al. (1998), 'RAMPs regulate the transport and ligand specificity of the calcitonin-receptor-like receptor', *Nature,* 393 (6683), 333-9.

Meister, A. and Anderson, M. E. (1983), 'Glutathione', *Annu Rev Biochem,* 52, 711-60.

Melillo, G., et al. (1995), 'A hypoxia-responsive element mediates a novel pathway of activation of the inducible nitric oxide synthase promoter', *J Exp Med,* 182 (6), 1683-93.

Mendez, O., et al. (2010), 'Knock down of HIF-1alpha in glioma cells reduces migration in vitro and invasion in vivo and impairs their ability to form tumor spheres', *Mol Cancer,* 9, 133.

Mery, L. and Boulay, F. (1993), 'Evidence that the extracellular N-terminal domain of C5aR contains amino-acid residues crucial for C5a binding', *Eur J Haematol,* 51 (5), 282-7.

Metellus, P., et al. (2011), 'Adrenomedullin expression and regulation in human glioblastoma, cultured human glioblastoma cell lines and pilocytic astrocytoma', *Eur J Cancer,* 47 (11), 1727-35.

Miller, M. J., et al. (1996), 'Adrenomedullin expression in human tumor cell lines. Its potential role as an autocrine growth factor', *J Biol Chem,* 271 (38), 23345-51.

Millonig, G., et al. (2009), 'Hypoxia-inducible factor 1 alpha under rapid enzymatic hypoxia: cells sense decrements of oxygen but not hypoxia per se', *Free Radic Biol Med,* 46 (2), 182-91.

Minet, E., et al. (2001), 'Transduction pathways involved in Hypoxia-Inducible Factor-1 phosphorylation and activation', *Free Radic Biol Med,* 31 (7), 847-55.

Miseki, T., et al. (2007), 'Suppression of tumor growth by intra-muscular transfer of naked DNA encoding adrenomedullin antagonist', *Cancer Gene Ther,* 14 (1), 39-44.

Moncada, S., Palmer, R. M., and Higgs, E. A. (1991), 'Nitric oxide: physiology, pathophysiology, and pharmacology', *Pharmacol Rev,* 43 (2), 109-42.

Montuenga, L. M., et al. (1997), 'Expression of adrenomedullin and its receptor during embryogenesis suggests autocrine or paracrine modes of action', *Endocrinology,* 138 (1), 440-51.

Moore, M. J., et al. (2007), 'Erlotinib plus gemcitabine compared with gemcitabine alone in patients with advanced pancreatic cancer: a phase III trial of the National Cancer Institute of Canada Clinical Trials Group', *J Clin Oncol,* 25 (15), 1960-6.

Morfis, M., Christopoulos, A., and Sexton, P. M. (2003), 'RAMPs: 5 years on, where to now?', *Trends Pharmacol Sci,* 24 (11), 596-601.

Morrish, D. W., et al. (1996), 'Identification by subtractive hybridization of a spectrum of novel and unexpected genes associated with in vitro differentiation of human cytotrophoblast cells', *Placenta,* 17 (7), 431-41.

Mundy, G. R. (2002), 'Metastasis to bone: causes, consequences and therapeutic opportunities', *Nat Rev Cancer,* 2 (8), 584-93.

Nag, K., et al. (2006), 'Molecular and functional characterization of adrenomedullin receptors in pufferfish', *Am J Physiol Regul Integr Comp Physiol,* 290 (2), R467-78.

Nagaya, N., et al. (2000), 'Hemodynamic, renal, and hormonal effects of adrenomedullin infusion in patients with congestive heart failure', *Circulation,* 101 (5), 498-503.

Nakamura, M., et al. (1997), 'Potent and long-lasting vasodilatory effects of adrenomedullin in humans. Comparisons between normal subjects and patients with chronic heart failure', *Circulation,* 95 (5), 1214-21.

Nakanishi, K., et al. (2004), 'Expressions of adrenomedullin mRNA and protein in rats with hypobaric hypoxia-induced pulmonary hypertension', *Am J Physiol Heart Circ Physiol,* 286 (6), H2159-68.

Nakayama, M., et al. (1999), 'Induction of adrenomedullin by hypoxia in cultured human coronary artery endothelial cells', *Peptides,* 20 (6), 769-72.

Nakazawa, I., et al. (2001), 'Human calcitonin receptor-like receptor for adrenomedullin: genomic structure, eight single-nucleotide polymorphisms, and haplotype analysis', *J Hum Genet,* 46 (3), 132-6.

Naot, D., et al. (2001), 'A potential role for adrenomedullin as a local regulator of bone growth', *Endocrinology,* 142 (5), 1849-57.

Narisawa-Saito, M. and Kiyono, T. (2007), 'Basic mechanisms of high-risk human papillomavirus-induced carcinogenesis: roles of E6 and E7 proteins', *Cancer Sci,* 98 (10), 1505-11.

Nguyen, S. V. and Claycomb, W. C. (1999), 'Hypoxia regulates the expression of the adrenomedullin and HIF-1 genes in cultured HL-1 cardiomyocytes', *Biochem Biophys Res Commun,* 265 (2), 382-6.

Nielsen, F. C., Gammeltoft, S., and Christiansen, J. (1990), 'Translational discrimination of mRNAs coding for human insulin-like growth factor II', *J Biol Chem,* 265 (23), 13431-4.

Nikitenko, L. L., et al. (2000), 'Adrenomedullin is an autocrine regulator of endothelial growth in human endometrium', *Mol Hum Reprod,* 6 (9), 811-9.

Nikitenko, L. L., et al. (2003), 'Transcriptional regulation of the CRLR gene in human microvascular endothelial cells by hypoxia', *FASEB J,* 17 (11), 1499-501.

Nishikimi, T., et al. (1997), 'Cardiac production and secretion of adrenomedullin are increased in heart failure', *Hypertension,* 30 (6), 1369-75.

Nishikimi, T., et al. (2003), 'Ventricular adrenomedullin system in the transition from LVH to heart failure in rats', *Hypertension,* 41 (3), 512-8.

Nishio, K., et al. (1997), 'Increased plasma concentrations of adrenomedullin correlate with relaxation of vascular tone in patients with septic shock', *Crit Care Med,* 25 (6), 953-7.

Nitta, K., et al. (2000), 'Increased plasma levels of adrenomedullin in patients with hemodialysis', *Nephron,* 85 (4), 360-2.

Nowak, W., et al. (2002), 'Novel regulation of adrenomedullin receptor by PDGF: role of receptor activity modifying protein-3', *Am J Physiol Cell Physiol,* 282 (6), C1322-31.

Nuki, C., et al. (1993), 'Vasodilator effect of adrenomedullin and calcitonin gene-related peptide receptors in rat mesenteric vascular beds', *Biochem Biophys Res Commun,* 196 (1), 245-51.

O'Reilly, K. M., et al. (2007), 'Asbestos-related lung disease', *Am Fam Physician,* 75 (5), 683-8.

O'Rourke, J. F., et al. (1996), 'Identification of hypoxically inducible mRNAs in HeLa cells using differential-display PCR. Role of hypoxia-inducible factor-1', *Eur J Biochem,* 241 (2), 403-10.

Obiri, N. I., et al. (1995), 'Receptor for interleukin 13. Interaction with interleukin 4 by a mechanism that does not involve the common gamma chain shared by receptors for interleukins 2, 4, 7, 9, and 15', *J Biol Chem,* 270 (15), 8797-804.

Obiri, N. I., et al. (1997), 'The IL-13 receptor structure differs on various cell types and may share more than one component with IL-4 receptor', *J Immunol,* 158 (2), 756-64.

Oehler, M. K., et al. (2001), 'Adrenomedullin inhibits hypoxic cell death by upregulation of Bcl-2 in endometrial cancer cells: a possible promotion mechanism for tumour growth', *Oncogene,* 20 (23), 2937-45.

Oehler, M. K., et al. (2003), 'Tissue and plasma expression of the angiogenic peptide adrenomedullin in breast cancer', *Br J Cancer,* 89 (10), 1927-33.

Oettle, H. and Neuhaus, P. (2007), 'Adjuvant therapy in pancreatic cancer: a critical appraisal', *Drugs,* 67 (16), 2293-310.

Ogoshi, M., Inoue, K., and Takei, Y. (2003), 'Identification of a novel adrenomedullin gene family in teleost fish', *Biochem Biophys Res Commun,* 311 (4), 1072-7.

Okumura, H., et al. (2004), 'Adrenomedullin infusion attenuates myocardial ischemia/reperfusion injury through the phosphatidylinositol 3-kinase/Akt-dependent pathway', *Circulation,* 109 (2), 242-8.

Onitsuka, H., et al. (2004), 'Differential gene expression of adrenomedullin receptors in pressure- and volume-overloaded heart--role of angiotensin II', *Peptides,* 25 (7), 1107-14.

Ono, Y., et al. (2000), 'Decreased gene expression of adrenomedullin receptor in mouse lungs during sepsis', *Biochem Biophys Res Commun,* 271 (1), 197-202.

Ornan, D. A., Chaudry, I. H., and Wang, P. (2002), 'Saturation of adrenomedullin receptors plays an important role in reducing pulmonary clearance of adrenomedullin during the late stage of sepsis', *Biochim Biophys Acta,* 1586 (3), 299-306.

Ouafik, L., Berenguer-Daize, C., and Berthois, Y. (2009), 'Adrenomedullin promotes cell cycle transit and up-regulates cyclin D1 protein level in human glioblastoma cells through the activation of c-Jun/JNK/AP-1 signal transduction pathway', *Cell Signal,* 21 (4), 597-608.

Ouafik, L., et al. (2002), 'Neutralization of adrenomedullin inhibits the growth of human glioblastoma cell lines in vitro and suppresses tumor xenograft growth in vivo', *Am J Pathol,* 160 (4), 1279-92.

Palmer, T. D., et al. (2011), 'Targeting tumor cell motility to prevent metastasis', *Adv Drug Deliv Rev,* 63 (8), 568-81.

Parameswaran, N. and Spielman, W. S. (2006), 'RAMPs: The past, present and future', *Trends Biochem Sci,* 31 (11), 631-8.

Parameswaran, N., et al. (1999a), 'SB203580 reverses adrenomedullin's effect on proliferation and apoptosis in cultured mesangial cells', *Eur J Pharmacol,* 371 (1), 75-82.

Parameswaran, N., et al. (1999b), 'Regulation of glomerular mesangial cell proliferation in culture by adrenomedullin', *Eur J Pharmacol,* 372 (1), 85-95.

Park, S. C., et al. (2008), 'Hypoxia-inducible adrenomedullin accelerates hepatocellular carcinoma cell growth', *Cancer Lett,* 271 (2), 314-22.

Peeters, M. C., et al. (2011), 'Importance of the extracellular loops in G protein-coupled receptors for ligand recognition and receptor activation', *Trends Pharmacol Sci,* 32 (1), 35-42.

Peinado, H., Lavotshkin, S., and Lyden, D. (2011), 'The secreted factors responsible for pre-metastatic niche formation: old sayings and new thoughts', *Semin Cancer Biol,* 21 (2), 139-46.

Perkins, S. N., Husten, E. J., and Eipper, B. A. (1990), 'The 108-kDA peptidylglycine alpha-amidating monooxygenase precursor contains two separable enzymatic activities involved in peptide amidation', *Biochem Biophys Res Commun,* 171 (3), 926-32.

Pinkel, D. and Albertson, D. G. (2005), 'Array comparative genomic hybridization and its applications in cancer', *Nat Genet,* 37 Suppl, S11-7.

Pinto, A., et al. (1996), 'Effects of adrenomedullin and calcitonin gene-related peptide on airway and pulmonary vascular smooth muscle in guinea-pigs', *Br J Pharmacol,* 119 (7), 1477-83.

Pio, R., et al. (2001), 'Complement factor H is a serum-binding protein for adrenomedullin, and the resulting complex modulates the bioactivities of both partners', *J Biol Chem,* 276 (15), 12292-300.

Ponta, H., Sherman, L., and Herrlich, P. A. (2003), 'CD44: from adhesion molecules to signalling regulators', *Nat Rev Mol Cell Biol,* 4 (1), 33-45.

Prado, M. A., et al. (2001), 'The role of the CGRP-receptor component protein (RCP) in adrenomedullin receptor signal transduction', *Peptides,* 22 (11), 1773-81.

Qi, T., et al. (2008), 'Identification of N-terminal receptor activity-modifying protein residues important for calcitonin gene-related peptide, adrenomedullin, and amylin receptor function', *Mol Pharmacol,* 74 (4), 1059-71.

Qi, T., et al. (2011), 'Structure-function analysis of amino acid 74 of human RAMP1 and RAMP3 and its role in peptide interactions with adrenomedullin and calcitonin gene-related peptide receptors', *Peptides,* 32 (5), 1060-7.

Qing, X., Svaren, J., and Keith, I. M. (2001), 'mRNA expression of novel CGRP1 receptors and their activity-modifying proteins in hypoxic rat lung', *Am J Physiol Lung Cell Mol Physiol,* 280 (3), L547-54.

Rabbitts, T. H. (1994), 'Chromosomal translocations in human cancer', *Nature,* 372 (6502), 143-9.

Rafii, S., et al. (2002), 'Vascular and haematopoietic stem cells: novel targets for anti-angiogenesis therapy?', *Nat Rev Cancer,* 2 (11), 826-35.

Rahman, N. and Stratton, M. R. (1998), 'The genetics of breast cancer susceptibility', *Annu Rev Genet,* 32, 95-121.

Ramachandran, V., et al. (2007), 'Adrenomedullin is expressed in pancreatic cancer and stimulates cell proliferation and invasion in an autocrine manner via the adrenomedullin receptor, ADMR', *Cancer Res,* 67 (6), 2666-75.

Rasheed, B. K., et al. (1995), 'Chromosome 10 deletion mapping in human gliomas: a common deletion region in 10q25', *Oncogene,* 10 (11), 2243-6.

Ray, K., et al. (1998), 'Identification of the sites of N-linked glycosylation on the human calcium receptor and assessment of their role in cell surface expression and signal transduction', *J Biol Chem,* 273 (51), 34558-67.

Richard, D. E., Berra, E., and Pouyssegur, J. (2000), 'Nonhypoxic pathway mediates the induction of hypoxia-inducible factor 1alpha in vascular smooth muscle cells', *J Biol Chem,* 275 (35), 26765-71.

Richard, D. E., et al. (1999), 'p42/p44 mitogen-activated protein kinases phosphorylate hypoxia-inducible factor 1alpha (HIF-1alpha) and enhance the transcriptional activity of HIF-1', *J Biol Chem,* 274 (46), 32631-7.

Richards, A. M., et al. (2001), 'Plasma N-terminal pro-brain natriuretic peptide and adrenomedullin: prognostic utility and prediction of benefit from carvedilol in chronic ischemic left ventricular dysfunction. Australia-New Zealand Heart Failure Group', *J Am Coll Cardiol,* 37 (7), 1781-7.

Rios, C. D., et al. (2001), 'G-protein-coupled receptor dimerization: modulation of receptor function', *Pharmacol Ther,* 92 (2-3), 71-87.

Risau, W. (1997), 'Mechanisms of angiogenesis', *Nature,* 386 (6626), 671-4.

Robert, C. and Dubertret, L. (1995), '[Cancers of the skin, relations to ultraviolet rays]', *Presse Med,* 24 (34), 1610-6.

Robinson, S. D., et al. (2009), 'Novel peptide antagonists of adrenomedullin and calcitonin gene-related peptide receptors: identification, pharmacological characterization, and interactions with position 74 in receptor activity-modifying protein 1/3', *J Pharmacol Exp Ther,* 331 (2), 513-21.

Rocchi, P., et al. (2001), 'Expression of adrenomedullin and peptide amidation activity in human prostate cancer and in human prostate cancer cell lines', *Cancer Res,* 61 (3), 1196-206.

Rolfs, A., et al. (1997), 'Oxygen-regulated transferrin expression is mediated by hypoxia-inducible factor-1', *J Biol Chem,* 272 (32), 20055-62.

Rosenes, Z., et al. (2012), 'The anti-cancer IgM monoclonal antibody PAT-SM6 binds with high avidity to the unfolded protein response regulator GRP78', *PLoS One,* 7 (9), e44927.

Roux, K. H. (1999), 'Immunoglobulin structure and function as revealed by electron microscopy', *Int Arch Allergy Immunol,* 120 (2), 85-99.

Ryan, H. E., Lo, J., and Johnson, R. S. (1998), 'HIF-1 alpha is required for solid tumor formation and embryonic vascularization', *EMBO J,* 17 (11), 3005-15.

Ryan, H. E., et al. (2000), 'Hypoxia-inducible factor-1alpha is a positive factor in solid tumor growth', *Cancer Res,* 60 (15), 4010-5.

Sahai, E. (2007), 'Illuminating the metastatic process', *Nat Rev Cancer,* 7 (10), 737-49.

Salaspuro, M. (2007), 'Interrelationship between alcohol, smoking, acetaldehyde and cancer', *Novartis Found Symp,* 285, 80-9; discussion 89-96, 198-9.

Salceda, S. and Caro, J. (1997), 'Hypoxia-inducible factor 1alpha (HIF-1alpha) protein is rapidly degraded by the ubiquitin-proteasome system under normoxic conditions. Its stabilization by hypoxia depends on redox-induced changes', *J Biol Chem,* 272 (36), 22642-7.

Sanz-Moreno, V., et al. (2008), 'Rac activation and inactivation control plasticity of tumor cell movement', *Cell,* 135 (3), 510-23.

Sarbassov, D. D., et al. (2005), 'Phosphorylation and regulation of Akt/PKB by the rictor-mTOR complex', *Science,* 307 (5712), 1098-101.

Sata, M., et al. (2000), 'Adrenomedullin and nitric oxide inhibit human endothelial cell apoptosis via a cyclic GMP-independent mechanism', *Hypertension,* 36 (1), 83-8.

Satoh, F., et al. (1995), 'Adrenomedullin in human brain, adrenal glands and tumor tissues of pheochromocytoma, ganglioneuroblastoma and neuroblastoma', *J Clin Endocrinol Metab,* 80 (5), 1750-2.

Schwartz, G. F., et al. (1993), 'Clinical applications of serum and tissue markers in malignant disease: breast cancer as the paradigm', *Clin Chem,* 39 (11 Pt 2), 2404-12.

Schwarz, N., et al. (2006), 'Adrenomedullin increases the expression of calcitonin-like receptor and receptor activity modifying protein 2 mRNA in human microvascular endothelial cells', *J Endocrinol,* 190 (2), 505-14.

Scott, A. M., Wolchok, J. D., and Old, L. J. (2012), 'Antibody therapy of cancer', *Nat Rev Cancer,* 12 (4), 278-87.

Semenza, G. L. (1999), 'Regulation of mammalian O2 homeostasis by hypoxia-inducible factor 1', *Annu Rev Cell Dev Biol,* 15, 551-78.

Semenza, G. L. (2003), 'Targeting HIF-1 for cancer therapy', *Nat Rev Cancer,* 3 (10), 721-32.

Semenza, G. L., et al. (1991), 'Hypoxia-inducible nuclear factors bind to an enhancer element located 3' to the human erythropoietin gene', *Proc Natl Acad Sci U S A,* 88 (13), 5680-4.

Semenza, G. L., et al. (1996), 'Hypoxia response elements in the aldolase A, enolase 1, and lactate dehydrogenase A gene promoters contain essential binding sites for hypoxia-inducible factor 1', *J Biol Chem,* 271 (51), 32529-37.

Serrano, J., et al. (2008), 'Adrenomedullin expression is up-regulated by acute hypobaric hypoxia in the cerebral cortex of the adult rat', *Brain Pathol,* 18 (3), 434-42.

Sexton, P. M., et al. (2001), 'Receptor activity modifying proteins', *Cell Signal,* 13 (2), 73-83.

Sharma, S. D., et al. (2009), 'Intermittent hypoxia activates peptidylglycine alpha-amidating monooxygenase in rat brain stem via reactive oxygen species-mediated proteolytic processing', *J Appl Physiol,* 106 (1), 12-9.

Shichiri, M. and Hirata, Y. (2003), 'Regulation of cell growth and apoptosis by adrenomedullin', *Hypertens Res,* 26 Suppl, S9-14.

Shichiri, M., et al. (1999), 'Induction of max by adrenomedullin and calcitonin gene-related peptide antagonizes endothelial apoptosis', *Mol Endocrinol,* 13 (8), 1353-63.

Shimekake, Y., et al. (1995), 'Adrenomedullin stimulates two signal transduction pathways, cAMP accumulation and Ca2+ mobilization, in bovine aortic endothelial cells', *J Biol Chem,* 270 (9), 4412-7.

Shimosawa, T., et al. (2003), 'Organ-protective effects of adrenomedullin', *Hypertens Res,* 26 Suppl, S109-12.

Shindo, T., et al. (2001), 'Vascular abnormalities and elevated blood pressure in mice lacking adrenomedullin gene', *Circulation,* 104 (16), 1964-71.

Shipley, W. U., et al. (1999), 'Radiation therapy for clinically localized prostate cancer: a multi-institutional pooled analysis', *JAMA,* 281 (17), 1598-604.

Shweiki, D., et al. (1992), 'Vascular endothelial growth factor induced by hypoxia may mediate hypoxia-initiated angiogenesis', *Nature,* 359 (6398), 843-5.

Siclari, V. A., Guise, T. A., and Chirgwin, J. M. (2006), 'Molecular interactions between breast cancer cells and the bone microenvironment drive skeletal metastases', *Cancer Metastasis Rev,* 25 (4), 621-33.

Siegrist, W., Stutz, S., and Eberle, A. N. (1994), 'Homologous and heterologous regulation of alpha-melanocyte-stimulating hormone receptors in human and mouse melanoma cell lines', *Cancer Res,* 54 (10), 2604-10.

Simms, J., et al. (2006), 'Characterization of the structure of RAMP1 by mutagenesis and molecular modeling', *Biophys J,* 91 (2), 662-9.

So, S., et al. (1996), 'Up-regulation of rat adrenomedullin gene expression by endotoxin: relation to nitric oxide synthesis', *Life Sci,* 58 (19), PL309-15.

Sodhi, A., et al. (2000), 'The Kaposi's sarcoma-associated herpes virus G protein-coupled receptor up-regulates vascular endothelial growth factor expression and secretion through mitogen-activated protein kinase and p38 pathways acting on hypoxia-inducible factor 1alpha', *Cancer Res,* 60 (17), 4873-80.

Soengas, M. S., et al. (1999), 'Apaf-1 and caspase-9 in p53-dependent apoptosis and tumor inhibition', *Science,* 284 (5411), 156-9.

Souhami, L., et al. (2009), 'Impact of the duration of adjuvant hormonal therapy in patients with locally advanced prostate cancer treated with radiotherapy: a secondary analysis of RTOG 85-31', *J Clin Oncol,* 27 (13), 2137-43.

Stacker, S. A., et al. (2002), 'Lymphangiogenesis and cancer metastasis', *Nat Rev Cancer,* 2 (8), 573-83.

Staller, P., et al. (2003), 'Chemokine receptor CXCR4 downregulated by von Hippel-Lindau tumour suppressor pVHL', *Nature,* 425 (6955), 307-11.

Stambolic, V., et al. (1998), 'Negative regulation of PKB/Akt-dependent cell survival by the tumor suppressor PTEN', *Cell,* 95 (1), 29-39.

Steeg, P. S. (2006), 'Tumor metastasis: mechanistic insights and clinical challenges', *Nat Med,* 12 (8), 895-904.

Steiner, S. (1975), '[Rheumatic fever in soldiers]', *Vojnosanit Pregl,* 32 (6), 619-22.

Strader, C. D., et al. (1994), 'Structure and function of G protein-coupled receptors', *Annu Rev Biochem,* 63, 101-32.

Stupp, R., et al. (2006), 'Changing paradigms--an update on the multidisciplinary management of malignant glioma', *Oncologist,* 11 (2), 165-80.

Stupp, R., et al. (2005), 'Radiotherapy plus concomitant and adjuvant temozolomide for glioblastoma', *N Engl J Med,* 352 (10), 987-96.

Su, A. I., et al. (2002), 'Large-scale analysis of the human and mouse transcriptomes', *Proc Natl Acad Sci U S A,* 99 (7), 4465-70.

Sugo, S., et al. (1995a), 'Effects of vasoactive substances and cAMP related compounds on adrenomedullin production in cultured vascular smooth muscle cells', *FEBS Lett,* 369 (2-3), 311-4.

Sugo, S., et al. (1994a), 'Production and secretion of adrenomedullin from vascular smooth muscle cells: augmented production by tumor necrosis factor-alpha', *Biochem Biophys Res Commun,* 203 (1), 719-26.

Sugo, S., et al. (1995b), 'Interleukin-1, tumor necrosis factor and lipopolysaccharide additively stimulate production of adrenomedullin in vascular smooth muscle cells', *Biochem Biophys Res Commun,* 207 (1), 25-32.

Sugo, S., et al. (1994b), 'Endothelial cells actively synthesize and secrete adrenomedullin', *Biochem Biophys Res Commun,* 201 (3), 1160-6.

Sullivan, R. and Graham, C. H. (2007), 'Hypoxia-driven selection of the metastatic phenotype', *Cancer Metastasis Rev,* 26 (2), 319-31.

Sylvester, P. W. (2011), 'Optimization of the tetrazolium dye (MTT) colorimetric assay for cellular growth and viability', *Methods Mol Biol,* 716, 157-68.

Takahashi, K., et al. (2003), 'Suppression of cytokine-induced expression of adrenomedullin and endothelin-1 by dexamethasone in T98G human glioblastoma cells', *Peptides,* 24 (7), 1053-62.

Takahashi, T., Ueno, H., and Shibuya, M. (1999), 'VEGF activates protein kinase C-dependent, but Ras-independent Raf-MEK-MAP kinase pathway for DNA synthesis in primary endothelial cells', *Oncogene,* 18 (13), 2221-30.

Takahashi, Y., et al. (2000), 'Hypoxic induction of prolyl 4-hydroxylase alpha (I) in cultured cells', *J Biol Chem,* 275 (19), 14139-46.

Taniguchi, T., et al. (1999), 'Ocular effects of adrenomedullin', *Exp Eye Res,* 69 (5), 467-74.

Tannock, I. F. (1996), 'Treatment of cancer with radiation and drugs', *J Clin Oncol,* 14 (12), 3156-74.

Taylor, M. M. and Samson, W. K. (2004), 'A possible mechanism for the action of adrenomedullin in brain to stimulate stress hormone secretion', *Endocrinology,* 145 (11), 4890-6.

ten Freyhaus, H., et al. 'Hypoxia enhances platelet-derived growth factor signaling in the pulmonary vasculature by down-regulation of protein tyrosine phosphatases', *Am J Respir Crit Care Med,* 183 (8), 1092-102.

Totsune, K., et al. (2000), 'Increased gene expression of adrenomedullin and adrenomedullin-receptor complexes, receptor-activity modifying protein (RAMP)2 and calcitonin-receptor-like receptor (CRLR) in the hearts of rats with congestive heart failure', *Clin Sci (Lond),* 99 (6), 541-6.

Tsujikawa, K., et al. (2007), 'Hypertension and dysregulated proinflammatory cytokine production in receptor activity-modifying protein 1-deficient mice', *Proc Natl Acad Sci U S A,* 104 (42), 16702-7.

Turk, H. M., et al. (2000), 'Relationship between plasma adrenomedullin levels and metabolic control, risk factors, and diabetic microangiopathy in patients with type 2 diabetes', *Diabetes Care,* 23 (6), 864-7.

Udawela, M., Hay, D. L., and Sexton, P. M. (2004), 'The receptor activity modifying protein family of G protein coupled receptor accessory proteins', *Semin Cell Dev Biol,* 15 (3), 299-308.

Udono, T., et al. (2000), 'Increased expression of adrenomedullin mRNA in the tissues of intraocular and orbital tumors', *Am J Ophthalmol,* 129 (4), 555-6.

Ueda, N., et al. (1994), 'G protein beta gamma subunits. Simplified purification and properties of novel isoforms', *J Biol Chem,* 269 (6), 4388-95.

Uemura, M., et al. 'Hypoxia-inducible adrenomedullin in colorectal cancer', *Anticancer Res,* 31 (2), 507-14.

Valastyan, S. and Weinberg, R. A. (2011), 'Tumor metastasis: molecular insights and evolving paradigms', *Cell,* 147 (2), 275-92.

Vaupel, P. (2004), 'The role of hypoxia-induced factors in tumor progression', *Oncologist,* 9 Suppl 5, 10-7.

Vengellur, A. and LaPres, J. J. (2004), 'The role of hypoxia inducible factor 1alpha in cobalt chloride induced cell death in mouse embryonic fibroblasts', *Toxicol Sci,* 82 (2), 638-46.

Veronesi, U., et al. (2002), 'Twenty-year follow-up of a randomized study comparing breast-conserving surgery with radical mastectomy for early breast cancer', *N Engl J Med,* 347 (16), 1227-32.

Vollmers, H. P. and Brandlein, S. (2006), 'Natural IgM antibodies: the orphaned molecules in immune surveillance', *Adv Drug Deliv Rev,* 58 (5-6), 755-65.

Walker, C. S., et al. (2010), 'Regulation of signal transduction by calcitonin gene-related peptide receptors', *Trends Pharmacol Sci,* 31 (10), 476-83.

Walsh, M. T., Foley, J. F., and Kinsella, B. T. (1998), 'Characterization of the role of N-linked glycosylation on the cell signaling and expression of the human thromboxane A2 receptor alpha and beta isoforms', *J Pharmacol Exp Ther,* 286 (2), 1026-36.

Wang, D., et al. (2008), 'Immunohistochemistry in the evaluation of neovascularization in tumor xenografts', *Biotech Histochem,* 83 (3), 179-89.

Wang, P., et al. (1999), 'Reduction in vascular responsiveness to adrenomedullin during sepsis', *J Surg Res,* 85 (1), 59-65.

Wang, S. M. and Yang, W. L. (2009), 'Circulating hormone adrenomedullin and its binding protein protect neural cells from hypoxia-induced apoptosis', *Biochim Biophys Acta,* 1790 (5), 361-7.

Ward, E. (1995), 'Overview of preventable industrial causes of occupational cancer', *Environ Health Perspect,* 103 Suppl 8, 197-203.

Wartenberg, M., et al. (2003), 'Regulation of the multidrug resistance transporter P-glycoprotein in multicellular tumor spheroids by hypoxia-inducible factor (HIF-1) and reactive oxygen species', *FASEB J,* 17 (3), 503-5.

Weber, G. F. (2008), 'Molecular mechanisms of metastasis', *Cancer Lett,* 270 (2), 181-90.

Weber, M. A. (2005), 'The role of the new beta-blockers in treating cardiovascular disease', *Am J Hypertens,* 18 (12 Pt 2), 169S-76S.

Weisberg, E., et al. (1997), 'Role of focal adhesion proteins in signal transduction and oncogenesis', *Crit Rev Oncog,* 8 (4), 343-58.

Wheatley, M., et al. (2011), 'Lifting The Lid On G-Protein-Coupled Receptors: The Role Of Extracellular Loops', *Br J Pharmacol*.

Withers, D. J., et al. (1996), 'Adrenomedullin stimulates DNA synthesis and cell proliferation via elevation of cAMP in Swiss 3T3 cells', *FEBS Lett,* 378 (1), 83-7.

Witschi, H., et al. (1997), 'The carcinogenicity of environmental tobacco smoke', *Carcinogenesis,* 18 (3), 575-86.

Wu, L. W., et al. (2000), 'Utilization of distinct signaling pathways by receptors for vascular endothelial cell growth factor and other mitogens in the induction of endothelial cell proliferation', *J Biol Chem,* 275 (7), 5096-103.

Wu, X., et al. (1998), 'The PTEN/MMAC1 tumor suppressor phosphatase functions as a negative regulator of the phosphoinositide 3-kinase/Akt pathway', *Proc Natl Acad Sci U S A,* 95 (26), 15587-91.

Wyckoff, J., et al. (2004), 'A paracrine loop between tumor cells and macrophages is required for tumor cell migration in mammary tumors', *Cancer Res,* 64 (19), 7022-9.

Wyckoff, J. B., et al. (2000), 'A critical step in metastasis: in vivo analysis of intravasation at the primary tumor', *Cancer Res,* 60 (9), 2504-11.

Wyckoff, J. B., et al. (2007), 'Direct visualization of macrophage-assisted tumor cell intravasation in mammary tumors', *Cancer Res,* 67 (6), 2649-56.

Yagoda, A. and Petrylak, D. (1993), 'Cytotoxic chemotherapy for advanced hormone-resistant prostate cancer', *Cancer,* 71 (3 Suppl), 1098-109.

Yamaga, J., et al. (2003), 'Direct measurement of glycine-extended adrenomedullin in plasma and tissue using an ultrasensitive immune complex transfer enzyme immunoassay in rats', *Hypertens Res,* 26 Suppl, S45-53.

Yamaguchi, H., Wyckoff, J., and Condeelis, J. (2005), 'Cell migration in tumors', *Curr Opin Cell Biol,* 17 (5), 559-64.

Yamaguchi, T., et al. (1995), 'Effect of adrenomedullin on aldosterone secretion by dispersed rat adrenal zona glomerulosa cells', *Life Sci,* 56 (6), 379-87.

Yang, B. C., et al. (1996), 'Adrenomedullin dilates rat pulmonary artery rings during hypoxia: role of nitric oxide and vasodilator prostaglandins', *J Cardiovasc Pharmacol,* 28 (3), 458-62.

Yang, M. H., et al. (2008), 'Direct regulation of TWIST by HIF-1alpha promotes metastasis', *Nat Cell Biol,* 10 (3), 295-305.

Yang, S., et al. (2002), 'Novel approach to prevent the transition from the hyperdynamic phase to the hypodynamic phase of sepsis: role of adrenomedullin and adrenomedullin binding protein-1', *Ann Surg,* 236 (5), 625-33.

Yin, H., Chao, L., and Chao, J. (2004), 'Adrenomedullin protects against myocardial apoptosis after ischemia/reperfusion through activation of Akt-GSK signaling', *Hypertension,* 43 (1), 109-16.

Yoshida, D., et al. (2006), 'Hypoxia inducible factor 1-alpha regulates of platelet derived growth factor-B in human glioblastoma cells', *J Neurooncol,* 76 (1), 13-21.

Yoshihara, F., et al. (2000), 'Ventricular adrenomedullin concentration is a sensitive biochemical marker for volume and pressure overload in rats', *Am J Physiol Heart Circ Physiol,* 278 (2), H633-42.

Yoshihara, F., et al. (2005), 'Upregulation of intracardiac adrenomedullin and its receptor system in rats with volume overload-induced cardiac hypertrophy', *Regul Pept,* 127 (1-3), 239-44.

Yu, A. Y., et al. (1999), 'Impaired physiological responses to chronic hypoxia in mice partially deficient for hypoxia-inducible factor 1alpha', *J Clin Invest,* 103 (5), 691-6.

Yu, C. M., et al. (2001a), 'Increase in plasma adrenomedullin in patients with heart failure characterised by diastolic dysfunction', *Heart,* 86 (2), 155-60.

Yu, F., et al. (2001b), 'HIF-1alpha binding to VHL is regulated by stimulus-sensitive proline hydroxylation', *Proc Natl Acad Sci U S A,* 98 (17), 9630-5.

Zelzer, E., et al. (1998), 'Insulin induces transcription of target genes through the hypoxia-inducible factor HIF-1alpha/ARNT', *EMBO J,* 17 (17), 5085-94.

Zhang, S. X., et al. (2003), 'Hypoxia induces an autocrine-paracrine survival pathway via platelet-derived growth factor (PDGF)-B/PDGF-beta receptor/phosphatidylinositol 3-kinase/Akt signaling in RN46A neuronal cells', *FASEB J,* 17 (12), 1709-11.

Zhang, X., et al. (2005), 'Adrenomedullin enhances invasion by trophoblast cell lines', *Biol Reprod,* 73 (4), 619-26.

Zhao, L., et al. (1996), 'Adrenomedullin activity in chronically hypoxic rat lungs', *Am J Physiol,* 271 (2 Pt 2), H622-9.

Zhao, Y., et al. (1998), 'PCR display identifies tamoxifen induction of the novel angiogenic factor adrenomedullin by a non estrogenic mechanism in the human endometrium', *Oncogene,* 16 (3), 409-15.

Zhong, H., et al. (1999), 'Overexpression of hypoxia-inducible factor 1alpha in common human cancers and their metastases', *Cancer Res,* 59 (22), 5830-5.

Zhou, M., et al. (2002), 'Adrenomedullin binding protein-1 modulates vascular responsiveness to adrenomedullin in late sepsis', *Am J Physiol Regul Integr Comp Physiol,* 283 (3), R553-60.

Zimmermann, U., et al. (1996), 'Identification of adrenomedullin receptors in cultured rat astrocytes and in neuroblastboma x glioma hybrid cells (NG108-15)', *Brain Res,* 724 (2), 238-45.

Zucker, S., et al. (2001), 'Tumorigenic potential of extracellular matrix metalloproteinase inducer', *Am J Pathol,* 158 (6), 1921-8.

Zudaire, E., Martinez, A., and Cuttitta, F. (2003), 'Adrenomedullin and cancer', *Regul Pept,* 112 (1-3), 175-83.

Books

1. C.K. Bomford, I.H. Kunkler, (2002). Walter and Miller's textbook of Radiotherapy: Radiation Physics, Therapy and Oncology. 6E, Churchill Linvingstone, UK.

2. Charles A Janeway, (1997). Immunobiology: The immune system in health and disease. 3E, Current Biology Limited.

Humphrey P Rang, Maureen M Dale, James M Ritter, Rod J Flower, Graeme Henderson, (2011). Rang & Dale's Pharmacology. 7E, Churchill Livinstone, UK.

Conferences

a) Rheumatology conference, SECC, Glasgow, UK.

www.rheumatology.org.uk/includes/documents/cm_docs/2012/0930_is_adrenomedullin_a_potential_therapeutic_forosteoarthritis_while_its_truncated_peptide_2252_acts_as_a.pdf